Year : 2016

Structural analysis of adult neural stem cells and their niche in the adult hippocampus

Gebara Elias Georges

UNIL | Université de Lausanne
Faculté de biologie et de médecine

Département des Neurosciences Fondamentales

Structural analysis of adult neural stem cells and their niche in the adult hippocampus

Thèse de doctorat en Neurosciences

présentée à la

Faculté de Biologie et de Médecine
de l'Université de Lausanne

par

Elias Georges Gebara

Neurobiologiste diplômé de l'Université Paris-Est Créteil (UPEC)

Jury

Prof. Jean-Pierre Hornung, Président
Prof. Nicolas Toni, Directeur
Prof. Andrea Volterra, Co-Directeur
Prof. Yvan Arsenijevic, Expert interne
Prof. Carmen Sandi, Expert externe

Lausanne 2016

Programme doctoral interuniversitaire en Neurosciences des Universités de Lausanne et Genève

LEMANIC NEURO SCIENCE DOCTORAL SCHOOL

UNIL | Université de Lausanne

UNIVERSITÉ DE GENÈVE

UNIL | Université de Lausanne

UNIVERSITÉ DE GENÈVE

Programme doctoral interuniversitaire en Neurosciences des Universités de Lausanne et Genève

Imprimatur

Vu le rapport présenté par le jury d'examen, composé de

Président	Monsieur Prof. Jean-Pierre **Hornung**
Directeur de thèse	Monsieur Prof. Nicolas **Toni**
Co-directeur de thèse	Monsieur Prof. Andrea **Volterra**
Experts	Madame Prof. Carmen **Sandi**
	Monsieur Prof. Yvan **Arsenijevic**

le Conseil de Faculté autorise l'impression de la thèse de

Monsieur Elias Georges Gebara

Neurobiologiste diplômé de l'Université de Paris-Est Créteil (UPEC)

intitulée

Structural analysis of adult neural stem cells and their niche in the adult hippocampus

Lausanne, le 7 juillet 2016

pour Le Doyen
de la Faculté de Biologie et de Médecine

Prof. Jean-Pierre Hornung

« The staircase of science is Jacob's ladder, it ends at the feet of God »

Albert Einstein

« As long as our brain is a mystery, the universe, the reflection of the structure of the brain will also be a mystery »

Santiago Ramón y Cajal

« Has it ever struck you… that life is all memory, except for the one present moment that goes by you so quickly you hardly catch it going? It's really all memory… except for each passing moment »

Eric kandell

Death of a Dogma

"Once development has ended, the fonts of growth of the cells, axons and dendrites dries up irrevocably. In adult centers, the nerve paths are fixed and immutable: everything may die, nothing may be regenerated."

Santiago Ramon y Cajal, 1928

ACKNOWLEDGMENTS

…It is impossible to start….

It cannot be argued with that the most influential person in my graduate career has been my advisor, Nicolas Toni. Nico's passion, guidance, and discipline have been indispensable to my growth as a scientist and as a person over these past four and a half years. I am especially grateful to Nico for his devotion to his students' education and success. I have not heard of another professor who goes so far out of his/her way to make sure students are prepared for whatever the next step in their journeys may be.

I am especially indebted to my thesis committee members. You have been very gracious and generous with your time. Thank you so much.

I have had the great pleasure of working on my project with Sébastien Sultan, Fréderic Cassé and Jonathan Moss. Seb was the single most influential person on my development as a bench scientist. He taught me everything he knew. I am also grateful to Seb for helping me to learn that there is more than one way to approach a problem. His hard work and friendship over the past years have been critical. He is a brilliant scientist, and I am sure he will have a successful carrier. Fred, it was great to know him for the last year of my thesis. He was always helpful and comforting. The various members of the lab have provided a diverse, if occasionally tumultuous, environment that has not only shaped me as a neuroscientist, but also as a person. I wouldn't replace any of the people I have had the opportunity to work with in the lab. The early lab members were instrumental to me in learning techniques and in how to think about neurosciences. I want also to thank my two students who become friends Florian Udry and Pieter-Jan Gijs.

I am more and more grateful to Michel Keilar every day as I write my thesis. Mitch is so thoughtful in always trying to make the annoying parts of lab life run more smoothly. His good mood and his humor were essential for me. He always makes me laugh and has the most quotable quotes.

A special thanks to Alexandre Pinault. Alex is one of the more unusual (in a good way) characters I've met. I've enjoyed getting to know him better over the last two years or so,

and I'm sad that it took so long. He is a really thoughtful person. We had so much fun together with the movie shooting and especially in Barcelona.

I want to thank also my training buddies Ossama, Paul, Ludo, Mitch (again), Flo (again), Gil, Tamara, and Kim without your support and our crazy running competitions I wouldn't be able to pass the writing obstacle. I believe that writing my thesis was the hardest obstacle to pass.

I need to make a separate paragraph here for the best secretary team ever. Maria, Francine and Kim, I want to thank you for being here, for all the hard work you did for me (residents permit, contract, bills...) and especially for the great time we spent together laughing.

I want to take the opportunity to thank the Department of Fundamental neurosciences for their support and the warm family atmosphere. A special thanks to the animal facility and the CIF.

Finally, to thank the people who shaped me into who I am. Toufic Saad, Pierre Boufayssal and Bahaa Roustom have been my best friends since I can remember, and it is always awesome to spend great time with you Bros. I am very happy to have you around. It's really nice to have some extended family nearby.

Mom, dad, I wish I could see you more, but I wanted to take this chance to thank you for working so hard to keep the family together over the years. I know it was challenging raising me as a kid and a teenage, and I'm amazed that you managed to do it so successfully.

I want take the advantage to thank Maïté and Regis for being here, and being supportive for all these years.

My two love life, Sophie and Nathanael. I love you both. Without your love and your support I would not have been able to accomplish all this. Sophie your support through all these years has been treasured. Your encouragement, quiet patience and unwavering love were undeniably the bedrock upon which the past ten years of my life have been built. Your tolerance of my occasional vulgar moods is a testament in itself of your unyielding devotion and love.

I cannot thank you enough.

TABLE OF CONTENTS

LIST OF FIGURES

LIST OF APPENDICES

English abstract

Structural analysis of adult neural stem cells and their niche in the adult hippocampus

New neurons are constantly produced at the sub-granular zone of the dentate gyrus, this phenomenon is called adult neurogenesis. This process is tightly regulated by several extrinsic factors such as physical activity, enriched environment, hippocampal-dependent learning tasks and a large number of molecules, as well as by intrinsic factors such as the neurogenic niche and the neuronal activity. The adult neural stem cell has a very specific morphology: The cell body is located in the sub-granular zone extend a long radial process that seeps into the granular layer and branches in the first third of the molecular layer. The complex morphology of the neural stem cell, suggests that close contacts with numerous cell types of the neurogenic niche may finely regulate of its proliferation and differentiation. The structure and interactions of the adult neural stem cell with the neurogenic niche are, however, very poorly described.

Thus, the work of my thesis was to:

- Study the complex morphology of the neural stem cell
- Clarify the link between morphology and activity
- Study the nature of contact between the components of the neurogenic niche and the RGL neural stem cell
- Assess the role of certain cells of the niche in the regulation of proliferation and differentiation of adult neural stem cell.

In the adult dentate gyrus, we discovered the existence of two subpopulations of cells with similar morphologies and related to the stem cell: the type α and type β. The type α represents 76 % of all RGL cells, has a long primary process with a small branch on the molecular layer of the dentate gyrus. The type β cell represents 24 % of the cells, has a short primary process with significant branching within the granular layer. The two subpopulations express stem cell markers, while the β cells also co-express astrocytic markers. Using clonal analysis, we showed that the type α divides and gives rise to all cell types (neurons, astrocytes and β cell), while the type β do not divide but is essentially transformed into astrocyte. Thus, a type α morphology contributes to the stem cell ability to capture stimuli within the molecular layer that regulate its proliferation and differentiation.

Then, we evaluated the role of glia in the regulation of stem cell in different physiological states: voluntary running and brain aging. We have established that there is an inverse correlation between the activation state of microglia and adult neurogenesis. Similarly, we analyzed the involvement of astrocytes in the regulation of the RGL neural stem cells by testing the effect of two molecules produced by astrocytes. We found that D-serine and taurine stimulate stem cells proliferation and the formation and maturation of new neurons. Our results emphasize the importance of the neurogenic niche in the regulation of the stem cell.

This knowledge is crucial for the understanding of homeostasis and brain plasticity, and for the development of brain repair strategies.

French abstract

L'analyse structurale des cellules souches neurales et leur niche dans l'hippocampe adulte

De nouveaux neurones sont constamment produits au niveau de la couche sous-granulaire du gyrus denté, ce phénomène est appelé la neurogenèse adulte. Ce processus est finement régulé par plusieurs facteurs extrinsèques tels que l'activité physique, l'environnement enrichi, les tâches d'apprentissage hippocampiques-dépendantes et un grand nombre de molécules, ainsi que par les facteurs intrinsèques tels que la niche neurogènique et l'activité neuronale. La cellule souche neurale adulte dispose d'une morphologie très particulière pour une cellule souche : Son corps cellulaire est situé dans la couche sous-granulaire et elle projette un long processus radial qui s'infiltre dans la couche granulaire et se ramifie dès le début de la couche moléculaire. La morphologie complexe de la cellule souche neurale, suggère qu'elle établit des contacts étroits avec différents types cellulaires de la niche neurogénique, qui contribuent à sa régulation. La structure et les interactions de la cellule souche neurale adulte avec la niche neurogénique sont cependant très peu décrites.

Ainsi, le travail de ma thèse consiste à :

- Etudier la morphologie complexe de la cellule souche neurale
- Clarifier le lien entre morphologie et activité
- Etudier la nature des contacts entre les composants de la niche neurogénique et la cellule souche
- Evaluer le rôle de certaines cellules de la niche dans la régulation de la prolifération et de la différenciation de la cellule souche neuronale adulte.

Dans le gyrus denté adulte, nous avons decouvert l'existence de deux sous-populations de cellules de morphologies similaires et apparentées à la cellule souche: la type α et la type β. La type α représente 76% de toutes les cellules à morphologie radiaire et possède un processus primaire long avec une ramification modeste au niveau de la couche moléculaire du gyrus denté. La type β représente 24% des cellules à morphologie radiaire et possède un processus primaire court avec une importante ramification à l'intérieur de la couche granulaire. Les deux sous-populations expriment les marqueurs de cellules souches, alors que la cellule β co-exprime également des marqueurs astrocytaires. A l'aide d'une analyse clonale, nous avons montré que la type α se divise et donne naissance à tous types de cellules (neurones, astrocytes et cellule β), alors que la type β ne se divise pas mais se transforme essentiellement en astrocyte. Ainsi, une morphologie de type α accorde à la cellule souche la possibilité de capter des stimuli régulant sa prolifération et sa différenciation au sein de la couche moléculaire.

Ensuite, nous avons évalué le rôle de la glie dans la régulation de la cellule souche dans différents états physiologiques : la course volontaire et le vieillissement cérébral. Nous avons établi qu'il existait une corrélation inverse entre l'état d'activation de la microglie et la neurogenèse adulte. De même, nous avons analysé l'implication des astrocytes dans la régulation de la cellule souche en testant l'effet de deux molécules produites par les astrocytes. Nous avons trouvé que la D-serine et la taurine stimulent la prolifération des cellules souches ainsi que la formation et la maturation des nouveaux neurones. Nos résultats soulignent l'importance de la niche neurogénique dans la régulation de la cellule souche.

Ces connaissances sont d'une importance cruciale pour la compréhension de l'homéostasie et de la plasticité du cerveau, ainsi que pour la mise en place des stratégies de réparation cérébrale.

CHAPTER 1: PREAMBLE

The adult central nervous system was supposed to be one of rare areas whereby new generation of neurons was impossible and imagined to be pointless and unfavorable to normal brain function. Actually, Santiago Ramón y Cajal believed that the adult brain is an organ where “everything may die, nothing may be regenerated” (1913). This dogma lived for almost 50 years until the early sixties’ where Joseph Altman first described putative proliferating cells in rat hippocampus. Regardless of these initial studies that described adult neurogenesis (Altman, 1962; Altman and Das, 1965), and its obvious occurrence across vertebrates, from birds to humans (Eriksson et al., 1998; Goldman and Nottebohm, 1983), the presumption that neurogenesis is restricted to embryonic development continued for a long time and the recognition of adult neurogenesis by the scientific community is a relatively recent advance (Kaplan, 2001).

In the past two decades, it has been progressively demonstrated that the mammalian adult brain, including humans (Eriksson et al., 1998; Spalding et al., 2013) retains stem cells that generate new, functional neurons (Bergmann and Frisen, 2013; Ming and Song, 2011). These findings promote the tempting vision of using adult neural stem cells to regenerate and repair brain tissue.

We must first understand the basic cellular mechanisms used to achieve adult neurogenesis, in order to use it for therapeutic purposes. Several questions remain unanswered, two of which captured my attention during my doctoral work: why the adult neural stem cells have this very complex morphology? How the adult neural stem cell is regulated inside its neurogenic niche?

CHAPTER 2: GENERAL INTRODUCTION

2.1 Introduction

This section summarizes key biological aspects of neurogenesis, including where it occurs, the main functions and how this process is regulated.

2.2 Neurogenesis in the adult brain

It is now firmly recognized that neurogenesis persists in the adult mammalian brain in at least two specific brain regions: the sub-ventricular zone (SVZ) of the lateral ventricles and in the sub-granular zone (SGZ) of the dentate gyrus (DG) of the hippocampus (Altman, 1963; Altman and Das, 1965; Lois and Alvarez-Buylla, 1994; Mirzadeh et al., 2008). While neurogenesis in these two regions has been considerably documented, the generation of new neurons may also occur in different brain regions such as the cortex, hypothalamus, striatum and cerebellum, although these finding are still controversial.(Gould et al., 2001; Luzzati et al., 2007; Migaud et al., 2010; Ponti et al., 2010). However, we will focus on here in the adult neurogenesis in the two main regions.

2.2.1 The Sub-ventricular Zone

The SVZ retains the largest number of proliferating cells in the adult brain of most mammals, including humans (Altman, 1963; Bernier et al., 2000; Gould et al., 1999; Kaplan, 1985; Kornack and Rakic, 2001). It is estimated that almost 30,000 neuroblasts are generated daily in the mouse SVZ (Lois and Alvarez-Buylla, 1994).

2.2.1.1 Proliferation and production of neural precursors

In the SVZ, a population of slowly dividing astrocytes with radial glial morphology act as the neural stem/precursor cells (Alvarez-Buylla and Lim, 2004; Doetsch et al., 1999). These cells are known as the type B cells. They occasionally send a process through the ependymal layer

to contact the ventricle, which might indicate an activated stem cell (Conover et al., 2000; Doetsch et al., 1999). The type B cells are multipotent. They give rise to fast dividing immature, transit amplifying precursor cells, the type C cells. Then, type C cells give rise to PSA-NCAM positive neuroblast, also called type A cells (Doetsch and Alvarez-Buylla, 1996) figure 1.

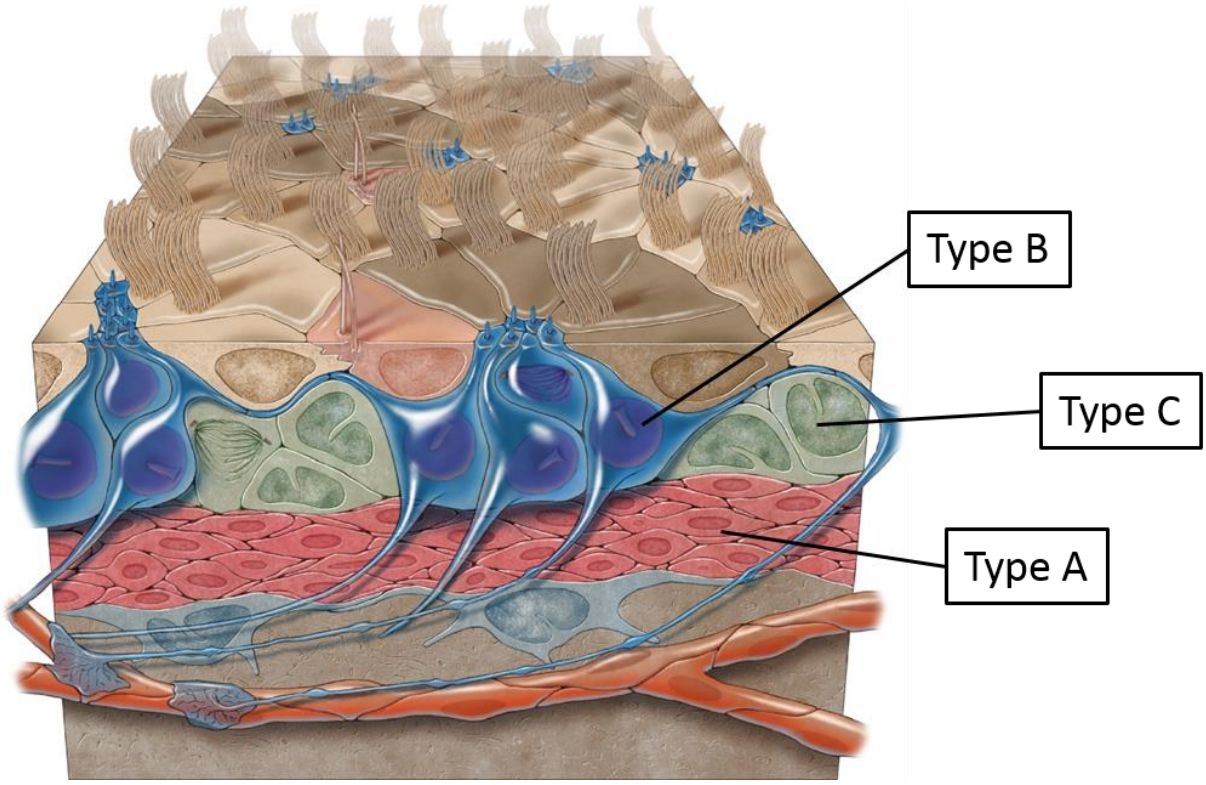

Figure 1: Model of the adult neurogenesis in the SVZ

3D model of the adult VZ neurogenic niche illustrating type B cells (blue), type C cells (green), and type A cells (red). Type B cells have a long basal process that terminates on blood vessels (orange) and an apical ending at the ventricle surface. Note the pinwheel organization (light and dark brown) composed of ependymal cells encircling type B apical surfaces (adapted from (Mirzadeh et al., 2008)).

2.2.1.2 Migration of neuroblasts to the olfactory bulb

In order to reach the olfactory bulb (OB), the newly generated neuroblasts undertake tangential migration in chains. They bind to each other using cell adhesion molecules such as integrins or PSA-NCAM (Murase and Horwitz, 2002). They migrate through an astrocyte lined migratory trail commonly called the rostral migratory stream (RMS) (Doetsch and Alvarez-Buylla, 1996; Kornack and Rakic, 2001; Lois and Alvarez-Buylla, 1994; Wichterle et

al., 1999). This migration is regulated by several repulsive and attractive factors, such as ephrins (Conover et al., 2000; Nguyen-Ba-Charvet et al., 2004), neurotransmitters like GABA (Bolteus and Bordey, 2004; Snapyan et al., 2009) and growth factors like GDNF, VEGF and BDNF (Paratcha et al., 2006; Snapyan et al., 2009; Wittko et al., 2009). Moreover, the neuroblasts take advantage of the position of blood vessels to use them as a scaffold for migration (Snapyan et al., 2009). Once they reach the OB, neuroblasts stop their tangential migration and begin a radial migration that allows them to integrate in the GCL and GL (Kriegstein and Alvarez-Buylla, 2009). This second migration is tightly regulated by several factors such as reelin, IGF1 (Insulin like growth factor 1), TNR (tenascin-R) and PK2 (prokineticin) (Hack et al., 2002; Hurtado-Chong et al., 2009; Ng et al., 2005; Saghatelyan et al., 2004) Figure 2.

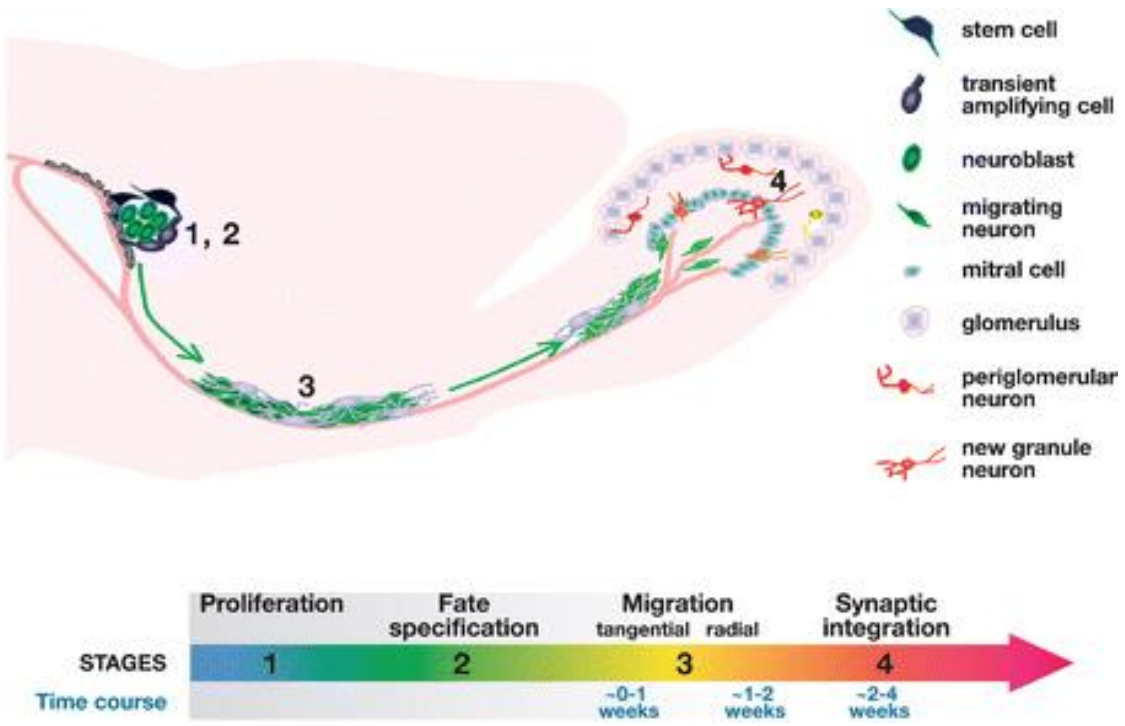

Figure 2: Generation of new interneurons in the OB

Adult neurogenesis in the SVZ/olfactory systems sustains four developmental stages. Stage1. Proliferation: adult neural stem cells give rise to transient amplifying cells. Stage2. Fate specification: transient amplifying cells differentiate into neuroblasts. Stage3. Migration: neuroblasts migrate in chains through the RMS to the OB. Stage4. Synaptic integration: neuroblasts differentiate into either granule neurons (Gr) or periglomerular neurons (PG) (Ming and Song, 2005).

2.2.1.3 Maturation and integration of newly generated interneurons

To reach the OB, neuroblasts migrate through the RMS for 4 to 10 days (Winner et al., 2002). Once they reach the OB these cells start to mature and integrate into the existing network, most of the neuroblasts will differentiate into granule cells (GCs), the remaining cells will differentiate into periglomerular neurons (PGs). GCs do not extend axons, have short basal dendrites that are confined within the granular cell layer, and a longer spiny apical dendrite that extend towards the external plexiform layer (EPL) where they form dendrodendritic synapses with lateral dendrites of the mitral cells (Shepherd et al., 2007) (Figure 3). These neurons play a role in olfactory function.

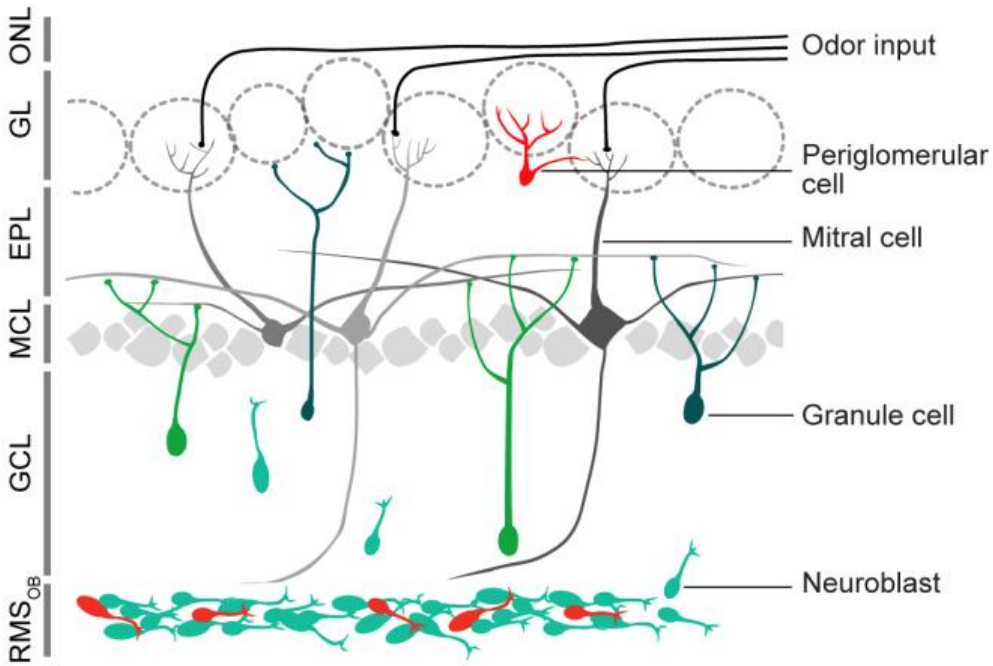

Figure 3: The laminar organization of the OB

Newly generated neuroblasts differentiate into granule and periglomerular neurons, adapted from (Breton-Provencher and Saghatelyan, 2012).

2.2.2 The dentate gyrus and the hippocampus

2.2.2.1 Anatomy and function of the hippocampus

The hippocampus is a major component of the brains of mammals including humans. It belongs to the limbic system and includes several distinct cytoarchitectural regions (Figure 4): the entorhinal cortex (EC), dentate gyrus (DG), hippocampus proper (including the Cornu Ammonis (CA), and subicular complex (Amaral et al., 2007; Amaral and Witter, 1989). The dentate gyrus contains the supra- (upper) and infra- (lower) pyramidal blades and the hilus, while the CA is differentiated into fields - CA1, CA2, and CA3 (Andersen et al., 2007).

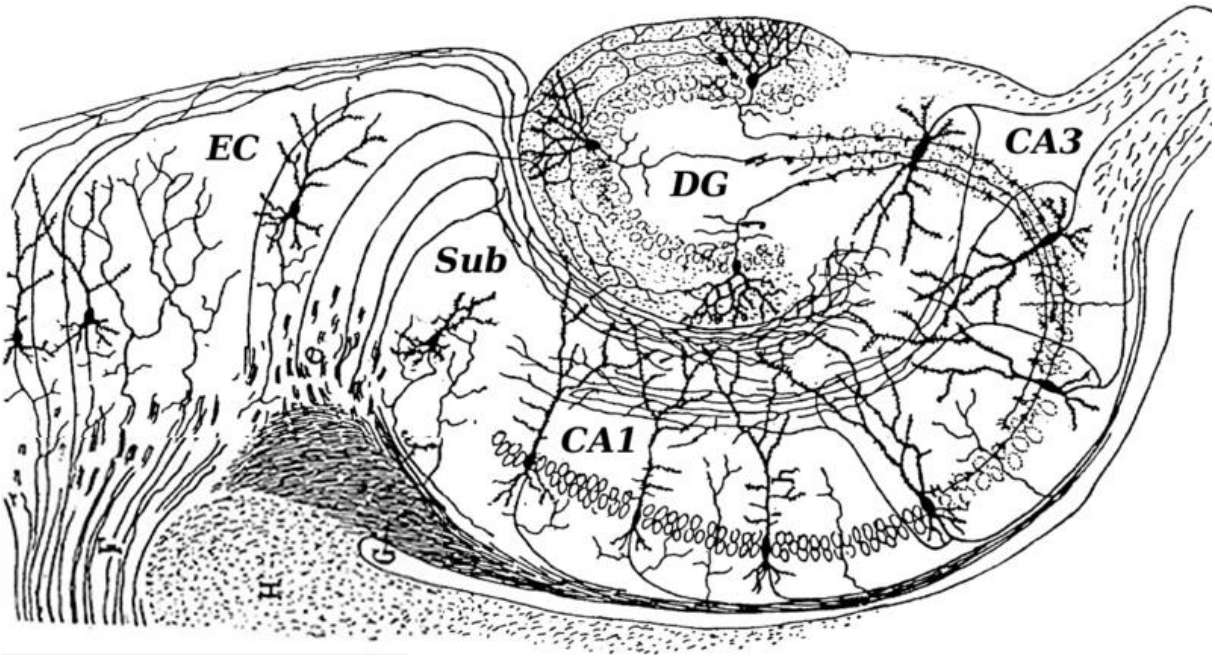

Figure 4: Drawing of the neural circuitry of the rodent hippocampus

Modified from Santiago Ramón y Cajal.

The main interest in the hippocampal function came after (Scoville and Milner, 1957) described a severe memory impairments in patient H.M. after the removal of his hippocampus in order to treat his epilepsy. H.M. patient showed deep anterograde amnesia and a temporally retrograde amnesia. He could not learn new explicit information or remember events that occurred recently prior to his surgery. However, H.M. patient was able to remember information from remote time periods from earlier in his life. These

findings suggest that the hippocampus is involved in encoding memories and retrieving recent memories. Then, several studies showed the importance of the hippocampus in the encoding and retrieval of explicit memory (Fuhs and Touretzky, 2007; Manns and Eichenbaum, 2009; Muller et al., 1996; Nadel and MacDonald, 1980). Moreover, studies revealed the role of the hippocampus in the development of allocentric spatial representations both in humans as well as animal models (O'Keefe, 1991).

The DG is formed mainly of excitatory granule neurons and a population of interneurons (Patton and McNaughton, 1995). The DG receives input from other structures in the hippocampal region, as well as the entorhinal cortex (EC), the thalamus, hypothalamus, medial septal complex and brainstem (Finch et al., 1986; Patton and McNaughton, 1995). The entorhinal cortex fibers project into the DG through the perforant pathway, previously described by Ramón y Cajal. This perforant pathway is the most important input to the DG and is responsible for most of the synaptic input onto dendrites in the ML (Witter, 2007).

The afferents from the lateral and medial perforant pathway make synapses with dendrites of granule neurons within the outer and medial ML (Ruth et al., 1982; Witter, 2007). Mossy fibers axons of granular neurons project into the hilus and stratum lucidum of CA3 in rodents. Mossy fiber axons establish synapses with inhibitory interneurons, hilar mossy cells, and CA3 pyramidal cells (Acsady et al., 1997), but only very rarely with other granule cells. These CA3 neurons project via the Schaffer collaterals to CA1 pyramidal neurons. These pyramidal neurons have axons that expand into the direction of the subiculum and then of the EC See figure 5 for a simplified illustration of hippocampal connectivity.

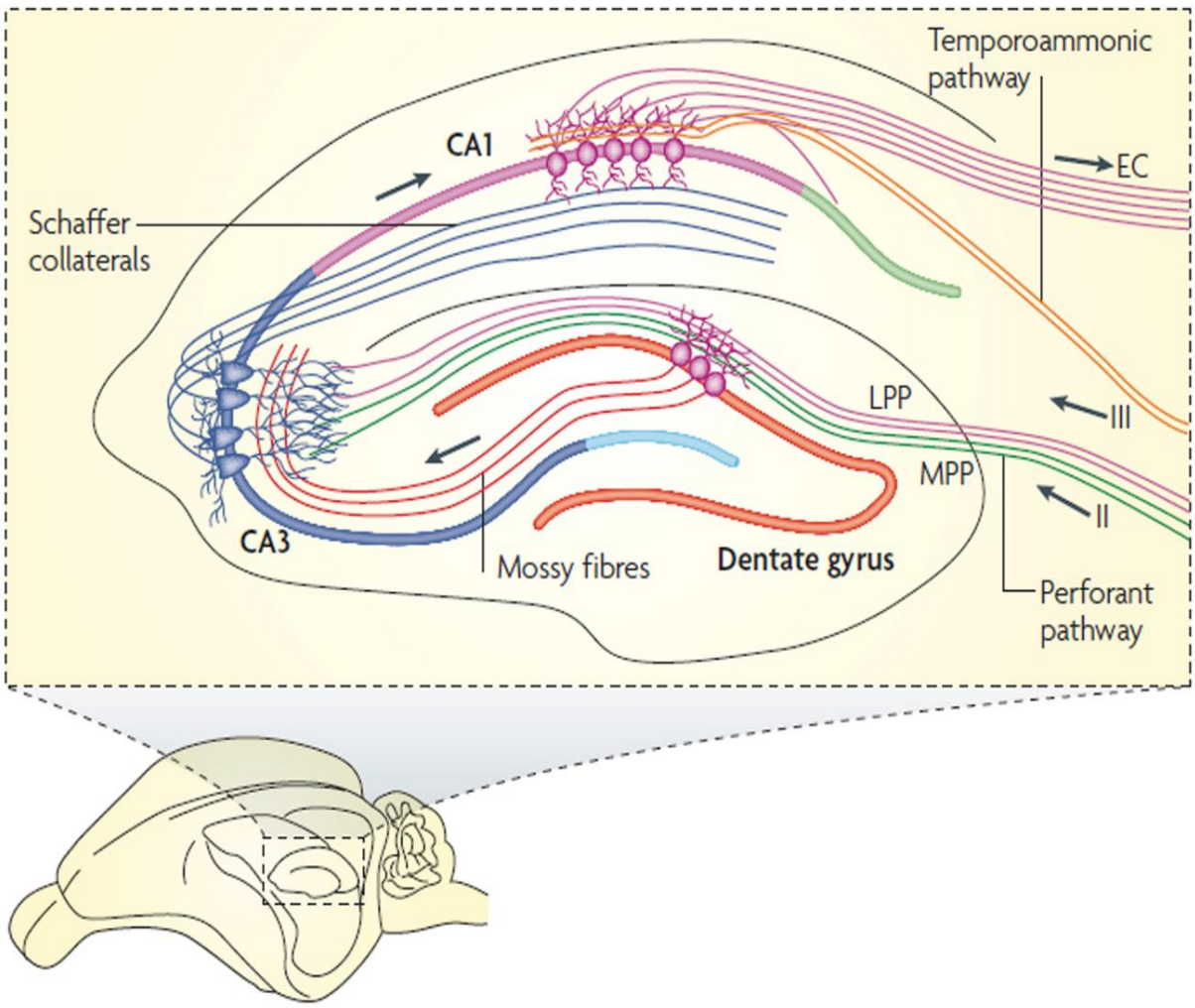

Figure 5: Anatomy and neuronal circuit of the hippocampus

The hippocampus receives synaptic input from the entorhinal cortex (EC) on the dentate gyrus (DG). Dentate granule neurons then project to CA3 neurons via the Mossy fibers. These CA3 neurons project via the Schaffer collaterals to CA1 pyramidal neurons. Their axons stretch into the direction of the EC. LPP, lateral perforant pathway; MPP, medial perforant pathway. From (Deng et al., 2010).

The DG is built from concentric layers. The first, the subgranular zone where reside the soma of the radial glia like cells (type 1 cells) and where adult hippocampal neurogenesis occurs. The second, the granule cell layer (GCL), contains the heavily packed soma of the granule neurons. The third, the molecular layer (ML), contains mainly the afferent fibers from the entorhinal cortex and the dendrites of granular neurons (Figure 6).

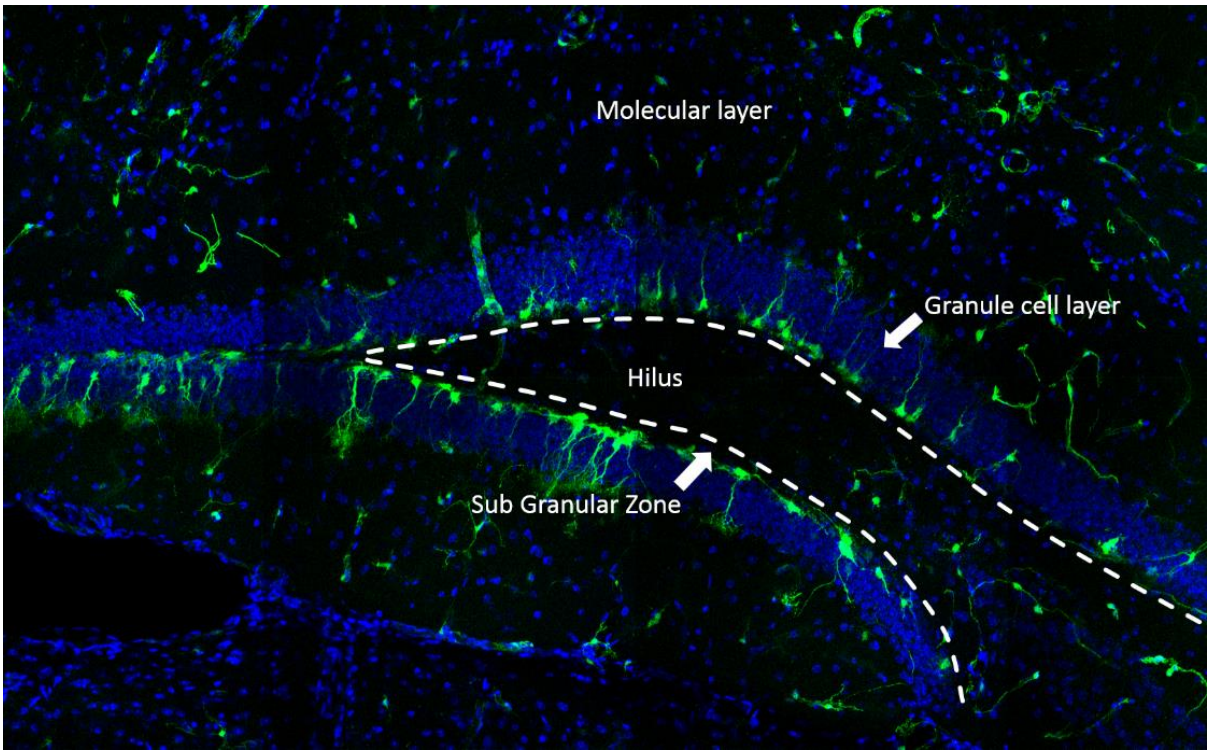

Figure 6: Structure of the mouse dentate gyrus

The mouse dentate gyrus is shaped in three layers and the hilus. The sub-granular zone (SGZ), encloses the soma of adult neural stem cell. The granule cell layer (GCL), encloses the cell bodies of the granular neurons. The molecular layer (ML) contains the dendrites of the granular cells and the afferent fiber from the entorhinal cortex. The hilus holds the axons of the granular neurons and interneurons.

2.2.2.2 Adult neurogenesis in the dentate gyrus: The process

Radial glia-like (RGL) neural stem cells reside in the SGZ of the DG, they are characterized by a long unique process that goes through the granular cell layer with an arborization spreading most of the time at the top of the GCL and in the inner third of the ML (Filippov et al., 2003) (figure 7).

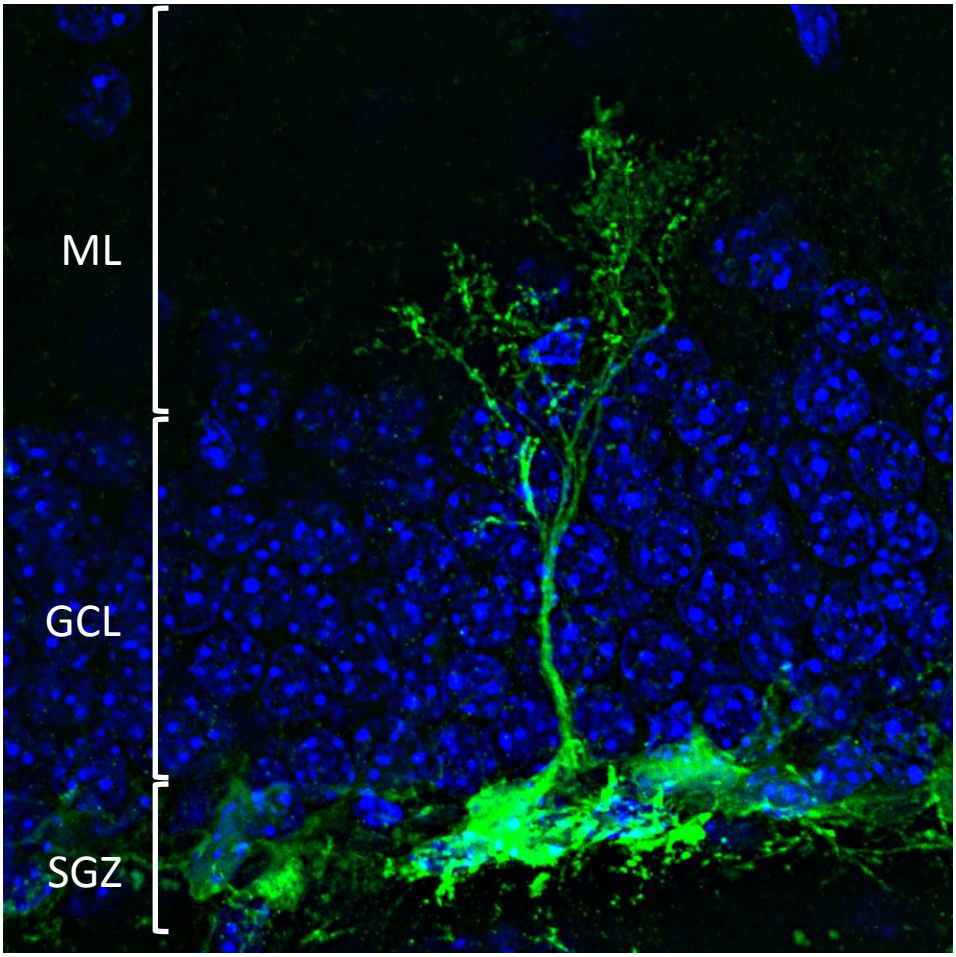

Figure 7: The radial Glia like (RGL) neural stem cell

RGL neural stem cells have a triangular soma located in the subgranular zone (SGZ), a radial process extending through the granule cell layer (GCL) that ends into a dense mesh of astrocyte-like processes in the molecular layer (ML).

RGL cells have astrocyte-like properties, they express GFAP and gap junction proteins and are coupled to neighbouring cells (Kunze et al., 2009; Seri et al., 2001). They also express Nestin, and Sox2 among other markers (Lagace et al., 2007; Suh et al., 2007) and are relatively quiescent. Isolated hippocampal progenitors cultured *in vitro* are able to generate neurons and astrocytes (Palmer et al., 1999) and recently, strong evidence indicated that *in vivo*, individual RGLs not only generate neurons, but also generate astrocytes either directly or through terminal differentiation (Bonaguidi et al., 2011; Encinas et al., 2011).

In the dentate gyrus, these RGL Nestin$^+$GFAP$^+$ stem cells give rise (by asymmetrical division) to type 2 cells also called Transit-amplifying progenitors (TAPs) that still express Nestin but not GFAP anymore. Their morphology and proliferative rate differs from RGL cells as they just have two small processes oriented tangentially to the SGZ and divide a lot (Fukuda et al., 2003; Kempermann et al., 2004; Kronenberg et al., 2003). They are divided in type 2a (Tbr2$^+$DCX$^-$PSA-NCAM$^-$) and type 2b (Tbr2$^+$DCX$^+$PSA-NCAM$^+$) (Kronenberg et al., 2003). DCX and PSA-NCAM are suggestive of neuronal lineage determination. Type 2b cells become neuroblasts as soon as they begin their axonal and dendritic growth.

At this stage, the early neuroblasts receive only GABAergic input from interneurons residing in the hilus (Zhao et al., 2008). Due to a high anion chloride intracellular concentration, the GABAergic signaling on early neuroblasts is excitatory, increasing intracellular Ca++ concentration and promoting neuronal differentiation (Piatti et al., 2006; Tozuka et al., 2005; Wang et al., 2005). Neuroblasts slowly migrate from the SGZ to the GCL and their dendrites reach the inner part of the molecular layer whereas their axon reaches the hippocampal CA3 region both around 10 days after generation from RGL cells (Piatti et al., 2006; Zhao et al., 2006).

Between two and four weeks after generation, the newborn neurons switch from excitatory to inhibitory GABA and receive glutamatergic inputs on dendritic spines that slowly mature (Piatti et al., 2006; Toni et al., 2007; Zhao et al., 2006). The main input on newborn neurons (and mature granular cells in general) comes from the entorhinal cortex through the perforant path (Laplagne et al., 2006; Toni et al., 2007; van Praag et al., 2002) whereas their outputs are in the CA3 region, and the hilus with glutamate as principal neurotransmitter (Toni et al., 2008; Zhao et al., 2006). Newborn neurons exhibit a lower threshold for the induction of long term potentiation (LTP), which results in a high synaptic plasticity (Schmidt-Hieber et al., 2004) and facilitate their integration into the hippocampus network. As a marker of maturation, newborn neurons express NeuN (Eriksson et al., 1998; Kuhn et al., 1996) and, 8 weeks after cell division, become indistinguishable from their neighbouring granule neurons (Laplagne et al., 2006)(Figure 8).

To become a mature neuron, the newly generated cells have to survive and their success depends on their integration in the pre-existing network. Thus, most of the TAPs die before they can become neuroblasts (Dayer et al., 2003; Kempermann et al., 1997a) if deprived of

GABAergic input. As previously mentioned, TAPs first receive GABAergic input that promotes their neuronal differentiation and therefore their survival (Ge et al., 2007; Tozuka et al., 2005). The remaining newborn neurons have to establish proper functional connections with the pre-existing network in order to survive. This inevitably leads to competition between newborn and probably also pre-existing neurons for available targets innervations (Bergami and Berninger, 2012; Tashiro et al., 2006; Toni et al., 2007). One of the hypothesis that emerges is that by increasing the local neuronal activity of the dentate gyrus (e.g. through learning), it is possible to increase the available connections with the pre-existing network and thus promote survival of newborn neurons through their integration.

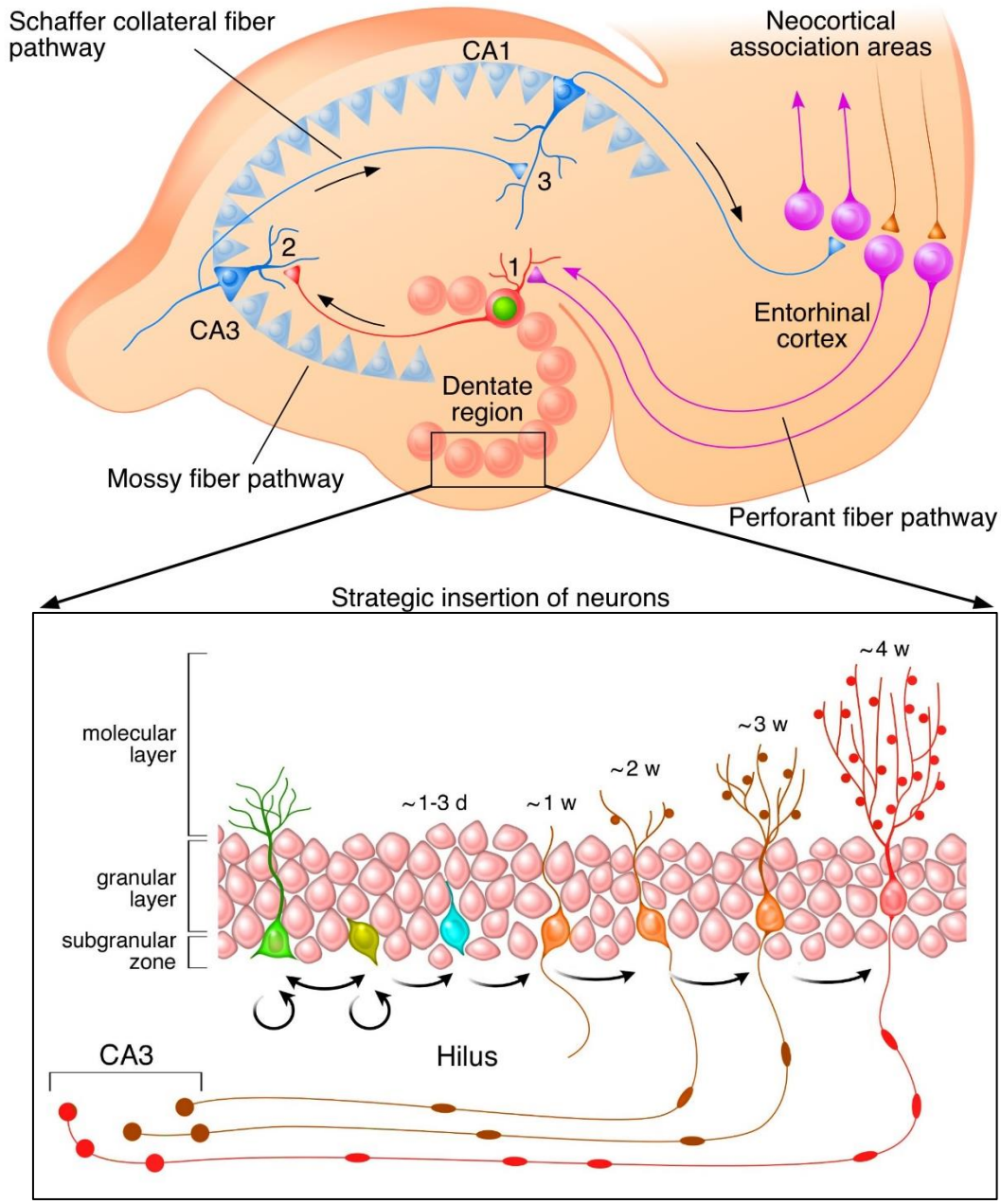

Figure 8: Neurogenesis in the dentate gyrus

Schematic of the hippocampus with CA1, CA3, dentate gyrus (DG), and hilus regions. The SGZ niche is comprised of radial and horizontal type 1 NSCs (green), early stage type 2a TAPs (yellow), late stage type 3 TAPs (bleu), immature granule neurons (orange), and mature granule neurons (red). The progression from type 1 NSCs to mature granule neurons in adult SGZ is a multistep process with distinct stages and is controlled by the sequential expression of transcription factors. (ML) Molecular layer; (GCL) granule cell layer.

2.2.2.3 Function of hippocampal neurogenesis

In the dentate gyrus, newly generated neurons display enhanced plasticity and a lower threshold for LTP (long term potentiation) initiation. Under identical conditions, LTP could be induced more easily in newly generated neurons than mature ones (Schmidt-Hieber et al., 2004). Moreover, newborn neurons, upon activation, showed fast and brief up-regulation of immediate early genes (such as Fos, Arc, Zif268) (Kee et al., 2007). The increase of immediate early genes expression in newly generated DGCs, suggests functional activation. Such results support the idea that adult-born neurons integrate into the pre-existing hippocampal circuits, and that they are preferentially activated during memory encoding and retrieval. A hyper-excitability and enhanced plasticity of newborn granule neurons can explain this preferential activation (Ge et al., 2007).

Reduced adult neurogenesis in rodents has consistently suggested a participation of adult newborn granule neurons in learning and memory (Deng et al., 2009; Snyder et al., 2005). Mice exposed to enriched environment and voluntary wheel running were shown to both have increased neurogenesis and memory performance (Kempermann et al., 1997b; van Praag et al., 1999). However, correlation doesn't mean causality. While, the correlation between cognition and stress is controversial (Shors, 2004), aged animals show impaired learning and memory in the Morris water maze for example. Additionally, a correlation between performance in the Morris water maze and adult neurogenesis was observed in individual aged animals in some but not in other studies (Groves et al., 2013). Therefore, whether hippocampal neurogenesis is a major causal factor for the changes in cognition is yet to be determined.

To directly assess the role of newly generated neurons in memory performance (Gu et al., 2012) aimed to reversibly silence adult-born hippocampal neurons during behavioral tasks by using optogentics. For this, they generated a retrovirus carrying the expression cassette of an inhibitory optogene, Archaerhodopsin-3. This retrovirus selectively infects dividing cells, therefore, selectively targeting a population of neurons born at the same time frame. With this approach, they were able to reversibly silence hippocampal adult-born neurons at different stage of their maturation, in behaving mice. During silencing, they challenged the

mice with two different behavioral assays: spatial learning in Morris water maze and contextual fear conditioning.

They found that silencing granule neurons 4 weeks after cell division, a time window where neurons display an increase synaptic integration, altered hippocampal memory performance in the two tests. Whereas, silencing these neurons after or before this time window had no effect on memory performance. This suggests that adult-born neurons play a specific role in learning and memory in the time window during which they display increased synaptic plasticity.

These results support the hypothesis that adult-born neurons become functional and play a role in learning and memory. Thus, understanding the mechanisms of regulation of adult neurogenesis is crucial for our ability to manipulate this process for the treatment of memory impairment in aging or disease.

2.3 Regulation of adult neurogenesis in the DG

Ultimately, adult neurogenesis is regulated by behavioral response to external stimuli (Glasper et al., 2012; Kempermann, 2011), which is logical from an evolutionary point of view. Indeed, such a plastic process able to impact learning and memory performance, and thus behavior, has to be responsive to environmental clues in order for the individual to better adapt to an ever-changing environment. However, in order to regulate adult neurogenesis, the behavioral responses to external stimuli has to eventually act at the transcriptional level. In-between, other regulatory levels are present, leaving a hierarchical model of adult neurogenesis regulation (figure 9), as described in Kempermann's review on the subject (Kempermann, 2011). For instance, in order to impact adult neurogenesis, the behavior of an individual responding to an external stimulus will obviously have to act on inner levels such as the hippocampal formation.

As adult neurogenesis can be regulated on so many levels, it is not surprising to have such a long and growing list of regulators. Indeed, starting from this hierarchical model of

regulation, an external stimulus able to act on one's behavior can possibly act on adult neurogenesis if it impacts inner levels until the transcriptional one.

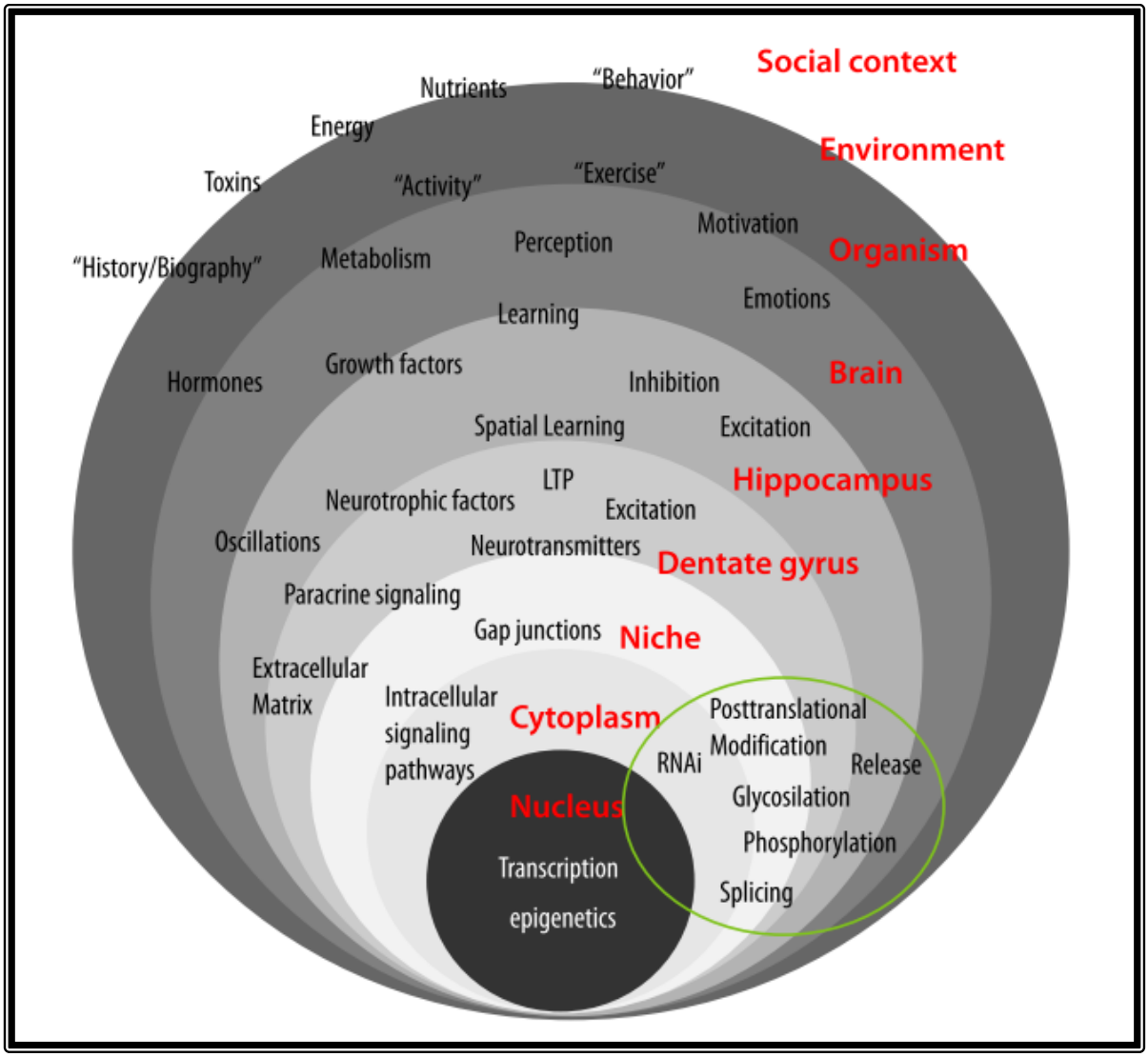

Figure 9: Hierarchical model of adult neurogenesis regulation

Adult neurogenesis regulation can occur at numerous levels as described by this scheme. Each outer level impacts the inner one until acting on transcriptional activity and eventually adult neurogenesis. Many regulators are able to act on different levels (e.g. neurotransmitter) showing the complexity of adult neurogenesis regulation. Although the scheme is simplified, the concept of a hierarchical organization of the regulation of adult neurogenesis is undisputable. Adapted from (Kempermann, 2011).

Neurogenesis is tightly regulated by the stem cells' highly specialized microenvironment, called the neurogenic niche (Mercier et al., 2002; Palmer et al., 2000; Tavazoie et al., 2008).

Shihabuddin and colleagues demonstrated the importance of the neurogenic niche by transplanting in the DG, stem/progenitor cells from a non-neurogenic area such as the spinal cord. These progenitor cells regain the ability to generate neurons and inversely, when grafted in a non-neurogenic area, DG stem cells lost their ability to differentiate into neurons (Figure 10) (Shihabuddin et al., 2000).

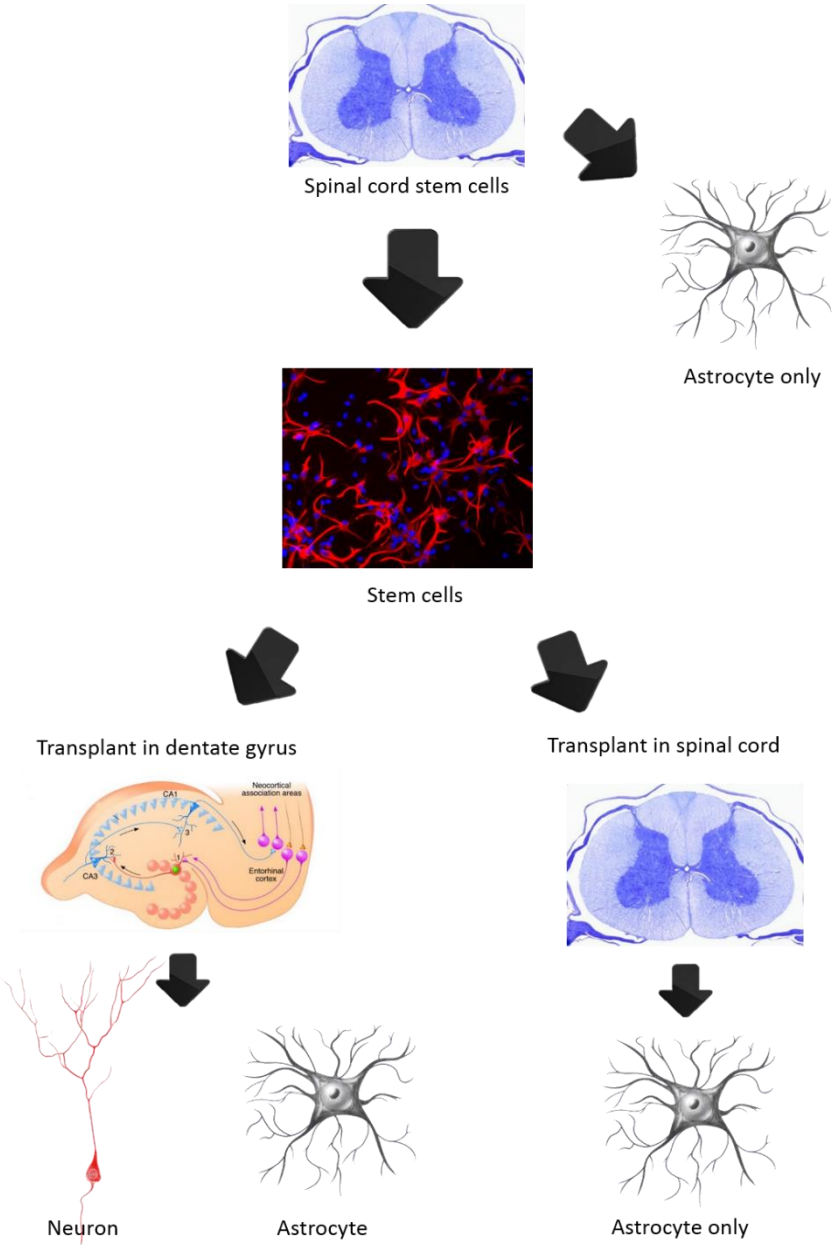

Figure 10: Schematic representation of the isolation and transplantation of adult-derived spinal cord stem cells

After isolation, when transplanted in the DG, stem/progenitor cells from a non-neurogenic area such

as the spinal cord regain the ability to generate neurons and inversely, when grafted in a non-neurogenic area, they lose their ability to differentiate into neurons.

The neurogenic niche is considered as a functional unit with the RGL neural stem cells. It contains cellular components (immature neurons, mature neurons, glial cells, blood vessels), as well as non-cellular factors such as secreted molecules and extracellular matrix. A wide variety of stimuli (or their absence) can regulate adult neurogenesis. These signals can influence different stages of development, from the stem cell to the new neuron. Since its discovery, most of the studies on adult neurogenesis were trying to discover its different regulators.

Understanding the mechanism by which the neurogenic niche regulate adult neurogenesis and identifying the factors that contribute to this regulation is crucial for the establishment of future brain repair strategies

2.3.1 Regulation of adult neurogenesis by neuronal activity

In the SGZ of the DG, immature and mature neurons are part of the niche and numerous studies suggest that the RGL neural stem cell respond directly to neuronal activity (Babu et al., 2009; Bengzon et al., 1997; Bruel-Jungerman et al., 2006; Deisseroth et al., 2004; Parent et al., 1997). Morpho-functional analysis has shown a localization dependent presence of AMPA receptors on their processes, glutamate transporters on the soma and gamma-aminobutyric acid (GABAA) receptors on the entire cell surface (Renzel et al., 2013). Actually, glutamate signaling has long been involved in the regulation of adult hippocampal neurogenesis. Activation of NMDA receptors by an injection of NMDA decreased cell proliferation in the adult DG, while injection of an NMDA receptor antagonist increased proliferation (Cameron et al., 1995; Nacher et al., 2001). Also, long-term potentiation (LTP) promotes proliferation and neuronal survival in an NMDA receptor-dependent manner (Bruel-Jungerman et al., 2006; Chun et al., 2006).

Moreover, in the SGZ of the DG, RGL neural stem cell are located in a region heavily innervated by serotonergic fibers expressing 5-HT1A receptors (Nishimura et al., 1995; Pompeiano et al., 1992). Studies have shown that an increased level of serotonin increases

DG proliferation. This increase of proliferation is mediated by 5-HT1A receptors (Brezun and Daszuta, 2000; Gould, 1999). However, reduction of the level of 5-HT decreased adult neurogenesis in the DG (Brezun and Daszuta, 1999; Ueda et al., 2005). Furthermore, adult neurogenesis is increased in mice treated with antidepressants acting through increasing synaptic 5-HT (Wang et al., 2008). Thus, the activity of the neuronal network regulates the RGL neural stem cell proliferation and differentiation.

2.3.2 Regulation of adult neurogenesis by glia

In addition to neurons, glial cells play a major role in the regulation of adult neurogenesis. They were described for the first time by Rudolf Virchow. Their designation is derived from the Greek word "γλία" for "glue". Today the importance of glia in the brain and especially in the DG is widely recognized (Barres, 2008; Herculano-Houzel, 2014; Lee et al., 2012; Sultan et al., 2015). Glial cells are divided into microglia, astrocytes, oligodendrocytes and NG2 cells. In my work, I have focused on microglia and astrocytes.

2.3.2.1 Microglia

Microglia is the primary immune-competent cells of the nervous system. They have a small soma and several processes that continuously scan their surroundings. Microglia are neuro-protective but they can become neurotoxic after a prolonged activation (Aloisi, 2001). Activation leads to morphological changes, including a more ramified structure. So microglia have a double role in the brain; it could promote neurogenesis by production growth factors (Ziv et al., 2006a; Ziv et al., 2006b)and when activated, it could impair neurogenesis by secreting pro-inflammatory cytokines like interleukin 1β, interleukin-6 or tumor necrosis factor (TNF)α. This increased microglial activation was associated also to a reduction of newborn neurons in the hippocampus (Ekdahl et al., 2003; Koo and Duman, 2008; Monje et al., 2003; Vallieres et al., 2002). Thus, microglia is critical for the development and differentiation of neural stem cells (Belmadani et al., 2006; Bhattacharyya et al., 2008; Gonzalez-Perez et al., 2010). Minocycline is a tetracycline antibiotic that has been shown to inhibit microglial cell activation (Stirling et al., 2005; Yoon et al., 2012). Anti-inflammatory treatment with minocycline results in enhanced hippocampal neurogenesis after cranial

irradiation, epilepsy, and ischemic stroke (Ekdahl et al., 2003; Liu et al., 2007; Monje et al., 2002). However, the role of microglia in absence of lesion or inflammation remains unclear. Recent studies suggest that resting microglia may be involved in the regulation of physiological mechanisms such as dendritic spine maintenance. In fact, they showed that microglia engulf and eliminate synapses during development (Paolicelli et al., 2011).

Moreover, microglial cells may be implicated in the maintenance of the homeostasis of the neurogenic niche by the removal of apoptotic newborn cells. It is a novel property of the cellular niche that modulates adult hippocampal neurogenesis (figure 11) (Sierra et al., 2010).

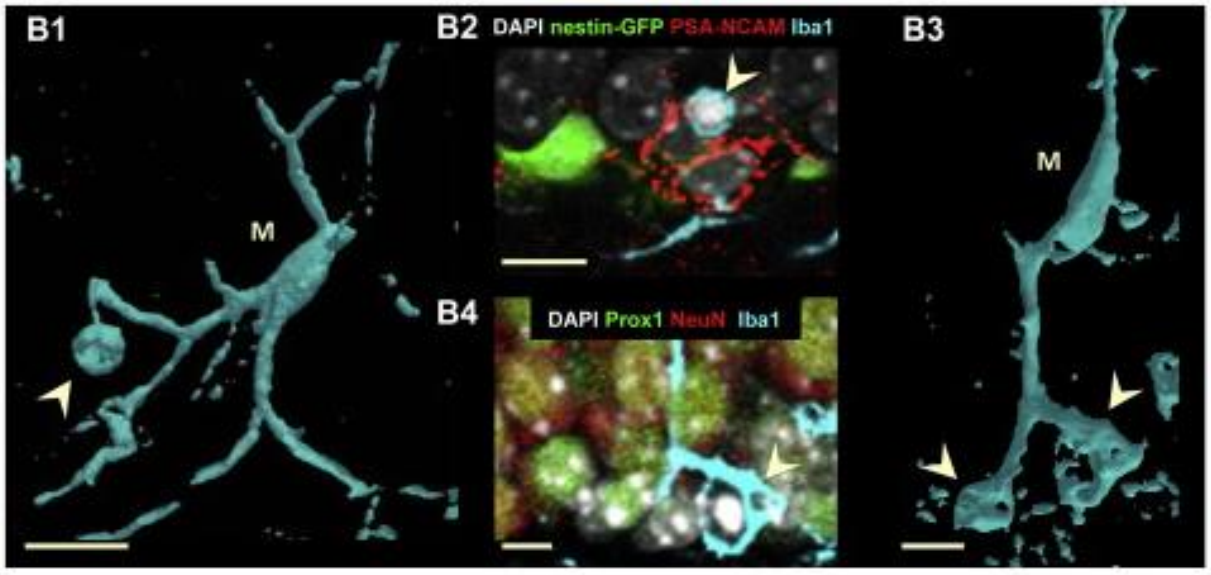

Figure 11: Unchallenged microglia phagocytose apoptotic cells in the normal adult SGZ
The phagocytic microglia shows ramified morphology typical of unchallenged microglia. Phagocytosis by unchallenged microglia occurs by a special modification of the microglial processes, a ball-and-chain structure (arrowhead, is shown in detail in B2), which form a phagocytic pouch that engulfs the apoptotic cell. (Scale bars represent 10 µm. (adapted from (Sierra et al., 2010))

2.3.2.2 Astrocytes

The name is derived from their star-like morphology. They have a ramified structure with fine processes; their morphology becomes increasingly complex with brain architecture. These cells are the major cell component of the brain; they provide support, protection and nutrients coming from the blood to neurons (Oberheim et al., 2012; Song et al., 2002). They regulate also the level of ions, hormones, growth factors and neurotransmitters in the neurogenic niche.

Astrocytes are in close contact to stem cells and neurons in the neurogenic niche. Song et al in 2002 have shown, using in vitro experiment, that astrocytes of the neurogenic niche control the proliferation and the fate of neural stem cells but more important, whereas astrocytes harvested from non-neurogenic regions do not support neurogenesis (Song et al., 2002) (figure 12). This study has shown the active regulatory role of astrocytes from the DG neurogenic niche in stem cell proliferation and differentiation (Steiner et al., 2006). Astrocytes in the neurogenic niche are capable of producing diffusible and membrane bound factors, which seems to be necessary to promote adult neurogenesis, but the exact mechanisms are still unknown (Steiner et al., 2006).

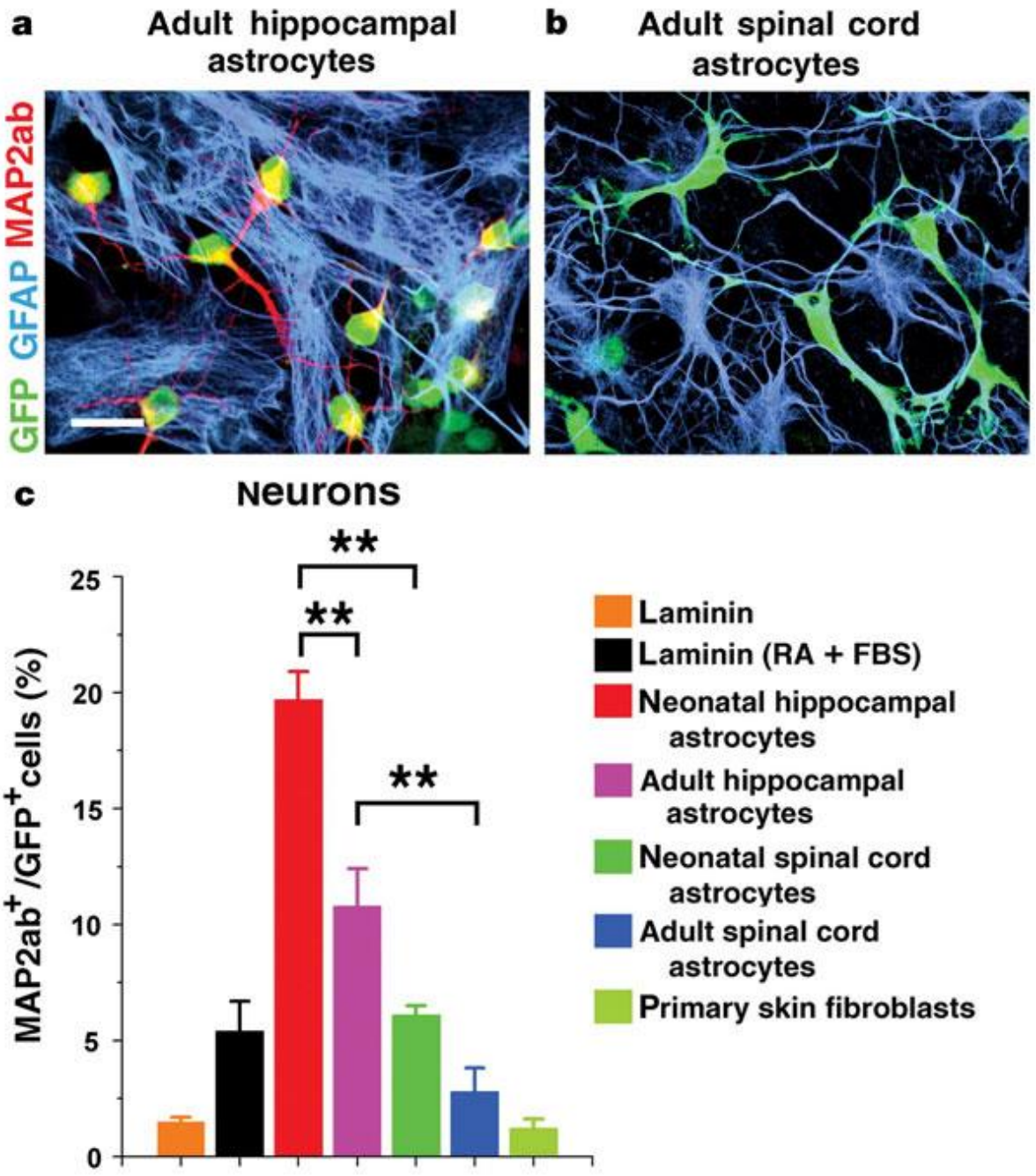

Figure 12: Mature astrocytes from adult hippocampus, but not adult spinal cord, promote neurogenesis from adult stem cells

Differentiation of GFP+ adult neural stem cells in co-culture with astrocytes derived from adult hippocampus (a) or adult spinal cord (b). Scale bar, 5 μm. Adult neural stem cells co-cultured with hippocampal astrocyte are more likely to differentiate into neurons. (adapted from (Song et al., 2002))

Astrocytes release different molecules such as neuromediators, growth factors, chemokines, cytokines and neurotrophins (Barkho et al., 2006; Brazel et al., 2005; Ford-Perriss et al., 2001; Juric et al., 2006; Riva et al., 1996; Wolosker et al., 1999). Additionally, recent studies in our lab showed the importance of astrocytic release in adult neurogenesis. Basically, blocking exocytosis of astrocytes decreases proliferation in the adult hippocampus and impairs dendritic spine formation on newly generated neurons (Sultan et al., 2015).

Therefore, mature astrocytes support the dendritic maturation, synaptic integration, and survival of new neurons in the adult hippocampus. And this regulation demonstrates a crucial role of the neurogenic niche in locally regulating and adjusting the late stages of adult neurogenesis, to fine tune network plasticity and hippocampal function.

2.4 Aim of the study

Over the past decades adult neurogenesis has been widely studied. But little is known about the morphology and the regulation of the adult neural stem cell. The present study aimed at increasing our knowledge about the link between the morphology and the activity of the adult neural stem and to identify the cellular components of the neurogenic niche and the nature of their contacts with the neural stem cell, to enable a better understanding of the function of the neurogenic niche. This gave the rationale in my thesis to focus on the following subjects:

- Understand and describe the structure of the neural stem cell
- Understand the structure and composition of the niche
- Define the role of astrocytes and microglia in the maintenance and function of the niche

The project proposed here aims at answering this question by providing the fine structural analysis of these cells and their interaction within the neurogenic niche. We believe it will yield a framework for understanding the regulation of adult neurogenesis but also reveal novel regulatory mechanisms. This knowledge is of essential importance for the understanding of brain homeostasis and plasticity, but also for the establishment of future brain repair strategies such as transplantation.

CHAPTER 3: STRUCTURE OF THE ADULT NEURAL STEM CELL

3.1 Introduction

The aim of this project is to examine the morphology of the adult neural stem cell and it's interaction with the components of the neurogenic niche.

During embryonic development, radial glia like stem cells play a scaffolding role for new born neurons, which migrate alongside the primary process to reach their final destination in the cortical plate (figure 10) (Noctor et al., 2001).

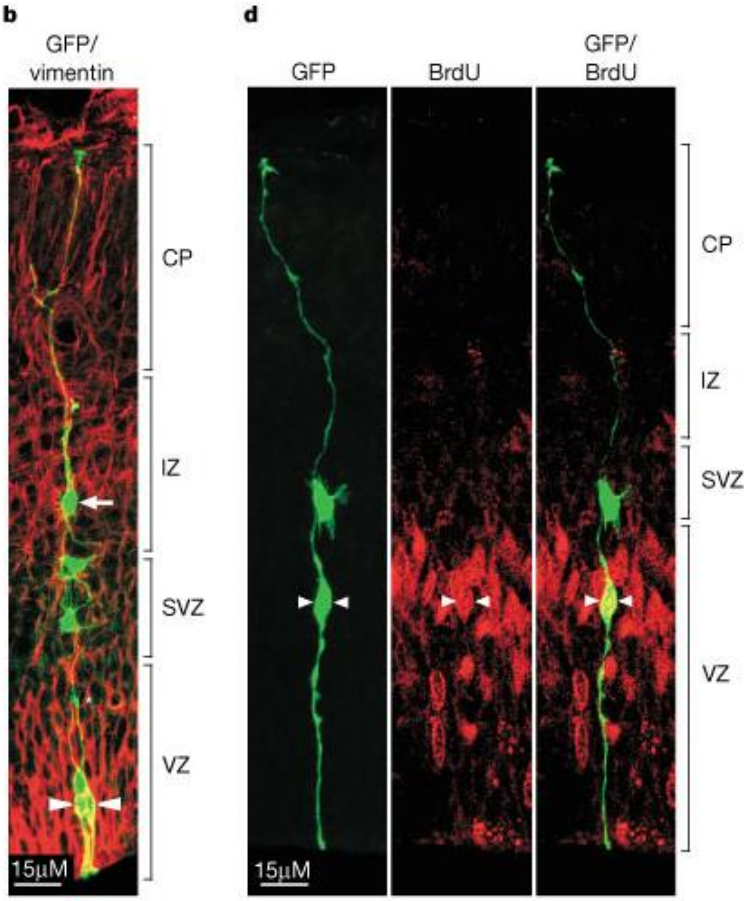

Figure 13: New born neurons migration through radial glial cells during embryonic development

b, At 72 h, radial clones include vimentin-positive radial glial cells (large arrowheads). A vimentin-negative cell resembling a migrating neuron (arrow) is apposed to the vimentin-positive radial fibre. **d**, S-phase clonal cells labelled with BrdU are radial glia. CP, cortical plate; IZ, intermediate zone. (adapted from (Noctor et al., 2001))

In adulthood, the RGL neural stem cells have very specific morphology (figure). The RGL are characterized by a long unique process that goes through the granular cell layer with an arborization spreading most of the time at the top of the GCL and in the inner third of the ML (figure 9). RGL cells express Nestin, GFAP (Seri et al., 2004; Steiner et al., 2006), Sox2 (Suh et al., 2007) and prominin 1 (Beckervordersandforth et al., 2014) among other markers and are relatively quiescent.

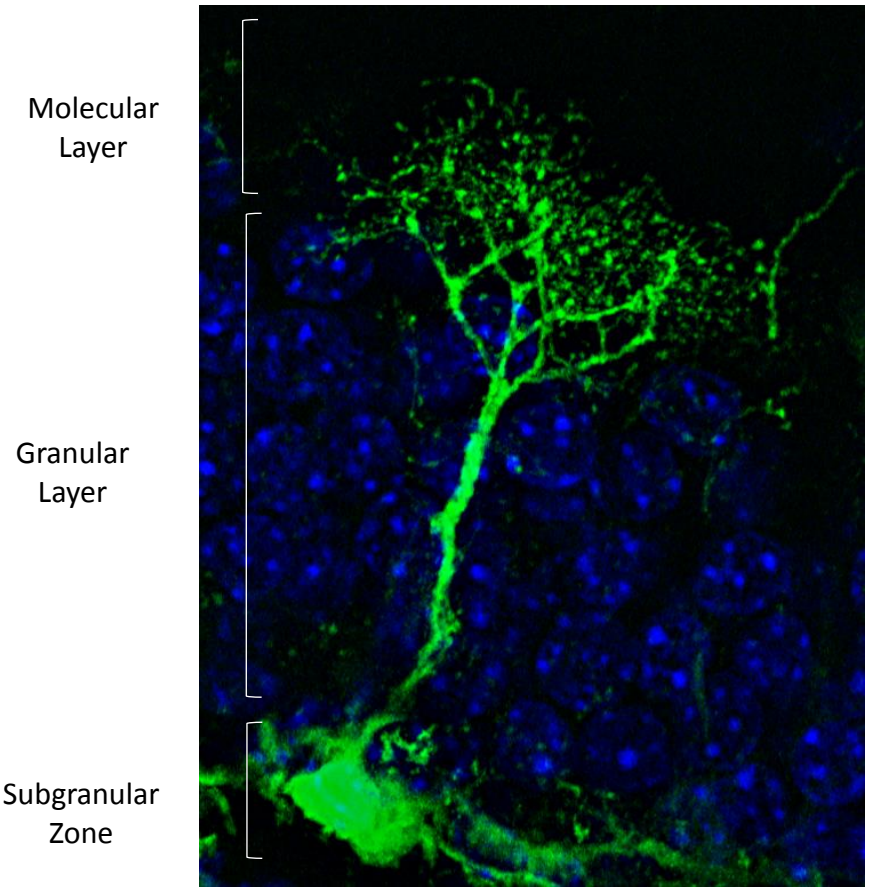

Figure 14: Adult neural stem cell/Radial Glia like cell

GFP expressing radial glia like cell in the dentate gyrus of Nestin-GFP mice. RGL stem cell display a long unique process that goes through the granular cell layer with an arborization spreading in the inner third of the ML. The nuclei are stained in bleu.

The function of the radial process is not clearly defined but we hypothesized that it could have a potential function in mediating their proliferation or fate by the local niche.

As introduced previously, neurogenesis is tightly regulated by the stem cells' highly specialized microenvironment, called the neurogenic niche. With neurogenic potential reside in the entire central nervous system; neurogenesis is restricted to the hippocampus and the

subventricular zone. However, when transplanted in the hippocampus, stem/progenitor cells from a non-neurogenic area such as the spinal cord regain the ability to generate neurons and inversely, when grafted in a non-neurogenic area, hippocampal neural stem cells lose their ability to differentiate into neurons (Shihabuddin et al., 2000).

Several cell types of the neurogenic niche have been shown to play a role in the regulation of the RGL proliferation, including astrocytes (Lie et al., 2005; Song et al., 2002), neurons (Song et al., 2012), microglia (Gebara et al., 2013; Sierra et al., 2010) or endothelial cells (Palmer et al., 2000). The influence of niche compounds on RGL cells may be mediated by the release of soluble molecules or by direct contact such as with microglia (Sierra et al., 2010) or astrocytes (Ashton et al., 2012). These previous observations advocate that the complex morphology of RGL stem cells allows the formation of numerous contacts with a variety of cell types of the hilus, GCL, and molecular layer of the dentate gyrus, all of which may participate to its regulation.

The structure of the RGL stem cell is still poorly described. Moreover, there is no evidence of a relationship between the structure and the function of the neural stem cells

The goal of this study is to examine the fine structure of RGL stem cells in the adult hippocampal niche and to examine the possibility of an association between morphology and activity.

3.2 Results

The results of this project were published in the following articles (Appendices 1-2):

Article 1

Elias Gebara, Michael Anthony Bonaguidi, Ruth Beckervordersandforth, Sébastien Sultan, Florian Udry, Pieter-Jan Gijs, Dieter Chichung Lie, Guo-Li Ming, Hongjun Song, Nicolas Toni (2016) **Heterogeneity of Radial Glia-Like Cells in the Adult Hippocampus,** *Stem cells.*

In this article, we characterized the morphology of radial glia-like (RGL) cells, their molecular identity (marker expression), proliferative activity (using BrdU and Ki-67), and fate determination (Lineage tracing) in the adult mouse hippocampus. We discovered the

cohabitation of two morphotypes of RGL cells: Type α cells, which displayed a long primary process modestly branching into the molecular layer and type β cells, with a shorter radial process highly branching into the outer granule cell layer-inner molecular layer border (figure 15).

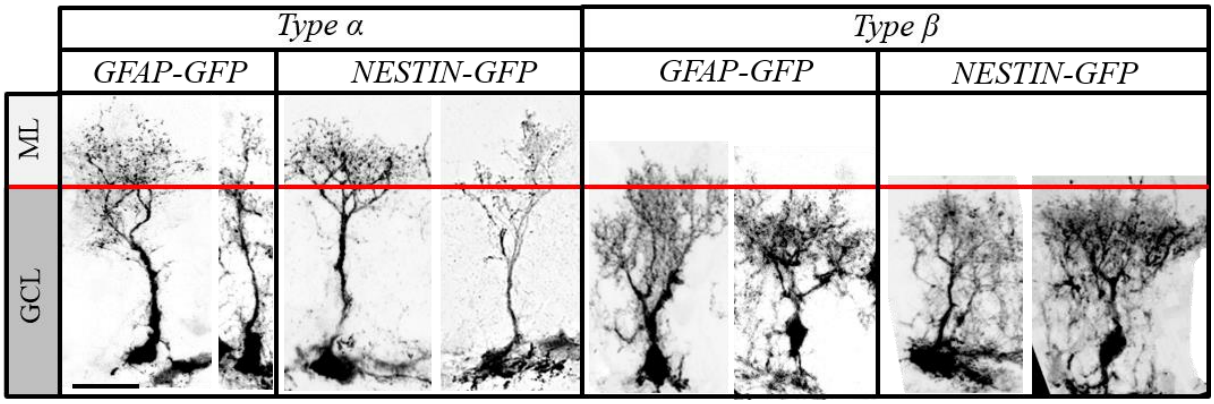

Figure 15: Morphometrical parameters of radial glia-like (RGL) cells

Confocal maximal projection micrographs of types α and β RGL cells in glial fibrillary acidic protein (GFAP)-green fluorescent protein (GFP) and Nestin-GFP mice.

Type α cells express all stem markers, are capable of self-renewal and production of neurons, astrocytes and type β cells. Type β cells co-express astrocytic and stem cell markers, do not proliferate and may represent an intermediate state in the transformation of type α, RGL stem cells, into astrocytes (Figure 16). Moreover, their population size did not change upon aging or exercise, but was increased by D-serine administration.

The strong association between morphology and function of RGL cells suggests that the processes of RGL cells play a potential role in regulating their activity Furthermore, these results indicate that the population of RGL cells is functionally heterogenous.

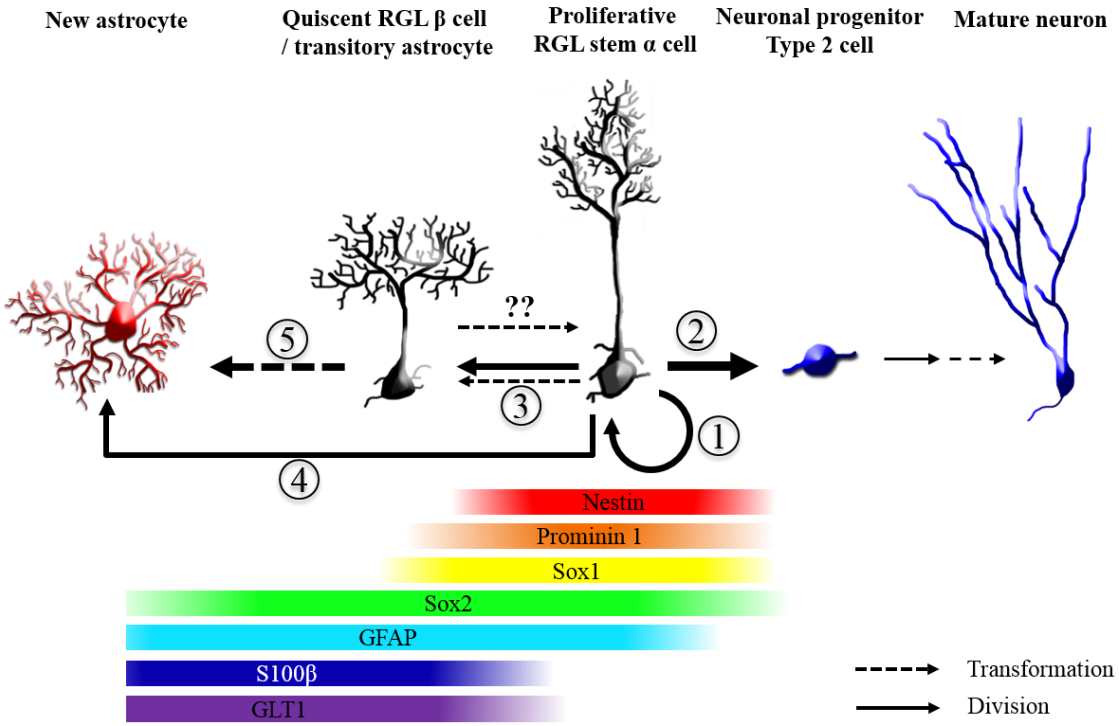

Figure 16: Model of type α and type β cells lineage relationship

Model of the lineage relationship of type α and type β cells in the adult mouse hippocampus under basal conditions. Type α cells can self-renew (1) and also generate type 2 neural progenitors (2), type β cells (3) and astrocytes (4). Type β cells do not divide, but may revert to type α cell (??) or transform into astrocytes (5). Also shown marker expression.

Contribution to article 1

I bred, genotyped and maintained transgenic mouse lines (GFAP-GFP, Nestin-GFP, GFAP Cre::Ert2 Rosa YFP, Nestin Cre::Ert2 and Td-tomato Flox mice). I produced the double transgenic Nestin Cre::Ert2 Td-tomato mice and set up the approach of clonal identification and with minimal tamoxifen injections. I performed the perfusions and tissue preparations, immunostainings, imaging and morphological analyses. I supervised a medical master student, Pieter-Jan Gijs. I analyzed the data and contributed to the writing of the article.

Article 2

Jonathan Moss, Elias Gebara, Eric A. Bushong, Irene Sánchez Pascual, Ruadhan O'Laoi, Imane El M'Ghari, Jacqueline Kocher-Braissant, Mark H. Ellisman, Nicolas Toni, (2016) **Fine Processes of Radial Glia-Like Stem Cells in the Hippocampal Adult Neurogenic Niche Ensheath Local Synapses and Vasculature**, PNAS.

In this study we used electron microscopy (TEM and SDF-TEM) to analyze the ultrastructure of the type α cells and to reveal the nature of their processes in 3D. We found that α RGL stem cells do not receive direct synaptic input. However, we found that their processes are closely apposed to, or even ensheathing asymmetric synapse, blood vessels, astrocytes and other α RGL stem cells. We were able to do a full reconstruction of the type α cell (Figure), including apical and basal processes. Our data support the hypothesis that the neurogenic niche plays an important role in the regulation of α RGL stem cells. While the resolution of EM was crucial to reveal the fine structure observed here, further studies are ongoing to understand the function of the perisynaptic and perivascular processes. By describing the fine structure of α RGL stem cells, and their relationships with elements of the dentate gyrus neurogenic niche, we provide a necessary structural framework linking adult neural stem cells and the signals that activate and modulate their activity, and a new perspective on the process of adult neurogenesis.

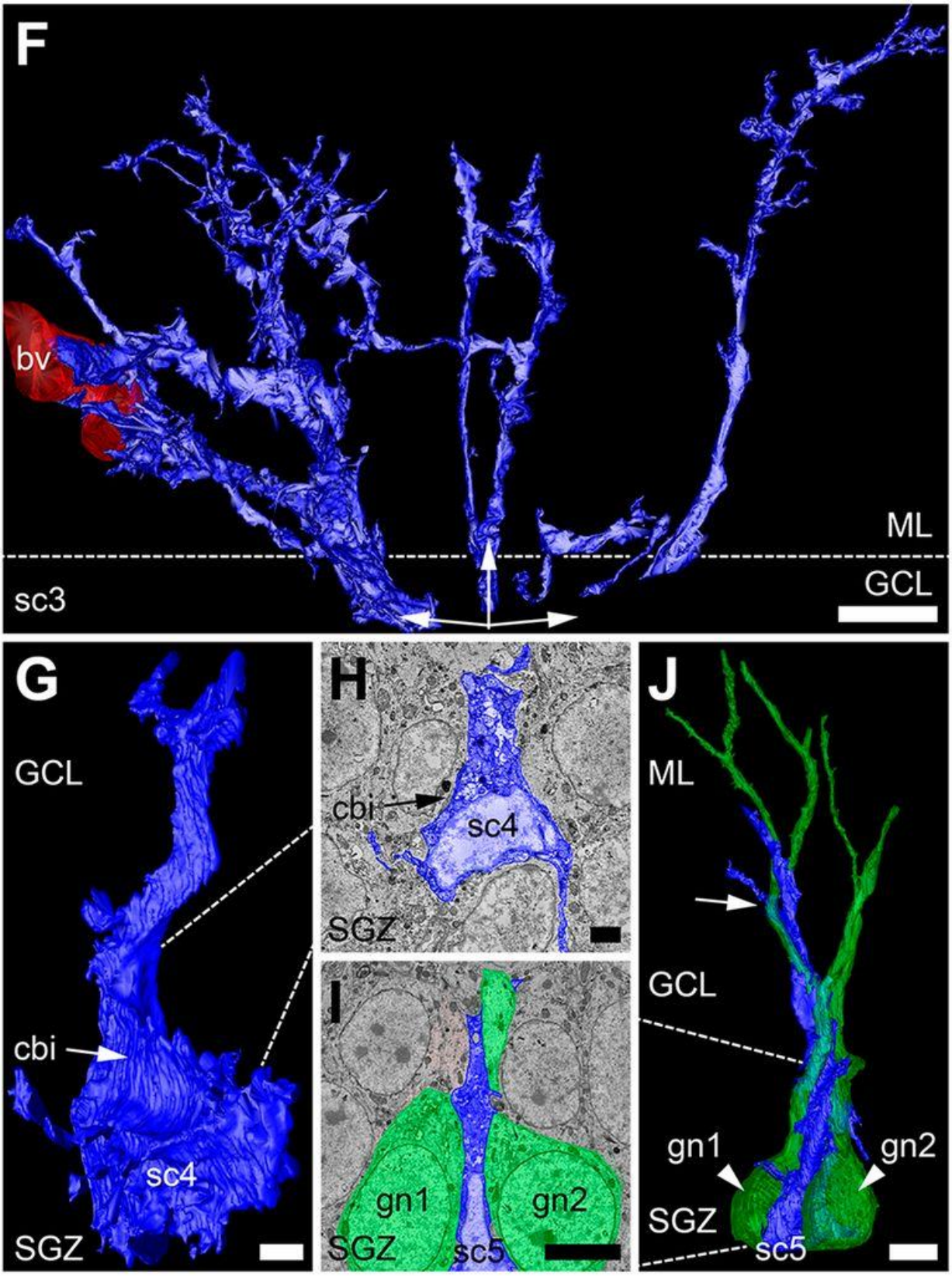

Figure 17: 3D reconstruction of a type α RGL stem cell

Processes of a single α RGL stem cell reconstructed from 178 SBF-SEM images. Three processes extend toward a local blood vessel (bv, red). (G and H) Three-dimensional reconstruction (G) from SBF-SEM images (H) of an α RGL stem cell with neighboring cell body indentations. (I and J) Three-

dimensional reconstruction of an α RGL stem cell and its primary process (arrow) alongside two granule neurons (Scale bars F, I, and J, 5 μm; G and H, 2 μm.)

Contribution to article 2

I maintained and bred the transgenic mouse line Nestin-GFP. I produced all the confocal images (figure 2). I analyzed some of the electron microscopy pictures and performed the 3D reconstruction of the entire type α cell (Figure 1 panel G-J and movies S2-S3).

CHAPTER 4: REGULATION OF ADULT NEUROGENESIS BY THE NEUROGENIC NICHE

4.1 General Introduction

The aim of this project is to examine the functional role of the niche, in particular microglia and astrocytes, on the structure of the niche and stem cell proliferation.

Neurogenesis is tightly regulated by the stem cells' highly specialized microenvironment, called the neurogenic niche. A clear understanding of the mechanism regulating adult neurogenesis is of crucial importance for the understanding of brain homeostasis and plasticity, but also for the establishment of future brain repair strategies.

In this work we are mostly interested in understanding the diverse contacts that adult neural stem cells establish with the different components of the neurogenic niche and factors produced by these components. Growing evidence suggests that the neurogenic niche has a major role on the proliferation and differentiation of the adult neural stem cells (Shihabuddin et al., 2000). Of particular interest, glia cells, they are the second most abundant cell type in the adult brain. Glial cells are divided into microglia, astrocytes, oligodendrocytes and NG2 cells. In my work, I focused specifically on microglia and astrocytes since several studies have showed the role of these cells types in pathological conditions but few have focused on their role in physiological conditions.

4.2 Regulation of adult neurogenesis by microglia

4.2.1 Introduction

Microglia are abundant and broadly distributed into the adult brain. These cells act as the resident immune cells of the brain and are involved in the inflammatory response. Their fine processes sample the entire brain parenchyma for infection. Upon activation, they are able to release cytokines and ensure phagocytosis. As we have seen in the general introduction microglia have a great impact on the regulation of the homeostasis of the brain.

In the healthy brain, studies have shown that microglia have extremely motile processes constantly scanning their local environment. Moreover, they interact with synaptic elements by direct contacts and exchanges of molecular. And also they contribute to the

rearrangement of neuronal circuits by phagocytosing newborn neurons or synaptic elements and thus are implicated in synaptic pruning ((Tremblay et al., 2011) for review). To elucidate if microglia, in the absence of inflammation or infection, participates in the regulation of neurogenesis we tested the correlation between the number of microglia in the hippocampus and the proliferation of adult neural stem cells, in physiological conditions, aging conditions (known to decrease adult neurogenesis) and Voluntary exercise (known to increase adult neurogenesis) (Encinas et al., 2011; Kempermann, 2011; Kuhn et al., 1996; van Praag et al., 1999; van Praag et al., 2005). Second we tested the effect of an antibiotic (doxycycline) on adult neurogenesis and microglia. Doxycycline is an activator for transgene control in inducible-reversible transgenic mouse model.

4.2.2 Results

The results of this project were published in the following articles (Appendices 3-4):

Article 1

Elias Gebara, Sébastien Sultan, Jaqueline Kocher-Braissant, Nicolas Toni (2013) **Adult hippocampal neurogenesis inversely correlates with microglia in conditions of voluntary running and aging**, *Frontiers in Neurosciences.*

In this study, we took advantage of the physiological variations of adult neurogenesis induced by voluntary running and aging to examine the correlation between microglia and adult hippocampal neurogenesis in absence of inflammatory stimulus. We found that aging decreased cell proliferation and the number of immature neurons whereas voluntary running had inverse effects. Moreover, we found that the decrease in adult neural RGL cells observed with aging, was rescued by voluntary running, suggesting that running may induce the symmetrical division of adult neural RGL cells and restore their population. Amazingly, both in running and aging conditions, the number of microglia but not of astroglia was inversely correlated with all measured parameters of neurogenesis. Similarly, *in vitro*, co-cultures of NPCs with an increasing proportion of microglia but not of astroglia reduced the number of NPCs after 4 days. These results indicate that, in physiological conditions,

microglia and neurogenesis are inversely correlated and suggest that microglia may inhibit adult neurogenesis by directly acting on stem/progenitor cells.

Contribution to article 1

I maintained and bred the transgenic mouse line (GFAP-GFP). Performed the BrdU injections, sacrificed mice at different timepoints and prepared the brain slices, immunostained the slices, took confocal micrographs and performed image and data analyses. Moreover, I performed the in vitro culture, microglia and astrocyte purification, and co-culture with NPCs. I contributed to the writing of the article.

Article 2

Sébastien Sultan*, Elias Gebara*, Nicolas Toni (2013) **Doxycycline increases neurogenesis and reduces microglia in the adult hippocampus**, *Frontiers in Neurosciences.* (*equally contributed to this work)

At first we were studying adult neurogenesis in transgenic mice, inducible with doxycycline. We found that the proliferation level in transgenic mice without doxycycline was significantly reduced compared to wild type mice with doxycycline. These two groups are considered as a control and should have the same amount of proliferation. In order to explain this unexpected results we decided to dig a little bit more about the effect of doxycycline on adult neurogenesis. We found that doxycycline reduced the number of RGL cells but increased the number of transit amplifying progenitors (TAPs) in the DG of adult mice. Once again we are confronted to intriguing results. Why we have a reduction of RGL neural cells but we had an increase proliferation? Actually, this may be explained by a shift in fate choice of the RGL cells leading to a depletion of the RGL cells pool in favor of the highly proliferative TAPs (Encinas et al., 2011). Moreover we found that the survival of newly generated neurons is increased and as a consequence, doxycycline treatment by increasing cell proliferation and survival of new neurons resulted in a net increase in neurogenesis. In addition, using viral injection, we were able to label the newly generated neurons and study their morphology. We found that doxycycline increased dendritic protrusions density on the

neurons formed during the treatment. But to this point, the mechanism of action of doxycycline on adult neurogenesis remains unclear. Studies showed that doxycycline is a synthetic antibiotic, with reported effects on pain, inflammation and neuroprotection (Cho et al., 2009; Clark et al., 1997; Jantzie and Todd, 2010). As Inflammatory microglia reduces neurogenesis (Ekdahl et al., 2003; Liu et al., 2007) and we reported that we have and inverse correlation between microglia and adult neurogenesis (Gebara et al., 2013), we decided to examine the effect of doxycycline on microglia both *in vitro* and *in vivo*. We found a dramatic reduction of microglia *in vitro* and *in vivo*, whereas no effect on astrocytes and NPC *in vitro*. Our data suggest that the effect of doxycycline on adult neurogenesis may be mediated by microglia.

Contribution to article 2

I maintained and bred the transgenic mouse lines (Nestin-GFP and GFAP-GFP). Together with Sebastien Sultan, I performed the BrdU injections, sacrificed mice at different timepoints, prepared the brain slices, immunostained the slices, took confocal micrographs and performed image analyses. Moreover, together with Sébastien Sultan, I performed the viral production and injection as well as the in vitro culture, astrocyte purification, and co-culture with NPCs. I contributed to the data analysis and writing of the article.

4.3 **Regulation of adult neurogenesis by astrocytes**

4.3.1 Introduction

Another major component of the neurogenic niche is the astroglia. As previously described, astrocytes have a crucial contribution in adult neurogenesis. They secrete several molecules, neurotransmitters and factors that regulate the proliferation and the differentiation of the RGL neural stem cell. Two amino-acids known to be released by astrocytes: D-serine (Bergersen et al., 2012; Martineau et al., 2013; Schell et al., 1995) and Taurine (Choe et al., 2012). D-serine is the major co-agonist of the NMDA receptor and is involved in different NMDAR-dependent processes such as neurotransmission (Bado et al., 2011), synaptic plasticity (Papouin et al., 2012) and long term potentiation in the hippocampus (Turpin et al.,

2011). Moreover, a recent study showed that, *in vitro,* D-serine induces the differentiation of SVZ progenitors into neurons (Huang et al., 2012). Taurine is a free amino-acid known to be involved in calcium homeostasis (El Idrissi, 2008; Wu et al., 2005), inflammation (Kim and Cha, 2014; Sun et al., 2012) and protection from glutamate excitotoxicity (Leon et al., 2009). In view of all these results, we decided to study the effect of D-serine and taurine on adult neurogenesis.

4.3.2 Results

The results of this project were published in the following articles (Appendices 5-6):

Article 1

Sébastien Sultan*, Elias Gebara*, Kristel Moullec, Nicolas Toni (2013) **D-serine increases adult hippocampal neurogenesis** *Frontiers in Neurosciences.* (*equally contributed to this work)

In the present study, we tested the effect of repeated injections of D-serine on hippocampal adult neurogenesis. We found that in vivo, consecutive ip injection for 8 days of D-serine increased cell proliferation as well as the number of both RGL cells (type-1) and TAP cells (type-2). Likewise, D-serine applied to adult hippocampal neural progenitors in culture also increased cell number supporting the hypothesis of a direct effect of D-serine on adult NSCs. Finally, when we inject D-serine during the critical phase for activity-dependent survival, it increased the survival of newborn neurons. Therefore, D-serine increased adult neurogenesis by acting on several steps of this process and may result in long-lasting changes in the granule cell layer.

Contribution to article 1

I maintained and bred the transgenic mouse line (Nestin-GFP). Sebastien Sultan and I performed the D-serine and BrdU injections, perfused the mice at different timepoints, prepared the brain slices, immunostained the slices, took confocal micrographs and

performed image and data analyses. Moreover, with Sébastien sultan we performed the in vitro culture, astrocyte purification, and co-culture with NPCs. I also co-supervised a master student, Kristel Moullec, who took some of the confocal micrographs. I contributed to the writing of the article.

Article 2

Elias Gebara, Florian Udry, Sébastien Sultan, Nicolas Toni (2015) **Taurine increases hippocampal neurogenesis in aging mice**, *Stem Cell Research.*

In this study, we studied the effect of chronic administration of taurine on hippocampal neurogenesis in aging mice known to have a decline of adult hippocampal neurogenesis. We found that taurine increased cell proliferation in the DG. More specifically, RGL stem cells showed enhanced proliferation. Taurine treatment on 10 month-old mice restored the number of RGL stem cells to values found in 2-months-old mice. This effect is mediated by the direct proliferation of RGL stem cells, since taurine increased the percentage of BrdU-expressing RGL stem cells. Taurine also significantly increased the total number of Tbr2+ intermediate progenitors and DCX+ immature neurons. Moreover, taurine increased the survival of new neurons, resulting in a net increase in adult neurogenesis. Taurine also a reduced microglia number and activity (tested with morphological parameters and marker expression). Furthermore, Taurine increased stem/progenitor cell proliferation in vitro. Together, these results show that, in the aging brain, taurine increases the proliferation of adult neural stem cell and thus the production of new neurons and plays a role in microglia function.

Contribution to article 2

I maintained and bred the transgenic mouse line (Nestin-GFP). Performed the taurine and BrdU injections, sacrificed mice at different timepoints and prepared brain slices, immunostained the slices, took confocal micrographs and performed image and data analyses. Moreover, I performed the in vitro culture. I supervised a master student, Florian Udry, who took confocal micrographs and did the analysis for figure 1. I contributed to the writing of the article.

CHAPTER 5: GENERAL DISCUSSION

General discussion

Historically, Humans have been fascinated by regeneration and the consequent possibility of becoming immortal. Already in Greek mythology, many episodes acted out the perpetual rebirth and the quest for immortality: Prometheus who stole the precious power of creation from Zeus, was chained on mount Caucasus and his liver was eaten daily by an eagle. But the liver was constantly regenerating. This myth revealed himself prodigiously visionary since today the tremendous capacity of the liver to regenerate is no more mythical.

It has long been firmly believed that neurons, unlike liver or skin cells, were no longer generated after birth. This dogma has now fallen, as many studies in animals and humans have provided evidence that neurons can also be renewed in some brain areas. So beyond development, neurogenesis continues in the adult hippocampus. This process plays a role in learning and memory and raises the hope that it may be targeted in the context of therapies against memory impairment.

Years of scientific investigation have significantly extended our knowledge of adult hippocampal neurogenesis. However, several questions on the regulation of this phenomenon remain unanswered. The objectives of this thesis work were to expand our knowledge on the role of the neurogenic niche in the regulation of the adult neural stem cell.

To this end, we initially combined advanced genetic labeling approaches with microscopy to examine the fine structure of the hippocampal stem cells and their niche, in vivo. We also examined the functional role of major niche cellular components, astrocytes and microglia, on stem cell proliferation and fate determination.

Morpho-functional characterization of adult neural hippocampal stem cells reveals two morphotypes of radial glia-like cells

Adult neural stem cells of the dentate gyrus share similarities with the radial glia neural stem cells of the embryonic brain (Kriegstein and Alvarez-Buylla, 2009) and have consequently been named radial glia-like stem cells (RGLs). RGLs express the astrocytic marker (GFAP) the stem cell marker (nestin and sox2) (Filippov et al., 2003; Fukuda et al., 2003), possess a triangular soma located at the subgranular zone and extend a primary radial process through the granule cell layer. However, unlike their embryonic counterpart, the main process of adult RGL stem cells ends into a dense network of fine processes in the first third of the molecular layer. These morphological features are commonly used to identify neural stem cell in the dentate gyrus.

By thoroughly analyzing the morphology of RGL cells in the adult dentate gyrus, we found that two morphotypes of RGL cells co-exist in the subgranular zone of the dentate gyrus. Considering the length of the primary process and the width of the arbor of secondary processes we found that type α cells, which represented 76.21% of all RGL cells, exhibited a long radial process and a narrow apical arbor spreading into the first third of the molecular layer. These cells expressed the well-known stem cell markers (nestin, Sox2, Sox1, Prominin1, GFAP), were able to self-renew and generate neurons, astrocyte and type β cells. Voluntary running and daily D-serine administration significantly increased their total number whereas aging decreased it. In contrast, type β cells represented 23.79% of all RGL cells. They had a short radial process and their secondary processes branched mainly in the granule cell layer. These cells co-expressed astrocytic and stem cell markers. Curiously, although these cells were continuously generated by the proliferation of type α cells, their total number remained unchanged, even upon stimulation by exercise or inhibition upon aging; and they did not proliferate.

We found a strong association between the morphology and the activity of the neural α stem cells. This association point to a probable role of the processes of the α RGL neural stem cell in the regulation of their activity. Even though the role of these processes remains unclear we found that the α RGL stem cell establish several contact with several cell types of the neurogenic niche, including microglia, astrocytes, NG2 cells and blood vessels. Previous

research have shown the importance of these cells type in the regulation of the proliferation and the differentiation of the neural stem cells (Ashton et al., 2012; Gebara et al., 2013; Palmer et al., 2000; Sierra et al., 2010; Villeda et al., 2011).

By using high resolution imaging such as electron microscopy (Moss et al., 2016) we were able to understand a little bit more about these contacts. Analyses revealed that α RGL stem cells send major processes toward blood vessels situated in the inner molecular layer, wrap them with thin sheets, and compete with local astrocytes for surface area contact. The α RGL neural stem cell processes also branch into finer filaments, consisting of mitochondria-containing varicosities, from which individual processes extend towards local asymmetrical synapses. This intimate relationship of the α RGL neural stem cell with both neuronal and vascular components of the local environment, suggests that it may be receiving signals to aid its survival or to activate the production of new neurons. The contacts that the α RGL stem cell establish may be involved in the regulation of it proliferation but the mechanism remain unclear and requires further investigation. In an ongoing, yet unpublished work, we started to elucidate the function of perisynaptic processes: Using EM, we found that α RGL neural stem cells at the presynaptic process level express the subunit1 Grin1 of the NMDA receptor. To check the functionality and the role of this receptor on the α RGL neural stem cell, we decided to knock it down specifically in adult neural stem cells, using cell-specific controllable transgenic mice. Our results show that the NMDA receptor regulates the proliferation and the fate of the α RGL neural stem cell. Further experiments will be done to consolidate these preliminary results and highlight the molecular mechanism of these regulations.

Using an in vivo clonal analysis approach, we studied the fate of RGL neural stem cells. Hence, we found that type α cells display all characteristics of RGL stem cells (Bonaguidi et al., 2011; Encinas et al., 2011; Filippov et al., 2003; Lugert et al., 2010). It is able to perform symmetric and asymmetric divisions. The symmetric division give rise to two new identical α cells, and the asymmetric division give rise to astrocyte, type β cells or Type II cells that undergo a neuronal differentiation. So type α may either transform into type β cells or produce type β cells upon division. Both possibilities are consistent with the mixed morphology and marker expression of type β cells and the incorporation of BrdU after

repeated injections supports the possibility that these cells are generated by the division of type α cells. However the identity of type β cells is less clear.

Based on the data we have and on the literature, we emitted two hypotheses concerning the fate of type β cells:

- As β cells express both stem cell and astrocytic markers, have an intermediate morphology between RGL stem cells and stellate, protoplasmic astrocytes and do not have the ability to divide (in our hand), we believe that these cells may be a transitory cell type involved in the formation of astroglia. Moreover, in line with our data, research has shown that during aging (Bonaguidi et al., 2011; Encinas et al., 2011) or epilepsy-induced hyperactivation (Sierra et al., 2015) neural stem cells are converted into astrocytes. After analyzing the morphology of the neural stem cells in aging and epilepsy-induced hyperactivation, we clearly see that they express morphological features of type β cells.

- However we cannot exclude the possibility that β cells may represent a highly quiescent pool of RGL stem cells that would return to type α cells upon proper stimulation. For example, in aging mice α cells are almost completely lost, but are then reinstated at normal level upon voluntary running. This restore may be due to conversion of type β cells into type α.

Thus, the fate of type β cells cannot be inferred from clonal analysis. However, the stable number of type β cells in conditions of increased proliferation, such as voluntary exercise, supports the possibility that type β cells either transform into other cell types and migrate out of the granule cell layer or are eliminated. Although the elimination of these cells by apoptosis is not excluded, the absence of microglia-dependent phagocytosis suggests it is unlikely. Time-lapse imaging may be necessary to examine whether type β cells can transform again into type α cells, or into astrocytes and migrate out of the granule cell layer.

To conclude, our results show that RGL cells in the dentate gyrus are heterogeneous in morphology and function and the morphological criteria provided here enable the easy identification of these two major morphotypes. Since the number of type α and type β cells can be modified by environmental conditions or pharmacological stimulation, the

morphological criteria we used are highly relevant to the status of the pool of RGL stem cells in the dentate gyrus.

Micro and astroglia tightly regulate the proliferation of the RGL neural stem cells

Microglia

The existence of activated microglia in the dentate gyrus of the hippocampus has been linked to inflammation. This microglia by producing cytokines reduces adult neurogenesis (Monje et al., 2003). In absence of inflammation, microglia contributes to the phagocytosis of early progenitors undergoing apoptotic elimination during the neuroprogenitors to neuroblasts transition (Sierra et al., 2010). We examined the correlation between microglia and adult hippocampal neurogenesis in physiological conditions known to increase or decrease neurogenesis, respectively voluntary running and aging. We found that aging decreased the number of proliferating cells (radial glia and transit-amplifying progenitors), cell proliferation in the granule cell layer and the number of immature neurons and increased microglia, whereas voluntary running had inverse effects. In both conditions, the amount of microglia was strongly inversely correlated with all parameters of neurogenesis. Similarly, in vitro, an increasing proportion of microglia but not of astroglia reduced the number of neural progenitor cells after 4 days of co-culture. Together, these results suggest that, in physiological conditions, microglia reduces neurogenesis.

These results are in contrast with previous studies showing that, under normal conditions, microglia promotes neurogenesis: In adult rats, Ziv et al showed that the increased neurogenesis induced by environmental enrichment was accompanied by an increase in microglia number, whereas immunodeficient mice had impaired neurogenesis (Ziv et al., 2006b). Similarly, voluntary running was shown to increase neurogenesis and microglia proliferation (Ehninger and Kempermann, 2003; Olah et al., 2009), without inducing a change in the total number of microglia cells or in their activation state (Olah et al., 2009).
In vitro too, neural progenitor cells co-cultured with microglia promote the proliferation of neural stem/progenitor cells, an effect believed to be mediated by factors released in the

culture medium since the proneurogenic effect can be mimicked by microglia-conditioned medium (Aarum et al., 2003; Morgan et al., 2004; Nakanishi et al., 2007; Walton et al., 2006).

However, in inflammatory conditions induced by epilepsy, ischemia or LPS injection, microglia undergo dramatic changes in their morphological and cytokine expression pattern and inhibit adult neurogenesis (Ekdahl et al., 2003; Kohman et al., 2013; Liu et al., 2007; Monje et al., 2002). Similarly, aging is associated with a reduced neurogenesis and mild, chronic inflammation and increased microglia proliferation that can be attenuated by voluntary running (Kohman et al., 2012). Inflammatory microglia is believed to directly inhibit neurogenesis, since anti-inflammatory treatments restore neurogenesis (Ekdahl et al., 2003; Kohman et al., 2013; Monje et al., 2003)and the exercise-induced increase and the age-dependent decline in neurogenesis are mediated by microglia in vitro (Vukovic et al., 2012).

Moreover, microglia contacts significantly more type β cells, than type α cells in sedentary conditions. However, we found no evidence of microglial engulfment of type α or type β cells and the contacts that these cells established with microglia occurred mainly on the fine, secondary processes rather than on the soma, as has been described for phagocytic engulfment (Sierra et al., 2010). In view of the previous studies, and our results we can conclude that microglia may regulate RGL stem cell proliferation using paracrine or juxtacrine signaling, independently from inflammatory pathway. These results are interesting, because they indicate that targeting microglia, even in absence of inflammation, can increase adult neurogenesis, as demonstrated by our results with taurine and doxycycline.
Still, further experiments will be needed to clarify the signaling between microglia and neurogenesis in the adult healthy brain.

Astrocytes

While microglia inhibits adult neurogenesis, astrocytes are known to secrete molecules that increase the proliferation of RGL stem cells (Barkho et al., 2006; Brazel et al., 2005; Juric et al., 2006; Steiner et al., 2006). Molecules can be released by passive diffusion through the

astrocytic membrane or by exocytosis due the presence of soluble N-ethylmaleimide sensitive fusion proteins (SNARE). Hippocampal astrocytes can stock and release D-serine, an endogenous D-amino acid (Martineau et al., 2013; Schell et al., 1995; Wolosker et al., 1999). D-serine is the major co-agonist of the NMDA receptor and is involved in different NMDAR-dependent processes including neurotransmission (Bado et al., 2011; Mothet et al., 2000) and long term potentiation (LTP) in the hippocampus through Calcium-dependent release (Henneberger et al., 2010; Turpin et al., 2011; Yang et al., 2013). In (Sultan et al., 2013b) we tested the effect of D-serine on hippocampal adult neurogenesis. We showed that D-serine not only increased the proliferation of α RGL neural stem cells but when it was injected during the critical period of activity-dependent cell death, it increased the survival of immature neurons. In fact, D-serine regulates several steps of hippocampal adult neurogenesis. Moreover, D-serine directly increased the proliferation of purified adult hippocampal progenitor cells *in vitro.*

Several studies showed that newly generated neurons play a role in hippocampal dependent learning and memory (Dupret et al., 2007; Gu et al., 2012; Ming and Song, 2011). Therefore, by increasing neurogenesis, D-serine may increase learning performances. Nevertheless, to investigate the role of D-serine in learning performances, behavioral experiments combined with D-serine treatment and ablation of neurogenesis are required.

Recently, in our lab we have shown the importance of D-serine in synaptic integration of adult-born neurons. Actually, during their maturation, new granule neurons first receive GABAergic excitatory innervation (Li et al., 2012). Then, granular neurons receive glutamatergic inputs, however they form silent synapses as they express only NMDA receptors but no AMPA receptors (Chancey et al., 2013). We found that at this stage, the release of the NMDAR co-agonist D-serine by astrocytes is crucial to contribute to the activity-dependent synaptic integration of newly generated neurons (Sultan et al., 2015). These observations are in line with previous observations on the role of the NR1 subunit of the NMDA receptor on new neuron survival (Tashiro et al., 2007; Tashiro et al., 2006). So, the observed effect of D-serine on neuronal survival may be linked to the role of NMDA receptor activation.

Moreover, in recent experiments, we found that the NMDA receptor is expressed on the surface of the α RGL neural stem cell and by knocking down this receptor specifically on the RGL we completely changed its regulation. Furthermore, electrophysiological recordings have shown the presence of NMDA receptors on RGL cells in acute hippocampal slices (Nacher et al., 2007; Shin et al., 2015; Wang et al., 2005). Therefore, D-serine may have a direct effect on neural stem cells, as shown in vitro. On the other hand, D-serine i.p. administration may enhance the hippocampal network activity and, as adult α RGL neural stem cells proliferation and newborn neurons survival are tightly regulated by hippocampal network activity (Bruel-Jungerman et al., 2006; Chun et al., 2006; Stone, 2011), may indirectly increase proliferation.
Further experiments will be needed to elucidate the role of D-serine and of the NMDA receptors on the proliferation of the stem/progenitor cells.

Another amino acid synthetized and secreted by astrocytes is taurine (Ripps and Shen, 2012). Taurine is produced from methionine and cysteine. It is not incorporated into proteins and this is the free amino acid with the highest concentration in tissue (Jacobsen and Smith, 1968). Taurine has been shown to be a neurotransmitter, although no specific taurine inotropic or metabotropic receptor has been clearly identified, several lines of evidences support the existence of one inotropic and maybe several metabotropic receptors able to modulate intracellular calcium levels and therefore the subsequent signalling pathways calcium is involved into and neurotransmission in general (Menzie et al., 2013; Wu et al., 2005; Wu et al., 1992). In (Gebara et al., 2015), we found that taurine injection increased the proliferation of α RGL stem cells. Besides, taurine increased the survival of newborn neurons, inducing a net increase of adult neurogenesis. We found also that taurine decreased the amount of hippocampal microglia but did not affect the number of GFAP-immunolabeled astrocytes. Together, these results indicate that, in the aged brain, taurine increases the production of new neurons by stimulating several steps of adult neurogenesis.

Furthermore, taurine may increase adult neurogenesis by modulating microglia. Indeed, the aging brain is accompanied by increased expression of genes involved in cellular stress and inflammation, microglia proliferation and activity (Kohman et al., 2012). Furthermore, we recently found that an increase in the number of microglia in the aging hippocampus

negatively correlates with the proliferation of α RGL stem cells, Tbr2-expressing intermediate progenitors and the number of DCX-expressing immature neurons suggesting a direct inhibitory effect of microglia on adult neurogenesis (Gebara et al., 2013). In support of this possibility, anti-inflammatory treatments that reduce microglia induce an increase in adult neurogenesis (Monje et al., 2003; Sultan et al., 2013a). Thus, the effect of taurine on adult neurogenesis may be mediated by its anti-inflammatory properties, as this molecule reduces the production of inflammatory cytokines such as TNFα or IL-1β (Kim and Cha, 2014) and its derivative, taurine-CL, reduces the activation of NFkb in several models of inflammation (Kim and Kim, 2005). Furthermore, taurine inhibits the development of chronic inflammation in animal models of arthritis, inflammatory bowel disease and lung fibrosis. In the brain, taurine reduces damage and cytokines expression after traumatic brain injury (Su et al., 2014) as well as lipopolysaccharide-induced inflammation and subsequent microglia activation and reduced neurogenesis in the hippocampus (Wu et al., 2013). Altogether, these data suggest that the effect of taurine on adult neurogenesis in the aged brain may be, at least partially, mediated by a reduction in microglia activation in the aged brain.

However, the diversity of action of taurine in vivo suggests that this molecule may use several molecular pathways to regulate adult neurogenesis. Indeed, consistently with previous reports (Ramos-Mandujano et al., 2014), we found that taurine increased the proliferation of purified adult hippocampal progenitor cells in vitro, in absence of microglia. Taurine is involved in cellular calcium homeostasis (El Idrissi, 2008), and has antioxidant (Schaffer et al., 2009)as well as antiapoptotic properties (Foos and Wu, 2002; Leon et al., 2009), all of which can potentially increase the proliferation or the survival rate of the highly proliferative and metabolically active neural stem cells and newborn neurons. Of particular interest, taurine has recently been shown to interact with the polyamine site of the NMDA receptor and reduce the action of spermine on NMDA receptor activity and the NMDA receptor affinity for glycine (Chan et al., 2014). The NMDA receptor is expressed by RGL cells (Muth-Kohne et al., 2010) and its activity regulates proliferation, as demonstrated by the stimulating effect of the antagonists memantine or MK-801 (Namba et al., 2009), or the inhibitory effects of the co-agonist D-serine (Sultan et al., 2013b). Thus, by directly modulating NMDA receptor activity on α RGL stem cells, taurine may increase the

proliferation of these cells and contribute to the increased neurogenesis observed in our study, a hypothesis that requires further testing.

Adult neurogenesis and the incorporation of new, particularly plastic neurons in the hippocampal network play a crucial role in learning and memory that underlie the age-related decrease in learning performances (Gil-Mohapel et al., 2013). The results presented here provide evidence that the age-related decrease in adult neurogenesis can be attenuated by the exogenous administration of taurine and provide a potential mechanism underlying the effect of taurine on cognition.

Conclusions and perspectives

The work of my thesis suggests that hippocampal RGL neural cells are a heterogeneous population. Still, how each of these subtypes of RGL cells is regulated has not been fully characterized, nevertheless we identified some important players.

- We offered a more detailed identification of different type of RGL neural cells in

the adult dentate gyrus. We clearly revealed that type α is an activated RGL neural stem cell available to divide, renew itself and give rise to neurons and astrocyte. However, the fate of type β cell remains unclear. Type β, is a very quiescent RGL cell, in physiological condition, does not divide and is only able to transform into astrocyte (figure 18).

Time-lapse imaging coupled with clonal analysis may be necessary to examine whether type β cells can transform again into type α cells, or only into astrocytes and migrate out of the granule cell layer. Elucidating the fate on type β is crucial. If type β is a very quiescent stem cell, it will be essential to reveal how to stimulate its proliferation in order to increase adult neurogenesis in pathological conditions where we have a complete depletion of type α cells.

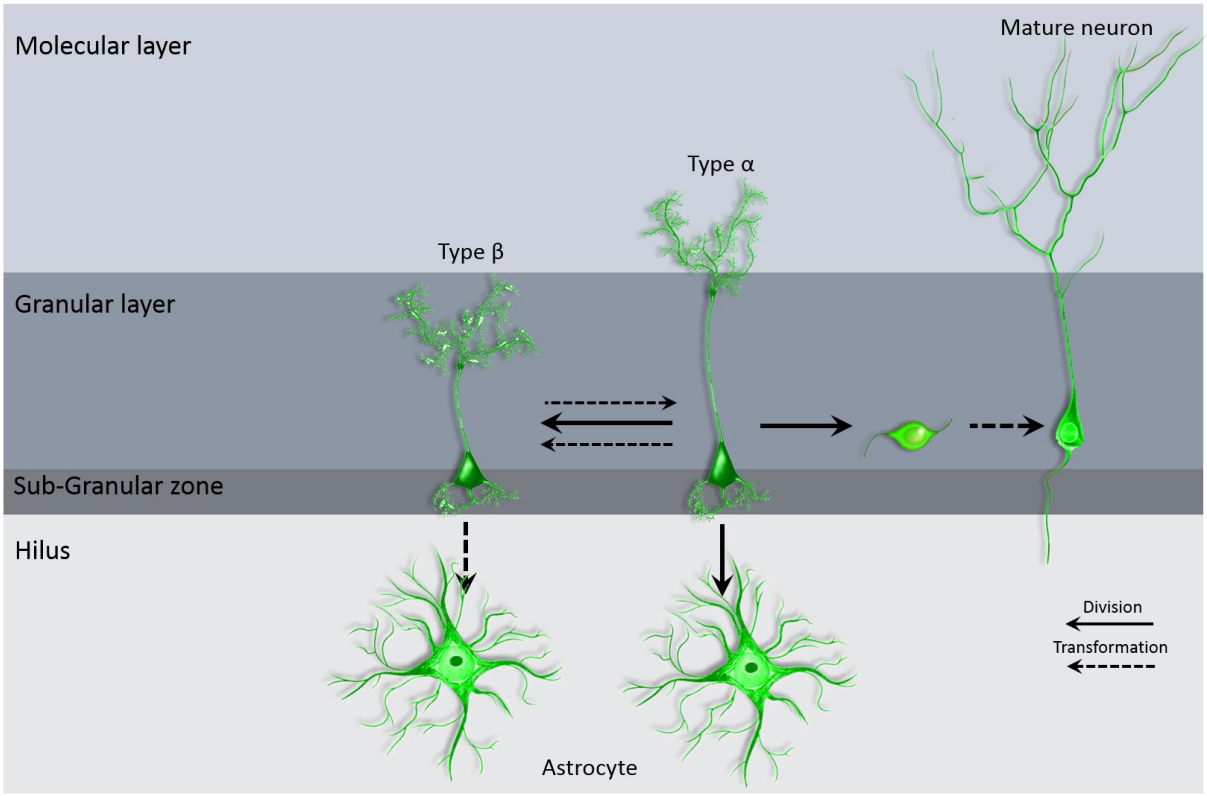

Figure 18: Heterogeneity of Radial Glia-Like cells in the adult hippocampus

Type α cells are able to do symmetric division to renew the stem cell pool. And it is able to do asymmetric division give rise to type 2 cells that differentiate into a mature neuron, to type β cells and astrocytes. Whereas type β cells do not divide and are prone to gliogenesis.

- We improved our knowledge on the role of microglia in regulating neurogenesis (Figure 19). We found that microglia decreases adult neurogenesis. However, the mechanism of action remains unclear and obviously additional experiments will be necessary to understand this mechanism. Time-lapse imaging in reporter mice for microglia and neural stem cells will elucidate the interactions between these two cell types and explain how these interactions play a role on the fate to the RGL neural cell. These experiments can be coupled with a deep analysis of the secretome of the microglia that permits to identify the key factors in these regulations.

- It is known that astrocytes play an important role in the homeostasis of the brain but very little is known about its role in the regulation of adult neurogenesis. Here, we elucidated the effect of two molecules intrinsic to the niche, normally released by astrocytes among load of others, which regulate adult neurogenesis (figure 19). The mechanism of

action is not completely clear, but several experiments that are ongoing or planned for the near future that will clarify this mechanism. Our data suggests a direct effect of D-serine on the α RGL neural stem cell. D-serine is a co-agonist of the NMDA receptor. To see if the effect is mediated by this receptor we decided to knock it down specifically in adult neural stem cells, using cell-specific controllable transgenic mice and then analyze the effect of D-serine both in vitro and in vivo.

The effect of Taurine on the adult RGL neural cell is even less clear. In fact, no specific inotropic or metabotropic receptor has been clearly identified. However, performing microarray on stem cell culture after Taurine treatment gives a hint about the genetic regulation. Moreover, it would be interesting to assess behavioral analysis coupled with the manipulation of the niche to check the effect on hippocampal function.

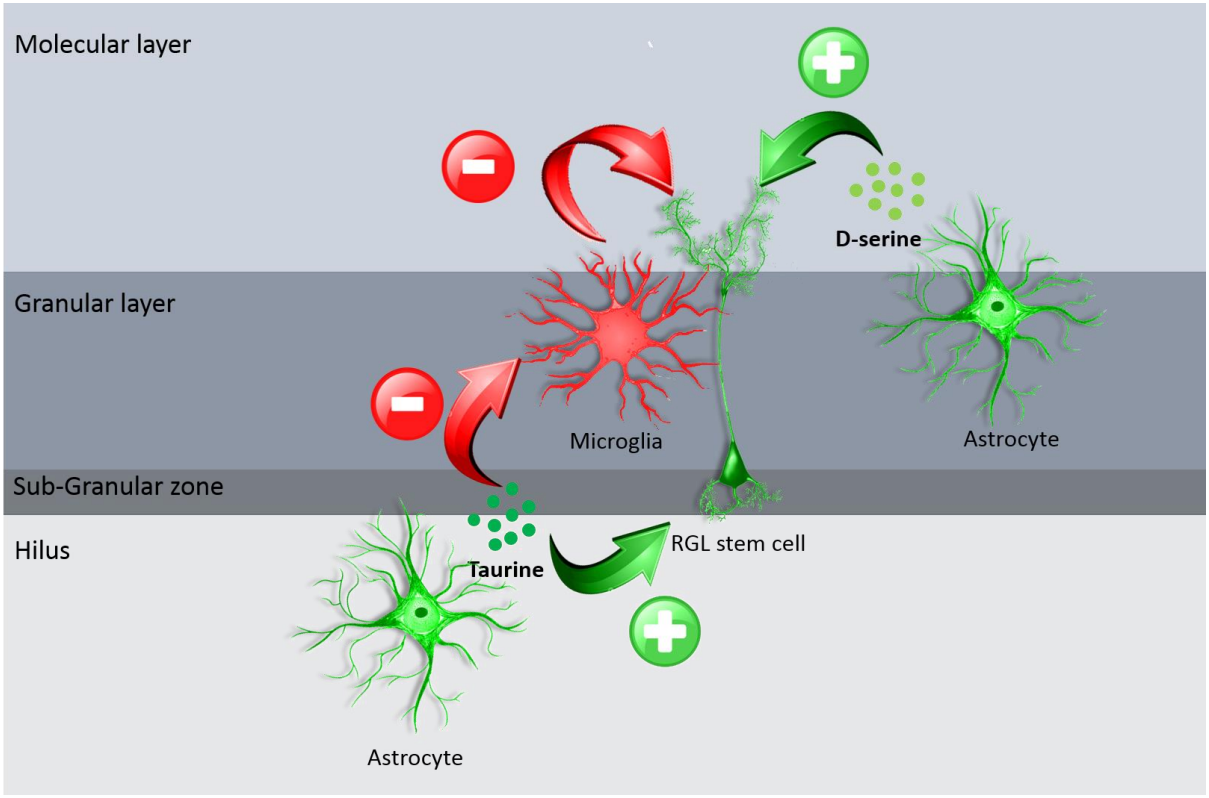

Figure 19: Regulation of the adult neural α RGL stem cells by micro and astroglia

Adult neurogenesis is tightly regulated by the neurogenic niche. Microglia by interacting with the RGL neural α RGL stem cell inhibits its proliferation. Astrocytes by secreting D-serine and taurine increase stem cells proliferation and neuronal differentiation. Moreover, Taurine decreases the number and the activation state of microglia.

In conclusion, adult neurogenesis is an important process of brain plasticity, which is highly regulated. A better understanding of the mechanisms of this regulation will help us to understand how the brain adapts to a constantly changing environment. Our findings are the first step of understanding how the neurogenic niche works and which factors are important for the regulation of the α RGL neural stem cell and the generation of neurons. This knowledge is crucial to be able, one day, to recreate a favorable environment for neurogenesis in other parts of the brain and thus produce neurons, which has huge therapeutic consequences.

REFERENCES

Aarum, J., Sandberg, K., Haeberlein, S.L., and Persson, M.A. (2003). Migration and differentiation of neural precursor cells can be directed by microglia. Proc Natl Acad Sci U S A 100, 15983-15988.

Acsady, L., Katona, I., Gulyas, A.I., Shigemoto, R., and Freund, T.F. (1997). Immunostaining for substance P receptor labels GABAergic cells with distinct termination patterns in the hippocampus. J Comp Neurol 378, 320-336.

Aloisi, F. (2001). Immune function of microglia. Glia 36, 165-179.

Altman, J. (1962). Are new neurons formed in the brains of adult mammals? Science 135, 1127-1128.

Altman, J. (1963). Autoradiographic investigation of cell proliferation in the brains of rats and cats. Anat Rec 145, 573-591.

Altman, J., and Das, G.D. (1965). Autoradiographic and histological evidence of postnatal hippocampal neurogenesis in rats. J Comp Neurol 124, 319-335.

Alvarez-Buylla, A., and Lim, D.A. (2004). For the long run: maintaining germinal niches in the adult brain. Neuron 41, 683-686.

Amaral, D.G., Scharfman, H.E., and Lavenex, P. (2007). The dentate gyrus: fundamental neuroanatomical organization (dentate gyrus for dummies). Prog Brain Res 163, 3-22.

Amaral, D.G., and Witter, M.P. (1989). The three-dimensional organization of the hippocampal formation: a review of anatomical data. Neuroscience 31, 571-591.

Andersen, M.L., Perry, J.C., Bignotto, M., Perez-Mendes, P., Cinini, S.M., Mello, L.E., and Tufik, S. (2007). Influence of chronic cocaine treatment and sleep deprivation on sexual behavior and neurogenesis of the male rat. Prog Neuropsychopharmacol Biol Psychiatry 31, 1224-1229.

Ashton, R.S., Conway, A., Pangarkar, C., Bergen, J., Lim, K.I., Shah, P., Bissell, M., and Schaffer, D.V. (2012). Astrocytes regulate adult hippocampal neurogenesis through ephrin-B signaling. Nat Neurosci 15, 1399-1406.

Babu, H., Ramirez-Rodriguez, G., Fabel, K., Bischofberger, J., and Kempermann, G. (2009). Synaptic Network Activity Induces Neuronal Differentiation of Adult Hippocampal Precursor Cells through BDNF Signaling. Front Neurosci 3, 49.

Bado, P., Madeira, C., Vargas-Lopes, C., Moulin, T.C., Wasilewska-Sampaio, A.P., Maretti, L., de Oliveira, R.V., Amaral, O.B., and Panizzutti, R. (2011). Effects of low-dose D-serine on recognition and working memory in mice. Psychopharmacology (Berl) 218, 461-470.

Barkho, B.Z., Song, H., Aimone, J.B., Smrt, R.D., Kuwabara, T., Nakashima, K., Gage, F.H., and Zhao, X. (2006). Identification of astrocyte-expressed factors that modulate neural stem/progenitor cell differentiation. Stem Cells Dev 15, 407-421.

Barres, B.A. (2008). The mystery and magic of glia: a perspective on their roles in health and disease. Neuron 60, 430-440.

Beckervordersandforth, R., Deshpande, A., Schaffner, I., Huttner, H.B., Lepier, A., Lie, D.C., and Gotz, M. (2014). In vivo targeting of adult neural stem cells in the dentate gyrus by a split-cre approach. Stem Cell Reports 2, 153-162.

Belmadani, A., Tran, P.B., Ren, D., and Miller, R.J. (2006). Chemokines regulate the migration of neural progenitors to sites of neuroinflammation. J Neurosci 26, 3182-3191.

Bengzon, J., Kokaia, Z., Elmer, E., Nanobashvili, A., Kokaia, M., and Lindvall, O. (1997). Apoptosis and proliferation of dentate gyrus neurons after single and intermittent limbic seizures. Proc Natl Acad Sci U S A 94, 10432-10437.

Bergami, M., and Berninger, B. (2012). A fight for survival: the challenges faced by a newborn neuron integrating in the adult hippocampus. Dev Neurobiol 72, 1016-1031.

Bergersen, L.H., Morland, C., Ormel, L., Rinholm, J.E., Larsson, M., Wold, J.F., Roe, A.T., Stranna, A., Santello, M., Bouvier, D., et al. (2012). Immunogold detection of L-glutamate and D-serine in small synaptic-like microvesicles in adult hippocampal astrocytes. Cereb Cortex 22, 1690-1697.

Bergmann, O., and Frisen, J. (2013). Neuroscience. Why adults need new brain cells. Science 340, 695-696.

Bernier, P.J., Vinet, J., Cossette, M., and Parent, A. (2000). Characterization of the subventricular zone of the adult human brain: evidence for the involvement of Bcl-2. Neurosci Res 37, 67-78.

Bhattacharyya, B.J., Banisadr, G., Jung, H., Ren, D., Cronshaw, D.G., Zou, Y., and Miller, R.J. (2008). The chemokine stromal cell-derived factor-1 regulates GABAergic inputs to neural progenitors in the postnatal dentate gyrus. J Neurosci 28, 6720-6730.

Bolteus, A.J., and Bordey, A. (2004). GABA release and uptake regulate neuronal precursor migration in the postnatal subventricular zone. J Neurosci 24, 7623-7631.

Bonaguidi, M.A., Wheeler, M.A., Shapiro, J.S., Stadel, R.P., Sun, G.J., Ming, G.L., and Song, H. (2011). In vivo clonal analysis reveals self-renewing and multipotent adult neural stem cell characteristics. Cell 145, 1142-1155.

Brazel, C.Y., Nunez, J.L., Yang, Z., and Levison, S.W. (2005). Glutamate enhances survival and proliferation of neural progenitors derived from the subventricular zone. Neuroscience 131, 55-65.

Breton-Provencher, V., and Saghatelyan, A. (2012). Newborn neurons in the adult olfactory bulb: unique properties for specific odor behavior. Behav Brain Res 227, 480-489.

Brezun, J.M., and Daszuta, A. (1999). Depletion in serotonin decreases neurogenesis in the dentate gyrus and the subventricular zone of adult rats. Neuroscience 89, 999-1002.

Brezun, J.M., and Daszuta, A. (2000). Serotonin may stimulate granule cell proliferation in the adult hippocampus, as observed in rats grafted with foetal raphe neurons. Eur J Neurosci 12, 391-396.

Bruel-Jungerman, E., Davis, S., Rampon, C., and Laroche, S. (2006). Long-term potentiation enhances neurogenesis in the adult dentate gyrus. J Neurosci 26, 5888-5893.

Cameron, H.A., McEwen, B.S., and Gould, E. (1995). Regulation of adult neurogenesis by excitatory input and NMDA receptor activation in the dentate gyrus. J Neurosci 15, 4687-4692.

Chan, C.Y., Sun, H.S., Shah, S.M., Agovic, M.S., Friedman, E., and Banerjee, S.P. (2014). Modes of direct modulation by taurine of the glutamate NMDA receptor in rat cortex. Eur J Pharmacol 728, 167-175.

Chancey, J.H., Adlaf, E.W., Sapp, M.C., Pugh, P.C., Wadiche, J.I., and Overstreet-Wadiche, L.S. (2013). GABA depolarization is required for experience-dependent synapse unsilencing in adult-born neurons. J Neurosci 33, 6614-6622.

Cho, Y., Son, H.J., Kim, E.M., Choi, J.H., Kim, S.T., Ji, I.J., Choi, D.H., Joh, T.H., Kim, Y.S., and Hwang, O. (2009). Doxycycline is neuroprotective against nigral dopaminergic degeneration by a dual mechanism involving MMP-3. Neurotox Res 16, 361-371.

Choe, K.Y., Olson, J.E., and Bourque, C.W. (2012). Taurine release by astrocytes modulates osmosensitive glycine receptor tone and excitability in the adult supraoptic nucleus. J Neurosci 32, 12518-12527.

Chun, S.K., Sun, W., Park, J.J., and Jung, M.W. (2006). Enhanced proliferation of progenitor cells following long-term potentiation induction in the rat dentate gyrus. Neurobiol Learn Mem 86, 322-329.

Clark, W.M., Lessov, N., Lauten, J.D., and Hazel, K. (1997). Doxycycline treatment reduces ischemic brain damage in transient middle cerebral artery occlusion in the rat. J Mol Neurosci 9, 103-108.

Conover, J.C., Doetsch, F., Garcia-Verdugo, J.M., Gale, N.W., Yancopoulos, G.D., and Alvarez-Buylla, A. (2000). Disruption of Eph/ephrin signaling affects migration and proliferation in the adult subventricular zone. Nat Neurosci 3, 1091-1097.

Dayer, A.G., Ford, A.A., Cleaver, K.M., Yassaee, M., and Cameron, H.A. (2003). Short-term and long-term survival of new neurons in the rat dentate gyrus. J Comp Neurol 460, 563-572.

Deisseroth, K., Singla, S., Toda, H., Monje, M., Palmer, T.D., and Malenka, R.C. (2004). Excitation-neurogenesis coupling in adult neural stem/progenitor cells. Neuron 42, 535-552.

Deng, P.Y., Xiao, Z., Jha, A., Ramonet, D., Matsui, T., Leitges, M., Shin, H.S., Porter, J.E., Geiger, J.D., and Lei, S. (2010). Cholecystokinin facilitates glutamate release by increasing the number of readily releasable vesicles and releasing probability. J Neurosci 30, 5136-5148.

Deng, W., Saxe, M.D., Gallina, I.S., and Gage, F.H. (2009). Adult-born hippocampal dentate granule cells undergoing maturation modulate learning and memory in the brain. J Neurosci 29, 13532-13542.

Doetsch, F., and Alvarez-Buylla, A. (1996). Network of tangential pathways for neuronal migration in adult mammalian brain. Proc Natl Acad Sci U S A 93, 14895-14900.

Doetsch, F., Garcia-Verdugo, J.M., and Alvarez-Buylla, A. (1999). Regeneration of a germinal layer in the adult mammalian brain. Proc Natl Acad Sci U S A 96, 11619-11624.

Dupret, D., Fabre, A., Dobrossy, M.D., Panatier, A., Rodriguez, J.J., Lamarque, S., Lemaire, V., Oliet, S.H., Piazza, P.V., and Abrous, D.N. (2007). Spatial learning depends on both the addition and removal of new hippocampal neurons. PLoS Biol 5, e214.

Ehninger, D., and Kempermann, G. (2003). Regional effects of wheel running and environmental enrichment on cell genesis and microglia proliferation in the adult murine neocortex. Cereb Cortex 13, 845-851.

Ekdahl, C.T., Claasen, J.H., Bonde, S., Kokaia, Z., and Lindvall, O. (2003). Inflammation is detrimental for neurogenesis in adult brain. Proc Natl Acad Sci U S A 100, 13632-13637.

El Idrissi, A. (2008). Taurine increases mitochondrial buffering of calcium: role in neuroprotection. Amino Acids 34, 321-328.

Encinas, J.M., Michurina, T.V., Peunova, N., Park, J.H., Tordo, J., Peterson, D.A., Fishell, G., Koulakov, A., and Enikolopov, G. (2011). Division-coupled astrocytic differentiation and age-related depletion of neural stem cells in the adult hippocampus. Cell Stem Cell 8, 566-579.

Eriksson, P.S., Perfilieva, E., Bjork-Eriksson, T., Alborn, A.M., Nordborg, C., Peterson, D.A., and Gage, F.H. (1998). Neurogenesis in the adult human hippocampus. Nat Med 4, 1313-1317.

Filippov, V., Kronenberg, G., Pivneva, T., Reuter, K., Steiner, B., Wang, L.P., Yamaguchi, M., Kettenmann, H., and Kempermann, G. (2003). Subpopulation of nestin-expressing progenitor cells in the adult murine hippocampus shows electrophysiological and morphological characteristics of astrocytes. Mol Cell Neurosci 23, 373-382.

Finch, D.M., Wong, E.E., Derian, E.L., and Babb, T.L. (1986). Neurophysiology of limbic system pathways in the rat: projections from the subicular complex and hippocampus to the entorhinal cortex. Brain Res 397, 205-213.

Foos, T.M., and Wu, J.Y. (2002). The role of taurine in the central nervous system and the modulation of intracellular calcium homeostasis. Neurochem Res 27, 21-26.

Ford-Perriss, M., Abud, H., and Murphy, M. (2001). Fibroblast growth factors in the developing central nervous system. Clin Exp Pharmacol Physiol 28, 493-503.

Fuhs, M.C., and Touretzky, D.S. (2007). Context learning in the rodent hippocampus. Neural Comput 19, 3173-3215.

Fukuda, S., Kato, F., Tozuka, Y., Yamaguchi, M., Miyamoto, Y., and Hisatsune, T. (2003). Two distinct subpopulations of nestin-positive cells in adult mouse dentate gyrus. J Neurosci 23, 9357-9366.

Ge, S., Yang, C.H., Hsu, K.S., Ming, G.L., and Song, H. (2007). A critical period for enhanced synaptic plasticity in newly generated neurons of the adult brain. Neuron 54, 559-566.

Gebara, E., Sultan, S., Kocher-Braissant, J., and Toni, N. (2013). Adult hippocampal neurogenesis inversely correlates with microglia in conditions of voluntary running and aging. Front Neurosci 7, 145.

Gebara, E., Udry, F., Sultan, S., and Toni, N. (2015). Taurine increases hippocampal neurogenesis in aging mice. Stem Cell Res 14, 369-379.

Gil-Mohapel, J., Brocardo, P.S., Choquette, W., Gothard, R., Simpson, J.M., and Christie, B.R. (2013). Hippocampal neurogenesis levels predict WATERMAZE search strategies in the aging brain. PLoS One 8, e75125.

Glasper, E.R., Schoenfeld, T.J., and Gould, E. (2012). Adult neurogenesis: optimizing hippocampal function to suit the environment. Behav Brain Res 227, 380-383.

Goldman, S.A., and Nottebohm, F. (1983). Neuronal production, migration, and differentiation in a vocal control nucleus of the adult female canary brain. Proc Natl Acad Sci U S A 80, 2390-2394.

Gonzalez-Perez, O., Jauregui-Huerta, F., and Galvez-Contreras, A.Y. (2010). Immune system modulates the function of adult neural stem cells. Curr Immunol Rev 6, 167-173.

Gould, E. (1999). Serotonin and hippocampal neurogenesis. Neuropsychopharmacology 21, 46S-51S.

Gould, E., Reeves, A.J., Fallah, M., Tanapat, P., Gross, C.G., and Fuchs, E. (1999). Hippocampal neurogenesis in adult Old World primates. Proc Natl Acad Sci U S A 96, 5263-5267.

Gould, E., Vail, N., Wagers, M., and Gross, C.G. (2001). Adult-generated hippocampal and neocortical neurons in macaques have a transient existence. Proc Natl Acad Sci U S A 98, 10910-10917.

Groves, J.O., Leslie, I., Huang, G.J., McHugh, S.B., Taylor, A., Mott, R., Munafo, M., Bannerman, D.M., and Flint, J. (2013). Ablating adult neurogenesis in the rat has no effect on spatial processing: evidence from a novel pharmacogenetic model. PLoS Genet 9, e1003718.

Gu, Y., Arruda-Carvalho, M., Wang, J., Janoschka, S.R., Josselyn, S.A., Frankland, P.W., and Ge, S. (2012). Optical controlling reveals time-dependent roles for adult-born dentate granule cells. Nat Neurosci 15, 1700-1706.

Hack, I., Bancila, M., Loulier, K., Carroll, P., and Cremer, H. (2002). Reelin is a detachment signal in tangential chain-migration during postnatal neurogenesis. Nat Neurosci 5, 939-945.

Henneberger, C., Papouin, T., Oliet, S.H., and Rusakov, D.A. (2010). Long-term potentiation depends on release of D-serine from astrocytes. Nature 463, 232-236.

Herculano-Houzel, S. (2014). The glia/neuron ratio: how it varies uniformly across brain structures and species and what that means for brain physiology and evolution. Glia 62, 1377-1391.

Huang, X., Kong, H., Tang, M., Lu, M., Ding, J.H., and Hu, G. (2012). D-Serine regulates proliferation and neuronal differentiation of neural stem cells from postnatal mouse forebrain. CNS Neurosci Ther 18, 4-13.

Hurtado-Chong, A., Yusta-Boyo, M.J., Vergano-Vera, E., Bulfone, A., de Pablo, F., and Vicario-Abejon, C. (2009). IGF-I promotes neuronal migration and positioning in the olfactory bulb and the exit of neuroblasts from the subventricular zone. Eur J Neurosci 30, 742-755.

Jacobsen, J.G., and Smith, L.H. (1968). Biochemistry and physiology of taurine and taurine derivatives. Physiol Rev 48, 424-511.

Jantzie, L.L., and Todd, K.G. (2010). Doxycycline inhibits proinflammatory cytokines but not acute cerebral cytogenesis after hypoxia-ischemia in neonatal rats. J Psychiatry Neurosci 35, 20-32.

Juric, D.M., Miklic, S., and Carman-Krzan, M. (2006). Monoaminergic neuronal activity up-regulates BDNF synthesis in cultured neonatal rat astrocytes. Brain Res 1108, 54-62.

Kaplan, M.S. (1985). Formation and turnover of neurons in young and senescent animals: an electronmicroscopic and morphometric analysis. Ann N Y Acad Sci 457, 173-192.

Kaplan, M.S. (2001). Environment complexity stimulates visual cortex neurogenesis: death of a dogma and a research career. Trends Neurosci 24, 617-620.

Kee, N., Teixeira, C.M., Wang, A.H., and Frankland, P.W. (2007). Preferential incorporation of adult-generated granule cells into spatial memory networks in the dentate gyrus. Nat Neurosci 10, 355-362.

Kempermann, G. (2011). Seven principles in the regulation of adult neurogenesis. Eur J Neurosci 33, 1018-1024.

Kempermann, G., Jessberger, S., Steiner, B., and Kronenberg, G. (2004). Milestones of neuronal development in the adult hippocampus. Trends Neurosci 27, 447-452.

Kempermann, G., Kuhn, H.G., and Gage, F.H. (1997a). Genetic influence on neurogenesis in the dentate gyrus of adult mice. Proc Natl Acad Sci U S A 94, 10409-10414.

Kempermann, G., Kuhn, H.G., and Gage, F.H. (1997b). More hippocampal neurons in adult mice living in an enriched environment. Nature 386, 493-495.

Kim, C., and Cha, Y.N. (2014). Taurine chloramine produced from taurine under inflammation provides anti-inflammatory and cytoprotective effects. Amino Acids 46, 89-100.

Kim, J.W., and Kim, C. (2005). Inhibition of LPS-induced NO production by taurine chloramine in macrophages is mediated though Ras-ERK-NF-kappaB. Biochem Pharmacol 70, 1352-1360.

Kohman, R.A., Bhattacharya, T.K., Kilby, C., Bucko, P., and Rhodes, J.S. (2013). Effects of minocycline on spatial learning, hippocampal neurogenesis and microglia in aged and adult mice. Behav Brain Res 242, 17-24.

Kohman, R.A., DeYoung, E.K., Bhattacharya, T.K., Peterson, L.N., and Rhodes, J.S. (2012). Wheel running attenuates microglia proliferation and increases expression of a proneurogenic phenotype in the hippocampus of aged mice. Brain Behav Immun 26, 803-810.

Koo, J.W., and Duman, R.S. (2008). IL-1beta is an essential mediator of the antineurogenic and anhedonic effects of stress. Proc Natl Acad Sci U S A 105, 751-756.

Kornack, D.R., and Rakic, P. (2001). The generation, migration, and differentiation of olfactory neurons in the adult primate brain. Proc Natl Acad Sci U S A 98, 4752-4757.

Kriegstein, A., and Alvarez-Buylla, A. (2009). The glial nature of embryonic and adult neural stem cells. Annu Rev Neurosci 32, 149-184.

Kronenberg, G., Reuter, K., Steiner, B., Brandt, M.D., Jessberger, S., Yamaguchi, M., and Kempermann, G. (2003). Subpopulations of proliferating cells of the adult hippocampus respond differently to physiologic neurogenic stimuli. J Comp Neurol 467, 455-463.

Kuhn, H.G., Dickinson-Anson, H., and Gage, F.H. (1996). Neurogenesis in the dentate gyrus of the adult rat: age-related decrease of neuronal progenitor proliferation. J Neurosci 16, 2027-2033.

Kunze, A., Congreso, M.R., Hartmann, C., Wallraff-Beck, A., Huttmann, K., Bedner, P., Requardt, R., Seifert, G., Redecker, C., Willecke, K., et al. (2009). Connexin expression by radial glia-like cells is required for neurogenesis in the adult dentate gyrus. Proc Natl Acad Sci U S A 106, 11336-11341.

Lagace, D.C., Whitman, M.C., Noonan, M.A., Ables, J.L., DeCarolis, N.A., Arguello, A.A., Donovan, M.H., Fischer, S.J., Farnbauch, L.A., Beech, R.D., et al. (2007). Dynamic contribution of nestin-expressing stem cells to adult neurogenesis. J Neurosci 27, 12623-12629.

Laplagne, D.A., Esposito, M.S., Piatti, V.C., Morgenstern, N.A., Zhao, C., van Praag, H., Gage, F.H., and Schinder, A.F. (2006). Functional convergence of neurons generated in the developing and adult hippocampus. PLoS Biol 4, e409.

Lee, Y., Morrison, B.M., Li, Y., Lengacher, S., Farah, M.H., Hoffman, P.N., Liu, Y., Tsingalia, A., Jin, L., Zhang, P.W., et al. (2012). Oligodendroglia metabolically support axons and contribute to neurodegeneration. Nature 487, 443-448.

Leon, R., Wu, H., Jin, Y., Wei, J., Buddhala, C., Prentice, H., and Wu, J.Y. (2009). Protective function of taurine in glutamate-induced apoptosis in cultured neurons. J Neurosci Res 87, 1185-1194.

Li, Y., Xiao, H., Chiou, T.T., Jin, H., Bonhomme, B., Miralles, C.P., Pinal, N., Ali, R., Chen, W.V., Maniatis, T., et al. (2012). Molecular and functional interaction between protocadherin-gammaC5 and GABAA receptors. J Neurosci 32, 11780-11797.

Lie, D.C., Colamarino, S.A., Song, H.J., Desire, L., Mira, H., Consiglio, A., Lein, E.S., Jessberger, S., Lansford, H., Dearie, A.R., et al. (2005). Wnt signalling regulates adult hippocampal neurogenesis. Nature 437, 1370-1375.

Liu, Z., Fan, Y., Won, S.J., Neumann, M., Hu, D., Zhou, L., Weinstein, P.R., and Liu, J. (2007). Chronic treatment with minocycline preserves adult new neurons and reduces functional impairment after focal cerebral ischemia. Stroke 38, 146-152.

Lois, C., and Alvarez-Buylla, A. (1994). Long-distance neuronal migration in the adult mammalian brain. Science 264, 1145-1148.

Lugert, S., Basak, O., Knuckles, P., Haussler, U., Fabel, K., Gotz, M., Haas, C.A., Kempermann, G., Taylor, V., and Giachino, C. (2010). Quiescent and active hippocampal neural stem cells with distinct morphologies respond selectively to physiological and pathological stimuli and aging. Cell Stem Cell 6, 445-456.

Luzzati, F., De Marchis, S., Fasolo, A., and Peretto, P. (2007). Adult neurogenesis and local neuronal progenitors in the striatum. Neurodegener Dis 4, 322-327.

Manns, J.R., and Eichenbaum, H. (2009). A cognitive map for object memory in the hippocampus. Learn Mem 16, 616-624.

Martineau, M., Shi, T., Puyal, J., Knolhoff, A.M., Dulong, J., Gasnier, B., Klingauf, J., Sweedler, J.V., Jahn, R., and Mothet, J.P. (2013). Storage and uptake of D-serine into astrocytic synaptic-like vesicles specify gliotransmission. J Neurosci 33, 3413-3423.

Menzie, J., Prentice, H., and Wu, J.Y. (2013). Neuroprotective Mechanisms of Taurine against Ischemic Stroke. Brain Sci 3, 877-907.

Mercier, F., Kitasako, J.T., and Hatton, G.I. (2002). Anatomy of the brain neurogenic zones revisited: fractones and the fibroblast/macrophage network. J Comp Neurol 451, 170-188.

Migaud, M., Batailler, M., Segura, S., Duittoz, A., Franceschini, I., and Pillon, D. (2010). Emerging new sites for adult neurogenesis in the mammalian brain: a comparative study between the hypothalamus and the classical neurogenic zones. Eur J Neurosci 32, 2042-2052.

Ming, G.L., and Song, H. (2005). Adult neurogenesis in the mammalian central nervous system. Annu Rev Neurosci 28, 223-250.

Ming, G.L., and Song, H. (2011). Adult neurogenesis in the mammalian brain: significant answers and significant questions. Neuron 70, 687-702.

Mirzadeh, Z., Merkle, F.T., Soriano-Navarro, M., Garcia-Verdugo, J.M., and Alvarez-Buylla, A. (2008). Neural stem cells confer unique pinwheel architecture to the ventricular surface in neurogenic regions of the adult brain. Cell Stem Cell 3, 265-278.

Monje, M.L., Mizumatsu, S., Fike, J.R., and Palmer, T.D. (2002). Irradiation induces neural precursor-cell dysfunction. Nat Med 8, 955-962.

Monje, M.L., Toda, H., and Palmer, T.D. (2003). Inflammatory blockade restores adult hippocampal neurogenesis. Science 302, 1760-1765.

Morgan, S.C., Taylor, D.L., and Pocock, J.M. (2004). Microglia release activators of neuronal proliferation mediated by activation of mitogen-activated protein kinase, phosphatidylinositol-3-kinase/Akt and delta-Notch signalling cascades. J Neurochem 90, 89-101.

Moss, J., Gebara, E., Bushong, E.A., Sanchez-Pascual, I., O'Laoi, R., El M'Ghari, I., Kocher-Braissant, J., Ellisman, M.H., and Toni, N. (2016). Fine processes of Nestin-GFP-positive radial glia-like stem cells in the adult dentate gyrus ensheathe local synapses and vasculature. Proc Natl Acad Sci U S A.

Mothet, J.P., Parent, A.T., Wolosker, H., Brady, R.O., Jr., Linden, D.J., Ferris, C.D., Rogawski, M.A., and Snyder, S.H. (2000). D-serine is an endogenous ligand for the glycine site of the N-methyl-D-aspartate receptor. Proc Natl Acad Sci U S A 97, 4926-4931.

Muller, R.U., Stead, M., and Pach, J. (1996). The hippocampus as a cognitive graph. J Gen Physiol 107, 663-694.

Murase, S., and Horwitz, A.F. (2002). Deleted in colorectal carcinoma and differentially expressed integrins mediate the directional migration of neural precursors in the rostral migratory stream. J Neurosci 22, 3568-3579.

Muth-Kohne, E., Terhag, J., Pahl, S., Werner, M., Joshi, I., and Hollmann, M. (2010). Functional excitatory GABAA receptors precede ionotropic glutamate receptors in radial glia-like neural stem cells. Mol Cell Neurosci 43, 209-221.

Nacher, J., Rosell, D.R., Alonso-Llosa, G., and McEwen, B.S. (2001). NMDA receptor antagonist treatment induces a long-lasting increase in the number of proliferating cells, PSA-NCAM-immunoreactive granule neurons and radial glia in the adult rat dentate gyrus. Eur J Neurosci 13, 512-520.

Nacher, J., Varea, E., Miguel Blasco-Ibanez, J., Gomez-Climent, M.A., Castillo-Gomez, E., Crespo, C., Martinez-Guijarro, F.J., and McEwen, B.S. (2007). N-methyl-d-aspartate receptor expression during adult neurogenesis in the rat dentate gyrus. Neuroscience 144, 855-864.

Nadel, L., and MacDonald, L. (1980). Hippocampus: cognitive map or working memory? Behav Neural Biol 29, 405-409.

Nakanishi, M., Niidome, T., Matsuda, S., Akaike, A., Kihara, T., and Sugimoto, H. (2007). Microglia-derived interleukin-6 and leukaemia inhibitory factor promote astrocytic differentiation of neural stem/progenitor cells. Eur J Neurosci 25, 649-658.

Namba, T., Maekawa, M., Yuasa, S., Kohsaka, S., and Uchino, S. (2009). The Alzheimer's disease drug memantine increases the number of radial glia-like progenitor cells in adult hippocampus. Glia 57, 1082-1090.

Ng, K.L., Li, J.D., Cheng, M.Y., Leslie, F.M., Lee, A.G., and Zhou, Q.Y. (2005). Dependence of olfactory bulb neurogenesis on prokineticin 2 signaling. Science 308, 1923-1927.

Nguyen-Ba-Charvet, K.T., Picard-Riera, N., Tessier-Lavigne, M., Baron-Van Evercooren, A., Sotelo, C., and Chedotal, A. (2004). Multiple roles for slits in the control of cell migration in the rostral migratory stream. J Neurosci 24, 1497-1506.

Nishimura, A., Ueda, S., Takeuchi, Y., Sawada, T., and Kawata, M. (1995). Age-related decrease of serotonergic fibres and S-100 beta immunoreactivity in the rat dentate gyrus. Neuroreport 6, 1445-1448.

Noctor, S.C., Flint, A.C., Weissman, T.A., Dammerman, R.S., and Kriegstein, A.R. (2001). Neurons derived from radial glial cells establish radial units in neocortex. Nature 409, 714-720.

O'Keefe, J. (1991). An allocentric spatial model for the hippocampal cognitive map. Hippocampus 1, 230-235.

Oberheim, N.A., Goldman, S.A., and Nedergaard, M. (2012). Heterogeneity of astrocytic form and function. Methods Mol Biol 814, 23-45.

Olah, M., Ping, G., De Haas, A.H., Brouwer, N., Meerlo, P., Van Der Zee, E.A., Biber, K., and Boddeke, H.W. (2009). Enhanced hippocampal neurogenesis in the absence of microglia T cell interaction and microglia activation in the murine running wheel model. Glia 57, 1046-1061.

Palmer, T.D., Markakis, E.A., Willhoite, A.R., Safar, F., and Gage, F.H. (1999). Fibroblast growth factor-2 activates a latent neurogenic program in neural stem cells from diverse regions of the adult CNS. J Neurosci 19, 8487-8497.

Palmer, T.D., Willhoite, A.R., and Gage, F.H. (2000). Vascular niche for adult hippocampal neurogenesis. J Comp Neurol 425, 479-494.

Paolicelli, R.C., Bolasco, G., Pagani, F., Maggi, L., Scianni, M., Panzanelli, P., Giustetto, M., Ferreira, T.A., Guiducci, E., Dumas, L., et al. (2011). Synaptic pruning by microglia is necessary for normal brain development. Science 333, 1456-1458.

Papouin, T., Ladepeche, L., Ruel, J., Sacchi, S., Labasque, M., Hanini, M., Groc, L., Pollegioni, L., Mothet, J.P., and Oliet, S.H. (2012). Synaptic and extrasynaptic NMDA receptors are gated by different endogenous coagonists. Cell 150, 633-646.

Paratcha, G., Ibanez, C.F., and Ledda, F. (2006). GDNF is a chemoattractant factor for neuronal precursor cells in the rostral migratory stream. Mol Cell Neurosci 31, 505-514.

Parent, J.M., Yu, T.W., Leibowitz, R.T., Geschwind, D.H., Sloviter, R.S., and Lowenstein, D.H. (1997). Dentate granule cell neurogenesis is increased by seizures and contributes to aberrant network reorganization in the adult rat hippocampus. J Neurosci 17, 3727-3738.

Patton, P.E., and McNaughton, B. (1995). Connection matrix of the hippocampal formation: I. The dentate gyrus. Hippocampus 5, 245-286.

Piatti, V.C., Esposito, M.S., and Schinder, A.F. (2006). The timing of neuronal development in adult hippocampal neurogenesis. Neuroscientist 12, 463-468.

Pompeiano, M., Palacios, J.M., and Mengod, G. (1992). Distribution and cellular localization of mRNA coding for 5-HT1A receptor in the rat brain: correlation with receptor binding. J Neurosci 12, 440-453.

Ponti, G., Crociara, P., Armentano, M., and Bonfanti, L. (2010). Adult neurogenesis without germinal layers: the "atypical" cerebellum of rabbits. Arch Ital Biol 148, 147-158.

Ramos-Mandujano, G., Hernandez-Benitez, R., and Pasantes-Morales, H. (2014). Multiple mechanisms mediate the taurine-induced proliferation of neural stem/progenitor cells from the subventricular zone of the adult mouse. Stem Cell Res 12, 690-702.

Renzel, R., Sadek, A.R., Chang, C.H., Gray, W.P., Seifert, G., and Steinhauser, C. (2013). Polarized distribution of AMPA, but not GABAA , receptors in radial glia-like cells of the adult dentate gyrus. Glia 61, 1146-1154.

Ripps, H., and Shen, W. (2012). Review: taurine: a "very essential" amino acid. Mol Vis 18, 2673-2686.

Riva, M.A., Molteni, R., Lovati, E., Fumagalli, F., Rusnati, M., and Racagni, G. (1996). Cyclic AMP-dependent regulation of fibroblast growth factor-2 messenger RNA levels in rat cortical astrocytes: comparison with fibroblast growth factor-1 and ciliary neurotrophic factor. Mol Pharmacol 49, 699-706.

Ruth, R.E., Collier, T.J., and Routtenberg, A. (1982). Topography between the entorhinal cortex and the dentate septotemporal axis in rats: I. Medial and intermediate entorhinal projecting cells. J Comp Neurol 209, 69-78.

Saghatelyan, A., de Chevigny, A., Schachner, M., and Lledo, P.M. (2004). Tenascin-R mediates activity-dependent recruitment of neuroblasts in the adult mouse forebrain. Nat Neurosci 7, 347-356.

Schaffer, S.W., Azuma, J., and Mozaffari, M. (2009). Role of antioxidant activity of taurine in diabetes. Can J Physiol Pharmacol 87, 91-99.

Schell, M.J., Molliver, M.E., and Snyder, S.H. (1995). D-serine, an endogenous synaptic modulator: localization to astrocytes and glutamate-stimulated release. Proc Natl Acad Sci U S A 92, 3948-3952.

Schmidt-Hieber, C., Jonas, P., and Bischofberger, J. (2004). Enhanced synaptic plasticity in newly generated granule cells of the adult hippocampus. Nature 429, 184-187.

Scoville, W.B., and Milner, B. (1957). Loss of recent memory after bilateral hippocampal lesions. J Neurol Neurosurg Psychiatry 20, 11-21.

Seri, B., Garcia-Verdugo, J.M., Collado-Morente, L., McEwen, B.S., and Alvarez-Buylla, A. (2004). Cell types, lineage, and architecture of the germinal zone in the adult dentate gyrus. J Comp Neurol 478, 359-378.

Seri, B., Garcia-Verdugo, J.M., McEwen, B.S., and Alvarez-Buylla, A. (2001). Astrocytes give rise to new neurons in the adult mammalian hippocampus. J Neurosci 21, 7153-7160.

Shepherd, G.M., Chen, W.R., Willhite, D., Migliore, M., and Greer, C.A. (2007). The olfactory granule cell: from classical enigma to central role in olfactory processing. Brain Res Rev 55, 373-382.

Shihabuddin, L.S., Horner, P.J., Ray, J., and Gage, F.H. (2000). Adult spinal cord stem cells generate neurons after transplantation in the adult dentate gyrus. J Neurosci 20, 8727-8735.

Shin, J., Berg, D.A., Zhu, Y., Shin, J.Y., Song, J., Bonaguidi, M.A., Enikolopov, G., Nauen, D.W., Christian, K.M., Ming, G.L., et al. (2015). Single-Cell RNA-Seq with Waterfall Reveals Molecular Cascades underlying Adult Neurogenesis. Cell Stem Cell 17, 360-372.

Shors, T.J. (2004). Memory traces of trace memories: neurogenesis, synaptogenesis and awareness. Trends Neurosci 27, 250-256.

Sierra, A., Encinas, J.M., Deudero, J.J., Chancey, J.H., Enikolopov, G., Overstreet-Wadiche, L.S., Tsirka, S.E., and Maletic-Savatic, M. (2010). Microglia shape adult hippocampal neurogenesis through apoptosis-coupled phagocytosis. Cell Stem Cell 7, 483-495.

Sierra, A., Martin-Suarez, S., Valcarcel-Martin, R., Pascual-Brazo, J., Aelvoet, S.A., Abiega, O., Deudero, J.J., Brewster, A.L., Bernales, I., Anderson, A.E., et al. (2015). Neuronal hyperactivity accelerates depletion of neural stem cells and impairs hippocampal neurogenesis. Cell Stem Cell 16, 488-503.

Snapyan, M., Lemasson, M., Brill, M.S., Blais, M., Massouh, M., Ninkovic, J., Gravel, C., Berthod, F., Gotz, M., Barker, P.A., et al. (2009). Vasculature guides migrating neuronal precursors in the adult mammalian forebrain via brain-derived neurotrophic factor signaling. J Neurosci 29, 4172-4188.

Snyder, J.S., Hong, N.S., McDonald, R.J., and Wojtowicz, J.M. (2005). A role for adult neurogenesis in spatial long-term memory. Neuroscience 130, 843-852.

Song, H., Stevens, C.F., and Gage, F.H. (2002). Astroglia induce neurogenesis from adult neural stem cells. Nature 417, 39-44.

Song, J., Zhong, C., Bonaguidi, M.A., Sun, G.J., Hsu, D., Gu, Y., Meletis, K., Huang, Z.J., Ge, S., Enikolopov, G., et al. (2012). Neuronal circuitry mechanism regulating adult quiescent neural stem-cell fate decision. Nature 489, 150-154.

Spalding, K.L., Bergmann, O., Alkass, K., Bernard, S., Salehpour, M., Huttner, H.B., Bostrom, E., Westerlund, I., Vial, C., Buchholz, B.A., et al. (2013). Dynamics of hippocampal neurogenesis in adult humans. Cell 153, 1219-1227.

Steiner, B., Klempin, F., Wang, L., Kott, M., Kettenmann, H., and Kempermann, G. (2006). Type-2 cells as link between glial and neuronal lineage in adult hippocampal neurogenesis. Glia 54, 805-814.

Stirling, D.P., Koochesfahani, K.M., Steeves, J.D., and Tetzlaff, W. (2005). Minocycline as a neuroprotective agent. Neuroscientist 11, 308-322.

Stone, J.M. (2011). Glutamatergic antipsychotic drugs: a new dawn in the treatment of schizophrenia? Ther Adv Psychopharmacol 1, 5-18.

Su, Y., Fan, W., Ma, Z., Wen, X., Wang, W., Wu, Q., and Huang, H. (2014). Taurine improves functional and histological outcomes and reduces inflammation in traumatic brain injury. Neuroscience 266, 56-65.

Suh, H., Consiglio, A., Ray, J., Sawai, T., D'Amour, K.A., and Gage, F.H. (2007). In vivo fate analysis reveals the multipotent and self-renewal capacities of Sox2+ neural stem cells in the adult hippocampus. Cell Stem Cell 1, 515-528.

Sultan, S., Gebara, E., and Toni, N. (2013a). Doxycycline increases neurogenesis and reduces microglia in the adult hippocampus. Front Neurosci 7, 131.

Sultan, S., Gebara, E.G., Moullec, K., and Toni, N. (2013b). D-serine increases adult hippocampal neurogenesis. Front Neurosci 7, 155.

Sultan, S., Li, L., Moss, J., Petrelli, F., Casse, F., Gebara, E., Lopatar, J., Pfrieger, F.W., Bezzi, P., Bischofberger, J., et al. (2015). Synaptic Integration of Adult-Born Hippocampal Neurons Is Locally Controlled by Astrocytes. Neuron 88, 957-972.

Sun, K., Chen, Y., Liang, S.Y., Liu, Z.J., Liao, W.Y., Ou, Z.B., Tu, B., and Gong, J.P. (2012). Effect of taurine on IRAK4 and NF-kappa B in Kupffer cells from rat liver grafts after ischemia-reperfusion injury. Am J Surg 204, 389-395.

Tashiro, A., Makino, H., and Gage, F.H. (2007). Experience-specific functional modification of the dentate gyrus through adult neurogenesis: a critical period during an immature stage. J Neurosci 27, 3252-3259.

Tashiro, A., Sandler, V.M., Toni, N., Zhao, C., and Gage, F.H. (2006). NMDA-receptor-mediated, cell-specific integration of new neurons in adult dentate gyrus. Nature 442, 929-933.

Tavazoie, M., Van der Veken, L., Silva-Vargas, V., Louissaint, M., Colonna, L., Zaidi, B., Garcia-Verdugo, J.M., and Doetsch, F. (2008). A specialized vascular niche for adult neural stem cells. Cell Stem Cell 3, 279-288.

Toni, N., Laplagne, D.A., Zhao, C., Lombardi, G., Ribak, C.E., Gage, F.H., and Schinder, A.F. (2008). Neurons born in the adult dentate gyrus form functional synapses with target cells. Nat Neurosci 11, 901-907.

Toni, N., Teng, E.M., Bushong, E.A., Aimone, J.B., Zhao, C., Consiglio, A., van Praag, H., Martone, M.E., Ellisman, M.H., and Gage, F.H. (2007). Synapse formation on neurons born in the adult hippocampus. Nat Neurosci 10, 727-734.

Tozuka, Y., Fukuda, S., Namba, T., Seki, T., and Hisatsune, T. (2005). GABAergic excitation promotes neuronal differentiation in adult hippocampal progenitor cells. Neuron 47, 803-815.

Tremblay, M.E., Stevens, B., Sierra, A., Wake, H., Bessis, A., and Nimmerjahn, A. (2011). The role of microglia in the healthy brain. J Neurosci 31, 16064-16069.

Turpin, F.R., Potier, B., Dulong, J.R., Sinet, P.M., Alliot, J., Oliet, S.H., Dutar, P., Epelbaum, J., Mothet, J.P., and Billard, J.M. (2011). Reduced serine racemase expression contributes to age-related deficits in hippocampal cognitive function. Neurobiol Aging 32, 1495-1504.

Ueda, S., Sakakibara, S., and Yoshimoto, K. (2005). Effect of long-lasting serotonin depletion on environmental enrichment-induced neurogenesis in adult rat hippocampus and spatial learning. Neuroscience 135, 395-402.

Vallieres, L., Campbell, I.L., Gage, F.H., and Sawchenko, P.E. (2002). Reduced hippocampal neurogenesis in adult transgenic mice with chronic astrocytic production of interleukin-6. J Neurosci 22, 486-492.

van Praag, H., Christie, B.R., Sejnowski, T.J., and Gage, F.H. (1999). Running enhances neurogenesis, learning, and long-term potentiation in mice. Proc Natl Acad Sci U S A 96, 13427-13431.

van Praag, H., Schinder, A.F., Christie, B.R., Toni, N., Palmer, T.D., and Gage, F.H. (2002). Functional neurogenesis in the adult hippocampus. Nature 415, 1030-1034.

van Praag, H., Shubert, T., Zhao, C., and Gage, F.H. (2005). Exercise enhances learning and hippocampal neurogenesis in aged mice. J Neurosci 25, 8680-8685.

Villeda, S.A., Luo, J., Mosher, K.I., Zou, B., Britschgi, M., Bieri, G., Stan, T.M., Fainberg, N., Ding, Z., Eggel, A., et al. (2011). The ageing systemic milieu negatively regulates neurogenesis and cognitive function. Nature 477, 90-94.

Vukovic, J., Colditz, M.J., Blackmore, D.G., Ruitenberg, M.J., and Bartlett, P.F. (2012). Microglia modulate hippocampal neural precursor activity in response to exercise and aging. J Neurosci 32, 6435-6443.

Walton, N.M., Sutter, B.M., Laywell, E.D., Levkoff, L.H., Kearns, S.M., Marshall, G.P., 2nd, Scheffler, B., and Steindler, D.A. (2006). Microglia instruct subventricular zone neurogenesis. Glia 54, 815-825.

Wang, J.W., David, D.J., Monckton, J.E., Battaglia, F., and Hen, R. (2008). Chronic fluoxetine stimulates maturation and synaptic plasticity of adult-born hippocampal granule cells. J Neurosci 28, 1374-1384.

Wang, L.P., Kempermann, G., and Kettenmann, H. (2005). A subpopulation of precursor cells in the mouse dentate gyrus receives synaptic GABAergic input. Mol Cell Neurosci 29, 181-189.

Wichterle, H., Garcia-Verdugo, J.M., Herrera, D.G., and Alvarez-Buylla, A. (1999). Young neurons from medial ganglionic eminence disperse in adult and embryonic brain. Nat Neurosci 2, 461-466.

Winner, B., Cooper-Kuhn, C.M., Aigner, R., Winkler, J., and Kuhn, H.G. (2002). Long-term survival and cell death of newly generated neurons in the adult rat olfactory bulb. Eur J Neurosci 16, 1681-1689.

Witter, M.P. (2007). The perforant path: projections from the entorhinal cortex to the dentate gyrus. Prog Brain Res 163, 43-61.

Wittko, I.M., Schanzer, A., Kuzmichev, A., Schneider, F.T., Shibuya, M., Raab, S., and Plate, K.H. (2009). VEGFR-1 regulates adult olfactory bulb neurogenesis and migration of neural progenitors in the rostral migratory stream in vivo. J Neurosci 29, 8704-8714.

Wolosker, H., Blackshaw, S., and Snyder, S.H. (1999). Serine racemase: a glial enzyme synthesizing D-serine to regulate glutamate-N-methyl-D-aspartate neurotransmission. Proc Natl Acad Sci U S A 96, 13409-13414.

Wu, G., Matsuwaki, T., Tanaka, Y., Yamanouchi, K., Hu, J., and Nishihara, M. (2013). Taurine counteracts the suppressive effect of lipopolysaccharide on neurogenesis in the hippocampus of rats. Adv Exp Med Biol 775, 111-119.

Wu, H., Jin, Y., Wei, J., Jin, H., Sha, D., and Wu, J.Y. (2005). Mode of action of taurine as a neuroprotector. Brain Res 1038, 123-131.

Wu, J.Y., Tang, X.W., and Tsai, W.H. (1992). Taurine receptor: kinetic analysis and pharmacological studies. Adv Exp Med Biol 315, 263-268.

Yang, J., Li, M.X., Luo, Y., Chen, T., Liu, J., Fang, P., Jiang, B., Hu, Z.L., Jin, Y., Chen, J.G., et al. (2013). Chronic ceftriaxone treatment rescues hippocampal memory deficit in AQP4 knockout mice via activation of GLT-1. Neuropharmacology 75, 213-222.

Yoon, S.Y., Patel, D., and Dougherty, P.M. (2012). Minocycline blocks lipopolysaccharide induced hyperalgesia by suppression of microglia but not astrocytes. Neuroscience 221, 214-224.

Zhao, C., Teng, E.M., Summers, R.G., Jr., Ming, G.L., and Gage, F.H. (2006). Distinct morphological stages of dentate granule neuron maturation in the adult mouse hippocampus. J Neurosci 26, 3-11.

Zhao, J., Peng, Y., Xu, Z., Chen, R.Q., Gu, Q.H., Chen, Z., and Lu, W. (2008). Synaptic metaplasticity through NMDA receptor lateral diffusion. J Neurosci 28, 3060-3070.

Ziv, Y., Avidan, H., Pluchino, S., Martino, G., and Schwartz, M. (2006a). Synergy between immune cells and adult neural stem/progenitor cells promotes functional recovery from spinal cord injury. Proc Natl Acad Sci U S A 103, 13174-13179.

Ziv, Y., Ron, N., Butovsky, O., Landa, G., Sudai, E., Greenberg, N., Cohen, H., Kipnis, J., and Schwartz, M. (2006b). Immune cells contribute to the maintenance of neurogenesis and spatial learning abilities in adulthood. Nat Neurosci 9, 268-275.

APPENDICES

A1

Heterogeneity of Radial Glia-Like Cells in the Adult Hippocampus

STEM CELLS®

TISSUE-SPECIFIC STEM CELLS

Heterogeneity of Radial Glia-Like Cells in the Adult Hippocampus

ELIAS GEBARA,[a] MICHAEL ANTHONY BONAGUIDI,[b] RUTH BECKERVORDERSANDFORTH,[c] SÉBASTIEN SULTAN,[a] FLORIAN UDRY,[a] PIETER-JAN GIJS,[a] DIETER CHICHUNG LIE,[c] GUO-LI MING,[b,d,e] HONGJUN SONG,[b,d,e] NICOLAS TONI[a]

Key Words. Adult stem cells • Nervous system • Neural stem cell • Somatic stem cells • Stem cell-microenvironment interactions

[a]Department of Fundamental Neuroscience, University of Lausanne, rue du Bugnon, Lausanne, Switzerland; [b]Institute for Cell Engineering, [d]Department of Neurology, [e]The Solomon Snyder Department of Neuroscience, Johns Hopkins University School of Medicine, Baltimore, Maryland, USA; [c]Institute of Biochemistry, Friedrich-Alexander Universität, Erlangen-Nürnberg, Fahrstrasse, Erlangen, Germany

Correspondence: Nicolas Toni, Ph.D., 9, rue du Bugnon, 1005 Lausanne, Switzerland. Telephone: 4121-692-5133; Fax: 4121-692-5105; e-mail: Nicolas.toni@unil.ch

Received July 3, 2015; accepted for publication November 8, 2015; first published online in STEM CELLS *EXPRESS* Month 00, 2015.

1066-5099/2016/$30.00/0

http://dx.doi.org/10.1002/stem.2266

ABSTRACT

Adult neurogenesis is tightly regulated by the neurogenic niche. Cellular contacts between niche cells and neural stem cells are hypothesized to regulate stem cell proliferation or lineage choice. However, the structure of adult neural stem cells and the contact they form with niche cells are poorly described. Here, we characterized the morphology of radial glia-like (RGL) cells, their molecular identity, proliferative activity, and fate determination in the adult mouse hippocampus. We found the coexistence of two morphotypes of cells with prototypical morphological characteristics of RGL stem cells: Type α cells, which represented 76% of all RGL cells, displayed a long primary process modestly branching into the molecular layer and type β cells, which represented 24% of all RGL cells, with a shorter radial process highly branching into the outer granule cell layer-inner molecular layer border. Stem cell markers were expressed in type α cells and coexpressed with astrocytic markers in type β cells. Consistently, in vivo lineage tracing indicated that type α cells can give rise to neurons, astrocytes, and type β cells, whereas type β cells do not proliferate. Our results reveal that the adult subgranular zone of the dentate gyrus harbors two functionally different RGL cells, which can be distinguished by simple morphological criteria, supporting a morphofunctional role of their thin cellular processes. Type β cells may represent an intermediate state in the transformation of type α, RGL stem cells, into astrocytes. STEM CELLS *2016; 00:000—000*

SIGNIFICANCE STATEMENT

Adult neurogenesis results in the formation of new neurons that play a role in learning and memory. The morphology of adult neural stem cells (ANSC) residing in the hippocampus is still poorly-described. The assessment of ANSC is usually performed using morphological criteria. Here, we discovered that ANSC are intermingled with cells of similar morphology but devoid of proliferative properties. These cells display hallmarks of immature astrocytes and are generated by ANSC, suggesting that they represent intermediates in the ANSC-astrocyte transition. Our results are relevant to the process of adult neurogenesis and will refine the assessment of ANSC status in vivo.

INTRODUCTION

The adult mammalian brain retains neural stem cells in two discrete areas, the subventricular zone and dentate gyrus of the hippocampus [1, 2]. Increasing evidence suggests that upon maturation, new neurons are involved in mechanisms of learning and indeed, the stimulation of adult hippocampal neurogenesis increases learning and memory performances [3, 4]. Thus, mechanisms involved in the regulation of adult neurogenesis are of great interest for our understanding of learning and memory and for the potential treatment of memory impairment.

In the hippocampus, adult neural stem cells reside in the subgranular zone (SGZ) of the dentate gyrus and may display a radial glia-like (RGL) morphology. They are characterized by a long process that extends through the granule cell layer (GCL) and widely branches in the outer GCL and in the inner third of the molecular layer [5–8]. Adult neural stem cells in the SGZ may also display shorter, horizontal processes [9, 10] greater proliferative activity than RGL stem cells [11], suggesting the existence of a morphofunctional component in the regulation of quiescence.

During embryonic development, time-lapse imaging showed that RGL stem cells generate neurons which use their parent cell's radial process to migrate to the cortical plate, a mechanism that may underlie the radial organization of the neocortex [12]. In adult neurogenesis, however, the function of the radial process in RGL stem cells is not clearly defined. Although the primary process is often seen alongside dendrites from nascent neurons [13], it is unclear whether it is used for the migration of the newborn neurons or for establishing contacts with the neurogenic niche. Furthermore, clonal analysis suggested that newly formed neurons in the adult hippocampus migrate away from their parent cells [14] and may use the vasculature for a tangential migration [15]. Thus, a potential function of the radial processes of adult RGL stem cells may rather be found in regulating their proliferation or fate through interactions with the local niche [16].

The direct cellular environment of neural stem cells plays a fundamental role in the regulation of adult neurogenesis. Indeed, although proliferating cells reside in the entire central nervous system, adult neurogenesis is restricted to the hippocampus and the subventricular zone. However, when transplanted in the hippocampus, progenitor cells from a non-neurogenic area such as the spinal cord regain the ability to generate neurons and inversely, when transplanted in a non-neurogenic area, hippocampal neural stem cells lose their ability to differentiate into neurons [17]. This indicates that the intrinsic neurogenic potential of central nervous system progenitor cells is controlled by the neurogenic niche.

Several cell types of the neurogenic niche have been shown to play a role in the regulation of the neural stem cell proliferation, including endothelial cells [18], astrocytes [19, 20], neurons [21], or microglia [22, 23]. The effect of niche cells on stem cells may be mediated by the release of soluble molecules such as Wnt3a [19] or GABA [21] or by direct contact such as with microglia [23] or astrocytes [24]. These observations suggest that the complex morphology of RGL stem cells enables the establishment of numerous contacts with a variety of cell types of the hilus, GCL, and molecular layer of the dentate gyrus, all of which may participate to its regulation.

The morphology of the RGL stem cells is still poorly described and in particular, it is still unknown whether there is a structure–function relationship among the population of this highly morphologically variable population of cells. The goal of this study is to examine the fine structure of RGL stem cells in the adult hippocampal niche and to test the possibility that the morphological characteristics of RGL stem cells may reflect their function.

Materials and Methods

Ethics Statement

This study was carried out in strict accordance with the recommendations in the Guidance for the Care and Use of Laboratory Animals of the National Institutes of Health. All experimental protocols were approved by the Swiss animal experimentation authorities (Service de la consommation et des affaires vétérinaires, Chemin des Boveresses 155, 1066 Epalinges, Switzerland). Every effort was made to minimize the number of animals used and their suffering.

Experimental Animals

Animals used for this study were adult male mice. *GFAP*-green fluorescent protein (GFP) mice were a kind gift from the laboratory of Helmut Kettenmann (Max-Delbruck center, Berlin, Germany) [25]. They express the GFP under the control of the human glial fibrillary acidic protein (GFAP) promoter. *Nestin*-GFP mice were a kind gift from the laboratory of K. Mori (PRESTO, Kyoto, Japan) [26]. These mice express the GFP under the stem cell-specific promoter Nestin. *Nestin*::CreER^{T2} and Z/EG$^{f/+}$ mice were purchased from The Jackson Laboratory (Maine, Bar Harbor, ME, USA, www.jax.org). The Rosa26tdTomato reporter mice [27] were a kind gift from the laboratory of Jean-Yves Chatton (Department of Fundamental Neurosciences, University of Lausanne, Switzerland). The *GFAP*::CreER^{T2}-Rosa YFP were a kind gift from the laboratory of Andrea Volterra (Department of Fundamental Neurosciences, University of Lausanne, Switzerland).

For clonal analysis, we used the *GFAP*::CreER^{T2} and the *Nestin*::CreER^{T2} mice. The *Nestin*::CreER^{T2} mice were crossed with fluorescent reporter mice Rosa-tdTomato or Z/EG$^{f/+}$. Tamoxifen (62 mg/ml; Sigma-Aldrich, Buchs, Switzerland www.sigmaaldrich.com; T5648) was prepared in a 5:1 ratio of corn oil to ethanol at 37 °C with occasional vortexing. A single tamoxifen or vehicle dose was injected into 8–10 weeks old mice (62 mg/kg intraperitoneally [i.p.]) for *Nestin*::CreER^{T2}-Z/EG$^{f/+}$ mice, 60 mg/kg for *Nestin*::CreER^{T2}-Rosa26tdtomato mice, or 86 mg/kg for the *GFAP*::CreER^{T2}-RosaYFP mice.

For exercise and aging experiments, young adult mice were 6-week-old and aged mice were 7.5-month-old at the beginning of the experiment. Runner mice were housed for 2 weeks in standard cages with free access to a running wheel (Fast-Trac; Bio-Serv). Non-runner mice were housed in similar, adjacent cages without running wheel. All mice were housed in a 12-hour light/dark cycle and controlled temperature of 22 °C. Food and water were available ad libitum.

BrdU and D-Serine Administration

All mice were injected i.p. with the thymidine analog bromodeoxyuridine (BrdU, Sigma-Aldrich, Buchs, Switzerland, www.sigmaaldrich.com), at doses of 100 mg/kg in saline. D-Serine was prepared fresh every day and diluted in water containing 0.9% NaCl. Seven-week-old mice were injected i.p. every day with 50 mg/kg of D-serine (Sigma-Aldrich, Buchs, Switzerland, www.sigmaaldrich.com) for 8 consecutive days or with the same volume of vehicle (0.9% NaCl in water).

Tissue Collection and Preparation

At the end of the experiment, mice received a lethal dose of pentobarbital (10 ml/kg, Sigma-Aldrich, Buchs, Switzerland, www.sigmaaldrich.com) and were perfusion-fixed with 50 ml of 0.9% saline followed by 100 ml of 4% paraformaldehyde (Sigma-Aldrich, Switzerland, www.sigmaaldrich.com) dissolved in phosphate buffer saline (PBS 0.1M, pH 7.4). Brains were then collected, postfixed overnight at 4 °C, cryoprotected 24 hours in 30% sucrose, and rapidly frozen. Coronal frozen sections of a thickness of 40 μm (50 μm for clonal analysis) were cut with a microtome-cryostat (Leica MC 3050S) and slices were kept in cryoprotectant (30% ethylene glycol and 25% glycerin in 1X PBS) at −20 °C until processed for immunostaining.

Immunohistochemistry

Immunochemistry was performed on 1-in-6 series of section. Sections were washed three times in PBS 0.1 M. BrdU detection required a DNA denaturation for 20 minutes in 2 M HCl at 37 °C and rinsed in 0.1 M borate buffer pH 8.5 for 15 minutes. Then, slices were incubated in blocking solution containing 0.3% Triton-X100 and 15% normal serum (normal goat serum (Gibco) or normal donkey serum (Sigma Aldrich, Buchs, Switzerland, www.sigmaaldrich.com depending on the secondary antibody) in PBS 0.1 M. Slices were then incubated 40 hours at 4 °C with the following primary antibodies: Chicken anti-GFP (1:500, AnaSpec Inc, Liege, Belgium, www.anaspec.com), Rabbit anti-GFP (1:500, AnaSpec Inc, Liege, Belgium, www.anaspec.com), mouse monoclonal anti-BrdU (1:250, Chemicon International, Schaffausen, Switzerland, www.merckmillipore.com), rabbit anti-K-i67 (1:200, Abcam, Cambridge, UK, www.abcam.com), rabbit anti-Sox1 (1:500, Abcam, Cambridge, UK, www.abcam.com), rabbit anti-GFAP (1:500, Invitrogen), goat anti-Iba1 (1:200, Abcam, Cambridge, UK, www.abcam.com), rabbit anti-Sox2 (1:500, Millipore, Schaffausen, Switzerland, www.merckmillipore.com), rabbit anti-NG2 (1:400, Chemicon, Schaffausen, Switzerland, www.merckmillipore.com) mouse anti-CD133 (Prominin 1, 1:500, Millipore, Schaffausen, Switzerland, www.merckmillipore.com), mouse anti-Nestin (1:200, Millipore, Schaffausen, Switzerland, www.merckmillipore.com), rabbit anti-S100B (1:500, Abcam, Cambridge, UK, www.abcam.com), rabbit anti-GLT1 (1:500, Abcam, Cambridge, UK, www.abcam.com). The sections were then incubated for 2 hours in either of the following secondary antibodies: Dylight 488 goat anti-chicken (1:500, Jackson ImmunoResearch, Newmarket, UK, www.jieurope.com), goat anti-rabbit Alexa-488 (1:250, Invitrogen, Zug, Switzerland, www.thermofischer.com) goat anti-mouse Alexa-594 (1:250, Invitrogen, Zug, Switzerland, www.thermofischer.com), goat anti-rabbit Alexa-594 (1:250, Invitrogen, Zug, Switzerland, www.thermofischer.com), donkey anti-goat Alexa-555 (1:250, Invitrogen, Zug, Switzerland, www.thermofischer.com), and donkey anti-rabbit Alexa 647 (1:250, Invitrogen, Zug, Switzerland, www.thermofischer.com). Blood vessels were labeled by Sulforhodamine 101 (Invitrogen, Zug, Switzerland, www.thermofischer.com). 4,6-Diamidino-2-phenylindole (DAPI) was used to reveal nuclei.

Image Analysis

Images were collected with a Zeiss confocal microscope (Zeiss LSM 710 Quasar Carl Zeiss, Oberkochen, Germany, www.zeiss.com) and cell counts were performed using stereology principles, as described previously [28]. Briefly, for each animal, a 1-in-6 series of section between −1.3 to −2.9 mm from the Bregma was stained with the nucleus marker DAPI and used to measure the volume of the GCL. The granule cell area was traced using Axiovision (Zeiss, Oberkochen, Germany, www.zeiss.com) software and the granule cell reference volume was determined by multiplying the area of the GCL by the distance between the sections sampled (240 μm). All cells were counted in the entire thickness of the sections in a 1-in-6 series of section (240 μm apart) with a 40 × objective. All cells were counted blind with regard to the mouse status. The number of immunolabeled cells was then related to GCL sectional volume and multiplied by the reference volume to estimate the total number of immunolabeled cells. RGL cells were counted in the SGZ of the dentate gyrus.

Clones were analyzed as described in Bonaguidi et al. [14]. Briefly, the tamoxifen dose was calibrated for each mouse line, so as to obtain a maximum of four clones per hippocampus. Clonal relation was then assessed within a distance of 150 μm from the type α RGL cell. Since progenies do not migrate more than 125 μm from the mother cell (as observed 2 months after tamoxifen injection in Bonaguidi et al. [14], Fig. 1F), this distance is sufficient to guarantee more than 90% probability as a clone.

Statistical Analysis

Hypothesis testing was two-tailed. All analyses were performed using JMP10 software. First, Shapiro-Wilk tests were performed on each group of data to test for distribution normality. For normal distribution we performed parametric tests. When the distribution was not normal, a nonparametric Kruskal-Wallis test was used. Homoscedasticity of variances was tested by Bartlett's test and adequate analysis of variance was performed, followed by a post hoc multiple comparisons procedure *t* test with Bonferonni correction. For two sample comparisons, when the distribution was normal, the equality of variances of the groups was tested by a bilateral F-test and the adequate unpaired *t* test was used. All data are presented as mean ± SEM.

Results

Morphometry Identifies Two Subtypes of RGL Cells with Distinct Molecular Marker Expression

RGL cells were identified using two common transgenic mouse lines: the *GFAP*-GFP mice [25] and the *Nestin*-GFP mice [26]. In these mice, the GFP is expressed under the control of the human *GFAP* promoter or the *Nestin* promoter, respectively. At 8 weeks of age, mice were prepared for histology and immunostaining against GFP was used to amplify the fluorescent signal. In both mice, GFP^+ RGL cells displayed a prototypical morphology, including a nucleus located in the SGZ of the DG, a radial process extending through the GCL and extensively branching into the outer GCL and the molecular layer and a few basal processes extending towards the hilus [5–8] (Fig. 1A).

We measured the following parameters in 2472 *GFAP*-GFP^+ and 1150 *Nestin*-GFP^+ RGL cells: position of the soma relative to the basal limit of the GCL, length of the primary process, number of secondary branches stemming from the primary process, projected surface of the territory encompassed by the whole cell or only by the secondary apical arbor, and maximal width of the territory covered by the apical arbor (Fig. 1; Supporting Information Fig. 1A). On average, the soma of RGL cells was found within 3.83 ± 0.07 μm of the base of the GCL. The length of their primary radial process was 75.82 ± 0.34 μm; the main process had 4.11 ± 0.03 branches; the secondary dendritic tree had a width of 25.14 ± 0.11 μm, covered a projected surface of 569.51 ± 36.83 μm^2 and the whole cell covered a surface area of 1485.75 ± 17.99 μm^2. There was no interstrain difference in the morphology of RGL cells, indicating that these parameters did not depend on the genetic background or the reporter, but rather reflected common features of RGL cells. Notably, there was a great variation in both the length and the width among RGL cells, which defined two distinct populations: a first group of cells, which we named type α, represented 75.46% of all RGL cells (73.8% in *Nestin*-GFP

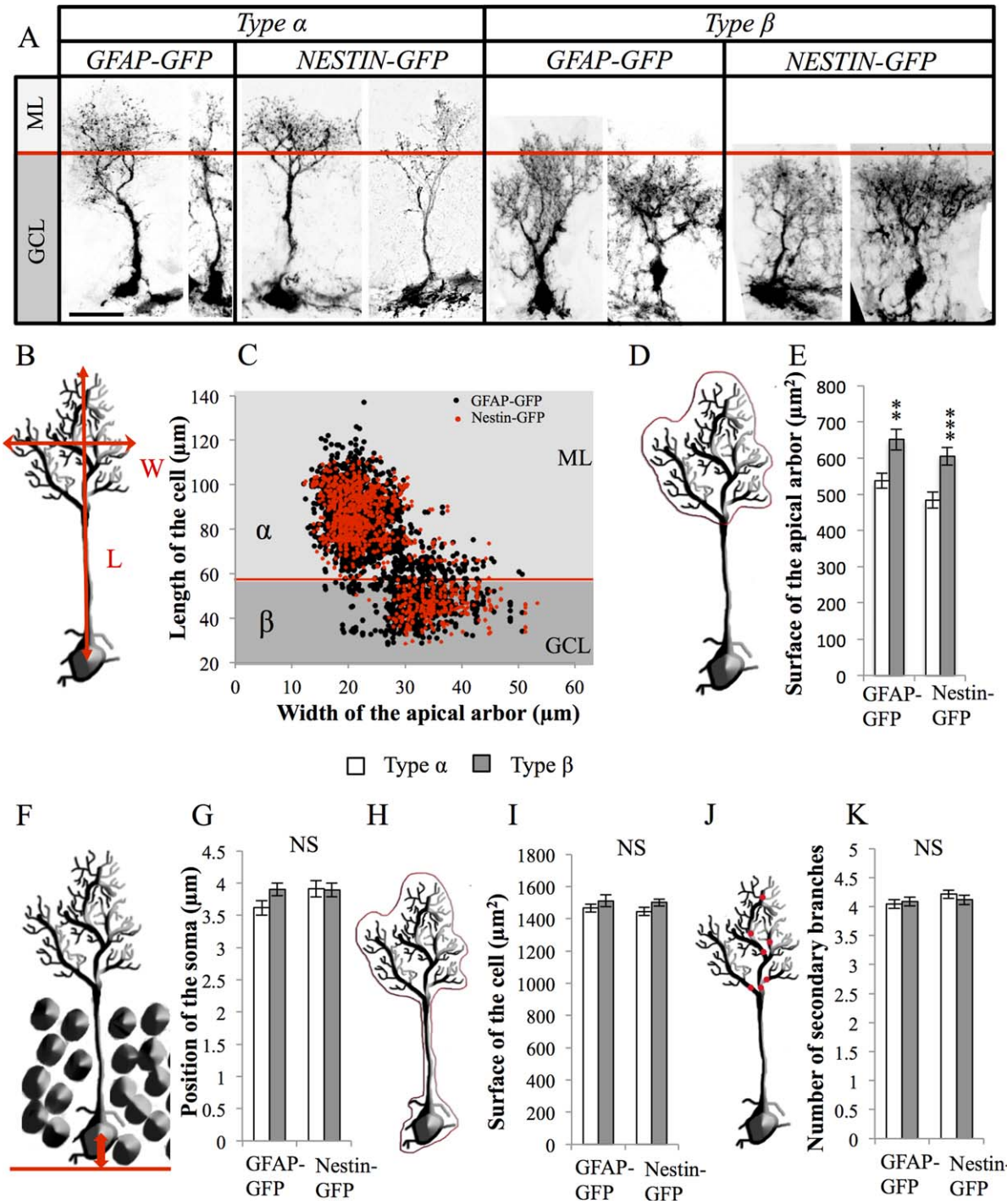

Figure 1. Morphometrical parameters of radial glia-like (RGL) cells. **(A)**: Confocal maximal projection micrographs of types α and β RGL cells in glial fibrillary acidic protein (*GFAP*)-green fluorescent protein (GFP) and *Nestin*-GFP mice. **(B)**: Drawing of a RGL neural stem cell illustrating the measurements of length and width of the cell. **(C)**: Scatter graph of all RGL cells analyzed morphometrically ($n = 2472$ for *GFAP*-GFP mice and $n = 1150$ for *Nestin*-GFP mice). **(D, E)**: Schematic illustration **(D)** and histogram **(E)** of the projected surface of the dendritic arbor of secondary processes in types α and β cells. **(F, G)**: Schematic illustration **(F)** and histogram **(G)** of the position of the soma of type α and the type β cells relative to the hilar border of the granule cell layer. **(H, I)**: Schematic illustration **(H)** and histogram **(I)** of the total surface of types α and β cells. **(J, K)**: Drawing **(J)** and histogram **(K)** of the number of branches of the main process of types α and β cells. Scale bar: 20 μm. Bilateral Student's t test **, $p < 0.01$; ***, $p < 0.001$. Each value represents the mean ± SEM. Abbreviations: GCL, granule cell layer; GFAP, glial fibrillary acidic protein; GFP, green fluorescent protein; ML, molecular layer.

mice and 76.2% in *GFAP*-GFP mice). They displayed a long radial process and a narrow arbor of secondary processes, which extended beyond the GCL, into the first third of the molecular layer. In contrast, a second group of cells named type β, which represented 24.54% of all RGL cells (26.2% in *Nestin*-GFP mice and 23.8% in *GFAP*-GFP mice), displayed a short primary process (shorter than 58 µm) and a broad arbor of secondary processes, most of which did not extend

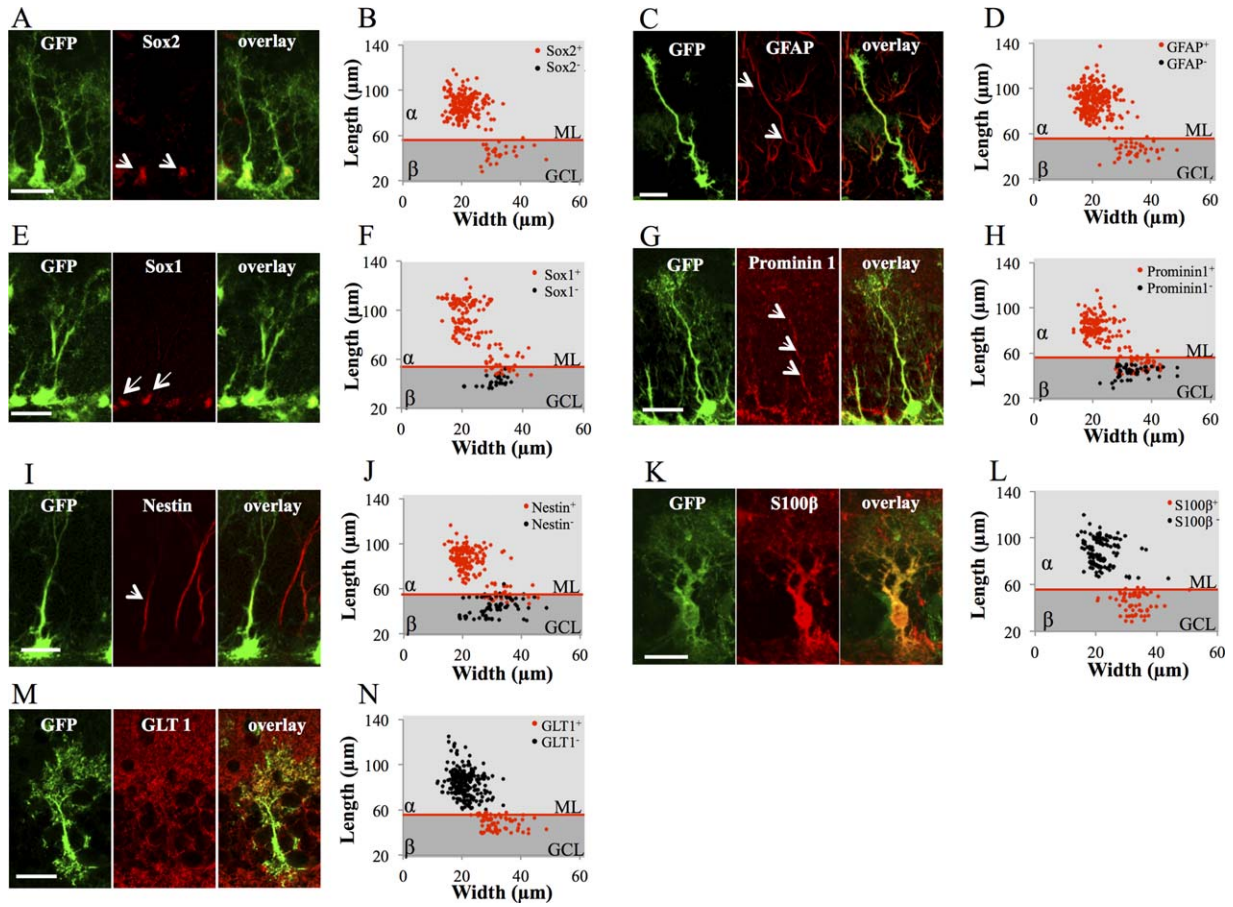

Figure 2. Molecular marker expression of type α and type β cells. **(A)**: Confocal maximal projection micrographs of glial fibrillary acidic protein (*GFAP*)-green fluorescent protein (GFP) radial glia-like (RGL) cells (green), immunostained for Sox2. **(B)** Scatter graphs representing the dimensions of RGL cells immunostained for Sox2. **(C)**: Confocal maximal projection micrographs of *GFAP*-GFP RGL cells (green), immunostained for GFAP. **(D)**: Scatter graphs representing the dimensions of RGL cells immunostained for GFAP. **(E)**: Confocal maximal projection micrographs of *GFAP*-GFP RGL cells (green), immunostained for Sox1. **(F)**: Scatter graphs representing the dimensions of RGL cells immunostained for Sox1. **(G)**: Confocal maximal projection micrographs of *GFAP*-GFP RGL cells (green), immunostained for Prominin1. **(H)**: Scatter graphs representing the dimensions of RGL cells immunostained for Prominin1. **(I)**: Confocal maximal projection micrographs of *GFAP*-GFP RGL cells (green), immunostained for Nestin. **(J)**: Scatter graphs representing the dimensions of RGL cells immunostained for Nestin. **(K)**: Confocal maximal projection micrographs of *GFAP*-GFP RGL cells (green), immunostained for S100β. **(L)**: Scatter graphs representing the dimensions of RGL cells immunostained for S100β. **(M)**: Confocal maximal projection micrographs of *GFAP*-GFP RGL cells (green), immunostained for GLT1. **(N)**: Scatter graphs representing the dimensions of RGL cells immunostained for GLT1. Scale bars = 20 μm. Abbreviations: GCL, granule cell layer; GFAP, glial fibrillary acidic protein; GFP, green fluorescent protein; ML, molecular layer.

beyond the limit of the GCL (Fig. 1A–1C). Due to their broader arbor of processes, type β cells displayed an increased projected surface of their apical arbor (Fig. 1D–1E). Types α and β cells were, however, similar in all other morphological criteria observed, regardless of the reporter mouse used to examine their morphology (Fig. 1F–1K). Thus, RGL cells are morphologically heterogeneous and are composed of two major morphotypes that can be clearly identified by the length of the primary process and the width of the arbor formed by the secondary processes.

We next examined the molecular identity of these two morphotypes using immunohistochemistry (Fig. 2; Supporting Information Fig. 1B). Types α and β cells expressed the neural stem cell markers GFAP and Sox2. However, although the stem cell markers Sox1, Prominin 1, and Nestin were expressed in 100% of type α cells, they were only expressed in a fraction of type β cells (49%, 32%, and 18%, respectively). Inversely, the astrocyte-specific glutamate transporter GLT1 and calcium binding protein S100β were expressed by all and virtually only type β cells. This indicates that a fraction of β cells coexpressed astrocytes-specific (GLT1, S100β) and stem cell-specific markers (Prominin1, Nestin, and Sox1). Intriguingly, the morphology of type β cells expressing Sox1, Prominin1, or Nestin was different than from immunonegative type β cells: Sox1, Prominin1, and Nestin were present in the cells with the longest processes, indicating that the length of the process was associated with a "stem-like" molecular identity of these cells (Fig. 2E–2J).

Thus, types α and β cells can be characterized by morphology and molecular markers: While type α cells extend processes well into the molecular layer and express stem cell markers such as Sox2, Sox1, Nestin, GFAP, and Prominin1, type β cells are restricted into the GCL and express S100β and GLT1, accompanied by Prominin1, Sox1, and Nestin for the longest cells.

Cellular Contacts with Niche Cells

The morphological differences between types α and β cells may enable them to interact with distinct niche cells which, in turn, may underlie different regulation mechanisms of their

activity. To examine the contacts between RGL cells and their cellular environment, as well as their relevance to proliferation, we examined mice in standard housing conditions and in cages containing a running wheel, a condition of voluntary exercise known to increase proliferation [4] (Fig. 3). After 2 weeks of exposure to a running wheel (or the same housing

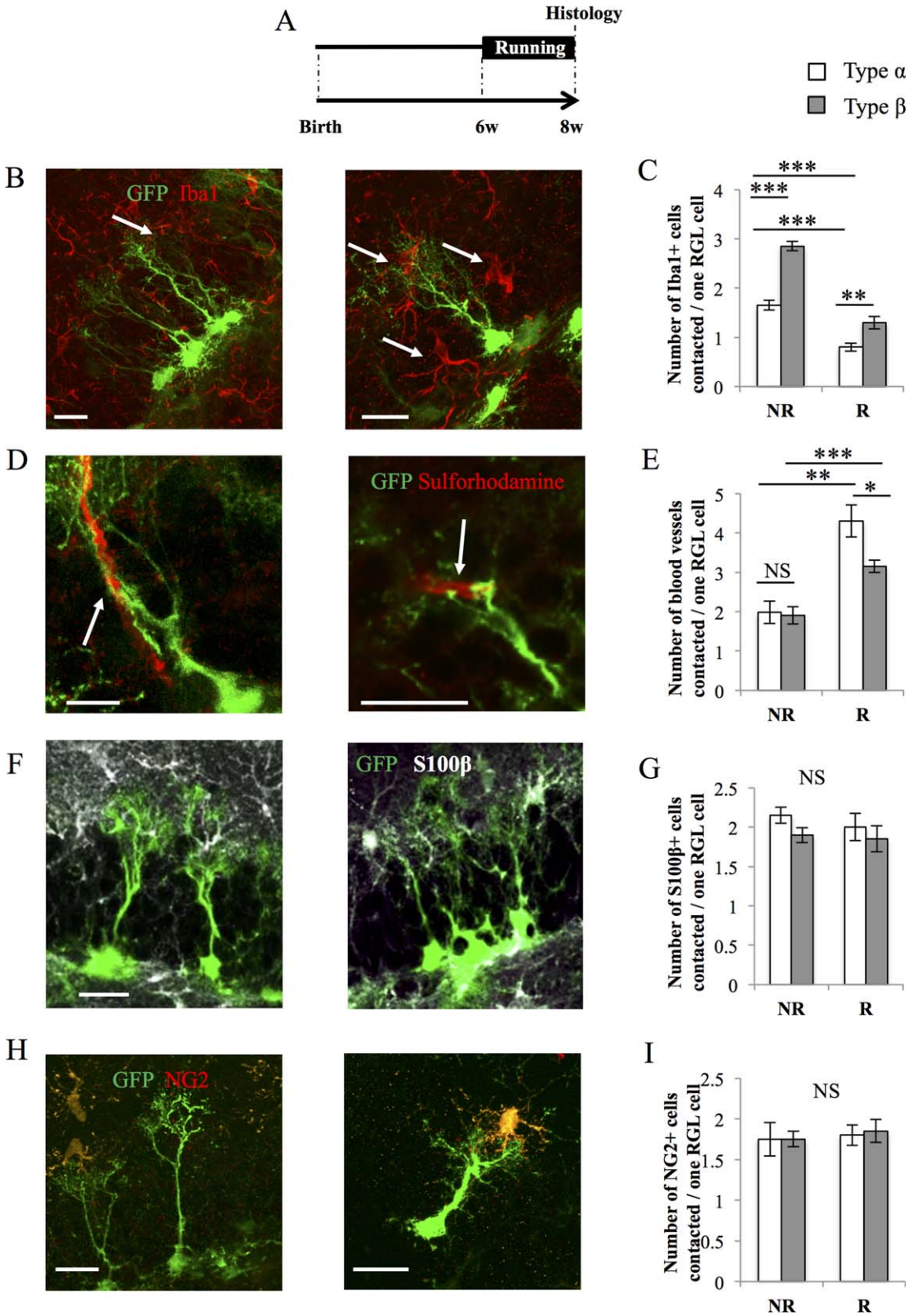

Figure 3.

cage without a running wheel), all mice were killed and immunohistochemistry was used to identify microglia (Iba1), astrocytes (S100β), and oligodendrocyte progenitor cells (NG2). Sulforhodamine 101 was used to identify blood vessels.

Under basal housing conditions (NR), individual RGL cell types contacted on average 2 blood vessels, 2.5 astrocytes, and 1.7 oligodendrocyte precursors, independently of their morphotype. In contrast, type β cells contacted significantly more microglia cells (2.8 microglia per type β cell) than by type α cells (1.6 microglia per type α cell, Fig. 3B–3I). The majority of the contacts with microglia occurred on the main process or the secondary processes of RGL cells, but no contact was observed on the soma (Fig. 3B). In running conditions (R), both types α and β cells contacted fewer microglia and more blood vessels than in nonrunning conditions. To test whether running affected RGL cells or niche cells, we examined the morphology of niche cells in running conditions. Consistent with our previous observations [22], running decreased the number of Iba1-expressing microglia, but increased the size of their territory and the number of branches (Supporting Information Fig. 2A–2C). Inversely, running increased the number and/or the size of blood vessels in the dentate gyrus, as reflected by increased number of pixels labeled by Sulforhodamine 101 (Supporting Information Fig. 2D–2F).

These results indicate that type β cells preferentially contacted microglia and that voluntary running increased the number of blood vessels and decreased the number of microglia, therefore, interfering with the contacts between types α and β cells with the niche.

Types α and β Cells Respond Differently to Proproliferative Stimuli

The proliferation of adult neural stem/progenitor cells is regulated by external stimuli and is increased by voluntary running [4] and decreases with aging [29]. To examine whether these conditions affected the number or the morphology of types α and β cells, 16 *GFAP*-GFP mice were divided in four experimental groups: young adult mice (8 weeks of age; Y) and older mice (8 months of age; O), that were housed individually in standard cages in presence (R) or absence (NR) of a running wheel for 2 weeks (Fig. 4A, 4 mice per group). The total number of RGL cells was significantly decreased by aging and increased by running (Fig. 4B, 4E). Similarly, voluntary running increased, whereas aging decreased the number of type α cells (Fig. 4C). In contrast, neither running, nor aging had any effect on the total number of type β cells (Fig. 4D). As a result, when the relative proportions of types α and β cells were calculated, Y, YR, and OR mice displayed mainly type α cells (66.6%, 80.6%, and 58%, respectively), whereas type β cells were more frequently observed on O mice (89%, Fig. 4B–4E). The length and width of types α and β cells were not modified by running or aging (Supporting Information Fig. 3). Thus, aging and exercise strongly modified the number of type α cells, but not the number of type β cells.

We next examined whether the pharmacological stimulation of adult neurogenesis cells may have a similar effect on the different morphotypes of cells. We recently reported that the administration of the NMDA receptor co-agonist D-serine increases the density of RGL stem cells [30]. Here, we repeated this experiment and injected four mice with D-serine (daily intraperitoneal injections 50 mg/kg, for 8 days during the eighth week of life) and four mice with the same volume of saline. All mice were examined 1 day after the last injection (Fig. 5A). Similarly to our previous observations, D-serine increased the total number of RGL cells. This increase was mediated by an increase in both the number of type α cells (120% increase) and type β cells (160% increase, Fig. 5B–5E). Moreover, the effect of D-serine was specific to RGL cells, since D-serine treatment did not change the number of GFAP-immunolabeled stellar astrocytes in the dentate gyrus [30]. To examine whether D-serine activated the proliferation of types α and β cells, we immunostained hippocampal slices for the cell proliferation marker Ki-67. Ki-67 is a nuclear protein associated with proliferation that is expressed during all active phases of the cell cycle. Of 545 cells analyzed, Ki-67 was expressed in about 10.45% of type α cells, but was not expressed in type β cells (Fig. 5F–5G). D-Serine significantly increased the proportion of Ki-67-expressing type α cells as compared to the proportion found in control, nontreated mice ($p < 0.01$, Fig. 6C).

Thus, D-serine increased the proliferation of type α and resulted in increased number of types α and β cells, but did not affect the proliferation of type β cells.

Proliferative Properties of Types α and β Cells

To examine the proliferative properties of types α and β cells, we immunostained hippocampal slices for the cell proliferation marker Ki-67 (Fig. 6A–6C). Of 1555 cells analyzed, Ki-67

Figure 3. Type α and β cells contact niche-forming cells. **(A)**: Experimental timeline. GFAP-GFP mice were housed in normal cages (NR) or in cages containing a running wheel (R) for 2 weeks before histological analysis. **(B)**: Confocal maximal projection micrographs of radial glia-like (RGL) cells (green) and Iba1-immunostained microglia (red). **(C)**: Histogram of the average number of microglia cells contacted per RGL cell. Type β cells contact more microglia than type α cells (one-way analysis of variance [ANOVA] $F(3, 15) = 73.12$; $p < 0.001$. Post hoc bilateral Student's t test: No Run [type α vs. type β] $p < 0.001$, Run [type α vs. type β] $p < 0.01$). Two weeks of running decrease the interaction of microglia with both types α and β cells (post hoc bilateral Student's t test: type α [No Run vs. Run] $p < 0.001$, type β [No Run vs. Run] $p < 0.001$). **(D)**: Confocal maximal projection micrographs of RGL cells (green) and blood vessels, identified with Sulforhodamine (red). **(E)**: Histogram of the number of blood vessels contacted per RGL stem cell. In sedentary mice, there is no difference between type α of a type β cell in sedentary conditions (one-way ANOVA $F(3, 15) = 16.10$; $p < 0.001$. Post hoc bilateral Student's t test: No Run [type α vs. type β] $p = 0.84$). In running mice, blood vessel are more contacted by type α than type β cells (post hoc bilateral Student's t test: Run [type α vs. type β] $p < 0.05$). Running, significantly increased the number of blood vessels contacted by both cell types (one-way ANOVA $F(3, 15) = 16.10$; $p < 0.001$. Post hoc bilateral Student's t test: type α [No Run vs. Run] $p < 0.001$, type β [No Run vs. Run] $p < 0.01$). **(F)**: Confocal maximal projection micrographs of RGL cells (green) and S100β-immunostained astrocytes (white). **(G)**: Histogram of the number of astrocytes contacted per type α or type β cells. **(H)**: Confocal maximal projection micrographs of RGL cells (green) and NG2-immunostained oligodendrocyte precursors cells (red). **(I)**: Histogram of the number of oligodendrocyte precursor cells contacted by types α or β cells. Scale bars = 20 μm. $N = 4$ animals per group. Each value represents the mean $\pm$ SEM. *, $p < 0.05$; **, $p < 0.01$; ***, $p < 0.001$. Abbreviations: GFP, green fluorescent protein; RGL, radial glia-like.

was expressed in about 5% of type α cells, but was not expressed in type β cells. Notably, type α-Ki-67^{+} cells displayed a longer process than type α-Ki-67^{-} cells (Fig. 6D). These results suggest that type β cells do not proliferate and support the possibility that the RGL cells' processes may play a role in proliferation.

To further examine cell proliferation, we performed pulse chase experiments with three different BrdU injection

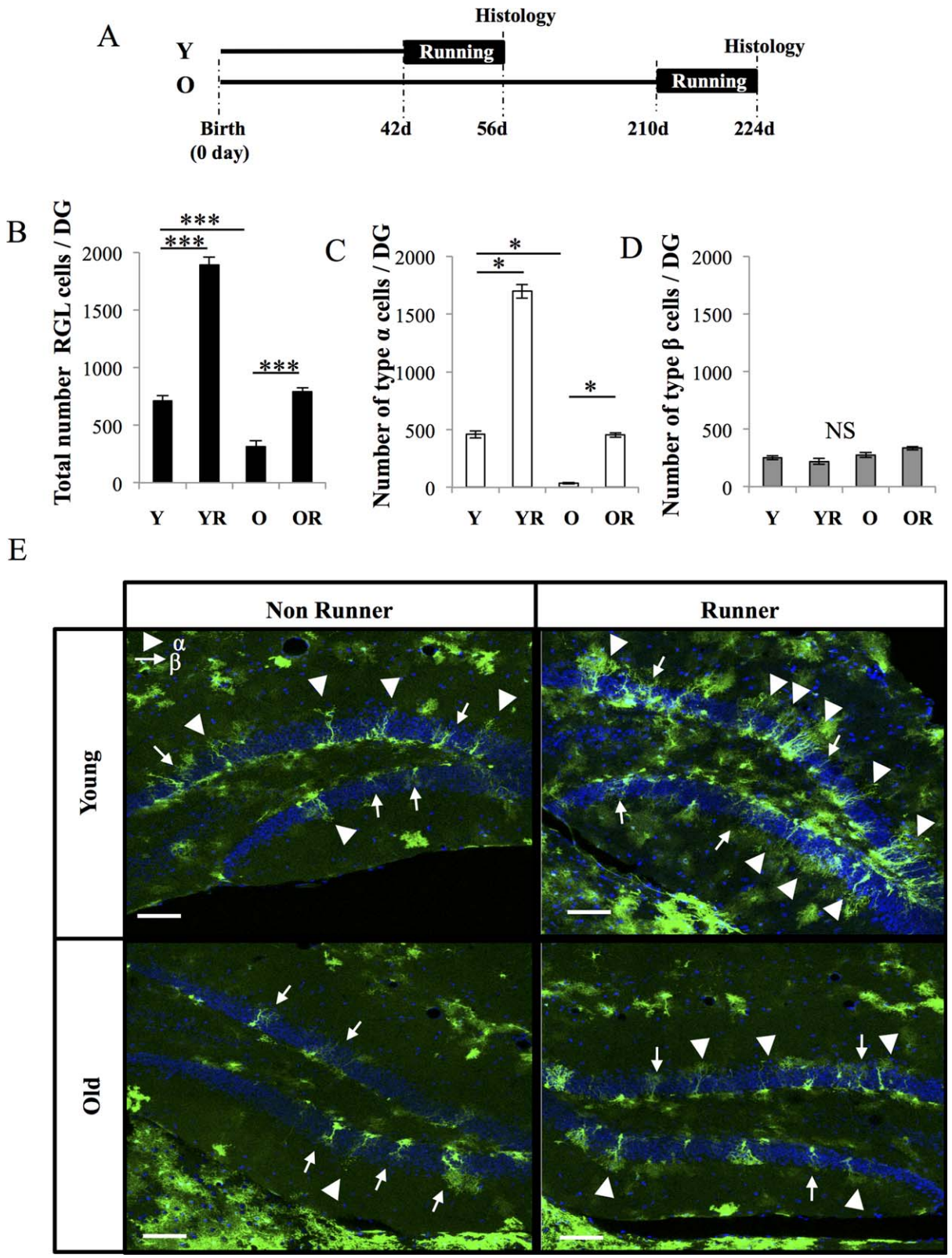

Figure 4.

protocols. By incorporating into the nascent DNA strand during mitosis, BrdU enables the labeling of dividing cells and their progenies. First, we injected mice with BrdU (1×100 mg/kg) and killed the mice 2 hours after the last BrdU-injection (Fig. 6E). This protocol enables the labeling of fast dividing progenitor cells, however, BrdU was incorporated in 3.9% type α cells, but was absent from type β cells (Fig. 6F). Then we injected mice with BrdU (3×100 mg/kg) and killed the mice 24 hours after the last BrdU-injection (Fig. 6G–6I). Of 500 cells, BrdU was incorporated in 3.64% of type α and 0.4% of type β. Moreover, the $BrdU^+$ type β cells were closely attached to $BrdU^+$ type α cells (Fig. 6H). In a third experiment, we injected mice with BrdU daily for 8 days (100 mg/kg) and killed the mice 1 day after the last BrdU-injection (Fig. 6J). Both types α and β cell types incorporated BrdU, although type α cells to a much greater extent than type β cells (Fig. 6K–6L, 527 cells analyzed, $BrdU^+$ type α: 5.69%, $BrdU^+$ type β: 0.94%). In contrast with Ki-67 labeling, the proportion of BrdU-labeled cells did not correlate with the dimensions of the cells (Fig. 6K).

Taken together, these results suggest that type β cells do not proliferate but are generated by the division of type α cells. To further examine this possibility, we performed a clonal analysis.

Fate Analysis of Type α and Type β Cells

To examine the fate of individual RGL cells, we used two transgenic mice, the *GFAP*::$CreER^{T2}$ and the Nestin::$CreER^{T2}$. We crossed the *Nestin*::$CreER^{T2}$ transgenic mouse (expressing the tamoxifen-inducible Cre recombinase under the control of the Nestin promoter) with reporter mice (ROSA-tdTomato or $Z/EG^{f/+}$) (Fig. 7A). The *GFAP*::$CreER^{T2}$ was crossed with the ROSA-YFP reporter mouse. A minimal tamoxifen injection resulted in the sparse labelling of adult neural stem cells, thereby enabling the identification and morphological analysis of individual clones [14]. To examine clones shortly after division, we killed the animals 1, 2, 3, or 7 days after tamoxifen injection (dpi, Fig. 7B).

In *Nestin*::$CreER^{T2}$ mice, we didn't detect any difference between the two reporter mice, therefore we combine the results of both mice. All clones are described and shown in Supporting Information Figures 4–6. Across all time points, we examined 227 clones that contained at least one RGL cell, which were most frequently accompanied by a neuronal progenitor/type 2 cell (N) or an astrocyte (A, Fig. 7; Supporting Information Fig. 4A). Astrocytes were defined by their typical stellar astrocytes morphology and their identity was confirmed by immunohistology against GFAP. Neuronal progenitor/type 2 cells were identified based on the absence of GFAP immunoreactivity and their short processes oriented horizontally or radially (Supporting Information Fig. 6). The most parsimonious clonal relationships between cells present in each clones revealed that 26.9% of the clones displayed an isolated RGL cell (all of which consisted of type α cells), suggesting no division, 37% of the clones divided once and 36.1% divided twice (Fig. 7F–7H; Supporting Information Fig. 4A). Of the 166 clones that divided at least once, 51.8% generated a neural progenitor/type 2 cell, 24.7% generated an astrocyte and 77.7% generated a RGL cell (including clones that contained neurons or astrocytes, Fig. 7C). Type β cells were more often observed in clones that contained astrocytes than in clones containing neurons, suggesting that they originated from α cells that were prone to gliogenesis (Fig. 7C). Finally, among the 129 clones in which a new RGL cell was observed, 44% generated 1 type β cell, 7% generated 2 type β cells and 49% generated a new type α cell (Fig. 7D). Thus, of 166 clones that divided at least once, 75 new type β cells and 63 new type α cells were generated (Fig. 7E; see summary table on Supporting Information Fig. 5A).

In *GFAP*::$CreER^{T2}$ mice, across all time points, we examined 93 clones. Similarly to *Nestin*::$CreER^{T2}$ mice, 5.3% of the clones did not divide, 46.3% divided once, and 48.4% divided twice (Supporting Information Figs. 4B, 5B). Of the 88 clones that divided, 56.8% generated a neuronal progenitor/type 2 cell, 12.5% generated and astrocyte, and 81.8% generated a RGL cell. Moreover similarly to Nestin::Cre mice, type β cells were more often observed in clones that contained astrocytes.

Thus, type α cells undergo numerous modes of division to generate type α cells, type β cells, neurons and astrocytes and new type β cells are frequently generated upon division of type α cells.

Discussion

Using a combination of morphometry, immunohistochemistry and clonal analysis, we found that two morphotypes of RGL cells coexist in the SGZ of the dentate gyrus, which can be characterized by two simple morphological features, the length of the primary process and the width of the arbor of secondary processes: Type α cells represented 76.21% of RGL cells and displayed a long radial process and a narrow arbor of secondary processes extending well into the first third of the molecular layer. These cells expressed stem cell markers, self-replicated and produced neurons, astrocytes and type β cells. Their total number was also greatly increased by voluntary running and D-serine administration and decreased by aging. In contrast, type β cells (which represented 23.79% of all RGL cells) had a short radial process and their secondary processes branched mainly in the GCL. Marker expression

Figure 4. Number of type α but not type β cells are changed by running and aging. **(A)**: Experimental timeline. GFAP-GFP mice were exposed to sedentary housing or cages with a running wheel (R), starting either at 42 days (Y) or 210 days (O) after birth. Mice were killed and examined 2 weeks after exposure to running wheel cages. **(B)**: Histogram of the total number of radial glia-like (RGL) cells in the dentate gyrus. Two-way analysis of variance (ANOVA) test showed that there is interaction between aging and running ($F(1, 12) = 35.50$; $p < 0.001$). The total number of RGL cells was significantly decreased with aging post hoc bilateral Student's *t* test (Y vs. O; $p < 0.001$) and increased by running (one-way ANOVA $F(3, 15) = 127.32$; $p < 0.001$). Post hoc bilateral Student's *t* test (Y vs. YR $p < 0.001$, O vs. OR $p < 0.001$). **(C)**: Histogram of the number of type α cells in the dentate gyrus. Voluntary running increased, whereas aging decreased the number of type α cells Kruskal-Wallis test $p < 0.01$. Post hoc Wilcoxon test (Y vs. O < 0.05; Kruskal-Wallis test $p < 0.01$). Post hoc Wilcoxon test (Y vs. YR $p < 0.05$, O vs. OR $p < 0.05$). **(D)**: Histogram of the number of type β cells in the dentate gyrus. **(E)**: Confocal maximal projection micrographs of hippocampal sections. Scale bars = 100 μm. *, $p < 0.05$; ***, $p < 0.001$, NS: Not significant. Abbreviations: DG, Dentate Gyrus; RGL, radial glia-like.

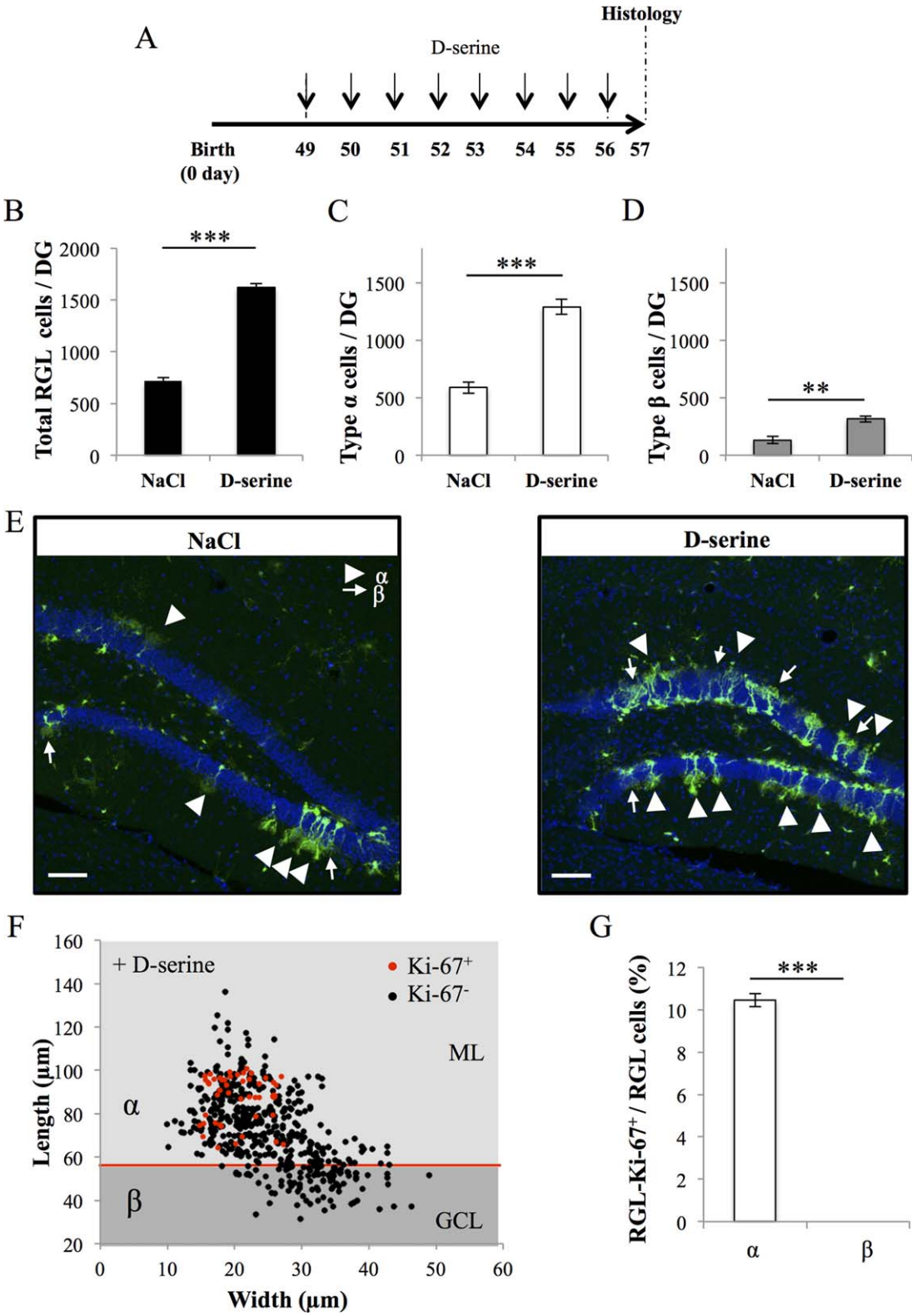

Figure 5. Number of types α and β cells are increased by D-serine injection. **(A)**: Experimental timeline: Nestin-GFP mice were injected with D-serine, daily for 8 days, starting at 49 days after birth and were killed 1 day after the last D-serine injection. **(B)**: Histogram of the total number of radial glia-like (RGL) cells in the dentate gyrus (bilateral Student's t test $p < 0.001$). **(C)**: Histogram of the number of type α cells in the dentate gyrus (bilateral Student's t test $p < 0.001$). **(D)**: Histogram of the number of the type β cells in the dentate gyrus (bilateral Student's t test $p < 0.01$). **(E)**: Confocal maximal projection micrographs of hippocampal sections. **(F)**: Scatter graph of RGL cells dimensions. Red dots: Ki-67$^+$ cells $N = 45$, black dots Ki-67$^-$ cells $N = 500$. **(G)**: Histogram showing the percentage of types α and β cells expressing Ki-67. Bilateral Student's t test. Scale bars = 100 μm. $N = 4$ animals per group. Each value represents the mean ± SEM. **, $p < 0.01$; ***, $p < 0.001$. Abbreviations: DG, Dentate Gyrus; GCL, granule cell layer; ML, molecular layer; RGL, radial glia-like.

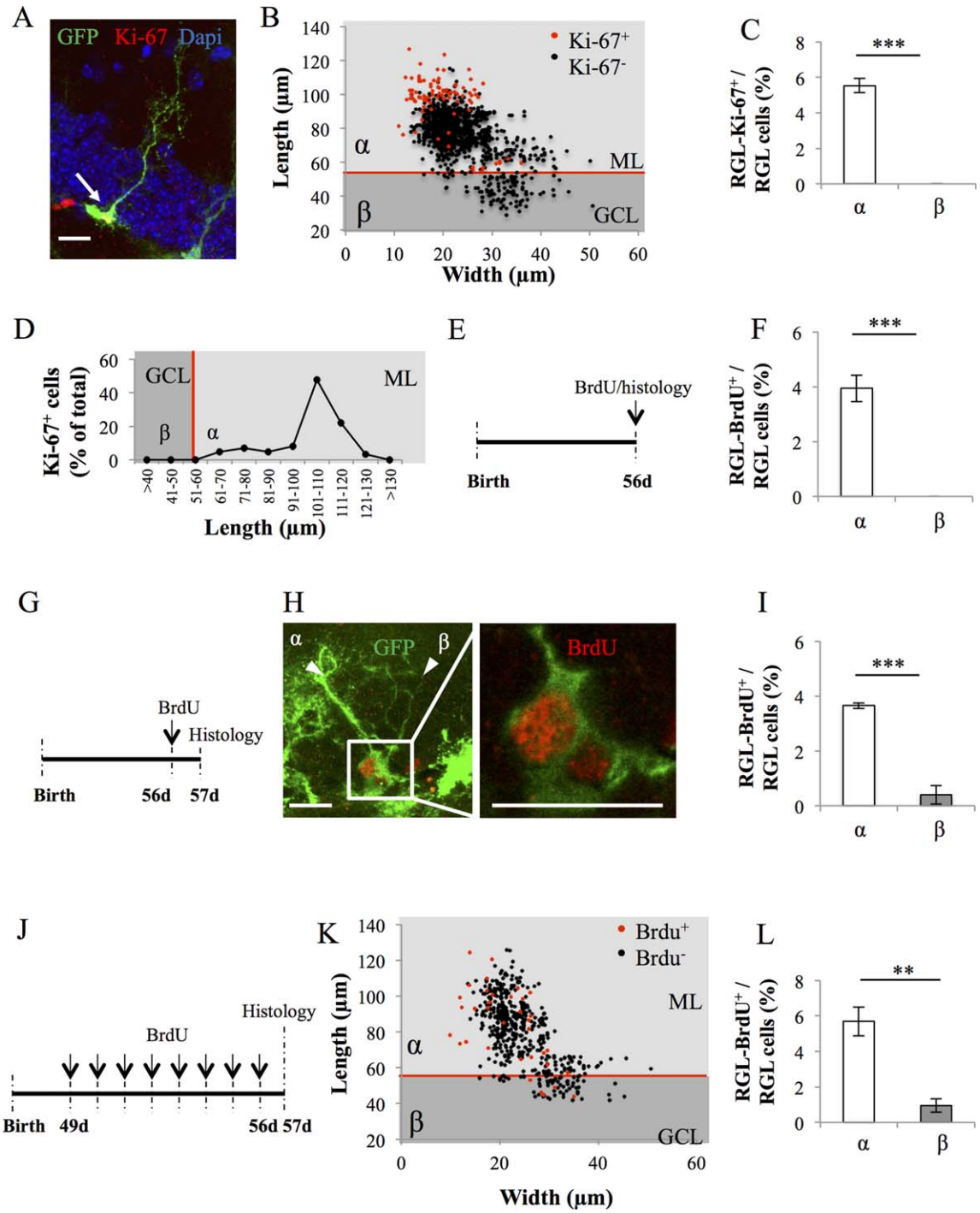

Figure 6. Proliferative properties of types α and β cells in GFAP-GFP mice. **(A)**: Confocal maximal projection micrograph of radial glia-like (RGL) cell (green), immunostained for Ki-67 (red). **(B)**: Scatter graph of RGL cell dimensions. Red dots: Ki-67$^+$ cells $N = 86$, black dots Ki-67$^-$ cells $N = 1469$. **(C)**: Histogram showing the percentage of types α and β cells expressing Ki-67. Bilateral Student's t test. **(D)**: Line graph representing the proportion of RGL cells expressing Ki-67 according to their length. **(E)**: Experimental timeline: mice were injected intraperitoneally (i.p.) at doses of 100 mg/kg in saline, three times at 2-hour intervals and killed 2 hours after the last injection. **(F)**: Histogram showing the percentage of types α and β cells expressing bromodeoxyuridine (BrdU). $N = 500$ cells. Bilateral Student's t test. **(G)**: Experimental timeline: mice were injected i.p. at doses of 100 mg/kg in saline, three times at 2-hour intervals and killed 24 hours after the last injection. **(H)**: Confocal maximal projection micrograph of types α and β cells expressing BrdU. Confocal micrograph of one focal plan showing the immunoreactive cells Scale bar: 20 μm **(I)** Histogram showing the percentage of types α and β cells expressing BrdU. $N = 500$ cells. Bilateral Student's t test. **(J)**: Experimental timeline: Mice were injected daily with BrdU for 8 consecutive days, starting at 49 days after birth. One day after the last injection, they were killed and prepared for histology. **(K)**: Scatter graphs representing the dimensions of RGL cells after immunostaining for BrdU (red dots: BrdU$^+$ cells $N = 35$, black dots BrdU$^-$ cells $N = 492$) **(L)**: Histogram showing the proportion of types α and β cells that incorporated BrdU. Bilateral Student's t test. Scale bar: 20 μm. Each value represents the mean $\pm$ SEM. **, $p < 0.01$ ***, $p < 0.001$. Abbreviations: BrdU, bromodeoxyuridine; GCL, granule cell layer; GFP, green fluorescent protein; ML, molecular layer; RGL, radial glia-like.

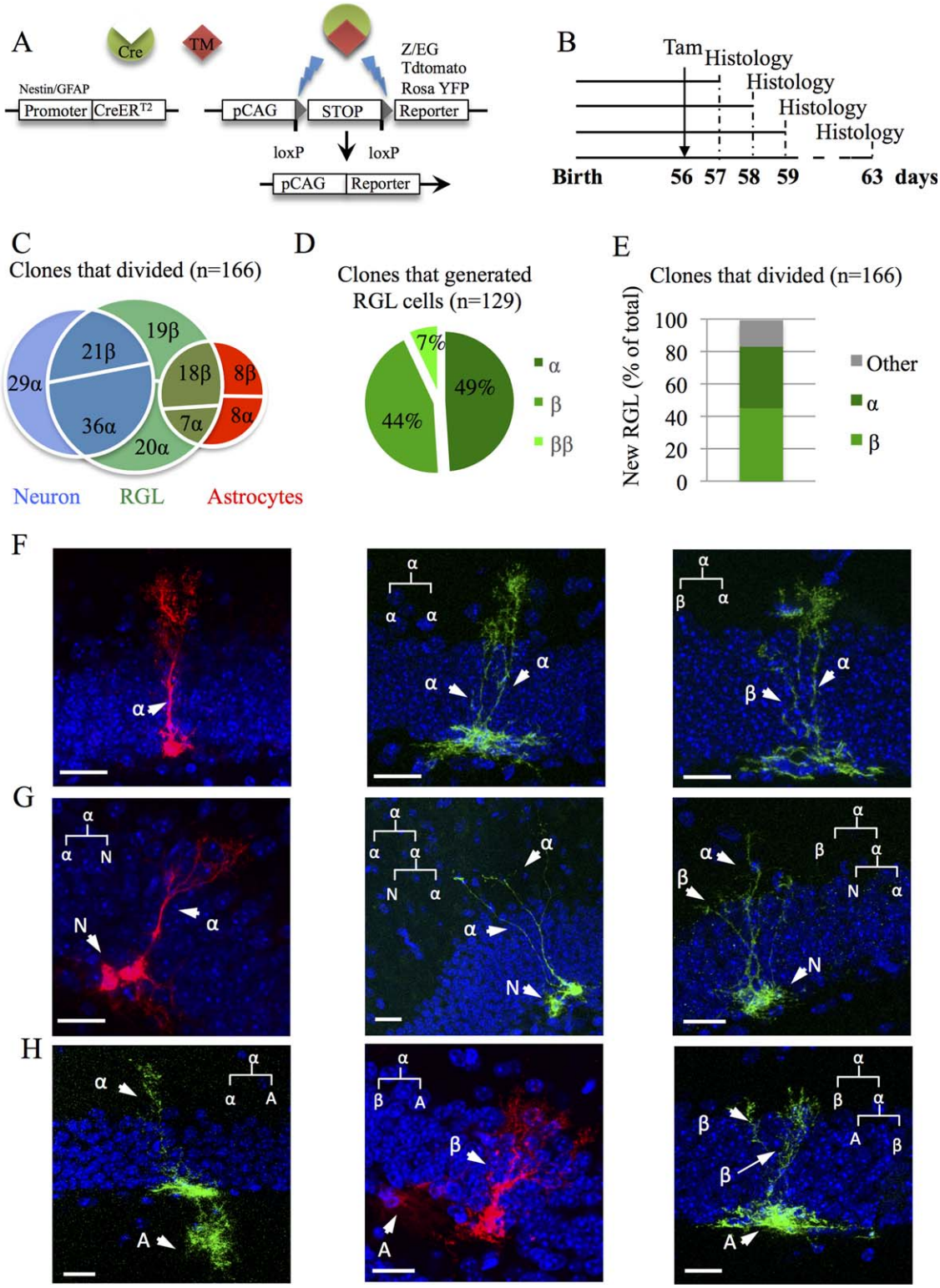

Figure 7. Clonal analysis of types α and β cells. **(A)**: Breeding scheme for clonal analysis: *Nestin*-CreER^{T2} mice were crossed to fluorescent reporter mice Rosa-tdTomato or Z/EG$^{f/+}$ and glial fibrillary acidic protein (*GFAP*)::CreER^{T2} were crossed with ROSA-YFP reporter mice **(B)**: Experimental timeline: Nestin::CreERt2 x Rosa-tdTomato or Z/EG$^{f/+}$ mice were injected with tamoxifen (Tam) at 56 days after birth and killed 1, 2, 3, and 7 day after Tam injection (dpi). **(C)**: Venn diagram showing the percentage of clones that generated neurons, astrocytes, or radial glia-like (RGL) cells out of all clones that divided. **(D)**: Pie chart representing the distribution of newly generated RGL cells among clones that generated new RGL cells. **(E)**: Histogram showing the percentage of newly generated RGL among the total number of dividing clones. **(F–H)**: Confocal micrographs of different clones with hypothetic (linkage) tree of fate. Clones generated either only new RGL cells **(F)**, neuronal progenitor/type 2 cell **(G)** or astrocytes **(H)**. (*N* = type 2/neuronal progenitor, A = astrocyte). Scale bars = 20 μm. Abbreviation: RGL, radial glia-like.

analyses revealed the coexpression of astrocytic and stem cell markers. These cells did not proliferate and their population size did not change upon aging or exercise, but was increased by D-serine administration. Together, these results reveal the coexistence within the dentate gyrus, of two populations of cells with prototypical morphology of RGL stem cells, but with radically different morphological and functional properties.

The strong association between morphology and function of RGL cells suggests that the processes of RGL cells play a potential role in regulating their activity. The shorter processes of type β cells do not reach the molecular layer. Although the role of the highly branched and long processes of RGL stem cells is still unclear, our results support the view that these processes establish specific contacts with the neurogenic niche [16]. We identified here that both types α and β cells established direct cellular contacts with several cell types of the neurogenic niche, including but not restricted to microglia, astrocytes, NG2-expressing glia, and blood vessels. Direct signaling with these cells are known to participate to the regulation stem cell proliferation and fate determination, as has recently been shown for astrocytes [24], blood vessels [18, 31], or microglia [22, 23]. Contacts with microglia seems of particular relevance to the identity of type β cells, since they contacted significantly more microglia than type α cells in normal (sedentary) conditions. The presence of microglia in the dentate gyrus has been associated with inflammation, which can reduce neurogenesis by the production of cytokines [32]. In absence of inflammation, microglia contribute to the phagocytosis of early progenitors undergoing apoptotic elimination during the neuroprogenitors to neuroblasts transition [23]. However, we found no evidence of microglial engulfment of type α or type β cells and the contacts that these cells established with microglia occurred mainly on the fine, secondary processes rather than on the soma, as has been described for phagocytic engulfment [23]. Our results therefore are consistent with the view that microglia may regulate RGL stem cell proliferation using paracrine or juxtacrine signaling, independently from inflammatory pathway [22]. Consistently, running modified the number and the structure of microglia cells (Supporting Information Fig. 2) and resulted in increased proliferation of type α cells (Fig. 3). Thus, cellular contacts established by RGL stem cells may be involved in the regulation of their proliferation. This possibility calls for a further examination of the specific contacts they form in the molecular layer, especially with microglia and blood vessels, with higher resolution imaging such as electron microscopy. Furthermore, whether the increased contacts between microglia and type β are a cause or consequence of their dormancy remains uncertain and this question will require further investigation with the use of live-cell imaging.

Type α cells display all characteristics of RGL stem cells [11, 14, 33, 34], but the identity of type β cells is less clear. Morphology and molecular marker expression suggest that these cells are intermediate between quiescent RGL stem cells and stellate, protoplasmic astrocytes. Indeed, type β cells express both stem cell markers such as Nestin, Prominin 1, Sox 1, and Sox 2, but also the mature astrocytic marker S100β and GLT1, which are normally not expressed in RGL stem cells [11]. Similarly, the morphology of type β cells is less polarized than type α cells, with shorter radial process and larger branches of secondary processes than type α cells, but not quite as round and branched as protoplasmic astrocytes. Furthermore, the absence of expression of the essential cell cycle marker Ki-67 from type β cells (Fig. 6A–6C), even upon activation by D-serine (Fig. 5F–5G) and the lack of BrdU incorporation in short (2 hours) pulses (Fig. 6D–6F) indicates that type β cells do not divide. Instead, we propose that type β cells are formed upon the division of type α cells. Consistent with this hypothesis, clonal analysis shows that type β cells were never found alone and all type β cells that incorporated BrdU after a 24 hours pulse were found apposed to a type α cell (Fig. 6G–6I). Although we cannot exclude that type β cells may represent a highly quiescent pool of RGL stem cells which may be converted into type α cells upon proper stimulation, this possibility is not supported by our results. Alternatively, type β cells may represent a transitional morphology of type α cells undergoing conversion into astrocytes, as has been proposed during aging [14, 33] or epilepsy-induced hyperactivation [35] (See schematic model in Supporting Information Fig. 7). In favor of this possibility, long primary processes in RGL cells were associated with Ki-67 expression (Figs. 5F, 6D) and type β cells that expressed stem cell markers (Sox 1, Prominin 1, and Nestin), had a longer primary process than cells not expressing these markers (Fig. 2). These correlations between marker expression and length of the primary process suggests the existence of a morphological continuum between RGL cells, with proliferation and the expression of stem cell markers decreasing with the shortening of the primary process.

Intriguingly, the frequent production of type β cells upon division of type α cells does not result in an increase in the number of type β cells over time or in conditions of increased proliferation such as voluntary exercise. This apparent stability in the population of type β cells, together with the absence of microglia engulfment of type β cells also supports the idea of a stable turnover, in which type β cells may transform into astrocytes and migrate out of the GCL. To maintain a stable population of type β cells under conditions of increased or decreased proliferation, the transformation into astrocytes would need to be regulated by the production of type β cells. Time-lapse imaging will shed light in the morphological dynamics and migratory pattern of type β cells.

Conclusion

Together, our results reveal the existence of two morphofunctionally distinct types of RGL cells in the adult dentate gyrus. The selective behavior of these cell types is relevant to the mechanisms of stem cell proliferation and self-renewal. Furthermore, the morphological criteria proposed here may be used to assess the status of the pool of RGL stem cells in the dentate gyrus.

Acknowledgments

We thank the Cellular Imaging Facility of the University of Lausanne and Jacqueline Kocher-Braissant for technical help. This work was supported by the Swiss National Science Foundation (to E.G., S.S., F.U., P.-J.G., and N.T.), the Deutsche Forschungsgemeinschaft (Grant DFG LI 858/9-1), and the Bavarian Research Network on Human-induced Pluripotent Stem Cells "ForIPS" (to D.C.L.), the Deutsche Forschungsgemeinschaft (Grant BE5136/1-1) (to R.B.), NIH (Grants

NS048271 and MH105128), Dr. Miriam and Sheldon G. Adelson Medical Research Foundation (to G.-L.M.), and NIH (NS047344; to H.S.). M.A.B. is currently affiliated with the Eli and Broad CIRM Center for regenerative Medicine and Stem Cell Research, University of Southern California, Los Angeles, California, USA.

Author Contributions

E.G.: conceived and designed the experiments, performed the experiments, analyzed the data, discussed the data, wrote the manuscript; M.A.B., R.B., and S.S.: performed the experiments, discussed the data; F.U. and P.-J.G.: performed the experiments; D.C.L.: discussed the data; G.-L.M.: provided financial support; H.S.: discussed the data, provided financial support; N.T.: conceived and designed the experiments, discussed the data, wrote the manuscript, provided financial support.

Disclosure of Potential Conflicts of Interest

The authors indicate no potential conflicts of interest.

References

1 Altman J, Das GD. Autoradiographic and histological evidence of postnatal hippocampal neurogenesis in rats. J Compar Neurol 1965;124:319–335.
2 Ming GL, Song H. Adult neurogenesis in the mammalian brain: Significant answers and significant questions. Neuron 2011;70: 687–702.
3 Sahay A, Scobie KN, Hill AS et al. Increasing adult hippocampal neurogenesis is sufficient to improve pattern separation. Nature 2011;472:466–470.
4 van Praag H, Christie BR, Sejnowski TJ et al. Running enhances neurogenesis, learning, and long-term potentiation in mice. Proc Natl Acad Sci USA 1999;96:13427–13431.
5 Beckervordersandforth R, Deshpande A, Schaffner I et al. In vivo targeting of adult neural stem cells in the dentate gyrus by a split-cre approach. Stem Cell Rep 2014;2: 153–162.
6 Huttmann K, Sadgrove M, Wallraff A et al. Seizures preferentially stimulate proliferation of radial glia-like astrocytes in the adult dentate gyrus: Functional and immunocytochemical analysis. Eur J Neurosci 2003; 18:2769–2778.
7 Kriegstein A, Alvarez-Buylla A. The glial nature of embryonic and adult neural stem cells. Ann Rev Neurosci 2009;32:149–184.
8 Mignone JL, Kukekov V, Chiang AS et al. Neural stem and progenitor cells in nestin-GFP transgenic mice. J Compar Neurol 2004; 469:311–324.
9 Steiner B, Klempin F, Wang L et al. Type-2 cells as link between glial and neuronal lineage in adult hippocampal neurogenesis. Glia 2006;54:805–814.
10 Suh H, Consiglio A, Ray J et al. In vivo fate analysis reveals the multipotent and self-renewal capacities of Sox2 + neural stem cells in the adult hippocampus. Cell Stem Cell 2007;1:515–528.
11 Lugert S, Basak O, Knuckles P et al. Quiescent and active hippocampal neural stem cells with distinct morphologies respond selectively to physiological and pathological stimuli and aging. Cell Stem Cell 2010;6:445–456.
12 Noctor SC, Flint AC, Weissman TA et al. Neurons derived from radial glial cells establish radial units in neocortex. Nature 2001; 409:714–720.
13 Shapiro LA, Korn MJ, Shan Z et al. GFAP-expressing radial glia-like cell bodies are involved in a one-to-one relationship with doublecortin-immunolabeled newborn neurons in the adult dentate gyrus. Brain Res 2005;1040:81–91.
14 Bonaguidi MA, Wheeler MA, Shapiro JS et al. In vivo clonal analysis reveals self-renewing and multipotent adult neural stem cell characteristics. Cell 2011;145:1142–1155.
15 Gerald J, Sun YZ, Ryan P et al. Tangential migration of neuronal precursors of glutamatergic neurons in the adult mammalian brain. PNAS 2015;112:9484–9489.
16 Fuentealba LC, Obernier K, Alvarez-Buylla A. Adult neural stem cells bridge their niche. Cell Stem Cell 2012;10:698–708.
17 Shihabuddin LS, Horner PJ, Ray J et al. Adult spinal cord stem cells generate neurons after transplantation in the adult dentate gyrus. J Neurosci 2000;20:8727–8735.
18 Palmer TD, Willhoite AR, Gage FH. Vascular niche for adult hippocampal neurogenesis. J Compar Neurol 2000;425:479–494.
19 Lie DC, Colamarino SA, Song HJ et al. Wnt signalling regulates adult hippocampal neurogenesis. Nature 2005;437:1370–1375.
20 Song H, Stevens CF, Gage FH. Astroglia induce neurogenesis from adult neural stem cells. Nature 2002;417:39–44.
21 Song J, Zhong C, Bonaguidi MA et al. Neuronal circuitry mechanism regulating adult quiescent neural stem-cell fate decision. Nature 2012;489:150–154.
22 Gebara E, Sultan S, Kocher-Braissant J et al. Adult hippocampal neurogenesis inversely correlates with microglia in conditions of voluntary running and aging. Front Neurosci 2013;7:145.
23 Sierra A, Encinas JM, Deudero JJ et al. Microglia shape adult hippocampal neurogenesis through apoptosis-coupled phagocytosis. Cell Stem Cell 2010;7:483–495.
24 Ashton RS, Conway A, Pangarkar C et al. Astrocytes regulate adult hippocampal neurogenesis through ephrin-B signaling. Nat Neurosci 2012;15:1399–1406.
25 Nolte C, Matyash M, Pivneva T et al. GFAP promoter-controlled EGFP-expressing transgenic mice: A tool to visualize astrocytes and astrogliosis in living brain tissue. Glia 2001;33:72–86.
26 Yamaguchi M, Saito H, Suzuki M et al. Visualization of neurogenesis in the central nervous system using nestin promoter-GFP transgenic mice. Neuroreport 2000;11:1991–1996.
27 Madisen L, Zwingman TA, Sunkin SM et al. A robust and high-throughput Cre reporting and characterization system for the whole mouse brain. Nat Neurosci 2010;13: 133–140.
28 Thuret S, Toni N, Aigner S et al. Hippocampus-dependent learning is associated with adult neurogenesis in MRL/MpJ mice. Hippocampus 2009;19:658–669.
29 Kuhn HG, Dickinson-Anson H, Gage FH. Neurogenesis in the dentate gyrus of the adult rat: Age-related decrease of neuronal progenitor proliferation. J Neurosci 1996;16: 2027–2033.
30 Sultan S, Gebara EG, Moullec K et al. D-Serine increases adult hippocampal neurogenesis. Front Neurosci 2013;7:155.
31 Villeda SA, Luo J, Mosher KI et al. The ageing systemic milieu negatively regulates neurogenesis and cognitive function. Nature 2011;477:90–94.
32 Monje ML, Toda H, Palmer TD. Inflammatory blockade restores adult hippocampal neurogenesis. Science 2003;302:1760–1765.
33 Encinas JM, Michurina TV, Peunova N et al. Division-coupled astrocytic differentiation and age-related depletion of neural stem cells in the adult hippocampus. Cell Stem Cell 2011;8:566–579.
34 Filippov V, Kronenberg G, Pivneva T et al. Subpopulation of nestin-expressing progenitor cells in the adult murine hippocampus shows electrophysiological and morphological characteristics of astrocytes. Mol Cell Neurosci 2003;23:373–382.
35 Sierra A, Martin-Suarez S, Valcarcel-Martin R et al. Neuronal hyperactivity accelerates depletion of neural stem cells and impairs hippocampal neurogenesis. Cell Stem Cell 2015;16:488–503.


See www.StemCells.com for supporting information available online.

Supplementary figure 1

A

	GFAP-GFP		Nestin-GFP	
	α	β	α	β
Width of the apical arbor	22.63 ± 0.11 (n=1884)	32.45 ± 0.23 (n=588)	22.00 ± 0.17 (n=849)	35.37 ± 0.32 (n=301)
Length of the cell	84.64 ± 0.29 (n=1884)	46.02 ± 0.27 (n=588)	87.59 ± 0.39 (n=849)	45.69 ± 0.36 (n=301)
Surface of the apical arbor	537.89 ± 21.10 (n=110)	651.33 ± 28.84 (n=110)	483.88 ± 22.15 (n=110)	604.93 ± 24.33 (n=110)
Position of the soma	3.61 ± 0.11 (n=500)	3.91 ± 0.12 (n=500)	3.90 ± 0.10 (n=500)	3.89 ± 0.10 (n=500)
Surface of the cell	1466.16 ± 24.02 (n= 300)	1444.66 ± 25.68 (n= 300)	1511.60 ± 35.98 (n=300)	1501.00 ± 22.07 (n=300)
Number of secondary branches	4.04 ± 0.076 (n= 500)	4.21 ±0.073 (n=500)	4.09 ± 0.077 (n=500)	4.11 ± 0.081 (n=500)

B

	Type α	Type β
Sox2	100% (n=165)	100% (n=62)
GFAP	100% (n=253)	100% (n=97)
Sox1	100% (n=166)	49% (n=52)
Prominin 1	100% (n=168)	32% (n=75)
Nestin	100% (n= 174)	18% (n= 75)
S100β	0.5% (n= 134)	100% (n=52)
Glt1	0% (n=248)	100% (n=69)

Supplementary figure 2

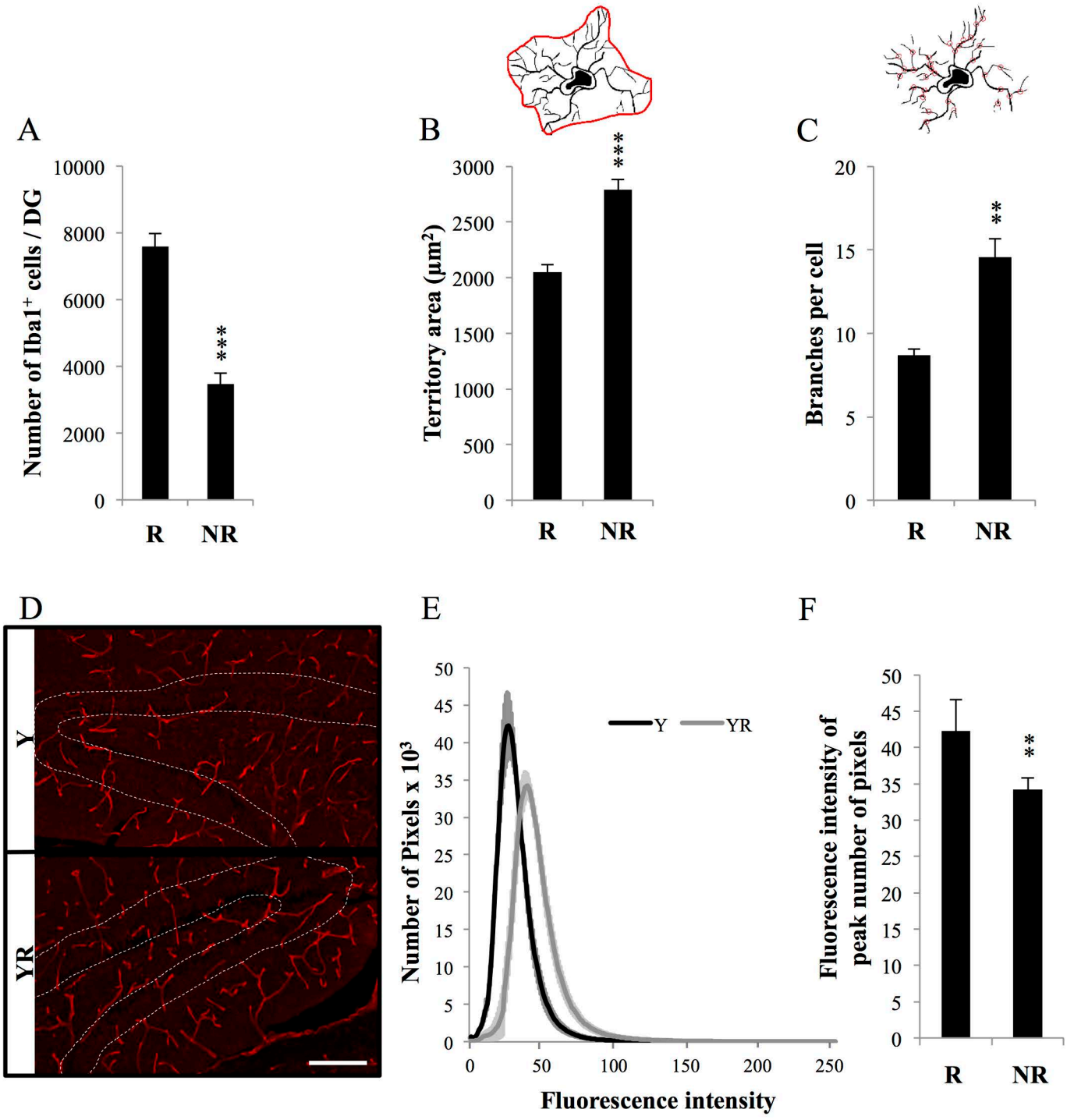

Supplementary figure 3

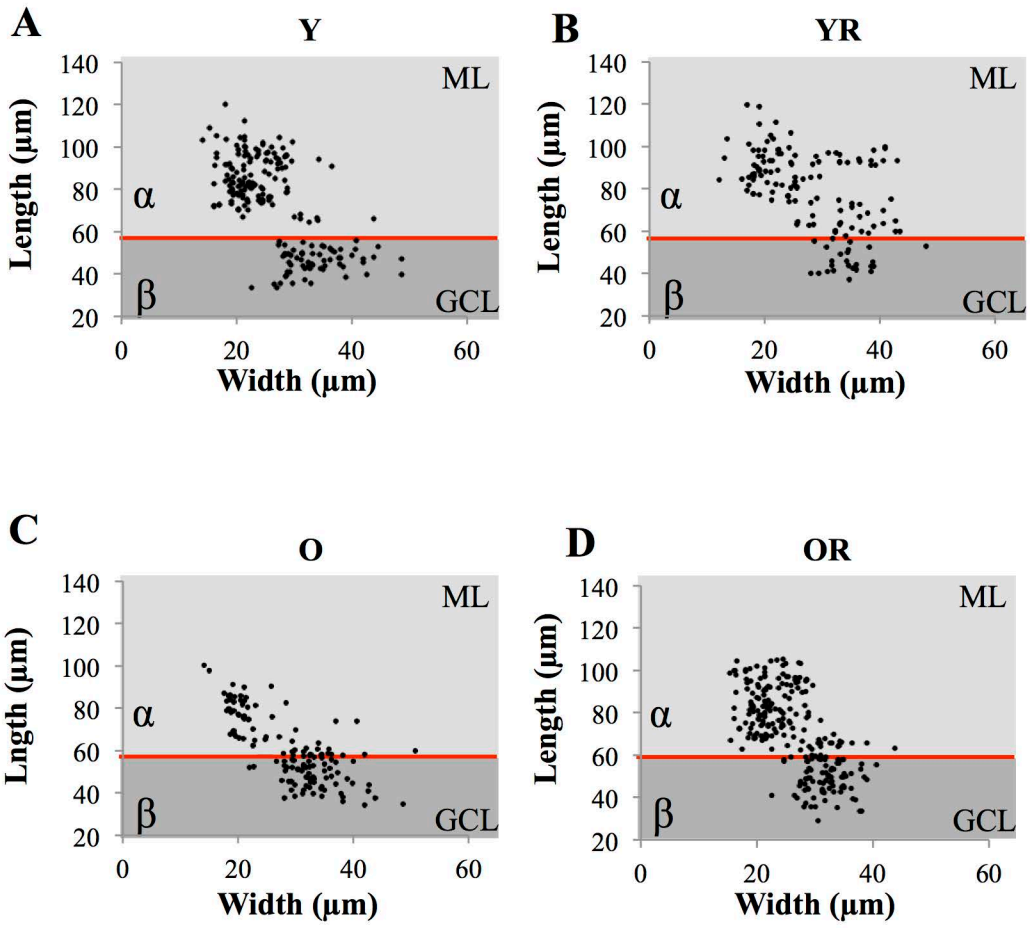

Supplementary figure 4

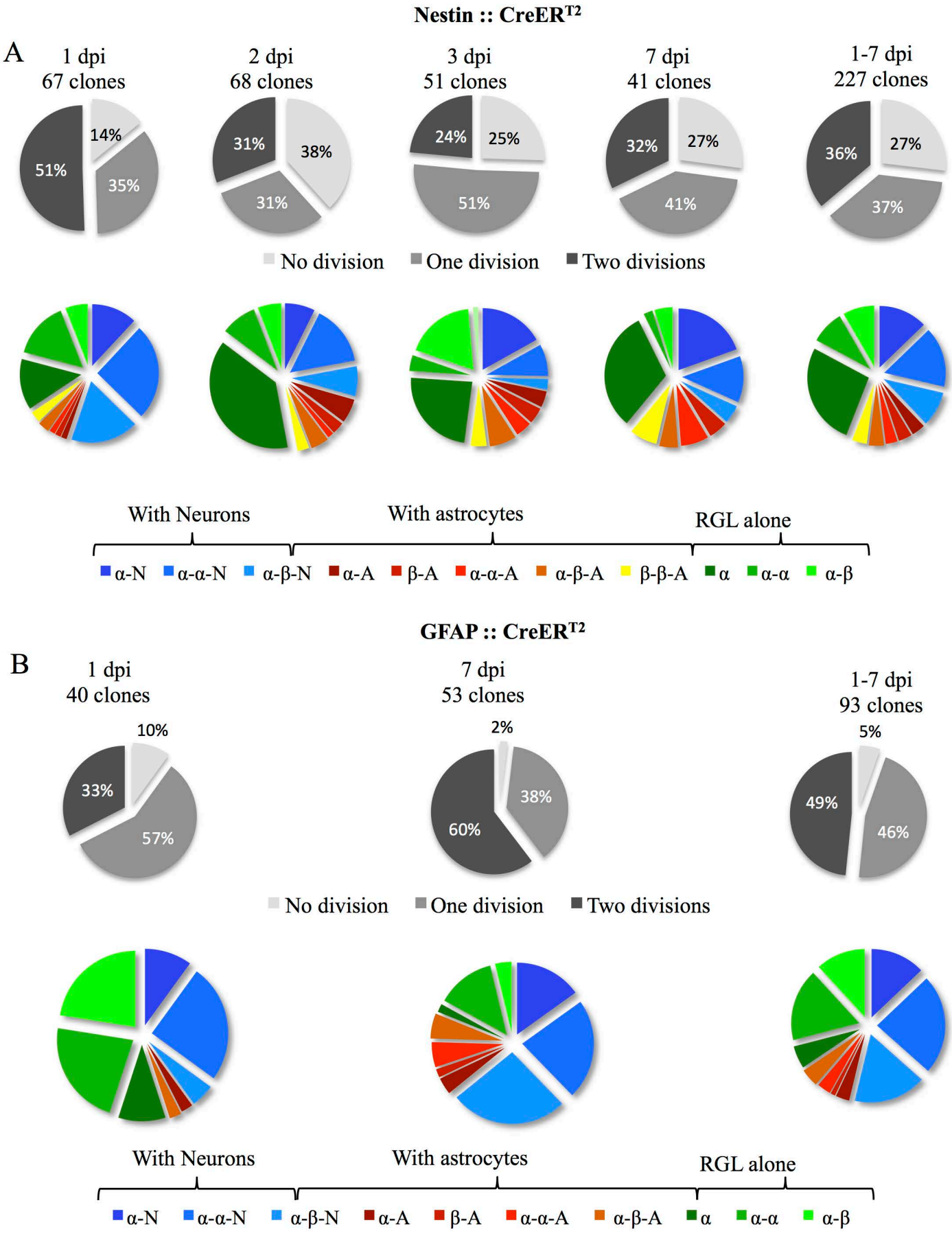

Supplementary figure 5

A

Nestin :: CreER^{T2}

	α-N	β-N	α-α-N	α-β-N	β-β-N	α-A	β-A	α-α-A	α-β-A	β-β-A	α	β	α-α	α-β	β-β
Dpi															
1	8 (3.52 %)	0	17 (7.49 %)	12 (5.29 %)	0	1 (0.44 %)	1 (0.44 %)	1 (0.44 %)	2 (0.88 %)	2 (0.88 %)	9 (3.96 %)	0	10 (4.41 %)	4 (1.76 %)	0
2	5 (2.20 %)	0	10 (4.41 %)	5 (2.20 %)	0	4 (1.76 %)	2 (0.88 %)	1 (0.44 %)	3 (1.32 %)	2 (0.88 %)	26 (11.45 %)	0	6 (2.64 %)	4 (1.76 %)	0
3	8 (3.52 %)	0	4 (1.76 %)	2 (0.88 %)	0	3 (1.32 %)	3 1.32	2 (0.88 %)	2 (0.88 %)	2 (0.88 %)	13 (5.73 %)	0	3 (1.32 %)	9 (3.96 %)	0
7	8 (3.52 %)	0	5 (2.20 %)	2 (0.88 %)	0	0	2 (0.88 %)	3 (1.32 %)	2 (0.88 %)	3 (1.32 %)	13 (5.73 %)	0	1 (0.44 %)	2 (0.88 %)	0
all	29 (12.78 %)	0	36 (15.86 %)	21 (9.25 %)	0	8 (3.52 %)	8 (3.52 %)	7 (3.08 %)	9 (3.96 %)	9 (3.96 %)	61 (26.87%)	0	20 (8.81 %)	19 (8.37 %)	0

B

GFAP :: CreER^{T2}

	α-N	β-N	α-α-N	α-β-N	β-β-N	α-A	β-A	α-α-A	α-β-A	β-β-A	α	β	α-α	α-β	β-β
Dpi															
1	4 (4.30 %)	0	10 (10.75 %)	2 (2.15 %)	0	1 (1.08 %)	0	0	1 (1.08 %)	0	4 (4.30 %)	0	9 (9.68 %)	9 (9.68 %)	0
7	8 (8.60 %)	0	12 (12.90 %)	14 (15.05 %)	0	1 (1.08 %)	1 (1.08 %)	2 (2.15 %)	5 (3.23 %)	0	1 (1.08 %)	0	7 (7.53 %)	2 (2.15 %)	0
all	12 (12.90 %)	0	22 (23.66 %)	16 (17.20 %)	0	2 (2.15 %)	1 (1.08 %)	2 (2.15 %)	6 (6.46 %)	0	5 (5.38 %)	0	16 (17.20 %)	11 (11.83%)	0

Supplementary figure 6

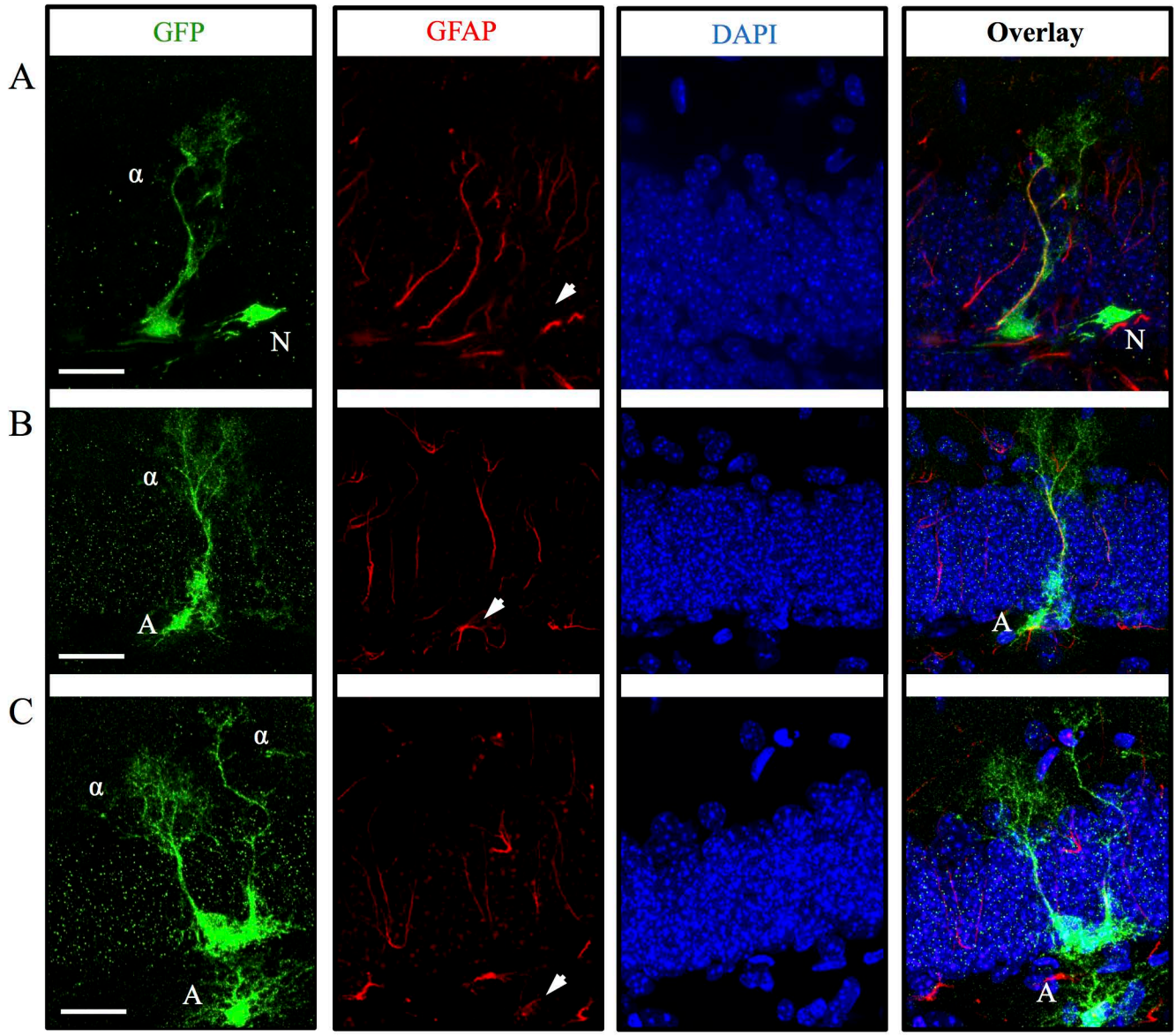

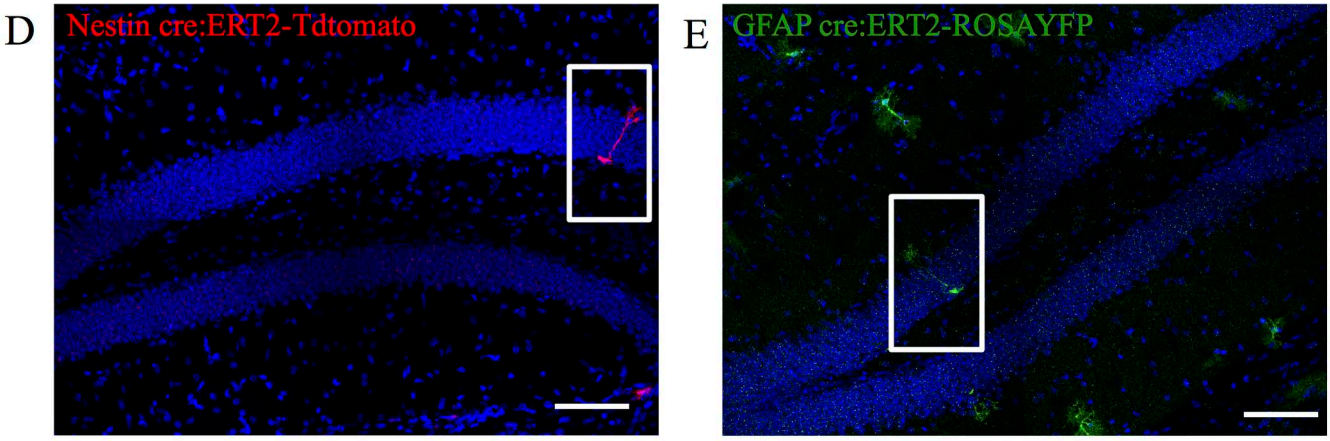

Supplementary figure 7

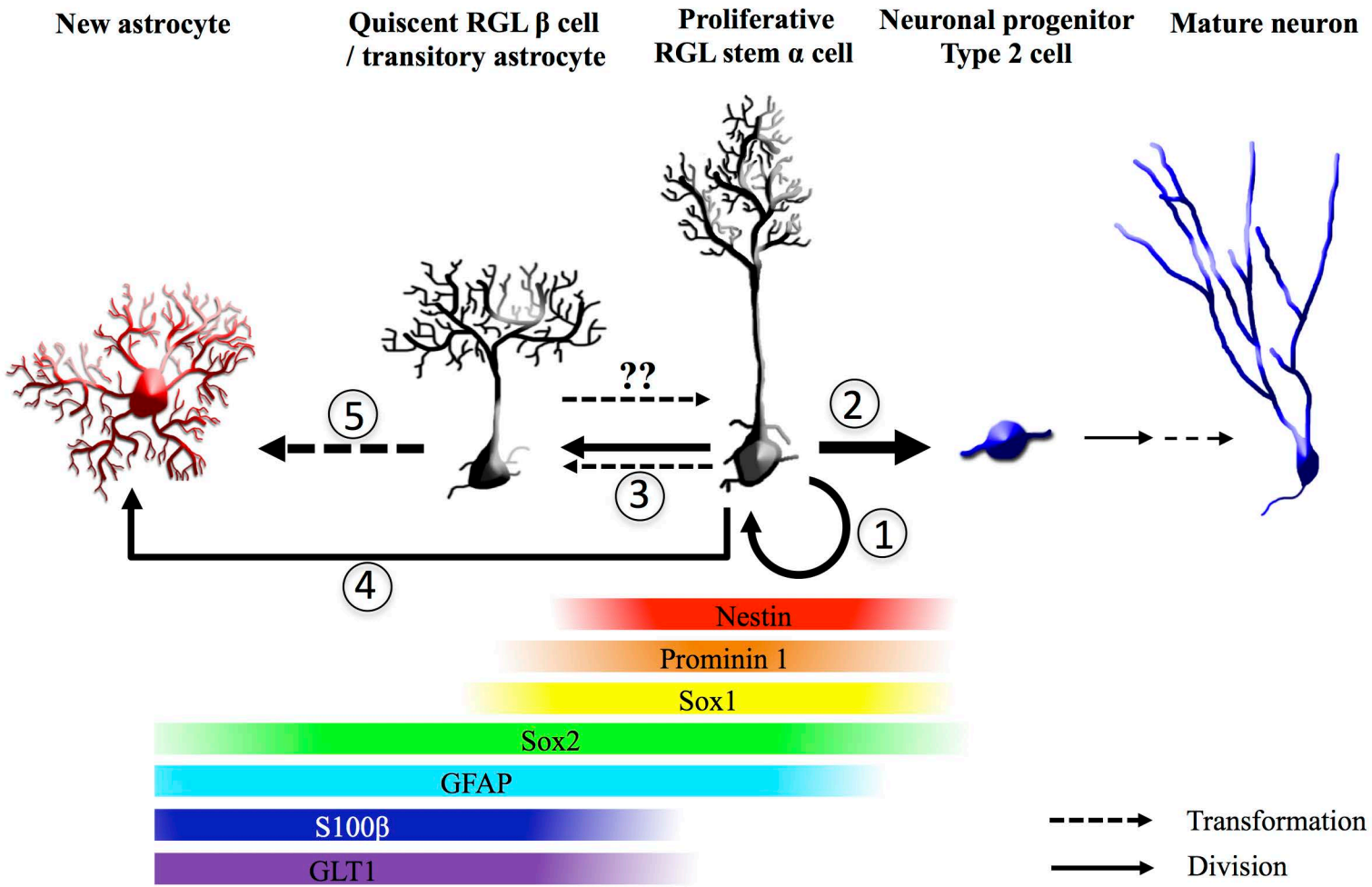

Supplementary Figure 1: Morphological and molecular characterization of type α and type β cells
(**A**) Table of the morphological parameters of type α and type β in both GFAP-GFP and Nestin-GFP mice. Data are the mean value ± SEM. (**B**) Table of the percentage of marker expression in type α and type β cells. In red: Number of cells analyzed.

Supplementary Figure 2: Effect of running on microglia and blood vessels
(**A**) Histogram of the number of $Iba1^+$ cells per dentate gyrus. Bilateral Student's t-test. (**B**) Histogram of the territory area occupied by microglial cells. Bilateral Student's t-test. (**C**) Histogram of the number of branches per microglial cell. Bilateral Student's t-test. (**D**) Confocal maximal projection micrographs of dentate gyrus stained for blood vessels. (**E**) Line graph of the number of pixels per fluorescence intensity of blood vessels in young and young runner mice. (**F**) Histogram of the fluorescence intensity of the peak number of pixels of blood vessels. Bilateral Student's t-test. **p<0.01. ***p<0.001. Scale bar: 100 μm.

Supplementary Figure 3: Effect of running or aging the morphology of type α and type β cells:
(A-D) Scatter graphs representing the dimensions of RGL cells in young mice (**A**), young mice exposed to running wheel (**B**), old mice (**C**) and old mice exposed to running wheel (**D**).

Supplementary Figure 4: Clonal analysis of type α and type β cells
(A) Pie charts of the quantitative comparison of the frequency of division (No division, one or two divisions), and the frequency of different clone types (α, α-α, α-β, α-N, α-α-N, α-β-N, α-A, β-A α-α-A, α-β-A, β-β-A) at 1, 2, 3,7dpi and all time points in Nestin::$CreER^{T2}$ mice **(B)** Pie charts of the quantitative comparison of the frequency of division (No division, one or two divisions), and the frequency of different clone types (α, α-α, α-β, α-N, α-α-N, α-β-N, α-A, β-A α-α-A, α-β-A, β-β-A) at 1,7dpi and all time points in GFAP::$CreER^{T2}$ mice.

Supplementary Figure 5: Clones containing type α and type β cells
(**A**-**B**) Table representing all clones analyzed in Nestin-GFP mice (**A**) and in GFAP-GFP mice (**B**). Numbers indicate number of clones analyzed and in brackets are the proportion of each clone.

Supplementary Figure 6: Identification of clones and progenies
(**A**) Confocal micrograph of type α cell with a $GFAP^-$/type 2 neural progenitor cell (N). (**B**) Confocal micrograph of type α cell with a $GFAP^+$/astrocyte. (**C**) Confocal micrograph of 2 type α cells with a $GFAP^+$/astrocyte. (**D**) Low magnification confocal micrograph of Nestin Cre::ER^{T2}-td-tomato mouse (left) and a GFAP Cre::ER^{T2}-ROSA-YFP mouse (right). Scale bars: 20 μm (panels A-C) and 100 μm (panels D, E).

Supplementary Figure 7: Model of type α and type β cells lineage relationship
Model of the lineage relationship of type α and type β cells in the adult mouse hippocampus under basal conditions. Type α cells can self-renew (1) and also generate type 2 neural progenitors (2), type β cells (3) and astrocytes (4). Type β cells do not divide, but may revert to type α cell (??) or transform into astrocytes (5). Also shown are marker expression.

A2

Fine processes of Nestin-GFP-positive radial glia-like stem cells in the adult dentate gyrus ensheathe local synapses and vasculature

Fine processes of Nestin-GFP–positive radial glia-like stem cells in the adult dentate gyrus ensheathe local synapses and vasculature

Jonathan Moss[a], Elias Gebara[a], Eric A. Bushong[b], Irene Sánchez-Pascual[a], Ruadhan O'Laoi[a], Imane El M'Ghari[a], Jacqueline Kocher-Braissant[a], Mark H. Ellisman[b], and Nicolas Toni[a,1]

[a]Department of Fundamental Neurosciences, University of Lausanne, 1005 Lausanne, Switzerland; and [b]National Center for Microscopy and Imaging Research, University of California, San Diego, La Jolla, CA 92093

Edited by Heather A. Cameron, National Institute of Mental Health/National Institutes of Health, Bethesda, MD, and accepted by the Editorial Board March 16, 2016 (received for review July 29, 2015)

Adult hippocampal neurogenesis relies on the activation of neural stem cells in the dentate gyrus, their division, and differentiation of their progeny into mature granule neurons. The complex morphology of radial glia-like (RGL) stem cells suggests that these cells establish numerous contacts with the cellular components of the neurogenic niche that may play a crucial role in the regulation of RGL stem cell activity. However, the morphology of RGL stem cells remains poorly described. Here, we used light microscopy and electron microscopy to examine Nestin-GFP transgenic mice and provide a detailed ultrastructural reconstruction analysis of Nestin-GFP–positive RGL cells of the dentate gyrus. We show that their primary processes follow a tortuous path from the subgranular zone through the granule cell layer and ensheathe local synapses and vasculature in the inner molecular layer. They share the ensheathing of synapses and vasculature with astrocytic processes and adhere to the adjacent processes of astrocytes. This extensive interaction of processes with their local environment could allow them to be uniquely receptive to signals from local neurons, glia, and vasculature, which may regulate their fate.

adult neurogenesis | adult neural stem cell | neurogenic niche | electron microscopy | hippocampus

Neurogenesis in the adult mouse brain primarily occurs within discrete niches, the subventricular zone (SVZ), and the subgranular zone (SGZ) of the dentate gyrus, supplying new neurons to the olfactory bulb and the dentate gyrus, respectively (1–3). Neural stem cells of these niches can be activated to divide and generate other stem cells, astrocytes, or new neurons (4, 5). Newborn neurons of the dentate gyrus have the capacity to integrate into the existing hippocampal circuitry (6–8), influencing processes such as learning and memory (9–11) as well as stress and depression (12).

Radial glia-like (RGL) neural stem cells of the SVZ, which supply the olfactory bulb with newborn neurons and astrocytes, express astrocytic markers and form elegant pinwheel structures (13–16). RGL neural stem cells of the adult dentate gyrus also express astrocytic markers, but comprise a heterogeneous population based on the molecular markers they express, the morphologies they exhibit (17–22), and their fate (23–28). Nestin-GFP–positive RGL stem cells account for more than 70% of RGL stem cells in the SGZ of the dentate gyrus (24), but it was recently found that not all Nestin-GFP–positive cells with RGL morphology have stem cell properties (29): type β cells, which arborize in the granule cell layer (GCL) but do not reach the molecular layer (ML) of the dentate gyrus, account for 26% of Nestin-GFP–positive RGL stem cells. They express stem cell (Sox1, Sox2, Prominin 1, GFAP, and Nestin) and astrocytic [GFAP, glial glutamate tranporter 1 (GLT1), and S100β] markers but do not proliferate. In contrast, type α cells, which extend across the GCL and arborize in the inner ML, account for 74% of Nestin-GFP–positive RGL cells. They express stem cell markers such as Sox1, Sox2, Prominin 1, GFAP, and Nestin, but neither S100β nor GLT1. Fate clonal analysis shows that these cells are able to proliferate and generate more type α cells, type 2 neuronal progenitors, astrocytes, and nonproliferative type β cells. In this study, we therefore focused on type α Nestin-GFP–positive RGL stem cells (hereafter referred to as NGPα RGL stem cells), which form dense arborizations of fine processes in the inner ML.

So why do these NGPα RGL stem cells have such a complex radial morphology? Embryonic cortical stem cells have smooth spheroid cell bodies that extend long smooth processes, which enable newly formed neurons to migrate into the cortical plate (30). In the adult dentate gyrus, however, the observation of individual clones suggest that adult-born neurons do not migrate alongside the radial process of their mother cells, but instead migrate tangentially away from it, before integrating into the GCL (24, 31). We therefore believe that the reasons for their complex radial morphologies lie in the regulatory mechanisms of the neurogenic niche. Adult neurogenesis is tightly regulated by the neurogenic niche, primarily restricting it to the SGZ and the SVZ, despite the neurogenic potential of progenitors that can be found throughout the central nervous system (32–34). The niche is vital for adult neurogenesis, and we suspect the elaborate morphology of RGL stem cells is key for their regulation by elements of the neurogenic niche (29, 35).

Significance

A population of adult neural stem cells supplies the dentate gyrus with new neurons that play a role in mechanisms of learning and memory. Radial glia-like stem cells have a unique morphology, including a dense arbor of fine processes that infiltrate the neurogenic niche. Here, we provide what is, to our knowledge, the first detailed ultrastructural description of these processes, and we reveal that these cells establish a variety of contacts with local blood vessels, synapses, and astrocytes. Given that signals derived from neurons, astrocytes, and blood vessels regulate the process of adult neurogenesis, the identification of these contacts provides a structural framework for elucidating the mechanisms by which this regulation occurs. These results contribute to a greater understanding of the adult hippocampal neurogenic niche.

Author contributions: J.M. and N.T. designed research; J.M., E.G., E.A.B., I.S.-P., R.O., I.E.M., and J.K.-B. performed research; E.A.B. and M.H.E. contributed new reagents/analytic tools; J.M. analyzed data; and J.M. and N.T. wrote the paper.

The authors declare no conflict of interest.

This article is a PNAS Direct Submission. H.A.C. is a guest editor invited by the Editorial Board.

[1]To whom correspondence should be addressed. Email: nicolas.toni@unil.ch.

This article contains supporting information online at www.pnas.org/lookup/suppl/doi:10.1073/pnas.1514652113/-/DCSupplemental.

We use a variety of light microscopy (LM) and EM techniques to probe the fine anatomical structure of NGPα RGL stem cells and their contacts with the neurogenic niche. We describe in detail the relationship of NGPα RGL stem cell processes with the local vasculature, glia, and neurons in an effort to better understand the role their structure could play in the context of adult neurogenesis.

Results

NGPα RGL Stem Cell Processes Reflect Their Environment. To examine the morphology of the NGPα RGL stem cells in the dentate gyrus, we used Nestin-GFP transgenic mice (36, 37). Immunohistochemistry allowed us to render the GFP-positive cells electron-dense with a 3,3′-diaminobenzidine (DAB)-peroxidase reaction for visualization at LM and EM levels (*Materials and Methods*). Strong labeling of cells in the dentate gyrus was evident at the LM level (Fig. 1*A*), with dark bands of NGP RGL stem cell bodies and type 2 precursors delineating the SGZ between the hilus and GCL. Single NGPα RGL stem cells ($n = 7$; *Materials and Methods*) were selected from the population for examination when the majority of their processes were contained within one 50-μm section (Fig. 1*B*). First, this allowed us to confirm the identity of the given NGPα RGL stem cell, as Nestin can label other cell types in the dentate gyrus (36), but none with the same distinctive morphology of NGPα RGL stem cells. Second, the systematic tracing in 3D of all processes in the ML until their point of origin in the main process of the identified NGPα RGL stem cell enabled us to confirm their identity. Third, restricting our analyses to cells contained within one section maximized the proportion of each cell that could be examined.

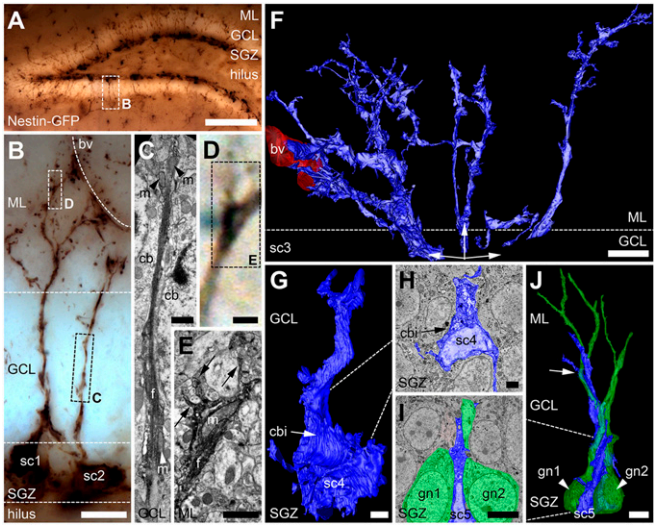

Fig. 1. RGL stem cell processes reflect their environment. (*A*) Dentate gyrus, immunoperoxidase-labeled for GFP, shows dark RGL stem cells and type 2 progenitor cells in the SGZ. (*B*) Two NGPα RGL stem cells (sc1 and sc2) from *A* extend their primary processes across the GCL that branch at the border of the ML, with some branches approaching a blood vessel (bv). (*C*) Detail from *B*: EM frame shows primary process of RGL stem cell (sc2) replete with filamentous fibers (f), constricted by two cell bodies (cb) in the GCL. Before and after the constriction, mitochondria (m) can be seen inside the process. (*D* and *E*) Detail from *B*: correlative LM (*D*) and EM (*E*) images of a mitochondria-containing portion of the process (m) where intracellular fibers (f) terminate, and finer processes (arrows) extend into the ML. (*F*) Processes of a single RGL stem cell (sc3) reconstructed from 178 SBF-SEM images. Three processes extend toward a local blood vessel (bv, red; Movie S1). (*G* and *H*) Three-dimensional reconstruction (*G*) from SBF-SEM images (*H*) of an RGL stem cell (sc4, blue) with neighboring cell body indentations (cbi; Movie S2). (*I* and *J*) Three-dimensional reconstruction of an RGL stem cell (sc5, blue) and its primary process (arrow) alongside two granule neurons (gn1 and gn2, green; Movie S3). (Scale bars: *A*, 100 μm; *B*, 10 μm; *C*–*E*, 1 μm; *F*, *I*, and *J*, 5 μm; *G* and *H*, 2 μm.)

Initial analyses showed that the primary processes of NGPα RGL stem cells, that extended across the GCL, were a key feature. Under the light microscope, they ostensibly appeared thicker and straighter than the subsequent secondary and tertiary processes in the ML (Fig. 1*B*). However, by using serial section transmission EM (TEM) and 3D reconstructions, primary processes were seen to twist and turn and expand and contract to infiltrate between the cell bodies of granule neurons (Fig. 1*C*). This is in contrast to the thinner and straighter processes of type 3, doublecortin-positive cells that also extend across the GCL (38). In the thinnest regions, only filamentous fibers occupied the process. Thicker, mitochondria-containing portions of the primary process gave rise to secondary branches (see also ref. 20). When the primary process had breached the border between the GCL and ML, extensive branching created large arbors of fine processes. Larger branches gravitated toward local blood vessels (Fig. 1*B*), whereas finer processes infiltrated the local neuronal and glial architecture (Fig. 1 *D* and *E*). The arborization of fine processes was generally confined to the inner third of the ML, but, occasionally, long fine threads reached as far as the outer third of the ML.

To complement our TEM observations, we used serial block-face scanning EM (SBF-SEM) (39) to image and reconstruct in 3D the fine ML processes of a single NGPα RGL stem cell (Fig. 1*F* and Movie S1). This reconstruction, and the individual frames from which it was created, revealed a great many features that could have been missed with the smaller sample sizes of TEM (Fig. S1*A*). The most obvious of these features was that larger ML secondary processes covered the surfaces of mature granule cell dendrites as they grew radially. This created the effect of processes forming a series of tunnels through which the mature dendrites extended (Fig. S1 *B*–*D*). Likewise, processes at the GCL–ML border displayed large concave surfaces, where they were positioned around the side of granule cell bodies (Fig. S1*E*). In addition to this main observation, several other features were worth noting: (*i*) a thick secondary process, on the edge of the ML, expanded to completely enclose a dendritic spine and the axons apposing the head of the spine (Fig. S1 *E* and *F*); (*ii*) a large process, extending toward a blood vessel, thinned into a sheet-like process between the edge of a cell body and large dendritic shaft (Fig. S1 *G* and *H*); and (*iii*) a thin sheet-like process extended tangentially, from a small radial process, and wrapped a number of axons along its path (Fig. S1 *I* and *J*).

The cell bodies of NGPα RGL stem cells took on three main morphologies: (*i*) they appeared pyramidal in nature, when their upper extreme was confined between the bases of granule neuron cell bodies of the GCL, and their lower extremes extended with greater freedom within the SGZ (Fig. 1 *G* and *H* and Movie S2); (*ii*) when their cell body sat entirely below the GCL, it appeared spheroid in shape (Fig. 1*B*, *sc2*); and (*iii*) on other occasions, the cell body was effectively sandwiched between two granule neuron cell bodies, and took on an hourglass-like conformation (Fig. 1 *I* and *J* and Movie S3). For all three morphologies, the surfaces of the stem cell body appeared concave, where granule neuron cell bodies impinged upon it, with ridges in between. Their nuclei almost completely filled the cytoplasm of the cell body and, as a result, took on the shape of the cell bodies themselves. Basal processes extended from the corners of their cell body, along the axis of the SGZ and into the hilus, and the primary process of the stem cell followed the dendrites of mature granule cells as they traversed the GCL.

Large NGPα RGL Stem Cell Processes Wrap Local Blood Vessels. One of most striking features of NGPα RGL stem cell morphology at LM and EM levels is their affinity to extend large processes toward local blood vessels (17, 19, 20, 29, 36), as visualized with

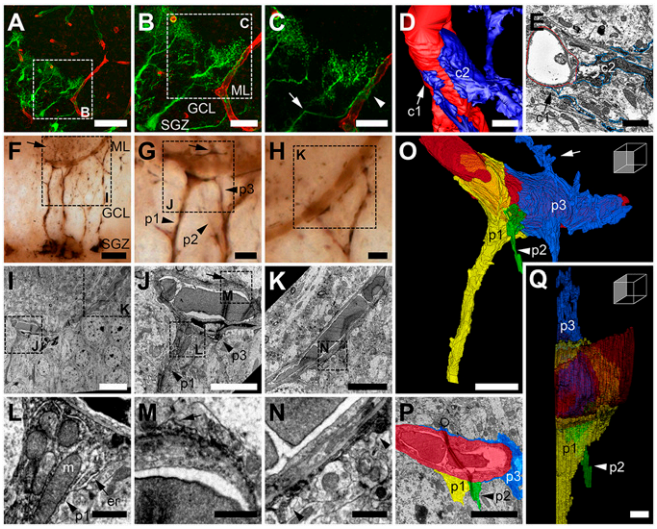

Fig. 2. RGL stem cell processes wrap blood vessels. (*A*–*C*) Confocal microscopy images of an NGPα RGL stem cell (green) branching toward (arrow) and contacting (arrowhead) a blood vessel (red; sulforhodamine 101). (*D*) Processes from a NGPα RGL stem cell (blue) making endfeet-like contacts (c1 and c2) with a local blood vessel (red); image 3D-reconstructed from SBF-SEM frames (*E*). (*F*) LM image of several NGPα, peroxidase-labeled RGL stem cells extending processes toward a blood vessel. (*G* and *H*) Higher-magnification images of *F*, with processes 3D-reconstructed in *O*–*Q* identified (p1–p3). (*I*–*K*) Correlative EM images of the interaction seen at the LM level in *F*–*H*. Arrows in *F*, *G*, *J*, *M*, and *O* show where the wrapping process (p3) extends beyond the blood vessel. (*L*) Detail from *J* shows mitochondria (m) and endoplasmic reticulum (er) clustered where process p1 spreads to ensheathe the blood vessel. (*M* and *N*) Detail from *J* and *K* showing thin wrapping of the blood vessel. (*O*–*Q*) Three-dimensional reconstruction (*O* and *Q*) and single EM frame (*P*) of the three processes (p1–p3) from two NGPα RGL stem cells (cell 1, p1, yellow; cell 2, p2, green; and cell 2, p3, blue) contacting/wrapping the blood vessel (red), originally seen in *F*, *G*, *I*, and *J* (Movie S4). (Scale bars: *A*, 50 μm; *B* and *F*, 20 μm; *C* and *I*, 10 μm; *D* and *E*, 2 μm; *G* and *H*, 5 μm; *J*, *K*, *O*, and *P*, 5 μm; *L*–*N* and *Q*, 1 μm.)

confocal microscopy (Fig. 2 *A*–*C*). For EM analyses of this interaction, we used DAB-peroxidase labeling of GFP in the Nestin-GFP mouse. Three-dimensional reconstruction of a single NGPα RGL stem cell (Fig. 2*D*) from serial SBF-SEM images (Fig. 2*E*) demonstrated its propensity to extend several large processes to contact the surface of a local blood vessel. These interactions ranged from small contacts (1–2 μm across), akin to astrocytic endfeet, up to larger sheet-like contacts that spread extensively (over 10 μm) across the surface of the blood vessel. NGPα RGL stem cells examined in a previous study were all shown to possess at least one interaction with a blood vessel (29). In the present study, we found that, if an ML blood vessel was situated only on one side of where the process emerged from the GCL, thick processes would polarize toward the blood vessel (Fig. 1 *B* and *F*). Conversely, stem cell process arbors would remain relatively symmetrical if blood vessels were (*i*) situated further from the emergence point, (*ii*) on both sides of the emergence point (at equal distances), or (*iii*) growing along the GCL–ML border (Fig. 2*F*).

To analyze how multiple NGPα RGL stem cell processes wrapped an individual blood vessel at the GCL–ML border, a region of tissue was selected for correlative LM/EM (Fig. 2*F*). This region contained an area where multiple processes from multiple NGPα RGL stem cells converged onto the blood vessel (Fig. 2*G*) and also an area where fewer processes approached the blood vessel (Fig. 2*H*). For larger processes, contacting or wrapping of the blood vessel did not represent the termination of their radial path, as finer processes branched beyond the blood vessel (Fig. 2 *F*, *G*, *J*, *M*, and *O*). EM analysis (i.e., TEM) of how the NGPα RGL stem cell process contacted the blood vessel revealed several key aspects of the interaction (Fig. 2 *I*–*N*). At the point where the primary process first met the blood vessel, the process expanded as it spread across the vessel surface (Fig. 2*J*), and within the expanded process sat a host of mitochondria and strings of endoplasmic reticulum (Fig. 2*L*). As processes wrapped the blood vessels, they thinned dramatically (Fig. 2 *J*, *K*, *M*, and *N*), but their coverage of the blood vessels was extensive.

Tracing these thin processes in serial EM sections and reconstructing them in 3D (Fig. 2 *O*–*Q*) revealed that they represented thin sheets of process that covered large areas of the blood vessel surface. Very few mitochondria were present within these thin sheets, perhaps explaining why so many were clustered at its point of origin (Fig. 2*L*), given the likely energy demands of possessing such an expansive morphology. The 3D reconstruction (Fig. 2 *O*–*Q* and Movie S4) showed three NGPα RGL stem cell processes, from two different cells, converging upon the same blood vessel and apposing each other along its surface. Of these three, two (Fig. 2 *O*–*Q*, p1 yellow and p3 blue) were larger processes that formed thin sheets and extended into fine processes beyond the blood vessel. The other (Fig. 2 *O*–*Q*, p2 green) branched from the same primary process as one of the larger processes (Fig. 2 *O*–*Q*, p3 blue) but had a much more restricted interaction with the blood vessel.

NGPα RGL Stem Cells and Astrocytes Share Blood Vessel Coverage. Processes of NGPα RGL stem cells covered much of the blood vessel surface, especially when the vessel was situated adjacent to the primary process emerging from the GCL. However, even in these regions, not all of the blood vessel was covered by the processes of a given labeled stem cell. The unlabeled processes covering the remainder of the blood vessel surface were similar in appearance to labeled processes, suggestive of a glial origin. Indeed, when they were examined in serial sections and 3D and traced to their larger processes and cell bodies in the ML, their morphologies were unmistakably those of astrocytes, characterized by bundles of filaments, granules of glycogen, a relatively pale cytoplasm, and condensations of chromatin inside the nuclear envelope (Fig. 3*A*) (40).

Astrocytes of the ML of the dentate gyrus and other regions of the hippocampus can position their cell bodies directly adjacent to blood vessels, completely enclosing large sections of a vessel (41, 42). However, in the vicinity of an NGPα RGL stem cell process emerging from the GCL, astrocytic coverage of the blood vessel was not always complete; the two types of process shared coverage of the blood vessel (Fig. 3*A*). The thickness of the stem cell process would expand and match the thickness of the astrocytic process, and form adhesion points where they met on the surface of the blood vessel, in direct contact with the basal lamina.

When blood vessels were more distant from the astrocyte cell body, multiple astrocytic processes shared the surface of the blood vessel, along with multiple NGPα RGL stem cell processes (Fig. 3 *B*–*D*). Examining the surface of a GCL–ML border blood vessel in cross-section, through 92 serial EM sections (each 70 nm thick), showed coverage by five stem cell processes and four astrocytic processes (Fig. 3 *E*–*R* and Movie S5). Along this section of blood vessel, the proportion of its surface covered by the stem cell process varied from approximately 50% to nearly 100% in individual sections (Fig. 3 *F*–*K*). Similar to the wrapping of the blood vessel by stem cell processes, astrocytic processes sometimes contacted the vessel with small endfeet (Fig. 3 *J* and *L*–*R*, astro2), and, on other occasions, contacts were made by large sheet-like processes (Fig. 3 *I* and *L*–*R*, astro3).

Fine Processes of NGPα RGL Stem Cells Approach Local Synapses. The primary or secondary processes of NGPα RGL stem cells split into a multitude of fine processes at the GCL–ML border, creating

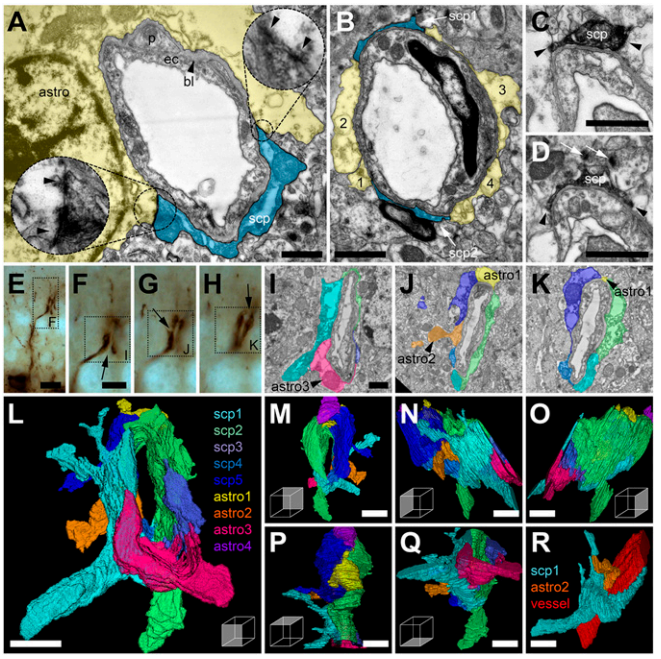

Fig. 3. RGL stem cell and astrocytic processes share coverage of blood vessels. (*A*) EM of an NGPα RGL stem cell process (scp, blue) wrapping a blood vessel in the inner ML that is also covered by astrocytic processes (astro, yellow): endothelial cell (ec), pericyte (p), basal lamina (bl). (*Insets*) Adhesion point densities (arrowheads) between astrocyte and stem cell processes. (*B*) Astrocytic processes (*1–4*, yellow) cover the blood vessel surface alongside NGPα RGL stem cell processes (scp1 and scp2, blue). (*C* and *D*) Serial sections of *B* show adhesion points (arrowheads) between NGPα RGL stem cell (scp) and astrocyte processes (*C*), and the same stem cell process extending toward synapses (arrows, *D*). (*E–H*) LM of an NGPα RGL stem cell wrapping a blood vessel at the GCL–ML border, seen at higher magnification in three different focal planes (*F–H*). Arrows in *F–H* point to the gaps in the stem cell process wrapping that correspond to the astrocytes seen in the EM frames (*I–K*). Processes are colored according to the key in *L*. (*L–R*) Three-dimensional reconstruction and alternate views of the five NGPα RGL stem cell processes and four astrocytic processes (Movie S5) that wrap the blood vessel depicted in *E–K*. (*R*) One astrocyte and one NGPα RGL stem cell process are shown with the blood vessel. (Scale bars: *A–D* and *I–K*, 1 μm; *E*, 10 μm; *F–H*, 5 μm; *L–R*, 2 μm.)

a dense arbor of intertwining fibers (Fig. 4 *A* and *B*) (17, 19, 20). Branching occurred abruptly, with stubs of large primary or secondary processes sprouting many fine processes. The fine processes took the form of long-reaching tendrils studded with varicosities (Fig. 4*B*). The varicosities were similar to those seen in the finest of thin neuronal dendrites, when the dendrite swells to incorporate small mitochondria at regular points along its length. When NGPα RGL stem cell process varicosities were analyzed at the EM level (Fig. 4 *C–E*), the vast majority contained a single mitochondrion, but notably the mitochondrion did not define the size of the varicosity. On average, the mitochondrion would only occupy 28% of the whole varicosity (±3%, SEM; $n = 10$; Fig. 4*F*). This raises the possibility that other intracellular machinery is occupying the remaining 72% of the varicosity, perhaps suggesting that varicosities represent a site for intercellular signaling.

To investigate this possibility further, we labeled NGPα RGL stem cells with immunogold particles. This allowed a greater visualization of the intracellular constituents than was possible with the DAB-peroxidase method, which fills the intracellular space with a dark diffuse reaction product. No evidence was found for any degree of synaptic contact with the immunogold-labeled varicosities, or any other part of the immunogold-labeled NGPα RGL stem cells. This does not rule out the presence of nonsynaptic receptors and associated intracellular machinery. Additionally, when a string of varicosities was viewed at the EM level, traced, and reconstructed in 3D (Fig. 4 *G–I* and Movie S6), three observations were made: (*i*) the radial process apposed and followed the primary and secondary dendrite of a mature granule neuron, as reported previously (38); (*ii*) fine processes extended from the varicosities to wrap local axons (Fig. 4 *J* and *K*); and (*iii*) some of these fine processes approached the synaptic cleft of local asymmetrical synapses, some of which were made with the spines of the granule cell dendrite the stem cell process was following (Fig. 4 *L* and *M*). It is possible that a common neuron-stem cell signaling mechanism underlies these three associations.

Fine Processes Ensheathe Asymmetrical Synapses. To more closely examine the association of fine NGPα RGL stem cell processes with local ML asymmetrical synapses, four NGPα RGL stem cells were selected from the dentate gyri of three Nestin-GFP DAB-peroxidase–labeled animals and then sectioned for EM analysis. It was possible to distinguish two types of interactions made by the varicosities with local asymmetrical synapses, although, in essence, they probably represent the extremes of a continuum. First, the varicosity itself wrapped its surfaces around

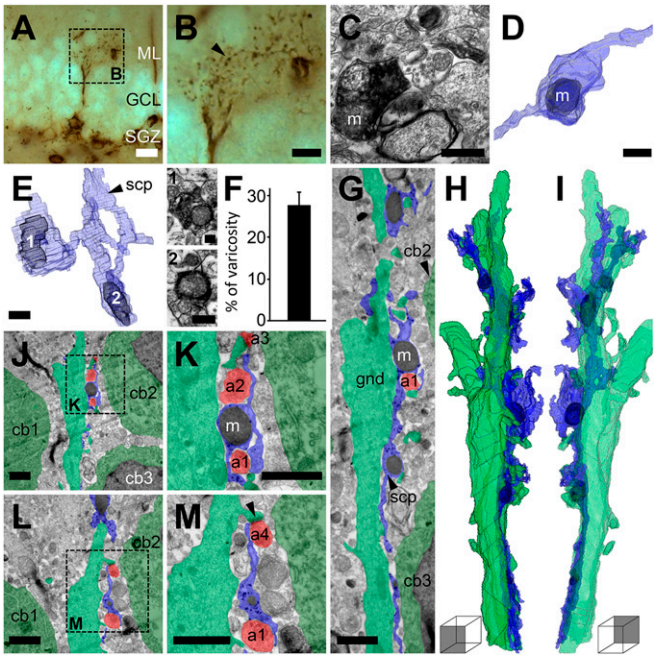

Fig. 4. Fine processes extend from varicosities of RGL stem cell processes to approach local synapses. (*A*) An NGPα DAB-peroxidase–labeled RGL stem cell selected for analysis of its fine process arbor at the GCL–ML border. (*B*) Higher-magnification view of the fine processes branching from primary and secondary processes. A fine process that resembles a long beaded string, because of the presence of varicose regions, extends toward a blood vessel (right). One mitochondrion-containing (m) varicosity from this string (arrowhead) was selected for EM analysis (*C*) and reconstruction in 3D (*D*). (*E*) Most varicosities included one mitochondrion, which rarely filled the varicosity (as in *E*, *2*), but more readily occupied one-quarter to one-third of the volume (*E*, *1*). (*F*) Mitochondria occupied 28 ± 3% (mean ± SEM) of the varicosity on average ($n = 10$). (*G*) Immunogold labeling of NGPα RGL stem cell processes (scp, blue) from the GCL–ML border (granule neuron cell bodies, cb1–cb3, dark green; nuclei in black) apposed to the side of a granule neuron dendrite (gnd, light green). Serial sections of image in *G* are reconstructed in 3D and shown from both sides (*H* and *I*; Movie S6). Mitochondria-containing (m, black) varicosities extend processes, which wrap local axons (a1 and a2, red; *J* and *K*) or approach the synapses (arrowhead) formed by local axons (a3 and a4, red) with the granule neuron dendrite (*J–M*). (Scale bars: *A*, 20 μm; *B*, 10 μm; *C–E*, 0.5 μm; *E*, *1*, and *E*, *2*, 0.2 μm; *G–M*, 1 μm.)

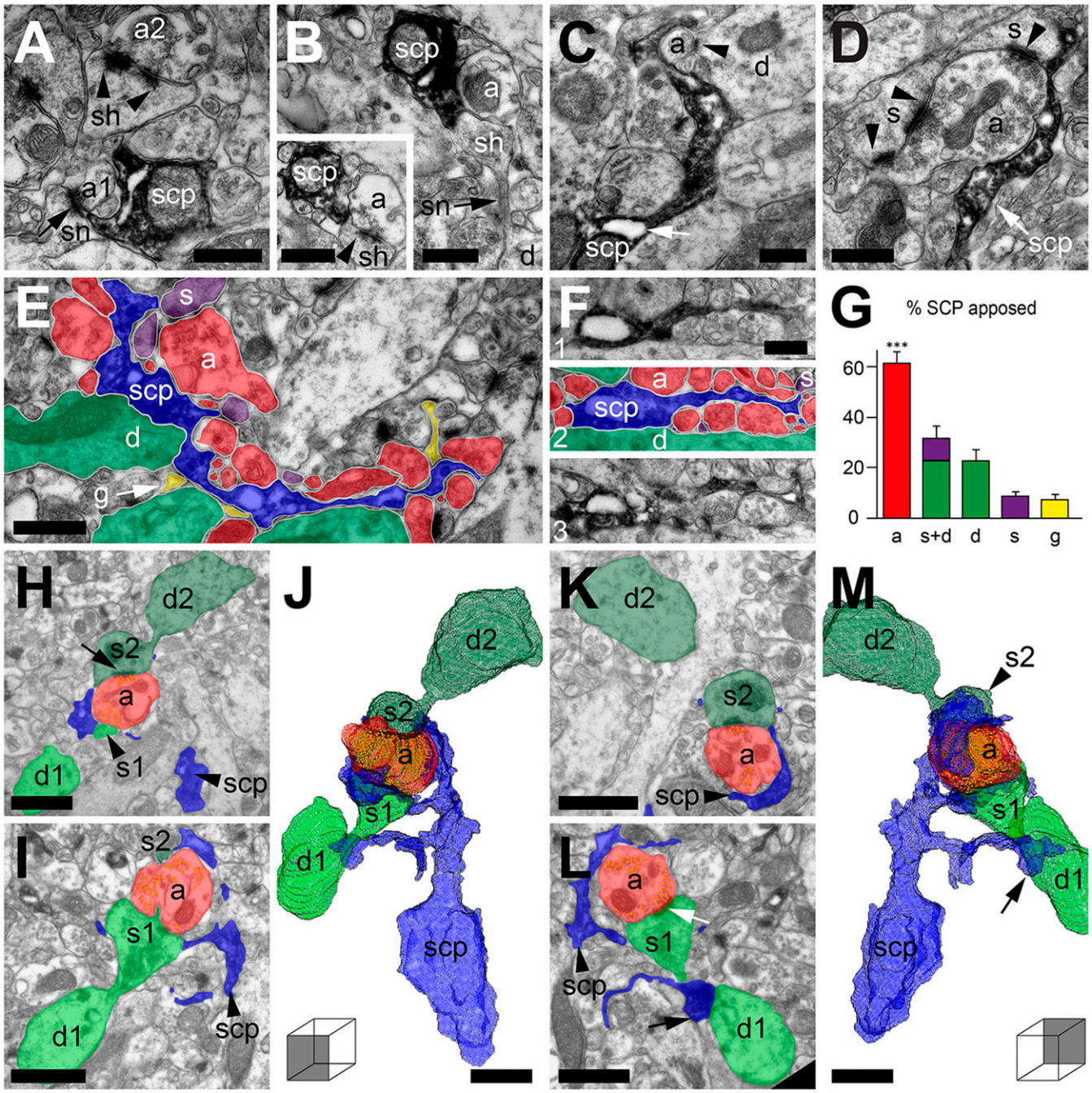

Fig. 5. RGL stem cell processes wrap local axons and synapses. (*A*) A DAB-labeled NGPα RGL stem cell process (scp) varicosity wrapping an axon (a1) forming an asymmetrical synapse (arrow) with a dendritic spine neck (sn). Arrowheads point to a second synapse made with the head of the same spine (sh). (*B*) An NGPα RGL stem cell varicosity directly apposing a spine head, extending from dendrite (d). (*Inset*) Adjacent section showing asymmetrical synapse (arrowhead). (*C*) A process from an NGPα RGL stem cell varicosity, wrapping an axon (a) and an asymmetrical synapse (arrowhead). Note also the reticulum-like inclusion (arrow) seen in the varicosity. (*D*) An NGPα RGL stem cell process wrapping a large axon terminal that forms asymmetrical synapses (arrowheads) with two dendritic spines (s). (*E*) An NGPα RGL stem cell process and the structures it apposes: axons (a), dendritic shafts (d), dendritic spines (s), and glia (g). (*F*) As for *E*, but the stem cell process (blue) apposes mainly axons (red) in its local vicinity. The adjacent serial sections (*1* and *3*) are shown without color overlays for comparison. (*G*) Proportion of varicosity membrane apposed by different structures [mean ± SEM of 10 varicosities, from four cells of three animals, 150 serial sections in total; one-way ANOVA with post hoc Dunnett test; $F_{(4,49)} = 31.38$, $P < 0.001$]. (*H–M*) Three-dimensional reconstruction (*J* and *M*; viewed from two angles; Movie S7) from serial EM frames, samples of which can be seen in *H*, *I*, *K*, and *L*. An NGPα RGL stem cell process (blue) wraps an inner ML axon terminal (red; vesicles in yellow), which forms asymmetrical synapses (arrows in *H* and *L*). (Scale bars: 0.5 μm.)

apposing synapses (Fig. 5 *A* and *B*). Varicosity surfaces therefore took on a concave form, as they arched around the mainly convex structures of small axon terminals and dendritic spines. Second, processes of varying lengths extended from the varicosities toward local asymmetrical synapses in a similar fashion to astrocytic processes (Fig. 5 *C* and *D*). Sometimes the association with the synapse was only one of apposing the edge of the synaptic cleft, but, other times, the process wrapped around the

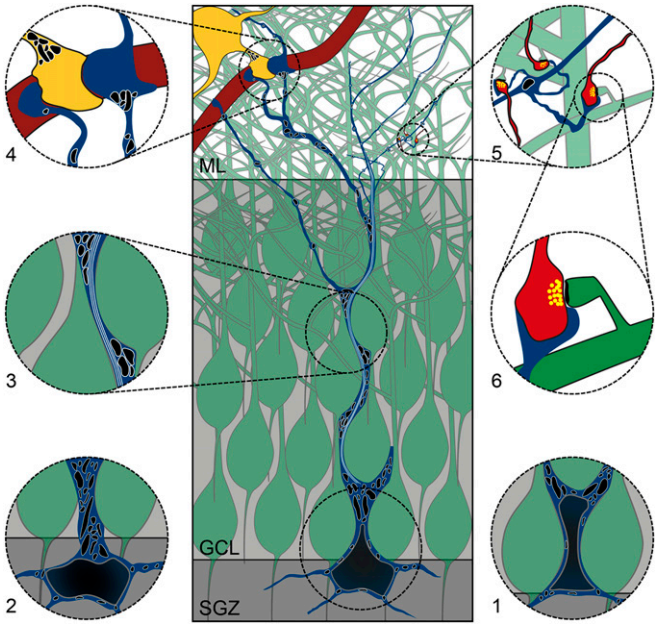

Fig. 6. RGL stem cell interactions with neuronal, vascular, and glial cells. The soma of the NGPα RGL stem cell (blue) sits above (*1*), across (*Center*), or below (*2*) the border of the SGZ and GCL, and takes different shapes. The primary process of the stem cell extends through the GCL (*3*), with its path and surface impacted on by granule neurons (green). Mitochondria (black) reside in the thicker parts of the process, but, in thinner regions, there is space only for the filaments (white) to grow through the process (*3*). Some processes in the ML make small endfeet-like contacts onto blood vessels (dark red) or wrap large thin sheets around them, sometimes continuing beyond the vessel after wrapping it (*4*). Astrocytic processes (yellow) share the blood vessel surface with the processes of the stem cell, with adhesion points where they meet. Thin processes possess regularly spaced mitochondria-filled varicosities along their length (*5*). Finer processes extend from these varicosities to approach and/or wrap around local asymmetrical synapses (light red; *5* and *6*).

whole axon terminal (Fig. 5*C*) and occasionally also the postsynaptic structure (Fig. 5*D*). The varicosities and their processes contained reticulum-like compartments into which the dark label could not penetrate. These were seen sitting next to mitochondria, in the varicosities themselves (Fig. 5 *A*–*C*, *E*, and *F*), or contained within the processes that extended from the varicosities (Fig. 5 *C*–*F*). It could be that these structures perform an important role related to the anatomical relationship of the stem cell processes with asymmetrical synapses.

Looking at individual EM frames of NGPα RGL stem cell varicosities, it was noticeable that the majority of their membranes were apposing neighboring axons. To quantify this relationship, we selected 10 varicosities at random (from four cells of three animals) and, across 150 serial sections, we measured the proportions of their membranes that were apposed by different structures. These structures included unmyelinated axons, dendritic shafts, dendritic spines, and glial processes. The varicosities more frequently apposed unmyelinated axons than any other individual structure [one-way ANOVA with a post hoc Dunnett test; $F_{(4,49)} = 31.38$, $P < 0.001$; Fig. 5*G*]. Seven of the 10 varicosities were analyzed further to establish their precise relationship with asymmetrical synapses of the ML. On average, these varicosities directly apposed the synaptic cleft of three asymmetrical synapses ($n = 7$; mean = 3.29 ± 0.35, SEM) and were within 0.5 μm of 13 asymmetrical synapses in 3D ($n = 7$; mean = 12.89 ± 1.43, SEM). Given that a typical NGPα RGL stem cell process arbor (Fig. 4 *A* and *B*) can possess 130 varicosities, this could suggest that its fine processes could appose ∼428 asymmetrical synapses in the inner ML and be within 0.5 μm of nearly four times as many ($n = 1,676$).

Many of the axons forming asymmetrical synapses in the inner third of the ML will be projections arriving from commissural fibers, hilar mossy cells, or the supramamillary nucleus (43), and the vast majority of postsynaptic structures will be the spines of granule cell dendrites. To demonstrate how tight the relationship of the NGPα RGL stem cell processes and these synapses could be, we traced an NGPα RGL stem cell process wrapping a large synapse-forming axon terminal in serial EM frames and reconstructed it in 3D (Fig. 5 *H*–*M* and Movie S7). The axon terminal formed asymmetrical synapses with the large mushroom spines of two dendrites (Fig. 5 *H* and *L*), and the stem cell process apposed both sides of each synapse, as well as the neck of one spine (Fig. 5 *L* and *M*). This tight association with local axons and synapses resembled the appositions seen for astrocytic processes (44), demonstrating yet another key feature of astrocytes mirrored by the processes of the NGPα RGL stem cell.

Discussion

The NGPα RGL stem cells of the mouse dentate gyrus have a highly complex and specialized morphology, with fine processes capable of invading all regions of the neurogenic niche, namely the GCL, the inner ML, the SGZ, and the hilus. In this study, we used Nestin-GFP transgenic mice and immunolabeling to identify NGPα RGL stem cells, and EM (TEM and SBF-SEM) to reveal the ultrastructure of their processes in 3D. Although no synaptic contacts were seen to be made with NGPα RGL stem cells, they were seen to directly appose asymmetrical synapses, blood vessels, granule neurons, astrocytes, and other NGPα RGL stem cells (Fig. 6). These structural interactions provide the anatomical framework for many of the factors identified as modulators of adult neurogenesis in the hippocampus.

Recent work has started to reveal heterogeneity within the population of dentate gyrus stem cells (22, 24, 28, 29). Stem cells with a horizontal morphology respond to various stimuli differently than those with a radial morphology (i.e., RGL stem cells) (22). RGL stem cells identified with different reporter mice (Nestin-GFP or GLAST-GFP) can play different roles in adult neurogenesis over different time scales (28). Even different Nestin-GFP mouse lines can label subtly different populations of Nestin-GFP–positive RGL stem cells (45–47). Using the same Nestin-reporter mouse as the present study, a previous study was able to characterize, by morphology, molecular marker expression, and clonal analysis, a Nestin-GFP–positive RGL stem cell that was able to proliferate and give rise to astrocytes, neurons, and other RGL cells: the type α Nestin-GFP–positive RGL stem cell (NGPα RGL stem cell) (29). By examining only Nestin-GFP–positive RGL stem cells with an NGPα RGL stem cell morphology, the present study focused on the proliferative population of Nestin-positive RGL stem cells. Further work will be required to assess whether the ultrastructural properties observed for NGPα RGL stem cells can be generalized to other dentate gyrus stem cells, such as (*i*) other Nestin-GFP–positive stem cells with different morphologies and fates, e.g., non-proliferative, NGPβ RGL stem cells (29) or stem cells with horizontal morphology (22), (*ii*) Nestin-GFP–positive RGL stem cells identified with different Nestin-GFP transgenic mouse lines (25, 45–47), (*iii*) RGL stem cells that are not Nestin-positive, approximately 30% of the total population (24) or those identified using other reporter mice (28), or (*iv*) RGL stem cells in the ventral hippocampus (48).

NGPα RGL Stem Cell Processes Define the Neurogenic Niche. Under the light microscope, the cell bodies of NGPα RGL stem cells appear distinct from those of their neighboring granule neurons and exhibit a variety of morphologies. When viewed in serial EM sections and reconstructed in 3D, NGPα RGL stem cell bodies

appear spheroid-, pyramidal-, or hourglass-shaped depending on whether they are in the SGZ, spanning the SGZ–GCL border, or entirely in the GCL, respectively (Fig. 6) (17, 19, 20). Their various morphologies are in sharp contrast to the relatively uniform morphologies of adjacent granule neuron cell bodies, whose tightly tessellated arrangement appears to impinge upon the more flexible shape of the stem cell. The imprints of granule neuron cell bodies also appear to contribute to the concave nature of the stem cell surfaces and the ridges present between them. Similar concave surfaces and ridges are seen for the primary process of the stem cell as it twists, turns, and curves around granule neuron cell bodies and primary dendrites en route to the ML (Fig. 6).

Similar morphological variety is seen in the contours of RGL stem cells in the tightly packed neurogenic niche of the SVZ (49), but this is not the case for embryonic cortical stem cells, which extend straight processes from smooth spheroid cell bodies, without the tight constraints of high cell body density (30). In the developing dentate gyrus, the first irregular contours of RGL stem cells appear at around postnatal day 3, when their radial processes begin to project across the more tightly packed GCL to the ML (50, 51). In the adult dentate gyrus, the NGPα RGL stem cell population is renewing (24, 29), and hence new primary processes are constantly extending through the GCL. The morphologies seen in the present study suggest that the flexible cytoskeleton of the NGPα RGL stem cell is exquisitely adapted to course its way through the more established architecture of the GCL.

At the edge of the ML, larger secondary and tertiary processes extend toward local blood vessels, wrapping them in large thin sheets, forming a patchwork coverage of the blood vessel surface alongside the processes of astrocytes (Fig. 6). Thin processes, with regular varicosities, extend finer processes toward local asymmetrical (i.e., putatively excitatory) synapses, approaching the synaptic cleft and/or ensheathing the synapse. The repeated nature of these process interactions with the surrounding vascular, glial, and neuronal environment is highly suggestive of underlying functions. As the vast majority of the NGPα RGL stem cell membrane comprises these processes, it could be argued that the neurogenic niche of the dentate gyrus is less rooted in the SGZ and more so in the inner third of the ML.

Synapse Wrapping by NGPα RGL Stem Cell Processes. In the present study, NGPα RGL stem cell processes in the ML are seen to approach and/or wrap asymmetrical synapses in a similar fashion to local astrocytes. This raises two key questions: (*i*) What function are NGPα RGL stem cell processes performing at the synapse? (*ii*) For which synapses are they performing this function?

Given their glia-like morphology, perisynaptic NGPα RGL stem cell processes could be acting as astrocytes. Astrocytes at the synapse take up excess glutamate, and are thought to release a host of factors, including neurotransmitters such as glutamate, ATP, and D-serine (52–55). These factors have the ability to regulate synaptic plasticity and contribute to the stability of synaptic connections, most notably those that are newly formed (56). If NGPα RGL stem cells could perform the same function in the inner third of the ML, they could promote the network integration of their own progeny by stabilizing their nascent synapses.

Alternatively, the function of perisynaptic NGPα RGL stem cell processes might be to gauge local network activity to regulate levels of neurogenesis. Single-cell RNA sequencing as well as subsequent electrophysiological analyses have recently shown that NGP RGL stem cells express functional glutamate receptors (ref. 57; but see also ref. 58 for contrast and ref. 59 for review). If these receptors are positioned perisynaptically, they might be able to detect fluctuations in local network activity via the amount of glutamate escaping from the synapse. A lower local network activity could result in less glutamate spillover and the activation of fewer glutamatergic receptors on the stem cell, and thus signal a greater need for new neurons. This could explain why blocking NMDA receptors in the dentate gyrus increases levels of adult neurogenesis in the dentate gyrus (60, 61, reviewed in ref. 62) and increases the numbers of RGL stem cells (63). Future experiments using immuno-EM approaches may help to identify and localize components crucial to these effects, such as glutamate receptors or transporters, in RGL stem cells.

NGPα RGL stem cell processes were seen to touch and/or ensheathe asymmetrical (putatively glutamatergic) synapses. Postsynaptic structures were identified as the dendritic spines of granule neurons, traced from the GCL, but the origin of presynaptic axons is less clear. The majority of glutamatergic inputs to the dentate gyrus originate from the entorhinal cortex (43), but cortical inputs mainly terminate in the outer two thirds of the ML (64–68). The dense arborizations of NGPα RGL stem cells are predominantly contained within the inner third of the ML and GCL, a region where subcortical inputs predominantly terminate (69). This might suggest that any glutamatergic signals received by stem cell processes would reflect the activity of subcortical inputs, such as long-range axons from the supramamillary nucleus (70). Notably, long-range serotonergic axons from the raphe arborize in the SVZ neurogenic niche and regulate the birth of new neurons (71). Other inputs to the inner ML emanate from commissural fibers or hilar mossy cells (72–74), which provide the first glutamatergic synapses onto newborn neurons of the dentate gyrus (75). Cell-specific stimulation of these neurons may help determine their action on the regulation of adult neuronal stem cells.

NGPα RGL Stem Cell Processes Within the Neurovascular Niche. In addition to the astrocyte-like wrapping of synapses, NGPα RGL stem cell processes also ensheathe blood vessels in an astrocyte-like manner (36). Thick processes branch toward local blood vessels, spreading across their surface, maximizing the surface area of the vessel they contact. This could suggest that signals released from the blood are attracting the stem cell process, stem cell process signals are attracting the blood vessel, or a mutual relationship exists whereby factors released from the blood and stem cell process benefit each other.

This relationship was first discussed in relation to whether a mitogenic signal, such as VEGF, was passed between the two structures to coregulate angiogenesis and neurogenesis (76). Although there are a collection of factors capable of influencing angiogenesis and neurogenesis, there are only a few neurogenic factors that are released from endothelial cells (77, 78). In addition, blood circulating factors have substantial effects over the process of neurogenesis (79–82). VEGF is one of these factors (83), and can stimulate neurogenesis (84–86) and reversibly modulate neuronal plasticity (87). Other blood-derived factors capable of affecting neurogenesis are glucocorticoids, which are necessary for the regulation of neuronal differentiation and migration (88). Adult neuronal stem cells themselves were recently shown to release a substantial VEGF-A signal (89), a signal that is received by other neuronal stem cells, via the VEGF receptor (VEGFR)2, and is necessary for maintenance of the RGL stem cell population. Additionally, a related VEGF ligand and receptor combination, VEGF-C and VEGFR3, respectively (90), was recently shown to directly control RGL stem cell activation in the hippocampus without effecting other cell types (91). Here, fine NGPα RGL stem cell processes were seen to appose the fine processes of neighboring stem cells, supporting the view that the autocrine secretion of proneurogenic factors may enable the autonomous regulation of stem cell activity.

As RGL stem cells secrete VEGF and their processes are comprehensively wrapping local blood vessels, it might be assumed that RGL stem cells are exerting a substantial control over angiogenesis and may participate in the formation of the

blood–brain barrier (BBB) on the newly formed blood vessels. Studies of physical exercise have shown that increases in neurogenesis with running (92) are coupled to increases in angiogenesis (93), and these factors are associated with an increase in cognitive function (94). Angiogenesis occurs alongside neurogenesis in embryonic development when the BBB is formed, but the BBB does not fully mature until 3 weeks postnatally, when cues from the neuroepithelium are thought to drive the wrapping of vessels by astrocytes (95). This gives plenty of opportunity to RGL stem cells in the developing dentate gyrus (50, 51) to receive similar cues and participate in the BBB via the wrapping of blood vessels. Furthermore, exogenous VEGF has been shown to increase the permeability of the BBB (96, 97). So the endogenous release of VEGF from perivascular RGL stem cell processes could participate in the induction of vasculogenesis and facilitate an increase in blood-to-brain signaling.

Blood vessels might also act as a site for the interaction between RGL stem cells and astrocytes. Here, we found that, where the two types of process met on the surface of the blood vessel, their membranes were of complementary thicknesses, and adhesion points existed between them. Astrocyte-expressed factors, such as Wnt3a, interleukins IL-1β and IL6, and ATP, promote differentiation of neural stem progenitor cells, whereas growth factor binding protein IGFBP6 and proteoglycan decorin inhibit their differentiation (98–100). Astrocyte–stem cell interactions have also been shown to regulate neurogenesis by secretion of ephrin-B2, which activates EphB4 receptors on the stem cell (101). Similar to the SVZ, where direct cell–cell contact between astrocytes and precursors stimulates neurogenesis (102), the extensive interaction between astrocytes and stem cell processes at the blood vessel surface in the dentate gyrus offers a stable structural platform through which astrocytic regulation of RGL stem cells could occur.

Conclusions

In this study, we have used a variety of LM and EM techniques to provide a detailed ultrastructural analysis of Nestin-GFP–positive adult RGL stem cells. The intimate relationship of their fine processes with synapses, blood vessels, and astrocytes provides a structural link between the local niche and the process of hippocampal neurogenesis. It supports the idea that the neurogenic niche plays an important role in the regulation of RGL stem cells, and that the niche itself could be considered to extend, with the processes of RGL stem cells, into the inner ML. Although the resolution of EM was required to reveal the fine elements observed here, further studies will be necessary to assess the function of the perisynaptic and perivascular structures described. By describing the fine structure of RGL stem cells, and their relationships with elements of the dentate gyrus neurogenic niche, we provide a necessary structural framework linking adult neural stem cells and the signals that activate and modulate their activity, and a new perspective on the process of adult neurogenesis.

Materials and Methods

Animal Handling. This study was carried out in strict accordance with the recommendations in the Guidance for the Care and Use of Laboratory Animals of the National Institutes of Health and was approved by the Swiss animal experimentation authorities. Every effort was made to minimize the number of animals used and their suffering. Nestin-GFP mice [male, P83-88; gift from the laboratory of K. Mori, Precursory Research for Embryonic Science and Technology (PRESTO), Japan Science and Technology Corporation, Soraku-gun, Kyoto] (37) were anesthetized, transcardially perfused with PBS solution (5 mL over 1 min) and then fixative [50 mL over 10 min, 4% paraformaldehyde (wt/vol); 0.1% glutaraldehyde (vol/vol) in 0.1 M phosphate buffer; (PB); Sigma], and kept at 4 °C for 24 h. Immunohistochemistry details are provided in *SI Materials and Methods*.

EM. Tissue was prepared as described in *SI Materials and Methods*. For TEM, seven NGPα RGL stem cells from Nestin-GFP transgenic mice were analyzed (four cells from three animals for DAB-peroxidase labeling and three cells from three animals for immunogold labeling), selected from 45 candidates identified at the LM level (29 DAB-peroxidase–labeled from three animals, 16 immunogold-labeled from three animals). For each of the seven cells, a mean of 10 regions of interest (ROIs; including cell bodies, primary processes, and blood vessel-wrapping or synapse-wrapping processes) were examined (±2 ROIs, SEM; 69 ROIs in total) in a mean of 29 serial sections each (±7 sections, SEM; 1,985 sections in total). For SBF-SEM, three RGL stem cells from three Nestin-GFP mice were microdissected from the tissue and processed.

ACKNOWLEDGMENTS. We thank Hongjun Song for comments on the manuscript and the Electron Microscope Facility and the Cellular Imaging Facility of the University of Lausanne. The SBF-SEM imaging performed at the University of California, San Diego, was supported by National Institutes of Health Grant GM103412 for the National Center for Microscopy and Imaging Research (to M.H.E.). J.M. and N.T. were funded by the IBRO-SSN Fellowship for Young Investigators, Fondation Leenaards, and the Swiss National Science Foundation. I.S-P. and R.O. were participants in the Summer Undergraduate Research Programme of the University of Lausanne.

1. Altman J, Das GD (1965) Autoradiographic and histological evidence of postnatal hippocampal neurogenesis in rats. *J Comp Neurol* 124(3):319–335.
2. Gould E (2007) How widespread is adult neurogenesis in mammals? *Nat Rev Neurosci* 8(6):481–488.
3. Ming GL, Song H (2011) Adult neurogenesis in the mammalian brain: Significant answers and significant questions. *Neuron* 70(4):687–702.
4. Kriegstein A, Alvarez-Buylla A (2009) The glial nature of embryonic and adult neural stem cells. *Annu Rev Neurosci* 32:149–184.
5. Bonaguidi MA, Song J, Ming GL, Song H (2012) A unifying hypothesis on mammalian neural stem cell properties in the adult hippocampus. *Curr Opin Neurobiol* 22(5): 754–761.
6. Toni N, Sultan S (2011) Synapse formation on adult-born hippocampal neurons. *Eur J Neurosci* 33(6):1062–1068.
7. Lee SW, Clemenson GD, Gage FH (2012) New neurons in an aged brain. *Behav Brain Res* 227(2):497–507.
8. Vivar C, van Praag H (2013) Functional circuits of new neurons in the dentate gyrus. *Front Neural Circuits* 7:15.
9. Braun SM, Jessberger S (2014) Adult neurogenesis: Mechanisms and functional significance. *Development* 141(10):1983–1986.
10. Deng W, Aimone JB, Gage FH (2010) New neurons and new memories: How does adult hippocampal neurogenesis affect learning and memory? *Nat Rev Neurosci* 11(5):339–350.
11. Marín-Burgin A, Schinder AF (2012) Requirement of adult-born neurons for hippocampus-dependent learning. *Behav Brain Res* 227(2):391–399.
12. O'Leary OF, Cryan JF (2014) A ventral view on antidepressant action: Roles for adult hippocampal neurogenesis along the dorsoventral axis. *Trends Pharmacol Sci* 35(12): 675–687.
13. Doetsch F, Caillé I, Lim DA, García-Verdugo JM, Alvarez-Buylla A (1999) Subventricular zone astrocytes are neural stem cells in the adult mammalian brain. *Cell* 97(6):703–716.
14. Mirzadeh Z, Merkle FT, Soriano-Navarro M, Garcia-Verdugo JM, Alvarez-Buylla A (2008) Neural stem cells confer unique pinwheel architecture to the ventricular surface in neurogenic regions of the adult brain. *Cell Stem Cell* 3(3):265–278.
15. Beckervordersandforth R, et al. (2010) In vivo fate mapping and expression analysis reveals molecular hallmarks of prospectively isolated adult neural stem cells. *Cell Stem Cell* 7(6):744–758.
16. Morrens J, Van Den Broeck W, Kempermann G (2012) Glial cells in adult neurogenesis. *Glia* 60(2):159–174.
17. Kosaka T, Hama K (1986) Three-dimensional structure of astrocytes in the rat dentate gyrus. *J Comp Neurol* 249(2):242–260.
18. Seri B, García-Verdugo JM, McEwen BS, Alvarez-Buylla A (2001) Astrocytes give rise to new neurons in the adult mammalian hippocampus. *J Neurosci* 21(18):7153–7160.
19. Seki T (2003) Microenvironmental elements supporting adult hippocampal neurogenesis. *Anat Sci Int* 78(2):69–78.
20. Seri B, García-Verdugo JM, Collado-Morente L, McEwen BS, Alvarez-Buylla A (2004) Cell types, lineage, and architecture of the germinal zone in the adult dentate gyrus. *J Comp Neurol* 478(4):359–378.
21. Seki T, Namba T, Mochizuki H, Onodera M (2007) Clustering, migration, and neurite formation of neural precursor cells in the adult rat hippocampus. *J Comp Neurol* 502(2):275–290.
22. Lugert S, et al. (2010) Quiescent and active hippocampal neural stem cells with distinct morphologies respond selectively to physiological and pathological stimuli and aging. *Cell Stem Cell* 6(5):445–456.
23. Namba T, et al. (2005) The fate of neural progenitor cells expressing astrocytic and radial glial markers in the postnatal rat dentate gyrus. *Eur J Neurosci* 22(8): 1928–1941.
24. Bonaguidi MA, et al. (2011) In vivo clonal analysis reveals self-renewing and multipotent adult neural stem cell characteristics. *Cell* 145(7):1142–1155.
25. Dranovsky A, et al. (2011) Experience dictates stem cell fate in the adult hippocampus. *Neuron* 70(5):908–923.

26. Encinas JM, et al. (2011) Division-coupled astrocytic differentiation and age-related depletion of neural stem cells in the adult hippocampus. *Cell Stem Cell* 8(5):566–579.
27. Kempermann G (2011) The pessimist's and optimist's views of adult neurogenesis. *Cell* 145(7):1009–1011.
28. DeCarolis NA, et al. (2013) In vivo contribution of nestin- and GLAST-lineage cells to adult hippocampal neurogenesis. *Hippocampus* 23(8):708–719.
29. Gebara E, et al. (2016) Heterogeneity of radial glia-like cells in the adult hippocampus. *Stem Cells*, 10.1002/stem.2266.
30. Noctor SC, Flint AC, Weissman TA, Dammerman RS, Kriegstein AR (2001) Neurons derived from radial glial cells establish radial units in neocortex. *Nature* 409(6821): 714–720.
31. Sun GJ, et al. (2015) Tangential migration of neuronal precursors of glutamatergic neurons in the adult mammalian brain. *Proc Natl Acad Sci USA* 112(30):9484–9489.
32. Shihabuddin LS, Horner PJ, Ray J, Gage FH (2000) Adult spinal cord stem cells generate neurons after transplantation in the adult dentate gyrus. *J Neurosci* 20(23): 8727–8735.
33. Song H, Stevens CF, Gage FH (2002) Astroglia induce neurogenesis from adult neural stem cells. *Nature* 417(6884):39–44.
34. Anthony TE, Klein C, Fishell G, Heintz N (2004) Radial glia serve as neuronal progenitors in all regions of the central nervous system. *Neuron* 41(6):881–890.
35. Silva-Vargas V, Crouch EE, Doetsch F (2013) Adult neural stem cells and their niche: A dynamic duo during homeostasis, regeneration, and aging. *Curr Opin Neurobiol* 23(6):935–942.
36. Filippov V, et al. (2003) Subpopulation of nestin-expressing progenitor cells in the adult murine hippocampus shows electrophysiological and morphological characteristics of astrocytes. *Mol Cell Neurosci* 23(3):373–382.
37. Yamaguchi M, Saito H, Suzuki M, Mori K (2000) Visualization of neurogenesis in the central nervous system using nestin promoter-GFP transgenic mice. *Neuroreport* 11(9):1991–1996.
38. Shapiro LA, Korn MJ, Shan Z, Ribak CE (2005) GFAP-expressing radial glia-like cell bodies are involved in a one-to-one relationship with doublecortin-immunolabeled newborn neurons in the adult dentate gyrus. *Brain Res* 1040(1-2):81–91.
39. Denk W, Horstmann H (2004) Serial block-face scanning electron microscopy to reconstruct three-dimensional tissue nanostructure. *PLoS Biol* 2(11):e329.
40. Peters A, Palay SL, Webster HdeF (1970) *The Fine Structure of the Nervous System* (Oxford Univ Press, Oxford, UK).
41. Hama K, Arii T, Katayama E, Marton M, Ellisman MH (2004) Tri-dimensional morphometric analysis of astrocytic processes with high voltage electron microscopy of thick Golgi preparations. *J Neurocytol* 33(3):277–285.
42. Mathiisen TM, Lehre KP, Danbolt NC, Ottersen OP (2010) The perivascular astroglial sheath provides a complete covering of the brain microvessels: An electron microscopic 3D reconstruction. *Glia* 58(9):1094–1103.
43. Leranth C, Hajszan T (2007) Extrinsic afferent systems to the dentate gyrus. *Prog Brain Res* 163:63–84.
44. Witcher MR, Kirov SA, Harris KM (2007) Plasticity of perisynapticastroglia during synaptogenesis in the mature rat hippocampus. *Glia* 55(1):13–23.
45. Encinas JM, Vaahtokari A, Enikolopov G (2006) Fluoxetine targets early progenitor cells in the adult brain. *Proc Natl Acad Sci USA* 103(21):8233–8238.
46. Balordi F, Fishell G (2007) Mosaic removal of hedgehog signaling in the adult SVZ reveals that the residual wild-type stem cells have a limited capacity for self-renewal. *J Neurosci* 27(52):14248–14259.
47. Lagace DC, et al. (2007) Dynamic contribution of nestin-expressing stem cells to adult neurogenesis. *J Neurosci* 27(46):12623–12629.
48. Jinno S (2011) Topographic differences in adult neurogenesis in the mouse hippocampus: A stereology-based study using endogenous markers. *Hippocampus* 21(5): 467–480.
49. Danilov AI, et al. (2009) Ultrastructural and antigenic properties of neural stem cells and their progeny in adult rat subventricular zone. *Glia* 57(2):136–152.
50. Brunne B, et al. (2010) Origin, maturation, and astroglial transformation of secondary radial glial cells in the developing dentate gyrus. *Glia* 58(13):1553–1569.
51. Nicola Z, Fabel K, Kempermann G (2015) Development of the adult neurogenic niche in the hippocampus of mice. *Front Neuroanat* 9:53.
52. Huang YH, Bergles DE (2004) Glutamate transporters bring competition to the synapse. *Curr Opin Neurobiol* 14(3):346–352.
53. Volterra A, Meldolesi J (2005) Astrocytes, from brain glue to communication elements: The revolution continues. *Nat Rev Neurosci* 6(8):626–640.
54. Bains JS, Oliet SH (2007) Glia: They make your memories stick! *Trends Neurosci* 30(8): 417–424.
55. Hamilton NB, Attwell D (2010) Do astrocytes really exocytose neurotransmitters? *Nat Rev Neurosci* 11(4):227–238.
56. Ota Y, Zanetti AT, Hallock RM (2013) The role of astrocytes in the regulation of synaptic plasticity and memory formation. *Neural Plast* 2013:185463.
57. Shin J, et al. (2015) Single-Cell RNA-seq with waterfall reveals molecular cascades underlying adult neurogenesis. *Cell Stem Cell* 17(3):360–372.
58. Tozuka Y, Fukuda S, Namba T, Seki T, Hisatsune T (2005) GABAergic excitation promotes neuronal differentiation in adult hippocampal progenitor cells. *Neuron* 47(6):803–815.
59. Jansson LC, Åkerman KE (2014) The role of glutamate and its receptors in the proliferation, migration, differentiation and survival of neural progenitor cells. *J Neural Transm (Vienna)* 121(8):819–836.
60. Cameron HA, McEwen BS, Gould E (1995) Regulation of adult neurogenesis by excitatory input and NMDA receptor activation in the dentate gyrus. *J Neurosci* 15(6): 4687–4692.
61. Nacher J, Rosell DR, Alonso-Llosa G, McEwen BS (2001) NMDA receptor antagonist treatment induces a long-lasting increase in the number of proliferating cells, PSA-NCAM-immunoreactive granule neurons and radial glia in the adult rat dentate gyrus. *Eur J Neurosci* 13(3):512–520.
62. Taylor CJ, He R, Bartlett PF (2014) The role of the N-methyl-D-aspartate receptor in the proliferation of adult hippocampal neural stem and precursor cells. *Sci China Life Sci* 57(4):403–411.
63. Namba T, Maekawa M, Yuasa S, Kohsaka S, Uchino S (2009) The Alzheimer's disease drug memantine increases the number of radial glia-like progenitor cells in adult hippocampus. *Glia* 57(10):1082–1090.
64. Bellocchio EE, et al. (1998) The localization of the brain-specific inorganic phosphate transporter suggests a specific presynaptic role in glutamatergic transmission. *J Neurosci* 18(21):8648–8659.
65. Fremeau RT, Jr, et al. (2001) The expression of vesicular glutamate transporters defines two classes of excitatory synapse. *Neuron* 31(2):247–260.
66. Fremeau RT, Jr, Voglmaier S, Seal RP, Edwards RH (2004) VGLUTs define subsets of excitatory neurons and suggest novel roles for glutamate. *Trends Neurosci* 27(2): 98–103.
67. Kaneko T, Fujiyama F (2002) Complementary distribution of vesicular glutamate transporters in the central nervous system. *Neurosci Res* 42(4):243–250.
68. Kaneko T, Fujiyama F, Hioki H (2002) Immunohistochemical localization of candidates for vesicular glutamate transporters in the rat brain. *J Comp Neurol* 444(1): 39–62.
69. Halasy K, Hajszan T, Kovács EG, Lam TT, Leranth C (2004) Distribution and origin of vesicular glutamate transporter 2-immunoreactive fibers in the rat hippocampus. *Hippocampus* 14(7):908–918.
70. Soussi R, Zhang N, Tahtakran S, Houser CR, Esclapez M (2010) Heterogeneity of the supramammillary-hippocampal pathways: Evidence for a unique GABAergic neurotransmitter phenotype and regional differences. *Eur J Neurosci* 32(5):771–785.
71. Tong CK, et al. (2014) Axonal control of the adult neural stem cell niche. *Cell Stem Cell* 14(4):500–511.
72. Amaral DG, Scharfman HE, Lavenex P (2007) The dentate gyrus: Fundamental neuroanatomical organization (dentate gyrus for dummies). *Prog Brain Res* 163:3–22.
73. Buckmaster PS, Wenzel HJ, Kunkel DD, Schwartzkroin PA (1996) Axon arbors and synaptic connections of hippocampal mossy cells in the rat *in vivo*. *J Comp Neurol* 366(2):271–292.
74. Frotscher M, Seress L, Schwerdtfeger WK, Buhl E (1991) The mossy cells of the fascia dentata: A comparative study of their fine structure and synaptic connections in rodents and primates. *J Comp Neurol* 312(1):145–163.
75. Chancey JH, Poulsen DJ, Wadiche JI, Overstreet-Wadiche L (2014) Hilar mossy cells provide the first glutamatergic synapses to adult-born dentate granule cells. *J Neurosci* 34(6):2349–2354.
76. Palmer TD, Willhoite AR, Gage FH (2000) Vascular niche for adult hippocampal neurogenesis. *J Comp Neurol* 425(4):479–494.
77. Goldman SA, Chen Z (2011) Perivascular instruction of cell genesis and fate in the adult brain. *Nat Neurosci* 14(11):1382–1389.
78. Shen Q, et al. (2004) Endothelial cells stimulate self-renewal and expand neurogenesis of neural stem cells. *Science* 304(5675):1338–1340.
79. Villeda SA, et al. (2011) The ageing systemic milieu negatively regulates neurogenesis and cognitive function. *Nature* 477(7362):90–94.
80. Villeda SA, Wyss-Coray T (2013) The circulatory systemic environment as a modulator of neurogenesis and brain aging. *Autoimmun Rev* 12(6):674–677.
81. Villeda SA, et al. (2014) Young blood reverses age-related impairments in cognitive function and synaptic plasticity in mice. *Nat Med* 20(6):659–663.
82. Stolp HB, Molnár Z (2015) Neurogenic niches in the brain: Help and hindrance of the barrier systems. *Front Neurosci* 9:20.
83. Leung DW, Cachianes G, Kuang WJ, Goeddel DV, Ferrara N (1989) Vascular endothelial growth factor is a secreted angiogenic mitogen. *Science* 246(4935): 1306–1309.
84. Schänzer A, et al. (2004) Direct stimulation of adult neural stem cells in vitro and neurogenesis in vivo by vascular endothelial growth factor. *Brain Pathol* 14(3): 237–248.
85. Jin K, et al. (2002) Vascular endothelial growth factor (VEGF) stimulates neurogenesis in vitro and in vivo. *Proc Natl Acad Sci USA* 99(18):11946–11950.
86. Fournier NM, Lee B, Banasr M, Elsayed M, Duman RS (2012) Vascular endothelial growth factor regulates adult hippocampal cell proliferation through MEK/ERK- and PI3K/Akt-dependent signaling. *Neuropharmacology* 63(4):642–652.
87. Licht T, et al. (2011) Reversible modulations of neuronal plasticity by VEGF. *Proc Natl Acad Sci USA* 108(12):5081–5086.
88. Fitzsimons CP, et al. (2013) Knockdown of the glucocorticoid receptor alters functional integration of newborn neurons in the adult hippocampus and impairs fear-motivated behavior. *Mol Psychiatry* 18(9):993–1005.
89. Kirby ED, Kuwahara AA, Messer RL, Wyss-Coray T (2015) Adult hippocampal neural stem and progenitor cells regulate the neurogenic niche by secreting VEGF. *Proc Natl Acad Sci USA* 112(13):4128–4133.
90. Ferrara N, Gerber HP, LeCouter J (2003) The biology of VEGF and its receptors. *Nat Med* 9(6):669–676.
91. Han J, et al. (2015) Vascular endothelial growth factor receptor 3 controls neural stem cell activation in mice and humans. *Cell Reports* 10(7):1158–1172.
92. van Praag H, Kempermann G, Gage FH (1999) Running increases cell proliferation and neurogenesis in the adult mouse dentate gyrus. *Nat Neurosci* 2(3):266–270.
93. Van der Borght K, et al. (2009) Physical exercise leads to rapid adaptations in hippocampal vasculature: Temporal dynamics and relationship to cell proliferation and neurogenesis. *Hippocampus* 19(10):928–936.
94. Clark PJ, Brzezinska WJ, Puchalski EK, Krone DA, Rhodes JS (2009) Functional analysis of neurovascular adaptations to exercise in the dentate gyrus of young adult mice associated with cognitive gain. *Hippocampus* 19(10):937–950.

95. Tam SJ, Watts RJ (2010) Connecting vascular and nervous system development: Angiogenesis and the blood-brain barrier. *Annu Rev Neurosci* 33:379–408.
96. Keck PJ, et al. (1989) Vascular permeability factor, an endothelial cell mitogen related to PDGF. *Science* 246(4935):1309–1312.
97. Jiang S, Xia R, Jiang Y, Wang L, Gao F (2014) Vascular endothelial growth factors enhance the permeability of the mouse blood-brain barrier. *PLoS One* 9(2):e86407.
98. Lie DC, et al. (2005) Wnt signalling regulates adult hippocampal neurogenesis. *Nature* 437(7063):1370–1375.
99. Barkho BZ, et al. (2006) Identification of astrocyte-expressed factors that modulate neural stem/progenitor cell differentiation. *Stem Cells Dev* 15(3):407–421.
100. Cao X, et al. (2013) Astrocytic adenosine 5′-triphosphate release regulates the proliferation of neural stem cells in the adult hippocampus. *Stem Cells* 31(8):1633–1643.
101. Ashton RS, et al. (2012) Astrocytes regulate adult hippocampal neurogenesis through ephrin-B signaling. *Nat Neurosci* 15(10):1399–1406.
102. Lim DA, Alvarez-Buylla A (1999) Interaction between astrocytes and adult subventricular zone precursors stimulates neurogenesis. *Proc Natl Acad Sci USA* 96(13):7526–7531.
103. Gebara E, Sultan S, Kocher-Braissant J, Toni N (2013) Adult hippocampal neurogenesis inversely correlates with microglia in conditions of voluntary running and aging. *Front Neurosci* 7:145.
104. Wilke SA, et al. (2013) Deconstructing complexity: Serial block-face electron microscopic analysis of the hippocampal mossy fiber synapse. *J Neurosci* 33(2):507–522.
105. Kremer JR, Mastronarde DN, McIntosh JR (1996) Computer visualization of three-dimensional image data using IMOD. *J Struct Biol* 116(1):71–76.

Supporting Information

Moss et al. 10.1073/pnas.1514652113

SI Materials and Methods

Immunohistochemistry. Brains were removed, postfixed for 24 h at 4 °C, washed in PBS solution, and cut in 50-μm coronal sections (VT1000S vibrating microtome; Leica Microsystems). Sections containing the dorsal dentate gyrus (from Bregma −1.7 mm to Bregma −2.3 mm) were washed (all washes and incubations performed while shaking at 20 rpm; Gyro Rocker; Stuart Scientific) in PBS solution and cryoprotectant [25% sucrose (wt/vol); Sigma; 10% glycerol (vol/vol); Sigma; in 0.05 M PB], incubated for 2 h in cryoprotectant, then freeze-thawed by immersion in liquid nitrogen, with further washes in cryoprotectant and PBS solution.

For the immunoperoxidase process, the tissue was blocked with three washes in 0.5% BSA (vol/vol in 0.1 M PB; Aurion) and the sections were incubated overnight in the primary antibody [rabbit anti-GFP; 1:1,000 (no. A11122; Invitrogen) in 0.1% BSA-PB with shaking at 25 °C]. Next, sections were washed in PBS solution and incubated in the secondary antibody [biotinylated goat anti-rabbit; 1:200 (no. 111–066-047; Jackson Laboratories) in 0.1% BSA-PB], shaking for 2 h at 25 °C. Sections were then washed in PBS solution and incubated in avidin–biotin–peroxidase complex (ABC Elite; Vector Laboratories) for 90 min shaking at 25 °C. They were then washed in PBS solution and 0.05 M Tris-buffered saline (TBS) solution (Sigma), reacted with DAB (6 min reaction; Vector Laboratories), with subsequent washes in TBS and PBS solutions.

For the immunogold process, the tissue was blocked by incubating for 2 h in 10% (vol/vol) normal goat serum (NGS) in PBS solution (Vector Laboratories), and the sections were then incubated overnight in the primary antibody [rabbit anti-GFP; 1:1,000; (no. A11122; Invitrogen) in 2% NGS-PBS solution; shaking at 25 °C]. Next, sections were washed in PBS solution and incubated in the gold-conjugated secondary antibody [goat anti-rabbit; 1:100 (Nanoprobes); 1.4 nm colloidal gold, 2004, Fab′ fragment; in 1% NGS-PBS solution], shaking for 2 h at 25 °C. Sections were then washed in PBS solution and 0.1 M sodium acetate 3-hydrate buffer (AB; Sigma), before the gold particles were silver-intensified (3–5-min reaction; 1 mL silver reagent; HQ Silver Kit; Nanoprobes), with further washes in AB and PBS solution.

For the immunofluorescence process, Nestin-GFP mice (P77) were intracardially injected with sulforhodamine 101 (200 μL; S359; Invitrogen) and then perfused/fixed with 0.9% saline solution and then 4% paraformaldehyde (wt/vol) in 0.1 M PBS solution. Brains were collected, postfixed overnight at 4 °C, cryoprotected for 24 h in 30% sucrose (wt/vol), and rapidly frozen. Coronal sections (40 μm) were cut (MC 3050S microtome-cryostat; Leica) and stored in cryoprotectant [30% (vol/vol) ethylene glycol and 25% (vol/vol) glycerin in PBS solution] at −20 °C. Immunochemistry was performed as previously described (103). Briefly, sections were washed in 0.1 M PBS solution and incubated in blocking solution containing 0.3% Triton-X100 and 15% normal goat serum (vol/vol, in 0.1 M PBS solution; no. 16210–064; Gibco). Sections were then incubated for 40 h at 4 °C in the primary antibody (chicken anti-GFP; 1:500; no. 55423; AnaSpec) and 2 h in the secondary antibody (DyLight 488 goat anti-chicken; 1:500; no. 103–485-155; Jackson Laboratories) before imaging. Images were acquired with a confocal microscope (Zeiss LSM 710 Quasar; Carl Zeiss), and 3D reconstructions were created with Bitplane IMARIS 7.2.3.

TEM. Both immunoperoxidase- and immunogold-labeled sections were then prepared for EM. Sections were washed in 0.1 M PB, postfixed with osmium tetroxide [1% (Electron Microscopy Sciences) in 0.1 M PB; 30 min for immunoperoxidase-labeled sections, 7 min for immunogold-labeled sections] and then washed in 0.1 M PB. They were then dehydrated with washes in an ascending series of ethanol dilutions [two washes in 50% ethanol; one wash in 70% ethanol with 1% uranyl acetate (wt/vol; Electron Microscopy Sciences); one wash in 95% ethanol; two washes in 100% ethanol]. Sections were then washed three times in acetone and infiltrated with resin (Durcupan ACM; Fluka; Sigma) and left overnight. The next day, the resin was heated, and sections were lifted onto microscope slides. Coverslips were applied, and the resin was cured at 65 °C over 3 d. ROIs were identified from the slides at the LM level, and then tissue was cut from the slide, and serial ultrathin sections (70 nm) were cut and collected onto Formvar-coated, single-slot copper grids (Electron Microscopy Sciences). The tissue was then contrasted with lead citrate and examined using a transmission electron microscope (CM10; Philips) at the Electron Microscope Facility at the University of Lausanne. Images were captured by using a digital camera (Morada SIS; Olympus) and processed by using Adobe Creative Suite and Fiji ImageJ software.

For the analysis of RGL stem cell process apposition,10 varicosties were selected at random from four DAB-labeled cells of three animals. Across a total of 150 serial sections (n = 9–21 sections per varicosity, depending on its size), we measured the proportion of their membranes that were apposed by different structures, in a fashion similar to techniques described previously (44). The lengths of membrane apposed by axons, dendritic shafts and spines, and glia were calculated as a percentage for each varicosity and then expressed as the mean of the 10 varicosities ± SEM. Comparisons were made between the mean apposition by axons and the mean apposition of each other structure by using a one-way ANOVA with a post hoc Dunnett test. For the analysis of mitochondrial occupation of the varicosity, the same 10 varicosities were used. The areas of each varicosity were measured in the same sets of serial sections (150 total; n = 9–21 per varicosity), as were the areas of each mitochondrion occupying the varicosity. The mitochondrial occupation of each varicosity was then calculated from the serial sections as a percentage and then expressed as the mean of all 10 varicosities ± SEM. Of the 10 varicosities mentioned earlier, seven had sufficient serial EM sections to assess the number of asymmetrical synapses within 0.5 μm. Fiji ImageJ software was used to measure distances from asymmetrical synapses to each varicosity in 3D, assuming an average section thickness of 70 nm. Those synaptic clefts lying directly adjacent to a varicosity with no intervening structures were considered to be apposed. The average number of asymmetrical synapses apposing and lying within 0.5 μm of a varicosity was expressed as the mean of the seven varicosities ± SEM.

SBF-SEM. To prepare samples for SBF-SEM, 50-μm coronal sections of three Nestin-GFP mouse brains were processed for immunoperoxidase labeling as described earlier (except for perfusion with fixative agent chilled on ice). Three RGL stem cells (one from each animal; sc3–sc5; *Results* and Fig. 1) were then microdissected from the tissue and processed for serial block-face SEM as previously described (104). Briefly, tissue was washed in cacodylate buffer (containing 2 mM $CaCl_2$) and then cacodylate buffer containing 2% osmium tetroxide and 1.5% potassium ferrocyanide (vol/vol). After washes in double-distilled (dd)H_2O, tissue was placed in 1% thiocarbohydrazide (wt/vol; in

ddH_2O), washed again in ddH_2O, and incubated in 2% osmium tetroxide. Further washes in ddH_2O were followed by an overnight incubation in 2% uranyl acetate overnight. After washes in ddH_2O, tissue was stained with a lead aspartate solution. Tissue was then washed in ddH_2O and dehydrated in a series of ascending alcohol concentrations (70% ethanol, 90%, twice in 100%), ice-cold dry acetone, and room temperature dry acetone. The tissue was then placed in ascending concentrations of Durcupan resin (Fluka; Sigma) before flat-embedding the tissue and curing the resin at 60 °C over 2 d.

Tissue was attached to the top of an aluminum specimen pin with silver epoxy and then trimmed. The pin was sputter-coated with gold-palladium (for enhanced conductivity), and specimens were then imaged by using a Merlin scanning electron microscope (Carl Zeiss) with a Gatan 3View SBF-SEM system. Accelerating voltages were 2.5, 1.8, and 1.8 kV for cells sc3–sc5, respectively. The *z*-steps for cells sc3–sc5 were 70, 60, and 60 nm, respectively. The *xy* pixel sizes for each cell were 7.5, 3.16, and 3.29 nm, respectively. Serial EM images of the tissue were viewed, traced, and 3D-reconstructed by using IMOD software (105) (bio3d.colorado.edu/imod/).

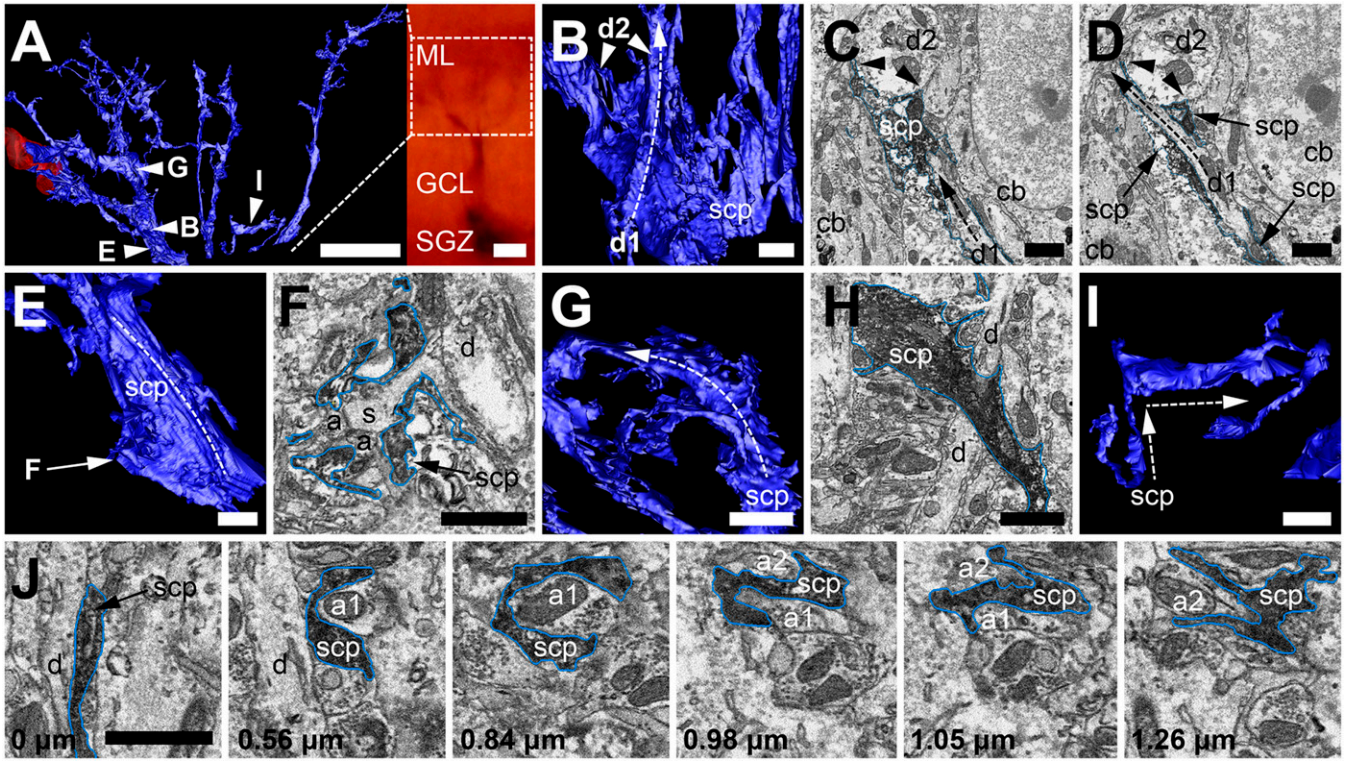

Fig. S1. Individual process features from a 3D reconstruction of a single RGL stem cell captured using SBF-SEM. (*A*) Three-dimensional reconstruction of the fine processes of an RGL stem cell as seen in Fig. 1*F* (and LM image, *Inset*; Movie S1), with ROIs marked and examined in more detail in *B*, *E G*, and *I*. (*B*) Two dendrites (d1 and d2) impinge upon the stem cell process (scp) as it extends radially; d1 forms a long concave indentation into the side of the process (dotted arrow), whereas the process splits around the larger d2 (arrowheads), resulting in a large concave surface on the process. (*C* and *D*) Consecutive EM sections of the 3D relationships seen in *B*, separated by 0.21 µm in the *z* axis. (*C*) Stem cell process (scp) sitting below dendrite d2, forming the large concave surface (arrowheads). Dendrite d1 approaches from below (dotted arrow), between two cell bodies (cb) on the edge of the GCL. (*D*) Dendrite d1 now splitting the stem cell process in two as it extends to the left of dendrite d2 (dotted arrow). (*E*) A large secondary process of the stem cell (scp) bends around a large dendrite and cell body at the GCL–ML border (dotted arrow), and some of the process extends to fill the space between GCL cell bodies (arrow). (*F*) Detail from *E* shows stem cell processes (scp) extending into the space between cell bodies and enclosing a dendritic spine (s, branching from dendrite d) and the two axons located at the spinehead (a). Low resolution of SBF-SEM images prevented the confirmation of presumed synaptic contacts in this instance. (*G*) A stem cell process, viewed from below (scp), thinning into a sheet as it extends out toward a blood vessel (dotted arrow). (*H*) In a single EM frame, the thin sheet of the process (scp) spreads between a large dendrite and a cell body, with a smaller dendrite (d) visible beneath the process. (*I*) A smaller process (scp), branching from the split of the primary process, stops extending radially and extends tangentially along the GCL–ML border (dotted arrows). (*J*) Serial sections of the tangentially-extending process (scp) show that it initially extends up the side of a dendrite (d) before wrapping a large axon terminal in one direction (a1) and another axon terminal (a2) in the opposite direction. (Scale bars: *A*, 10 µm; *B–J*, 2 µm.)

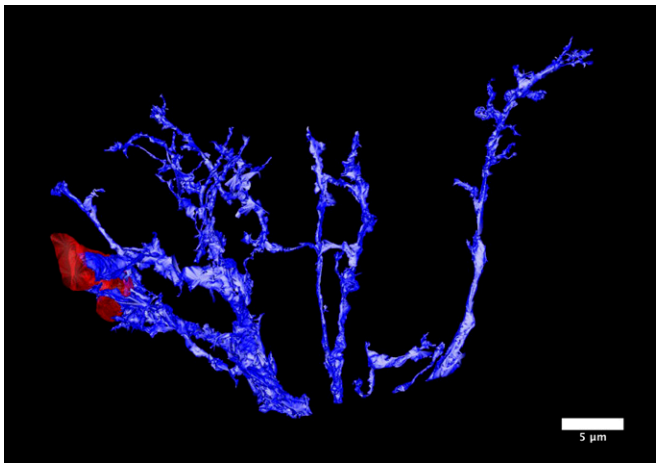

Movie S1. Three-dimensional reconstruction of NGPα RGL stem cell processes in the ML of the dentate gyrus. Secondary processes of an NGPα RGL stem cell (blue) emerge from the GCL after splitting from the same primary process. Thicker processes branch toward a local blood vessel (red) and form small endfeet-like contacts or wrap thin sheets around the vessel. Thinner processes from all secondary processes branch extensively, sending finer processes toward local synapses. Throughout the process arbor, the impressions of surrounding neuronal, vascular, and glial architecture are seen across its surface contours. Images from this reconstruction are provided in Fig. 1*F* and Fig. S1.

Movie S1

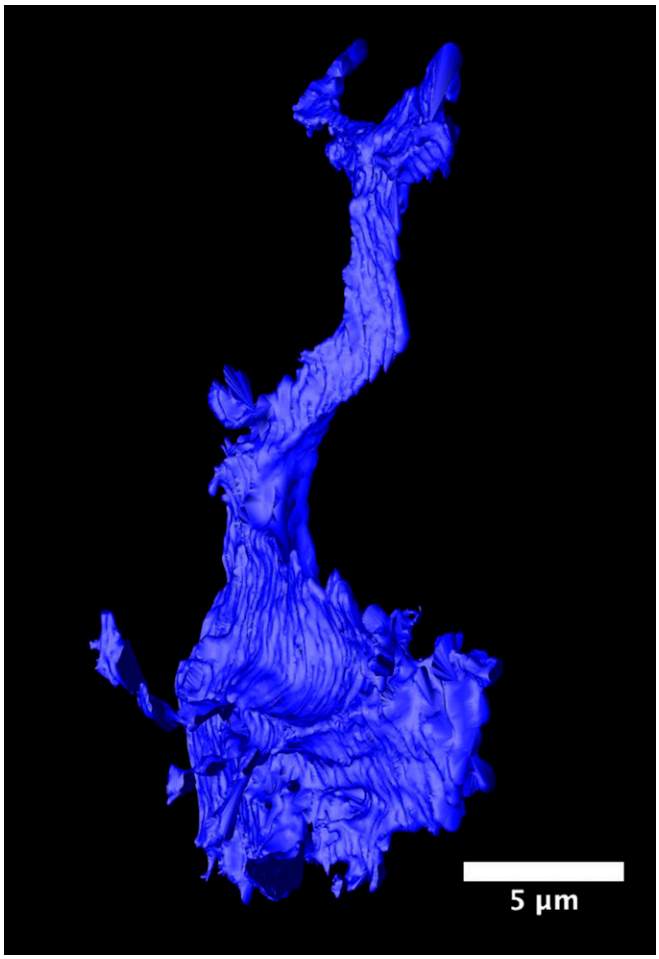

Movie S2. Three-dimensional reconstruction of an NGPα RGL stem cell body and primary process in the SGZ and GCL. As shown in Fig. 1 *G* and *H*, the shape of the cell body (blue) is defined by the base of granule neurons on the SGZ–GCL border. Basal processes extend along the SGZ and into the hilus, and its primary process begins to wind its way through the granule neurons of the GCL.

Movie S2

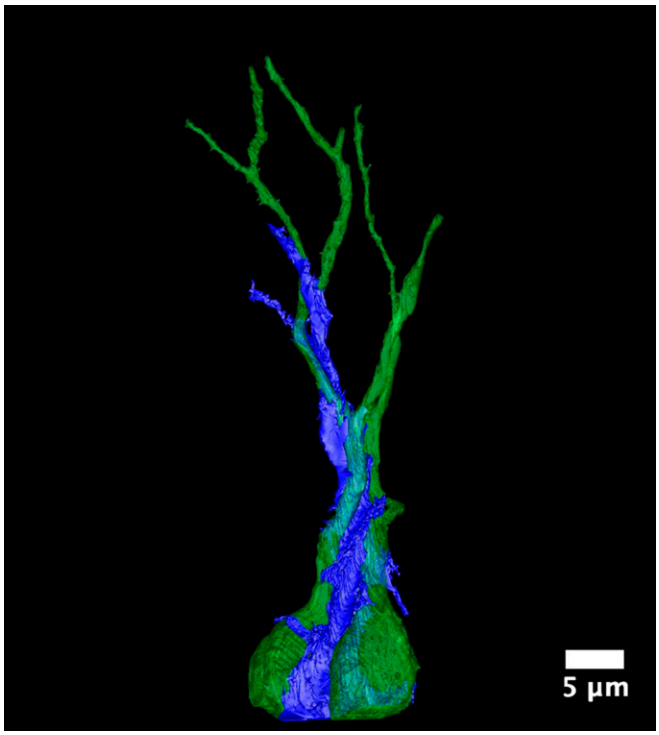

Movie S3. Three-dimensional reconstruction of an NGPα RGL stem cell sandwiched between two granule neurons at the base of the GCL. The NGPα RGL stem cell body (blue) is seen compressed into an hourglass-like morphology between two granule neurons (green) at the base of the GCL. As the primary process of the stem cell rises through the GCL, it follows the dendrites of one granule neuron toward the border with the ML, as shown in Fig. 1 *I* and *J*.

Movie S3

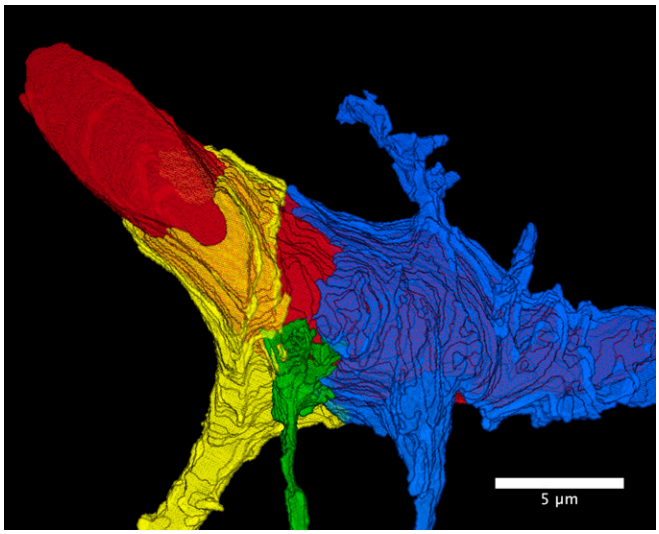

Movie S4. Three-dimensional reconstruction of three NGPα RGL stem cell processes making contacts with and/or wrapping a local blood vessel. In this section through a blood vessel (red), three stem cell processes from two NGPα RGL stem cells are shown contacting a blood vessel. The yellow- and blue-colored processes wrap the vessel more extensively than the green-colored process, which forms a small endfoot-like contact. The space between the three processes with no stem cell process coverage is covered by the processes of an astrocyte. This is also shown in Fig. 2.

Movie S4

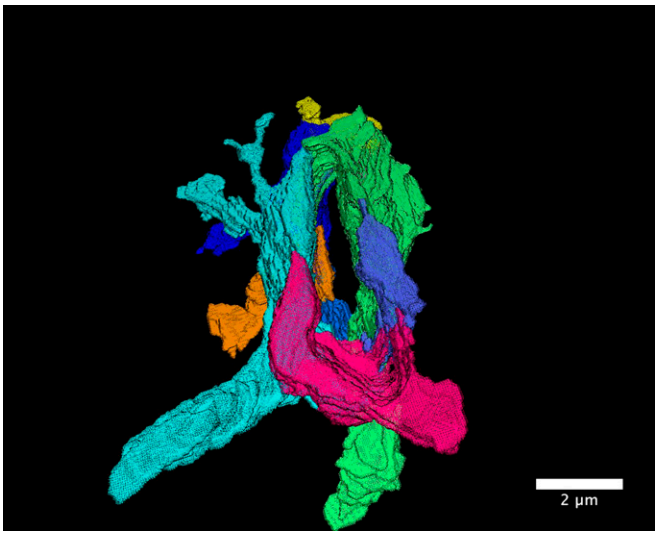

Movie S5. Three-dimensional reconstruction of multiple NGPα RGL stem cell and astrocytic processes wrapping an ML blood vessel. Stem cell processes ("cold" colors; key provided in Fig. 3) and astrocytic processes ("warm" colors) share the wrapping of a blood vessel (uncolored). Adhesions are made between the two types of process and between processes of similar types. Fig. 3 shows more detail.

Movie S5

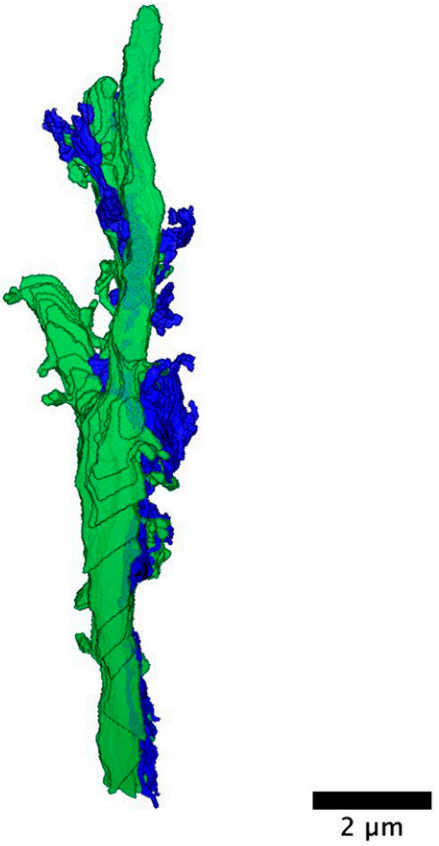

Movie S6. Three-dimensional reconstruction of a fine NGPα RGL stem cell process following the dendrites of a granule neuron. On the ML–GCL border, a fine process of an NGPα RGL stem cell (blue) can be seen following the primary and secondary dendrites of a granule neuron (green). Mitochondria-containing (black) varicosities are seen at regular intervals along the process, and finer processes branch out from these toward local asymmetrical synapses (Fig. 4).

Movie S6

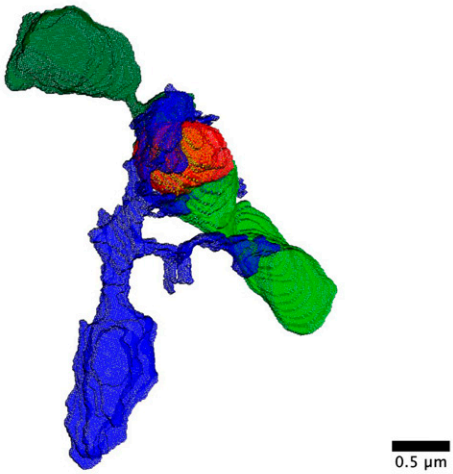

Movie S7. Three-dimensional reconstruction of NGPα RGL stem cell processes wrapping asymmetrical synapses and an axon. An NGPα RGL stem cell process (blue) branches from the thicker primary process and wraps around an axon (red), which is forming asymmetrical synaptic contacts with the large mushroom heads of two dendritic spines (greens). Pools of vesicles (yellow) cluster at the synapses, which are approached from multiple angles by the stem cell processes. Another branch of the process is directed toward the base of the spine neck. Further information is shown in Fig. 5.

Movie S7

A3

Adult hippocampal neurogenesis inversely correlates with microglia in conditions of voluntary running and aging

frontiers in NEUROSCIENCE

ORIGINAL RESEARCH ARTICLE
published: 20 August 2013
doi: 10.3389/fnins.2013.00145

Adult hippocampal neurogenesis inversely correlates with microglia in conditions of voluntary running and aging

Elias Gebara, Sebastien Sultan, Jacqueline Kocher-Braissant and Nicolas Toni*

Department of Fundamental Neurosciences, University of Lausanne, Lausanne, Switzerland

Edited by:
Jack M. Parent, University of Michigan, USA

Reviewed by:
Djoher N. Abrous, Institut des Neurosciences de Bordeaux, France
Amanda Sierra, University of the Basque Country EHU/UPV, Spain

***Correspondence:**
Nicolas Toni, Department of Fundamental Neurosciences, University of Lausanne, 9, rue du Bugnon, 1005 Lausanne, Switzerland
e-mail: nicolas.toni@unil.ch

Adult hippocampal neurogenesis results in the formation of new neurons and is a process of brain plasticity involved in learning and memory. The proliferation of adult neural stem or progenitor cells is regulated by several extrinsic factors such as experience, disease or aging and intrinsic factors originating from the neurogenic niche. Microglia is very abundant in the dentate gyrus (DG) and increasing evidence indicates that these cells mediate the inflammation-induced reduction in neurogenesis. However, the role of microglia in neurogenesis in physiological conditions remains poorly understood. In this study, we monitored microglia and the proliferation of adult hippocampal stem/progenitor cells in physiological conditions known to increase or decrease adult neurogenesis, voluntary running and aging respectively. We found that the number of microglia in the DG was strongly inversely correlated with the number of stem/progenitor cells and cell proliferation in the granule cell layer. Accordingly, co-cultures of decreasing neural progenitor/glia ratio showed that microglia but not astroglia reduced the number of progenitor cells. Together, these results suggest that microglia inhibits the proliferation of neural stem/progenitor cells despite the absence of inflammatory stimulus.

Keywords: adult neurogenesis, dentate gyrus, microglia, running, aging

INTRODUCTION

In the mammalian brain, adult neural stem cells reside in the subventricular zone and subgranular zone (SGZ) of the hippocampus and continue to produce new neurons throughout life (Altman, 1969). Adult neurogenesis has been observed in all mammalian species including humans (Eriksson et al., 1998) and results in the formation of new neurons in the olfactory bulb and the dentate gyrus (DG) of the hippocampus. Radial glia-like (RGL) neural stem cells that reside in the SGZ of the DG, proliferate and give rise to transit-amplifying progenitors (TAP) expressing the T-box brain gene 2 (Tbr2) antigen which then give rise to doublecortin (DCX)-expressing immature neurons (Gage, 2000; Yao et al., 2012). After a phase of maturation, newly-formed neurons express the mature neuronal marker Neu N, functionally integrate into the hippocampal network (Toni and Sultan, 2011) and participate to mechanisms of learning and memory (Aimone et al., 2010). Each of these steps is highly regulated by signaling from the neurogenic niche, and an increasing number of pro-neurogenic factors are being discovered, with great potential interest for cell-replacement therapeutic approaches. The neurogenic niche is constituted by stem cells and their progenies, astrocytes, oligodendrocytes, endothelial cells, microglia, mature and immature neurons (Shihabuddin et al., 2000; Song et al., 2002; Zhao et al., 2008; Bonaguidi et al., 2011). These cells release a wide array of factors that control adult neurogenesis. However, the contribution of specific cell types on the processes of adult neurogenesis remains poorly determined.

Of particular interest, microglia are abundant and widely distributed throughout the adult brain. These cells are involved in the inflammatory reaction and act as the resident immune cells of the brain. Their fine extensions and dynamic nature enable microglia to survey the entire brain parenchyma for potential infection or cell damage and, upon activation, they release cytokines and proceed to the phagocytosis of cell debris or infectious micro-organisms. The experimental activation of microglia by the administration of the bacterial endotoxin lipopolysaccharide (LPS) has been shown to decrease adult neurogenesis, by specifically inhibiting the proliferation or the survival of the new cells (Ekdahl et al., 2003; Monje et al., 2003; Fujioka and Akema, 2010). These effects may be mediated by the release of cytokines such as IL-6, TNFα, IL-1β, since these molecules show an inhibitory effect on adult neurogenesis *in vitro* or *in vivo* (Vallieres et al., 2002; Monje et al., 2003; Keohane et al., 2010; Kohman and Rhodes, 2013).

Recently, the role of microglia in absence of lesion or inflammation has started to raise interest. Indeed, recent studies suggest that resting microglia may be involved in the regulation of physiological mechanisms such as dendritic spine maintenance (Paolicelli et al., 2011) or the homeostasis of the neurogenic niche by the removal of apoptotic newborn cells (Sierra et al., 2010). Furthermore, neural progenitor cells (NPCs) regulate microglia function *in vitro*, by the secretion of growth factors (Mosher et al., 2012). However, the role of microglia on adult neurogenesis in physiological conditions remains unclear.

Here, we examined the correlation between the amount of microglia in the hippocampus and the proliferation of adult neural stem cells, in physiological conditions. To increase the variability in progenitor proliferation, we used aging and voluntary

exercise, as these parameters are known to decrease and increase neurogenesis respectively (Kuhn et al., 1996; van Praag et al., 1999, 2005; Encinas et al., 2011; Kempermann, 2011).

MATERIALS AND METHODS

ETHICS STATEMENT

This study was carried out in strict accordance with the recommendations in the Guidance for the Care and Use of Laboratory Animals of the National Institutes of Health. All experimental protocols were approved by the Swiss animal experimentation authorities (Service de la consommation et des affaires vétérinaires, Chemin des Boveresses 155, 1066 Epalinges, Switzerland, permit number: 2301). Every effort was made to minimize the number of animals used and their suffering.

EXPERIMENTAL ANIMALS

All animals used for this study were adult male mice. GFAP-GFP mice were a kind gift from the laboratory of Helmut Kettenmann (Max-Delbruck center, Berlin, Germany) (Nolte et al., 2001). They express the green fluorescent protein (GFP) under the control of the human glial fibrillary acidic protein promoter (GFAP). At the beginning of the experiment, the first group of mice was 6-week-old and the second group 7.5-month-old. Runner mice were housed for 2 weeks in standard cages equipped with a running wheel (Fast-Trac; Bio-Serv, USA) and were allowed free access to the running wheel. Non-runner mice were housed in similar, adjacent cages without running wheel. All mice were housed in a 12-h light/dark cycle and controlled temperature of 22°C. Food and water were available *ad-libitum*.

BrdU ADMINISTRATION

Immediately at the end of the running period, all mice were injected intraperitoneally with the DNA replication marker, Bromodeoxyuridine (BrdU, Sigma-Aldrich, Buchs, Switzerland), at doses of 100 mg/kg in saline, 3 times at 2-h intervals. Two hours after the last injection, mice were sacrificed and the number of BrdU cell was counted to assess cell proliferation (Mandyam et al., 2007; Taupin, 2007; Yang et al., 2011; Gao and Chen, 2013).

TISSUE COLLECTION AND PREPARATION

At the end of the experiment, mice received a lethal dose of pentobarbital (10 mL/kg, Sigma-Aldrich, Buchs, Switzerland) and were perfusion-fixed with 50 ml of 0.9% saline followed by 100 mL of 4% paraformaldehyde (Sigma-Aldrich, Switzerland) dissolved in phosphate buffer saline (PBS 0.1M, pH 7.4). Brains were then collected, postfixed overnight at 4°C, cryoprotected 24 h in 30% sucrose and rapidly frozen. Coronal frozen sections of a thickness of 40 µm were cut with a microtome-cryostat (Leica MC 3050S) and slices were kept in cryoprotectant (30% ethylene glycol and 25% glycerin in 1X PBS) at –20°C until processed for immunostaining.

IMMUNOHISTOCHEMISTRY

Immunochemistry was performed on 1-in-6 series of section. Sections were washed 3 times in PBS 0.1 M. BrdU detection required formic acid pretreatment (formamide 50% in 2X SSC buffer; 2X SSC is 0.3 M NaCl and 0.03 M sodium citrate, pH 7.0) at 65°C for 2 h followed by DNA denaturation for 30 min in 2 M HCl for 30 min at 37°C and rinsed in 0.1 M borate buffer pH 8.5 for 10 min. Then, slices were incubated in blocking solution containing 0.3% Triton-X100 and 15% normal serum normal goat serum (Gibco, 16210-064) or normal donkey serum (Sigma Aldrich, D-9663), depending on the secondary antibody in PBS 0.1 M. Slices were then incubated 40 h at 4°C with the following primary antibodies: mouse monoclonal anti-BrdU (1:250, Chemicon International, Dietikon, Switzerland), rabbit anti-Ki-67 (1:200, Abcam, ab15580), goat anti-DCX (1:500, Santa Cruz biotechnology, sc-8066), rabbit anti-GFAP (1:500, Invitrogen, 180063), rabbit anti-Tbr2 (1:200, Abcam, ab23345), goat anti-Iba1 (1:200, Abcam, ab5076), mouse anti-MHC-II (1:200 Abcam, ab23990). The sections were then incubated for 2 h in either of the following secondary antibodies: goat anti-mouse Alexa-594 (1:250, Invitrogen), goat anti-rabbit Alexa-594 (1:250, Invitrogen), donkey anti-goat Alexa-555 (1:250, Invitrogen). 4,6 diamidino-2-phenylindole (Dapi) was used to reveal nuclei.

CELL CULTURE

Adult NPCs expressing the red fluorescent protein (RFP) are a kind gift from the laboratory of Fred Gage (Salk Institute, San Diego, USA). They were isolated from the DG of adult Fisher 344 rats and cultured as previously described (Palmer et al., 1997). Microglia and astrocyte primary culture were purified from postnatal day 3 rats. Cerebral cortices, including the hippocampus, were mechanically triturated for homogenization and seeded onto poly-D-lysine coated 75 cm^2 flasks in Dulbecco's Modified Eagle Medium (DMEM) glutamax (Invitrogen, USA), 10% normal calf serum with penicillin/streptomycin (Invitrogen, USA). Cells were grown for 5–7 days in a humidified 5% CO2 incubator at 37°C. At confluence, flasks were shaken at 250 rpm on an orbital shaker for 2 h to separate microglia from astrocytes. Detached microglia were seeded in poly-D-lysine coated 6-well microplates in culture medium supplemented with 30% astrocyte conditioned medium, to enhance the survival of microglia (personal communication from Dr. Romain Gosselin, University of Lausanne). Different numbers of microglia or astrocytes were plated on coated 12 mm coverslips in a 24-well culture plate (20,000, 40,000, 60,000 cells per well). Three hours later, a fixed number of RFP-expressing NPCs (20,000 cells per well) were plated on the same culture wells, at a (NPCs/Glia) ratio of 1/0, 1/1, 1/2, 1/3. Three wells per condition were used. Ninety-six hours after plating, cells were fixed with 4% paraformaldehyde for 20 min, briefly washed and immunostained for Iba1 or GFAP and mounted.

CELL NUMBER QUANTIFICATION

All images were acquired using a confocal microscope (Zeiss LSM 710 Quasar Carl Zeiss, Oberkochen, Germany). The total number of immunoreactive cells was estimated throughout the entire granule cell layer using stereological sampling, as previously described (Thuret et al., 2009), between –1.3 to –2.9 mm from the Bregma. For each animal, a 1-in-6 series of sections was stained with the nucleus marker DAPI and used to measure the volume of the granule cell layer. The granule cell area was traced using Axiovision (Zeiss, Germany) software and the

granule cell volume was determined by multiplying the traced granule cell layer area by the thickness of the corresponding section and the distance between the sections sampled (240 μm). For all mice analyzed in this study, no difference of volume was found between groups [One-Way ANOVA, $F_{(3,\ 15)} = 0.29$, $p = 0.82$], (data not shown). All cells were counted blind with regard to the mouse status. The number of labeled cells was counted for each section, in the entire thickness of the granular cell layer of the DG with a 40x objective. RGL cells and cells expressing BrdU, Ki-67, DCX or Tbr2 were counted in an area containing the granule cell layer and the subgranular zone, whereas cells expressing Iba1, MHC-II and GFAP (**Figures 2A,D,F**) were counted in an area including the sub-granular cell layer, the granule cell layer, the molecular layer and the hilus. Cells expressing Iba1 (**Figure 2B**) were also counted in the primary somatosensory cortex (S1).

For *in vitro* cell quantification, images were acquired using confocal microscopy. The numbers of RFP-expressing NPCs, Iba1-expressing microglia and GFAP-expressing astrocytes were counted in 4 selected fields, systematically placed in the same positions relative to the coverslips' edges. The total number of cells per selected field was divided by the total area of the selected fields to obtain an average cell density per well that was then multiplied by the total surface area of the coverslip to obtain an estimate of the total number of cells per coverslip. This number of cells was then compared to the number of cells that were plated in the wells to obtain a percentage of increase in NPCs number.

STATISTICAL ANALYSIS

Hypothesis testing was two-tailed. All analyses were performed using JMP10 software. First, Shapiro-Wilk tests were performed on each dataset to test for distribution normality. The distribution was normal for all data. To test for possible interaction between the 2 groups (Aging and Running) a Two-Way ANOVA was performed. When an interaction was found, a One-Way ANOVA test was performed, if no interaction was found, we analyzed each variable independently using a Two-Way ANOVA. All analyses were followed by a *post-hoc* Tukey HSD test. In order to test linear correlation, Spearman correlation test was performed. Results are expressed by the Spearman correlation coefficient (ρ) and the *p*-value. Data is presented as mean ± standard error of the mean (SEM).

RESULTS

EFFECT OF AGING AND RUNNING ON CELL PROLIFERATION AND IMMATURE NEURONS

We tested the effect of running and aging on GFAP-GFP mice (Nolte et al., 2001), which are commonly-used mice models for the examination of adult neurogenesis and enable the identification of stem cells (Huttmann et al., 2003; Ehninger and Kempermann, 2008). Sixteen GFAP-GFP mice were divided in 4 experimental groups: young adult mice (8 weeks of age; 8 W) and older mice (8 months of age; 8 M), that were previously housed individually in standard cages in presence (R) or absence (NR) of a running wheel for 2 weeks (4 mice per group). At the end of the 2 weeks period, all mice received 3 intraperitoneal injections of BrdU (100 mg/kg) at 2 h intervals and were sacrificed 2 h after the last BrdU injection (**Figure 1A**). Brains were sectioned and immunostained for BrdU and markers for adult neurogenesis and microglia. We first assessed cell proliferation in the granule cell layer of the DG. A Two-Way ANOVA test revealed that there is interaction between aging and running for Ki-67 marker [$F_{(1,\ 12)} = 5.74$; $p < 0.05$]. The density of Ki-67-expressing cells was significantly decreased by aging [**Figures 1B,C**, One-Way ANOVA $F_{(3,\ 15)} = 22.65$; $p < 0.001$. *Post-hoc* Tukey HSD test: NR 8 W vs. NR 8M $p < 0.05$] and increased by running [One-Way ANOVA $F_{(3,\ 15)} = 22.65$; $p < 0.001$. *Post-hoc* Tukey HSD test NR 8 W vs. R 8 W $p < 0.001$, NR 8 M vs. R 8 M $p = 0.24$].

Similarly, there is interaction between aging and running for BrdU marker [Two-Way ANOVA $F_{(1,\ 12)} = 17.6$; $p < 0.01$]. The density of BrdU-expressing cells was significantly decreased with aging [**Figures 1D,E**, One-Way ANOVA $F_{(3,\ 15)} = 62.19$; $p < 0.001$. *Post-hoc* Tukey HSD test: NR 8 W vs. NR 8 M, $p < 0.05$] and increased by running [One-Way ANOVA $F_{(3,\ 15)} = 62.19$; $p < 0.001$. *Post-hoc* Tukey HSD test: NR 8 W vs. R 8 W $p < 0.001$, NR 8 M vs. R 8 M $p < 0.01$]. Thus, cell proliferation was increased by voluntary running and reduced by aging.

In the DG, proliferative cells are divided in 2 main cell populations: the type 1, radial glia-like (RGL) stem cells and the type 2, TAPs. RGL cells were identified by the expression of GFP, their nucleus located in the subgranular zone and a radial process extending through the granule cell layer and branching into the molecular layer (Huttmann et al., 2003; Mignone et al., 2004; Kriegstein and Alvarez-Buylla, 2009; Beckervordersandforth et al., 2010). They expressed the self-renewal factor Sox2 (data not shown). For RGL, Two-Way ANOVA test showed that there is interaction between aging and running [$F_{(1,\ 12)} = 5.3$; $p < 0.05$]. The density of RGL cells was significantly decreased by aging (**Figures 1F,G**, One-Way ANOVA $F_{(3,\ 15)} = 35.81$; $p < 0.001$. *Post-hoc* Tukey HSD test: NR 8 W vs. NR 8 M $p < 0.05$] and increased by running [One-Way ANOVA $F_{(3,\ 15)} = 35.81$; $p < 0.001$. *Post-hoc* Tukey HSD test: NR 8 W vs. R 8 W $p < 0.001$, NR 8 M vs. R 8 M $p < 0.01$]. TAPs were identified by immunostaining against Tbr2 (Hodge et al., 2008). Similarly, there is interaction between aging and running for Tbr2 marker [Two-Way ANOVA $F_{(1,12)} = 5.2$ $p < 0.05$]. The density of Tbr2-expressing cells was decreased by aging [**Figures 1H,I**, One-Way ANOVA $F_{(3,\ 15)} = 27.32$; $p < 0.001$. *Post-hoc* Tukey HSD test: NR 8 W vs. NR 8 M $p < 0.05$] and increased by running [One-Way ANOVA $F_{(3,\ 15)} = 27.32$; $p < 0.001$. *Post-hoc* Tukey HSD test NR 8 W vs. R 8 W $p < 0.001$, NR 8 M vs. R 8 M $p = 0.2$]. Thus, running increased and aging decreased the density of stem and progenitor cells.

Finally, we examined the effect of aging and running on immature neurons identified by immunohistochemistry against doublecortin (DCX). A Two-Way ANOVA test revealed that there is no interaction between aging and running for DCX marker [$F_{(1,\ 12)} = 2.21$; $p = 0.16$]. Although, The density of DCX-expressing cells decreased with aging [**Figures 1J,K**, Anova $F_{(1,\ 12)} = 52.90$; $p < 0.001$. *Post-hoc* Tukey HSD test: NR 8 W vs. NR 8 M $p < 0.01$] and increased with running [$F_{(1,\ 12)} = 29.97$; $p < 0.001$. *Post-hoc* Tukey HSD test NR 8 W vs. R 8 W $p < 0.001$,

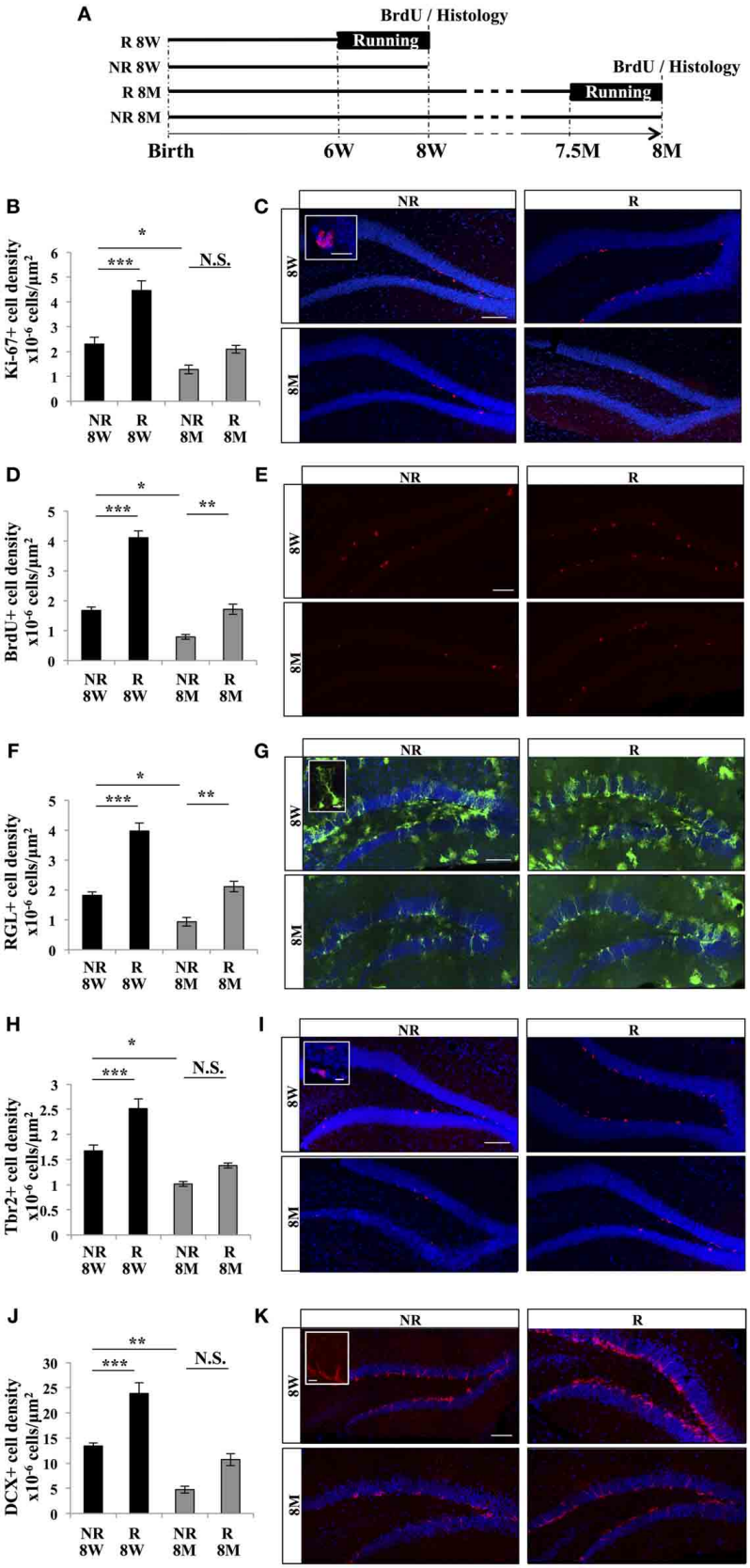

FIGURE 1 | Continued

FIGURE 1 | Effect of running and aging on cell proliferation in the dentate gyrus. (A) Experimental timeline. **(B)** Histogram of the density (cells/μm^2) of Ki-67–expressing cells in the granule cell layer of the dentate gyrus of 8-week-old animals (8 W) and 8-month-old animals (8 M) housed with (R), or without (NR) a running wheel. **(C)** Confocal maximal projection micrographs of hippocampal sections immunostained for Ki-67. Inset: Higher magnification confocal micrograph of a Ki-67-expressing cell. **(D)** Histogram of the density of BrdU-positive cells in the granule cell layer of the dentate gyrus. **(E)** Confocal maximal projection micrographs of hippocampal sections immunostained for BrdU. **(F)** Quantification of the density of RGL cells in the granule cell layer of the dentate gyrus. **(G)** Confocal maximal projection micrographs of hippocampal sections. Inset: Higher magnification confocal micrograph of a RGL cell. **(H)** Histogram showing the density of Tbr2-expressing cells in the granule cell layer of the dentate gyrus. **(I)** Confocal maximal projection micrographs of hippocampal sections immunostained for Tbr2. Inset: Higher magnification confocal micrograph of a Tbr2-expressing cell. **(J)** Histogram of the density of DCX-immunolabeled cells in the granule cell layer of the dentate gyrus. **(K)** Confocal micrographs of hippocampal sections immunostained for DCX. Inset: Higher magnification confocal micrograph of a DCX-immunolabeled group of cells. Blue: Dapi staining. Animals, $n = 4$ per group. Scale bars: 100 μm, insets 10 μm, *post-hoc* Tukey HSD test $^{*}p < 0.05$; $^{**}p < 0.01$; $^{***}p < 0.001$; NS: $p > 0.05$. Each value represents the mean ± SEM.

NR 8 M vs. R 8 M $p = 0.06$]. Together, these results indicate that the density of proliferative cells, cell proliferation and the density of immature neurons decreased with aging and increased with voluntary running.

EFFECT OF AGING AND RUNNING ON MICROGLIA

Next we examined the effect of aging and running on microglia, using the immunomarker Iba1. Iba1-expressing cells displayed an oval cell body and numerous ramified processes (**Figures 2A–C**). A Two-Way ANOVA revealed that there is interaction between aging and running for Iba1 marker [$F_{(1,\ 12)} = 5.65$; $p < 0.05$]. The density of Iba 1-expressing cells in the DG was decreased by running [**Figures 2A–C**, One-Way ANOVA $F_{(3,\ 15)} = 75.94$; $p < 0.001$. *Post-hoc* Tukey HSD test: NR 8 W vs. R 8 W $p < 0.001$, NR 8 M vs. R 8 M $p < 0.001$] and increased by aging [One-Way ANOVA $F_{(3,\ 15)} = 75.94$; $p < 0.001$. *Post-hoc* Tukey HSD test: NR 8 W vs. NR 8 M $p < 0.001$]. To examine whether the effect of running and aging on microglia was restricted to the hippocampus, we measured microglia in the primary somato-sensory cortex of all mice. Contrary to what we observed in the DG, in the primary somato-sensory cortex, there was no interaction between aging and running in the level of Iba1 marker [Two-Way ANOVA $F_{(1,\ 12)} = 2.1$; $p = 0.17$]. Anova showed that running increased [**Figure 2B**, $F_{(1,\ 12)} = 92.47$; $p < 0.001$. *Post-hoc* Tukey HSD test: NR 8 W vs. R 8 W $p < 0.001$, NR 8 M vs. R $p < 0.001$] whereas aging decreased the density of microglia in the cortex [$F_{(1,\ 12)} = 52.49$; $p < 0.001$. *Post-hoc* Tukey HSD test: NR 8 W vs. NR 8 M $p < 0.001$].

To test whether the expression of the antigen presentation protein MHC II was also regulated by aging and running, we immunostained brain slices for MHC II. A Two-Way ANOVA revealed that there is interaction between aging and running for MHC II marker [$F_{(1,\ 12)} = 8.08$ $p < 0.01$]. The density of MHC II-expressing cells was decreased by running [**Figures 2D,E**, One-Way ANOVA $F_{(3,\ 15)} = 145.19$; $p < 0.001$. *Post-hoc* Tukey HSD test: NR 8 W vs. R 8 W $p < 0.001$, NR 8 M vs. R 8 M $p < 0.001$] and increased by aging [One-Way ANOVA $F_{(3,\ 15)} = 145.19$, $p < 0.001$. *Post-hoc* Tukey HSD test: NR 8 W vs. NR 8 M $p < 0.001$]. Finally, we examined whether astroglia was similarly affected by running or aging by immunostaining against GFAP. The density of GFAP-expressing astrocytes was constant throughout all conditions [**Figures 2F,G**; Two-Way ANOVA $F_{(3,\ 12)} = 0.49, p = 0.69$], indicating that the effect of aging and running was specific to microglia.

CORRELATION BETWEEN MICROGLIA AND ADULT NEUROGENESIS

The opposite effects of running and aging on microglia and adult neurogenesis suggest that microglia and adult neurogenesis may be inversely correlated. We therefore plotted, for each mouse, the number of Iba-expressing microglia and the number of cells expressing markers for neurogenesis. The number of Iba1-expressing microglia was inversely correlated with the number of Ki-67-expressing cells (**Figure 3**; $\rho = -0.92$, $p < 0.001$), RGL cells ($\rho = -0.98$, $p < 0.001$), Tbr2-expressing cells ($\rho = -0.85$, $p < 0.001$), BrdU-immunolabeled cells ($\rho = -0.95$, $p < 0.001$), and DCX-expressing cells ($\rho = -0.88$, $p < 0.001$). Similarly, the number of MCH II-expressing microglia inversely correlated with the number of Ki-67-expressing cells (Data not shown; $\rho = -0.95$, $p < 0.001$), RGL cells ($\rho = -0.92$, $p < 0.001$), Tbr2-expressing cells ($\rho = -0.97$, $p < 0.001$), BrdU-immunolabeled cells ($\rho = -0.94$, $p < 0.001$), and DCX-expressing cells ($\rho = -0.97$, $p < 0.001$). These results indicate that microglia density was inversely correlated with stem/progenitor cell proliferation.

To test the possibility that microglia number could directly affect stem/progenitor cell proliferation, we co-cultured microglia and NPCs. We plated a constant number of NPCs with an increasing proportion of microglia and 4 days later, we counted the number of remaining NPCs. The number of NPCs significantly decreased with the increasing proportion of co-cultured microglia [**Figure 4**; One-Way ANOVA $F_{(6,\ 20)} = 82.58$, $p < 0.001$; 1/0 vs. 1/1 *post-hoc* Student's *t*-test $p < 0.001$, 1/0 vs. 1/2 *post-hoc* Student's *t*-test $p < 0.001$, 1/0 vs. 1/3 *post-hoc* Student's *t*-test $p < 0.001$]. To test whether this effect was specific to microglia, we repeated this experiment with increasing proportion of astrocytes instead of microglia. In contrast to microglia, astrocytes did not decrease the number of NPCs in co-cultures [One-Way ANOVA $F_{(6,\ 20)} = 82.58$, $p < 0.001$; 1/0 vs. 1/2 *post-hoc* Student's *t*-test $p = 0.53$, 1/0 vs. 1/3 *post-hoc* Student's *t*-test $p = 0.13$]. Thus, increasing microglia density inhibited NPCs growth and/or survival *in vitro* and resulted in a corresponding decrease in NPCs number.

DISCUSSION

In this study, we exploited the physiological variations of adult neurogenesis induced by voluntary running and aging to examine the correlation between microglia and adult hippocampal neurogenesis in absence of inflammatory stimulus. In line with previous studies, we found that aging decreased cell proliferation and the

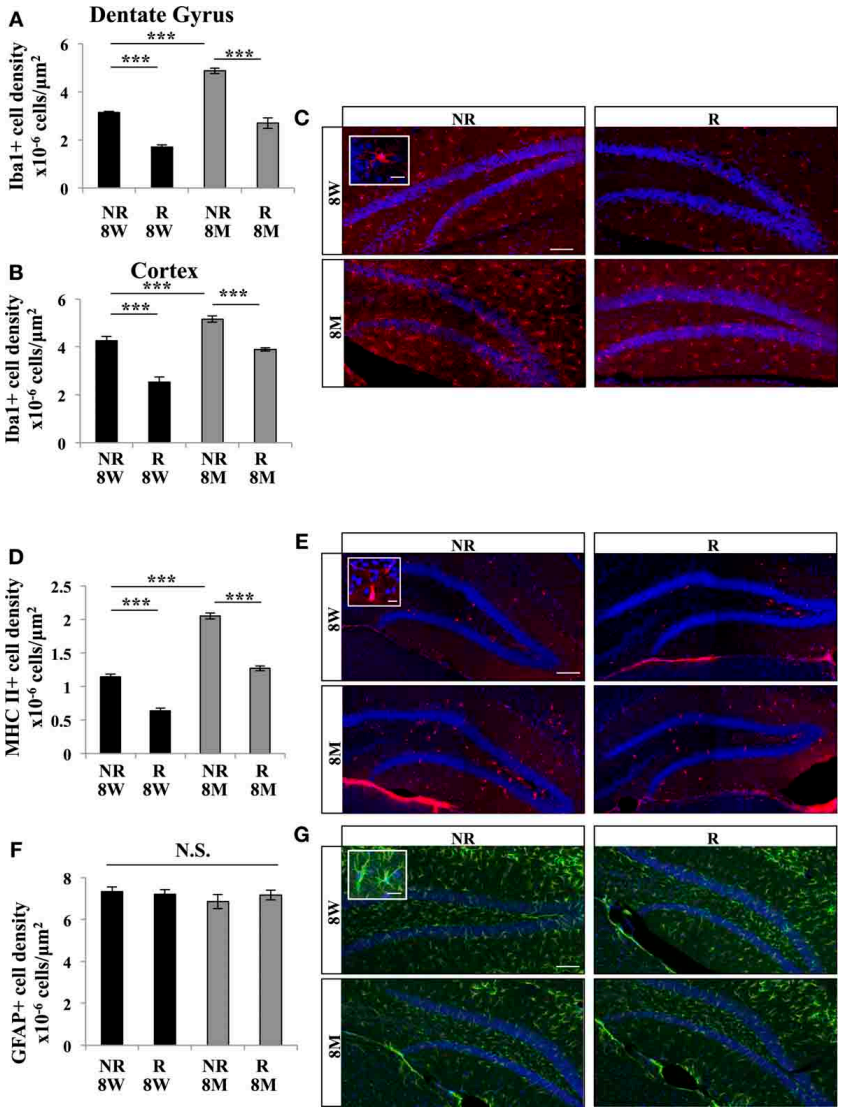

FIGURE 2 | Effect of running and aging on the density of microglia. **(A)** Histogram showing the density (cells/μm^2) of Iba1-expressing cells in the dentate gyrus (including hilus, granule cell layer and molecular layer). **(B)** Histogram of the density of Iba1-expressing cells in the cortex. **(C)** Confocal maximal projection micrographs of hippocampal sections immunostained for Iba1. Inset: Higher magnification confocal micrograph of an Iba1-immunolabeled cell. **(D)** Histogram of the density of MHC II-expressing cells in the dentate gyrus. **(E)** Confocal maximal projection micrographs of hippocampal sections immunostained for MHC II. Inset: Higher magnification confocal micrograph of a MHC II-immunolabeled cell. **(F)** Histogram of the density of GFAP-expressing astrocytes in the dentate gyrus of mice for each experimental condition. **(G)** Confocal maximal projection micrographs of hippocampal sections immunostained for GFAP. Inset: Higher magnification confocal micrograph of a GFAP-immunolabeled cell. Blue: Dapi staining. Animals: $n = 4$ per group. Scale bars: 100 µm, insets 10 µm. *post-hoc* Tukey HSD test: N.S.: $p > 0.05$; $^{***}p < 0.001$. Each value represents the mean ± SEM.

number of immature neurons whereas voluntary running had inverse effects (Kuhn et al., 1996; van Praag et al., 1999, 2005; Encinas et al., 2011; Kempermann, 2011). In addition, we found that the decrease in RGL cells observed with aging (Encinas et al., 2011), was reversed by voluntary running, suggesting that running may induce the symmetrical division of RGL cells and restore their population. Strikingly, in both conditions, the amount of microglia but not of astroglia was strongly inversely correlated with all measured parameters of neurogenesis. Similarly, *in vitro*, co-cultures of NPCs with an increasing proportion of microglia but not of astroglia reduced the number of NPCs after 4 days. Together, these results indicate that, in physiological conditions, microglia and neurogenesis are inversely correlated and suggest that microglia may inhibit adult neurogenesis by directly acting on stem/progenitor cells.

These observations are in line with previous experiments showing that, in inflammatory conditions induced by epilepsy, ischemia or LPS injection, microglia undergo dramatic changes in their morphological and cytokine expression pattern and inhibit adult neurogenesis (Monje et al., 2002; Ekdahl et al., 2003; Liu

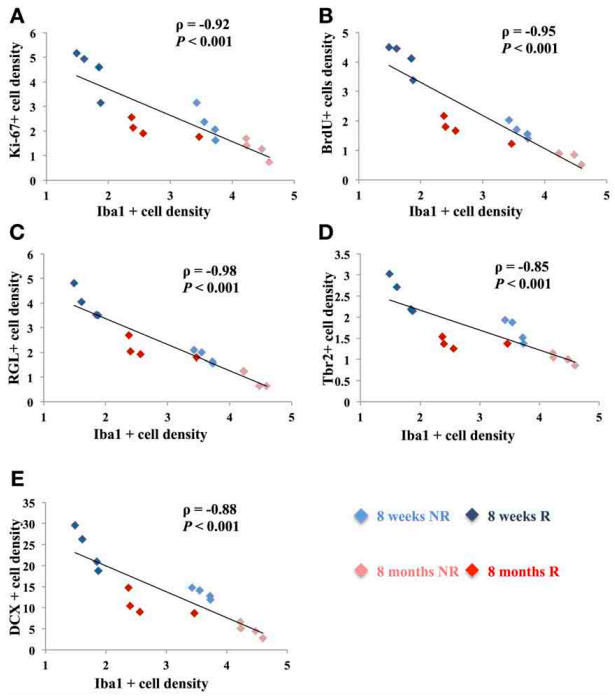

FIGURE 3 | Correlation between cell proliferation and Iba1-expressing microglia. (A–E) Plots showing the density of Ki-67-expressing cells **(A)**, BrdU-labeled cells **(B)**, RGL cells **(C)**, Tbr2-expressing cells **(D)** and DCX-expressing cells **(E)**, as a function of the density of Iba1-expressing cells, in the dentate gyrus. Each point represents the density of cells for one animal. Spearman's correlation test was used to study the correlation, ρ: coefficient of Spearman; p: value of significance.

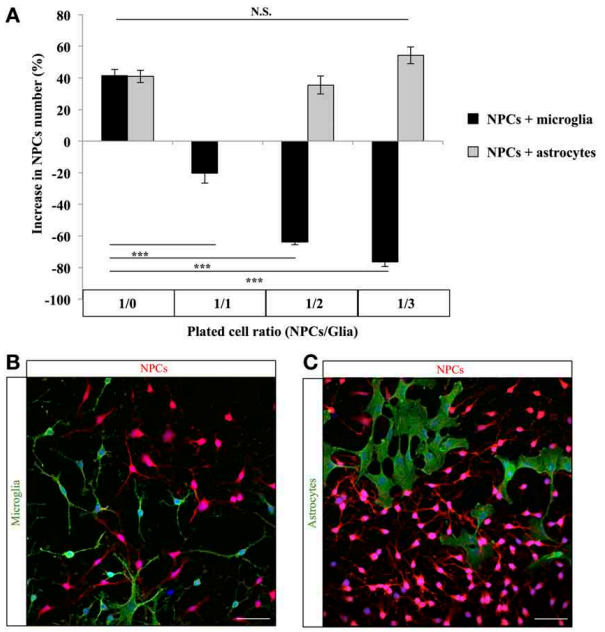

FIGURE 4 | Effect of microglia on progenitor cells *in vitro*. (A) Histogram of the change in NPCs number when cultured with microglia or astrocytes (% from the number of plated cells). $N = 3$ culture wells per group. **(B)** Confocal maximal projection micrographs of NPCs-microglia co-cultures. **(C)** Confocal maximal projection micrographs of NPCs-astrocytes co-cultures. N.S.: $p > 0.05$, $^{***}p < 0.001$. Each value represents the mean ± SEM.

et al., 2007; Kohman et al., 2012). Similarly, aging is associated with a reduced neurogenesis, mild, chronic inflammation and increased microglia proliferation that can be attenuated by voluntary running (Kohman et al., 2012). In these experimental paradigms, inflammatory microglia is believed to directly inhibit neurogenesis, since anti-inflammatory treatments restore neurogenesis (Ekdahl et al., 2003; Monje et al., 2003; Liu et al., 2007; Kohman and Rhodes, 2013) and the exercise-induced increase and the age-dependent decline in neurogenesis are mediated by microglia *in vitro* (Vukovic et al., 2012).

However, in our study, we did not induce inflammation and in absence of activation, microglia has been reported to promote neurogenesis: In adult rats, the increased neurogenesis induced by environmental enrichment was accompanied by an increase in microglia number, whereas immunodeficient mice had impaired neurogenesis (Ziv et al., 2006). Similarly, voluntary running was shown to increase neurogenesis (van Praag et al., 1999) and microglia proliferation (Ehninger and Kempermann, 2008; Encinas et al., 2011), without inducing changes in the total number of microglia cells or in their activation state (Encinas et al., 2011). *In vitro* too, microglia was shown to promote the proliferation of co-cultured NPCs, an effect believed to be mediated by released factors, since the pro-neurogenic effect was mimicked by microglia-conditioned medium (Morgan et al., 2004; Aarum et al., 2003; Walton et al., 2006; Nakanishi et al., 2007). Thus, it is surprising that in our study, we observed an inverse correlation between microglia number and neurogenesis, in absence of inflammatory stimulus, in particular in running and non-running young mice. This discrepancy may partly result from differences in housing conditions, diet or animal strain. Indeed, while our study examined transgenic mice in the FVB/N background, the Ziv study used adult male rats (Ziv et al., 2006) and the Olah study used adult male C57Bl/6 mice (Olah et al., 2009). FVB/N mice are known to have reduced cell proliferation in the adult DG, as compared to C57Bl/6 mice (Schauwecker, 2006) and may therefore respond differently to microglia regulation, or have increased basal inflammatory state. However, the absence of inflammatory stimulus in our *in vivo* experiments as well as the morphological aspect of microglia suggestive of a resting state, indicate no overt inflammation in GFAP-GFP mice. Furthermore, the observation that microglia reduced the number of NPCs *in vitro* supports the idea of a direct inhibition of progenitor cell proliferation by microglia. Finally, in a recent study, we found that doxycycline treatment decreased microglia cell number and increased neurogenesis and cell proliferation in C57Bl/6 mice (Sultan et al., 2013), suggesting that environmental factors and housing conditions may interfere with the effect of microglia on adult neurogenesis, rather than mouse strain.

However, correlation does not imply causality and the signaling between microglia and neurogenesis in the adult healthy brain remains unclear. Although activated microglia can directly inhibit neurogenesis by releasing a number of pro-inflammatory

cytokines (Monje et al., 2003; Nakanishi et al., 2007), external factors such as voluntary running may act on neurogenesis independently from microglia. For example, the exercise-induced increase in neurogenesis depends on peripheral VEGF (Fabel et al., 2003) that acts directly on NPCs of the hippocampus (Fournier et al., 2012). Running can also affect microglia by reducing the expression of pro-inflammatory cytokines such as TNF-α, and increasing the expression of the anti-inflammatory cytokines such as IL-1ra (Pervaiz and Hoffman-Goetz, 2011) or the chemokine CX_3CL1, that induces a neuroprotective microglia phenotype and promotes neurogenesis (Vukovic et al., 2012). Inversely, gene expression analysis in the hippocampus showed that running induced the transcription of genes involved in inflammation, including genes related to MHC I (β2-microglobulin, H2-D1) and elements of the complement system (C4A, C3, C1q) or in the inflammatory response (COX-2, CX3C), suggesting that running may increase inflammation (Tong et al., 2001; Kohman et al., 2011).

Depending on its activation state, microglia may have opposite effects on adult neurogenesis and it is likely that in the same brain, pro-neurogenic and anti-neurogenic microglia co-exist, with a different response to external stimulus, such as voluntary running and housing conditions. The combined action of external factors and microglia state may then result in unexpected effects on adult neurogenesis. Clearly, further experiments will be necessary to elucidate the regulation of neurogenesis by microglia and the role played by environmental factors such as stress and activity on both microglia and neurogenesis. This knowledge is crucial for the understanding of the regulation of adult neurogenesis by the neurogenic niche as well as for the therapeutic use of neural stem cells in inflammatory context such as lesions or neurodegenerative disorders.

AUTHOR CONTRIBUTIONS

Conceived and designed the experiments: Elias Gebara, Sebastien Sultan and Nicolas Toni. Performed the experiments: Elias Gebara, Sebastien Sultan and Jacqueline Kocher-Braissant Analyzed the data: Elias Gebara and Sebastien Sultan Wrote the paper: Elias Gebara, Sebastien Sultan and Nicolas Toni.

ACKNOWLEDGMENTS

The authors wish to thank Romain Gosselin (Department of Fundamental Neurosciences, University of Lausanne, Switzerland) for critical insight on *in vitro* experiments. Images acquisition was performed at the Cellular Imaging Facility of the University of Lausanne (Lausanne, Switzerland). This work was supported by the Swiss National Science Foundation and the Leenaards Foundation.

REFERENCES

Aarum, J., Sandberg, K., Haeberlein, S. L., and Persson, M. A. (2003). Migration and differentiation of neural precursor cells can be directed by microglia. *Proc. Natl. Acad. Sci. U.S.A.* 100, 15983–15988. doi: 10.1073/pnas.2237050100

Aimone, J. B., Deng, W., and Gage, F. H. (2010). Adult neurogenesis: integrating theories and separating functions. *Trends Cogn. Sci.* 14, 325–337. doi: 10.1016/j.tics.2010.04.003

Altman, J. (1969). Autoradiographic and histological studies of postnatal neurogenesis. 3. Dating the time of production and onset of differentiation of cerebellar microneurons in rats. *J. Comp. Neurol.* 136, 269–293. doi: 10.1002/cne.901360303

Beckervordersandforth, R., Tripathi, P., Ninkovic, J., Bayam, E., Lepier, A., Stempfhuber, B., et al. (2010). *In vivo* fate mapping and expression analysis reveals molecular hallmarks of prospectively isolated adult neural stem cells. *Cell Stem Cell* 7, 744–758. doi: 10.1016/j.stem.2010.11.017

Bonaguidi, M. A., Wheeler, M. A., Shapiro, J. S., Stadel, R. P., Sun, G. J., Ming, G. L., et al. (2011). *In vivo* clonal analysis reveals self-renewing and multipotent adult neural stem cell characteristics. *Cell* 145, 1142–1155. doi: 10.1016/j.cell.2011.05.024

Ehninger, D., and Kempermann, G. (2008). Neurogenesis in the adult hippocampus. *Cell Tissue Res.* 331, 243–250. doi: 10.1007/s00441-007-0478-3

Ekdahl, C. T., Claasen, J. H., Bonde, S., Kokaia, Z., and Lindvall, O. (2003). Inflammation is detrimental for neurogenesis in adult brain. *Proc. Natl. Acad. Sci. U.S.A.* 100, 13632–13637. doi: 10.1073/pnas.2234031100

Encinas, J. M., Michurina, T. V., Peunova, N., Park, J. H., Tordo, J., Peterson, D. A., et al. (2011). Division-coupled astrocytic differentiation and age-related depletion of neural stem cells in the adult hippocampus. *Cell Stem Cell* 8, 566–579. doi: 10.1016/j.stem.2011.03.010

Eriksson, P. S., Perfilieva, E., Bjork-Eriksson, T., Alborn, A. M., Nordborg, C., Peterson, D. A., et al. (1998). Neurogenesis in the adult human hippocampus. *Nat. Med.* 4, 1313–1317. doi: 10.1038/3305

Fabel, K., Fabel, K., Tam, B., Kaufer, D., Baiker, A., Simmons, N., et al. (2003). VEGF is necessary for exercise-induced adult hippocampal neurogenesis. *Eur. J. Neurosci.* 18, 2803–2812. doi: 10.1111/j.1460-9568.2003.03041.x

Fournier, N. M., Lee, B., Banasr, M., Elsayed, M., and Duman, R. S. (2012). Vascular endothelial growth factor regulates adult hippocampal cell proliferation through MEK/ERK- and PI3K/Akt-dependent signaling. *Neuropharmacology* 63, 642–652. doi: 10.1016/j.neuropharm.2012.04.033

Fujioka, H., and Akema, T. (2010). Lipopolysaccharide acutely inhibits proliferation of neural precursor cells in the dentate gyrus in adult rats. *Brain Res.* 1352, 35–42. doi: 10.1016/j.brainres.2010.07.032

Gage, F. H. (2000). Mammalian Neural Stem Cells. *Science* 287, 1433–1438. doi: 10.1126/science.287.5457.1433

Gao, X., and Chen, J. (2013). Moderate traumatic brain injury promotes neural precursor proliferation without increasing neurogenesis in the adult hippocampus. *Exp. Neurol.* 239, 38–48. doi: 10.1016/j.expneurol.2012.09.012

Hodge, R. D., Kowalczyk, T. D., Wolf, S. A., Encinas, J. M., Rippey, C., Enikolopov, G., et al. (2008). Intermediate progenitors in adult hippocampal neurogenesis: Tbr2 expression and coordinate regulation of neuronal output. *J. Neurosci.* 28, 3707–3717. doi: 10.1523/JNEUROSCI.4280-07.2008

Huttmann, K., Sadgrove, M., Wallraff, A., Hinterkeuser, S., Kirchhoff, F., Steinhauser, C., et al. (2003). Seizures preferentially stimulate proliferation of radial glia-like astrocytes in the adult dentate gyrus: functional and immunocytochemical analysis. *Eur. J. Neurosci.* 18, 2769–2778. doi: 10.1111/j.1460-9568.2003.03002.x

Kempermann, G. (2011). Seven principles in the regulation of adult neurogenesis. *Eur. J. Neurosci.* 33, 1018–1024. doi: 10.1111/j.1460-9568.2011.07599.x

Keohane, A., Ryan, S., Maloney, E., Sullivan, A. M., and Nolan, Y. M. (2010). Tumour necrosis factor-alpha impairs neuronal differentiation but not proliferation of hippocampal neural precursor cells: role of hes1. *Mol. Cell. Neurosci.* 43, 127–135. doi: 10.1016/j.mcn.2009.10.003

Kohman, R. A., Deyoung, E. K., Bhattacharya, T. K., Peterson, L. N., and Rhodes, J. S. (2012). Wheel running attenuates microglia proliferation and increases expression of a proneurogenic phenotype in the hippocampus of aged mice. *Brain Behav. Immun.* 26, 803–810. doi: 10.1016/j.bbi.2011.10.006

Kohman, R. A., and Rhodes, J. S. (2013). Neurogenesis, inflammation and behavior. *Brain Behav. Immun.* 27, 22–32. doi: 10.1016/j.bbi.2012.09.003

Kohman, R. A., Rodriguez-Zas, S. L., Southey, B. R., Kelley, K. W., Dantzer, R., and Rhodes, J. S. (2011). Voluntary wheel running reverses age-induced changes in hippocampal gene expression.*PLoS ONE* 6:e22654. doi: 10.1371/journal.pone.0022654

Kriegstein, A., and Alvarez-Buylla, A. (2009). The glial nature of embryonic and adult neural stem cells. *Annu. Rev. Neurosci.* 32, 149–184. doi: 10.1146/annurev.neuro.051508.135600

Kuhn, H. G., Dickinson-Anson, H., and Gage, F. H. (1996). Neurogenesis in the dentate gyrus of the adult rat: age-related decrease of neuronal progenitor proliferation. *J. Neurosci.* 16, 2027–2033.

Liu, Z., Fan, Y., Won, S. J., Neumann, M., Hu, D., Zhou, L., et al. (2007). Chronic treatment with minocycline preserves adult new neurons and reduces functional impairment after focal cerebral ischemia. *Stroke* 38, 146–152. doi: 10.1161/01.STR.0000251791.64910.cd

Mandyam, C. D., Harburg, G. C., and Eisch, A. J. (2007). Determination of key aspects of precursor cell proliferation, cell cycle length and kinetics in the adult mouse subgranular zone. *Neuroscience* 146, 108–122. doi: 10.1016/j.neuroscience.2006.12.064

Mignone, J. L., Kukekov, V., Chiang, A. S., Steindler, D., and Enikolopov, G. (2004). Neural stem and progenitor cells in nestin-GFP transgenic mice. *J. Comp. Neurol.* 469, 311–324. doi: 10.1002/cne.10964

Monje, M. L., Mizumatsu, S., Fike, J. R., and Palmer, T. D. (2002). Irradiation induces neural precursor-cell dysfunction. *Nat. Med.* 8, 955–962. doi: 10.1038/nm749

Monje, M. L., Toda, H., and Palmer, T. D. (2003). Inflammatory blockade restores adult hippocampal neurogenesis. *Science* 302, 1760–1765. doi: 10.1126/science.1088417

Morgan, S. C., Taylor, D. L., and Pocock, J. M. (2004). Microglia release activators of neuronal proliferation mediated by activation of mitogen-activated protein kinase, phosphatidylinositol-3-kinase/Akt and delta-Notch signalling cascades. *J. Neurochem.* 90, 89–101. doi: 10.1111/j.1471-4159.2004.02461.x

Mosher, K. I., Andres, R. H., Fukuhara, T., Bieri, G., Hasegawa-Moriyama, M., He, Y., et al. (2012). Neural progenitor cells regulate microglia functions and activity. *Nat. Neurosci.* 15, 1485–1487. doi: 10.1038/nn.3233

Nakanishi, M., Niidome, T., Matsuda, S., Akaike, A., Kihara, T., and Sugimoto, H. (2007). Microglia-derived interleukin-6 and leukaemia inhibitory factor promote astrocytic differentiation of neural stem/progenitor cells. *Eur. J. Neurosci.* 25, 649–658. doi: 10.1111/j.1460-9568.2007.05309.x

Nolte, C., Matyash, M., Pivneva, T., Schipke, C. G., Ohlemeyer, C., Hanisch, U. K., et al. (2001). GFAP promoter-controlled EGFP-expressing transgenic mice: a tool to visualize astrocytes and astrogliosis in living brain tissue. *Glia* 33, 72–86.

Olah, M., Ping, G., De Haas, A. H., Brouwer, N., Meerlo, P., Van Der Zee, E. A., et al. (2009). Enhanced hippocampal neurogenesis in the absence of microglia T cell interaction and microglia activation in the murine running wheel model. *Glia* 57, 1046–1061. doi: 10.1002/glia.20828

Palmer, T. D., Takahashi, J., and Gage, F. H. (1997). The adult rat hippocampus contains primordial neural stem cells. *Mol. Cell Neurosci.* 8, 389–404. doi: 10.1006/mcne.1996.0595

Paolicelli, R. C., Bolasco, G., Pagani, F., Maggi, L., Scianni, M., Panzanelli, P., et al. (2011). Synaptic pruning by microglia is necessary for normal brain development. *Science* 333, 1456–1458. doi: 10.1126/science.1202529

Pervaiz, N., and Hoffman-Goetz, L. (2011). Freewheel training alters mouse hippocampal cytokines. *Int. J. Sports Med.* 32, 889–895. doi: 10.1055/s-0031-1279780

Schauwecker, P. E. (2006). Genetic influence on neurogenesis in the dentate gyrus of two strains of adult mice. *Brain Res.* 1120, 83–92. doi: 10.1016/j.brainres.2006.08.086

Shihabuddin, L. S., Horner, P. J., Ray, J., and Gage, F. H. (2000). Adult spinal cord stem cells generate neurons after transplantation in the adult dentate gyrus. *J. Neurosci.* 20, 8727–8735.

Sierra, A., Encinas, J. M., Deudero, J. J., Chancey, J. H., Enikolopov, G., Overstreet-Wadiche, L. S., et al. (2010). Microglia shape adult hippocampal neurogenesis through apoptosis-coupled phagocytosis. *Cell Stem Cell* 7, 483–495. doi: 10.1016/j.stem.2010.08.014

Song, H., Stevens, C. F., and Gage, F. H. (2002). Astroglia induce neurogenesis from adult neural stem cells. *Nature* 417, 39–44. doi: 10.1038/417039a

Sultan, S., Gebara, E., and Toni, N. (2013). Doxycycline increases neurogenesis and reduces microglia in the adult hippocampus. *Front. Neurosci*. 7:131. doi: 10.3389/fnins.2013.00131

Taupin, P. (2007). BrdU immunohistochemistry for studying adult neurogenesis: paradigms, pitfalls, limitations, and validation. *Brain Res. Rev.* 53, 198–214. doi: 10.1016/j.brainresrev.2006.08.002

Thuret, S., Toni, N., Aigner, S., Yeo, G. W., and Gage, F. H. (2009). Hippocampus-dependent learning is associated with adult neurogenesis in MRL/MpJ mice. *Hippocampus* 19, 658–669. doi: 10.1002/hipo.20550

Tong, L., Shen, H., Perreau, V. M., Balazs, R., and Cotman, C. W. (2001). Effects of exercise on gene-expression profile in the rat hippocampus. *Neurobiol. Dis.* 8, 1046–1056. doi: 10.1006/nbdi.2001.0427

Toni, N., and Sultan, S. (2011). Synapse formation on adult-born hippocampal neurons. *Eur. J. Neurosci.* 33, 1062–1068. doi: 10.1111/j.1460-9568.2011.07604.x

Vallieres, L., Campbell, I. L., Gage, F. H., and Sawchenko, P. E. (2002). Reduced hippocampal neurogenesis in adult transgenic mice with chronic astrocytic production of interleukin-6. *J. Neurosci.* 22, 486–492.

van Praag, H., Kempermann, G., and Gage, F. H. (1999). Running increases cell proliferation and neurogenesis in the adult mouse dentate gyrus. *Nat. Neurosci.* 2, 266–270. doi: 10.1038/6368

van Praag, H., Shubert, T., Zhao, C., and Gage, F. H. (2005). Exercise enhances learning and hippocampal neurogenesis in aged mice. *J. Neurosci.* 25, 8680–8685. doi: 10.1523/JNEUROSCI.1731-05.2005

Vukovic, J., Colditz, M. J., Blackmore, D. G., Ruitenberg, M. J., and Bartlett, P. F. (2012). Microglia modulate hippocampal neural precursor activity in response to exercise and aging. *J. Neurosci.* 32, 6435–6443.

Walton, N. M., Sutter, B. M., Laywell, E. D., Levkoff, L. H., Kearns, S. M., Marshall, G. P., et al. (2006). Microglia instruct subventricular zone neurogenesis. *Glia* 54, 815–825. doi: 10.1002/glia.20419

Yang, C. P., Gilley, J. A., Zhang, G., and Kernie, S. G. (2011). ApoE is required for maintenance of the dentate gyrus neural progenitor pool. *Development* 138, 4351–4362. doi: 10.1242/dev.065540

Yao, J., Mu, Y., and Gage, F. H. (2012). Neural stem cells: mechanisms and modeling. *Protein Cell* 3, 251–261.

Zhao, C., Deng, W., and Gage, F. H. (2008). Mechanisms and functional implications of adult neurogenesis. *Cell* 132, 645–660. doi: 10.1016/j.cell.2008.01.033

Ziv, Y., Ron, N., Butovsky, O., Landa, G., Sudai, E., Greenberg, N., et al. (2006). Immune cells contribute to the maintenance of neurogenesis and spatial learning abilities in adulthood. *Nat. Neurosci.* 9, 268–275. doi: 10.1038/nn1629

Conflict of Interest Statement: The authors declare that the research was conducted in the absence of any commercial or financial relationships that could be construed as a potential conflict of interest.

Received: 23 June 2013; paper pending published: 13 July 2013; accepted: 30 July 2013; published online: 20 August 2013.
Citation: Gebara E, Sultan S, Kocher-Braissant J and Toni N (2013) Adult hippocampal neurogenesis inversely correlates with microglia in conditions of voluntary running and aging. Front. Neurosci. 7:145. doi: 10.3389/fnins.2013.00145
This article was submitted to Neurogenesis, a section of the journal Frontiers in Neuroscience.

A4

Doxycycline increases neurogenesis and reduces microglia in the adult hippocampus.

frontiers in
NEUROSCIENCE

ORIGINAL RESEARCH ARTICLE
published: 25 July 2013
doi: 10.3389/fnins.2013.00131

Doxycycline increases neurogenesis and reduces microglia in the adult hippocampus

Sebastien Sultan†, Elias Gebara† and Nicolas Toni*

Department of Fundamental Neurosciences, University of Lausanne, Lausanne, Switzerland

Edited by:
João O. Malva, University of Coimbra, Portugal

Reviewed by:
Jorge Valero, University of Coimbra, Portugal
William Gray, Cardiff University, UK

***Correspondence:**
Nicolas Toni, Department of Fundamental Neurosciences, University of Lausanne, 9, rue du Bugnon, 1005 Lausanne, Switzerland
e-mail: nicolas.toni@unil.ch

† These authors have contributed equally to this work.

Adult hippocampal neurogenesis results in the continuous formation of new neurons and is a process of brain plasticity involved in learning and memory. Although inducible-reversible transgenic mouse models are increasingly being used to investigate adult neurogenesis, transgene control requires the administration of an activator, doxycycline (Dox), with unknown effects on adult neurogenesis. Here, we tested the effect of Dox administration on adult neurogenesis *in vivo*. We found that 4 weeks of Dox treatment at doses commonly used for gene expression control, resulted in increased neurogenesis. Furthermore, the dendrites of new neurons displayed increased spine density. Concomitantly, Iba1-expressing microglia was reduced by Dox treatment. These results indicate that Dox treatment may interfere with parameters of relevance for the use of inducible transgenic mice in studies of adult neurogenesis or brain inflammation.

Keywords: dentate gyrus, hippocampus, adult neurogenesis, doxycycline, tetracycline, gene expression regulation

INTRODUCTION

Adult neurogenesis occurs mainly in two discrete areas: the olfactory bulb and the dentate gyrus (DG) of the hippocampus (Altman, 1969). The process of adult neurogenesis consists in several steps: First, the division of adult neural stem cells, residing in the subgranular zone (SGZ) of the DG (Gage, 2000). Adult neural stem cells display a radial glia like (RGL) morphology, characterized by a unique radial process extending through the granule cell layer and branching into the molecular layer and by the expression of several markers such as the astrocytic glial fibrillary acidic protein (GFAP) and nestin (Huttmann et al., 2003; Ehninger and Kempermann, 2008). RGL cells divide asymmetrically to self-renew and yield highly proliferative transit-amplifying progenitors (TAPs), which do not have a radial morphology and express nestin and the T-box brain gene 2 (Tbr2), but not GFAP. TAPs give rise to immature neurons, which express the immature neuronal marker doublecortin (DCX) and differentiate into mature, NeuN-expressing neurons (Gage, 2000; Ma et al., 2009; Yao et al., 2012). During their maturation, young neurons project their dendrites into the molecular layer, form dendritic spines, which receive synaptic inputs from perforant path afferences from the entorhinal cortex (Gage, 2000; Van Praag et al., 2002; Laplagne et al., 2006; Toni et al., 2007; Toni and Sultan, 2011). They also project their axons to the hippocampal CA3 area and establish synaptic connections with postsynaptic inhibitory interneurons and excitatory pyramidal neurons (Toni et al., 2008). After 8 weeks, new neurons are morphologically and functionally indistinguishable from neighboring neurons and are completely integrated into the hippocampal network (Laplagne et al., 2006; Ge et al., 2008).

The mechanisms regulating adult neurogenesis are highly relevant for our understanding of brain plasticity and for the potential use of these cells as therapeutic targets. Indeed, although their role remains unclear, increasing evidence suggests that new neurons are involved in mechanisms of learning and memory (Van Praag et al., 1999, 2002; Saxe et al., 2006, 2007; Dupret et al., 2007; Trouche et al., 2009; Massa et al., 2011; Gu et al., 2012; Shors et al., 2012; Tronel et al., 2012) as well as in depression and mood control (Santarelli et al., 2003; Samuels and Hen, 2011). However, one of the great difficulties in studying adult neurogenesis *in vivo*, is that the mechanisms regulating neuronal proliferation, differentiation and survival also play a role during brain development and therefore, their manipulation leads to prenatal death or morbidity. This experimental caveat can be circumvented by the use of inducible transgene expression, such as the tetracycline regulatory system, controlled with the administration of doxycycline (Dox) (Gossen and Bujard, 1992; Zhou et al., 2006; Chow et al., 2012). This elegant system enables the bi-directional and non-invasive regulation of gene expression. Furthermore, by controlling the timing of the genetic manipulation, genes necessary for cell survival can be manipulated without affecting brain development. However, although inducible transgenic mouse models are increasingly being used for studies of adult neurogenesis, the effect of Dox on adult neurogenesis is unknown. Dox is a synthetic antibiotic of the tetracycline inhibitors group, with reported effects on pain, inflammation and neuroprotection (Clark et al., 1997; Cho et al., 2009; Jantzie and Todd, 2010; Yoon et al., 2012). Thus, the use of Dox to control gene expression may potentially bias phenotypic analysis of adult neurogenesis with the introduction of confounding factors.

The aim of the present study was to examine the potential effects of Dox on adult neurogenesis *in vivo*. We have used a *per os* administration route, which corresponds to the main experimental protocol for the control of transgene expression. Using immunohistochemistry and viral-mediated labeling, we have analyzed the effect of Dox on RGL cells, TAPs and on the

differentiation, survival and synaptic maturation of new neurons, as well as on microglia.

MATERIALS AND METHODS

ETHICS STATEMENT

This study was carried out in strict accordance with the recommendations in the Guidance for the Care and Use of Laboratory Animals of the National Institutes of Health. All experimental protocols were approved by the Swiss animal experimentation authorities (Service de la consommation et des affaires vétérinaires, Chemin des Boveresses 155, 1066 Epalinges, Switzerland, permit number: 2301). Every effort was made to minimize the number of animals used and their suffering.

EXPERIMENTAL ANIMALS

Animals used for the study were adult males of 6 weeks of age at the beginning of the experiment. All animals were housed in standard cages under a 12-h light/dark cycle and temperature-controlled (22°C) conditions. Food and water were available *ad libitum*. C57Bl/6 mice were purchased from Janvier (le Genest Saint Isle, France), GFAP-GFP mice were a kind gift from the laboratory of Helmut Kettenmann (Max-Delbruck center, Berlin, Germany) (Nolte et al., 2001). They express the green fluorescent protein (GFP) under the control of the astrocyte-specific human GFAP promoter. Nestin-GFP mice were a kind gift from the laboratory of K. Mori (PRESTO, Kyoto, Japan) (Yamaguchi et al., 2000). They express GFP under the control of the stem cell-specific promoter nestin. Food pellets containing 40-ppm of Dox were purchased from Harlan Laboratory (WI, USA). Control mice were fed with the same food pellets without Dox, purchased from the same source.

BrdU ADMINISTRATION

Bromodeoxyuridine (BrdU, Sigma-Aldrich, Buchs, Switzerland) was injected intraperitoneally at doses of 100 mg/kg in saline, 3 times at 2-h intervals. Mice were then sacrificed either 2 h after the last injection, to examine cell proliferation (Mandyam et al., 2007; Taupin, 2007; Yang et al., 2011; Gao and Chen, 2013) or 30 days after injections, to examine newborn cells survival (Taupin, 2007).

RETROVIRUS-MEDIATED LABELING

We used a retroviral vector derived from the Moloney murine leukemia virus (MoMuLv) containing a GFP-expression cassette under the control of the cytomegalovirus early enhancer and chicken beta-actin promoter (cag) (Zhao et al., 2006). The final virus titer was 10E8 pfu/ml, as measured by GFP–expressing colony formation on 293T cells. Mice were anesthetized with a mixture of 90 mg/kg ketamine and 4.5 mg/kg xylazine (i.p.) and then placed in a stereotaxic instrument (Narishige Scientific Instruments, Tokyo, Japan). 1.5 µl of virus was injected bilaterally at the following coordinates from the Bregma: anteroposterior −2 mm, lateral 1.75 mm and dorsoventral −2.25 mm. GFP signal was amplified by immunohistochemistry using chicken anti-GFP IgY (AnaSpec Inc. CA 94555, 1:1000) and dylight 488 goat anti-chicken IgY (Jackson ImmunoResearch Europe ltd., Suffolk, United Kingdom; 1:250).

TISSUE COLLECTION AND PREPARATION

Mice were deeply anesthetized with a lethal dose of pentobarbital (10 mL/kg, Sigma-Aldrich, Buchs, Switzerland) and perfusion-fixed with 50 ml of 0.9% saline immediately followed by 100 mL of 4% paraformaldehyde (Sigma-Aldrich, Switzerland) dissolved in phosphate buffer saline (PBS 0.1 M, pH 7.4). Brains were then dissected, post-fixed overnight at 4°C, cryoprotected 24 h in 30% sucrose and rapidly frozen. Coronal frozen sections of a thickness of 40 µm were cut with a microtome-cryostat (Leica MC 3050S) and slices were stored in cryoprotectant (30% ethylene glycol and 25% glycerin in 1X PBS) at −20°C until processing for immunostaining, as described previously (Thuret et al., 2009).

IMMUNOHISTOCHEMISTRY

Sections were washed 3 times in PBS 0.1M. BrdU detection required formic acid pretreatment (formamide 50% in 2× SSC buffer; 2× SSC is 0.3 M NaCl, and 0.03 M sodium citrate, pH 7.0) at 65°c for 2 h followed by DNA denaturation for 30 min in 2 M HCl at 37°C and rinsed in 0.1 M borate buffer pH 8.5 for 10 min. Nonspecific binding was blocked with 0.25% Triton-X100 and 15% normal serum [normal goat serum (Gibco, 16210-064) or normal donkey serum (Sigma Aldrich, D-9663), depending on the secondary antibody] in PBS 0.1 M. Slices were then incubated 48 h at 4°C with the primary antibodies described below. Then sections were incubated for 2 h with the corresponding secondary antibodies in PBS 0.1 M. 4,6 diamidino-2-phenylindole (DAPI) was used to reveal nuclei.

Primary antibodies used for immunohistochemistry were as follows: rabbit anti-Ki-67 (1:200, Abcam, ab15580), goat anti-DCX (1:500, Santa Cruz biotechnology, sc-8066), rabbit anti-Tbr2 (1:200, Abcam, ab23345), mouse monoclonal anti-BrdU (1:250, Chemicon International, Dietikon, Switzerland), mouse anti-NeuN (Chemicon international 1:1000), goat anti-Iba1 (1:200, Abcam, ab5076), rabbit anti-GFAP (1:500, Invitrogen, 180063).

Secondary antibodies were used as follows: goat anti-mouse Alexa-594 (1:250, Invitrogen), goat anti-rabbit Alexa-594 (1:250, Invitrogen), goat anti-rabbit Alexa-488 (1:250, Invitrogen), donkey anti-goat Alexa-555 (1:250, Invitrogen).

IMAGE ANALYSIS

All images were acquired using a confocal microscope (Zeiss LSM 710 Quasar Carl Zeiss, Oberkochen, Germany). The total numbers of immunoreactive cells throughout the entire granule cell layer were estimated using stereological sampling, as previously described (Thuret et al., 2009), between −1.3 and −2.9 mm from the Bregma. However, no guard zones were used, which may lead to possible bias in the counting of cells at the edge of each section, spread across control and Dox groups. For each animal, a 1-in-6 series of sections was stained with the nucleus marker DAPI and used to measure the volume of the granule cell layer. The granule cell area was traced using Axiovision (Zeiss, Germany) software and the granule cell volume was determined by multiplying the traced granule cell layer area by the thickness of the corresponding section and the distance between the sections sampled (240 µm). For all mice analyzed in this study, no difference was found between Dox-treated and control animals. All

cells were counted blind with regard to the mouse status. Cells were counted in the entire thickness of the sections in a 1-in-6 series of section (240 μm apart) with a 40× objective. The number of immunolabeled cells was then related to granule cell layer sectional volume and multiplied by the reference volume to estimate the total number of immunolabeled cells. Cells expressing BrdU, Ki-67, DCX or Tbr2 were counted in the granule cell layer, whereas cells expressing Iba1 and GFAP (**Figure 6**) were counted in the whole DG.

BrdU colocalization with the neuronal marker NeuN was analyzed by confocal microscopy and was confirmed on single optical sections, for 50–60 cells per animal. The proportion of double-labeled cells was then obtained for each animal and then averaged for each group. DCX-expressing cells were counted on confocal stack images using the colocalization with the nuclear stain DAPI and/or the presence of processes as visual landmarks for their identification. This approach may lead to a slight underestimation of DCX-expressing cell numbers. Spine density was assessed as previously described (Krzisch et al., 2013). Dendrites were imaged with confocal microscopy in the second third of the molecular layer and their length as well as spine density (number of spines divided by dendritic length) was measured using image J software, for 40–50 neurons per group.

Spine morphology was classified in three groups based on the maximal diameter of the spine head, as measured on maximal projections with Image J software: Filopodia <0.25μm, thin spines 0.25–0.45 μm and mushroom spines >0.45 μm. The percentage of each type of dendritic spine was then expressed by neuron and averaged for each mouse (25–30 neurons per group, 800 spines per group).

CELL CULTURE

Adult neural progenitor cells (NPC) expressing the red fluorescent protein (RFP) are a kind gift from the laboratory of Fred Gage (Salk Institute, San Diego, USA). They were originally isolated from the DG of adult Fisher 344 rats and cultured as previously described (Palmer et al., 1997).

Microglia and astrocyte primary culture were purified from postnatal day 2 rats. Cerebral cortices were mechanically triturated for homogenization and seeded onto poly-D-lysine coated 75 cm^2 flasks in Dulbecco's Modified Eagle Medium (DMEM) glutamax (Invitrogen, USA), 10% normal calf serum with penicillin/streptomycin (Invitrogen, USA). Cells were grown for 5–7 days in a humidified 5% CO2 incubator at 37°C. At confluence, flasks were shaken at 250 rpm on an orbital shaker for 2 h to separate microglia from astrocytes. Detached microglia were seeded in poly-D-lysine coated 6-well microplates in culture medium supplemented with 30% astrocyte conditioned medium.

All three cell types were cultured separately and, one day after plating, were treated with Dox or vehicle (PBS). Dox was purchased from Sigma-Aldrich (St Louis, MO, USA) and dissolved in PBS to prepare a stock solution of 10 mg/ml. The stock solution was stored at −20°C. Upon use, the stock solution was diluted 10 times in PBS and 1 μl of the solution was added daily to the culture medium, at a concentration of 1 μg/ml. This regimen of Dox treatment is commonly used for the induction of tetracycline-dependent gene expression in cell culture (Stegmeier et al., 2005; Richter et al., 2013).

After the treatment, cells were fixed and mounted for cell quantification. The number of Iba1+, RFP+, and GFAP+ cells was counted in twelve randomly selected fields per condition (three culture wells per groups, four fields per culture well) on confocal micrographs. The number of cells was then divided by the surface area of the selected fields, to obtain cell density. The density was then averaged between the four fields to obtain the average density per culture well.

STATISTICAL ANALYSIS

Hypothesis testing was two-tailed. All analyses were performed using JMP10 software. First, Shapiro-Wilk tests were performed on each group of data to test for distribution normality. The distribution was normal for all data. For two-sample comparisons, the equality of variances of the groups was tested and the adequate unpaired *t*-test was used. For the analysis of dendritic spine morphology (**Figure 5C**), parametric tests were used (two-way ANOVA followed by a *post-hoc* Student's *t*-test). Data are presented as mean ± SEM.

RESULTS

Dox EXPOSURE INCREASED CELL PROLIFERATION

To examine the effect of Dox treatment on cell proliferation, 6 weeks old C57Bl/6 mice were fed for 4 weeks with unlimited supply of food pellets containing either 40 ppm of Dox or no Dox (**Figure 1A**). At the end of the treatment, mice were sacrificed and brain slices were immunostained for the proliferation marker Ki-67 (Kee et al., 2002). Treated animals showed a higher number of Ki-67 labeled cells in the granule cell layer of the DG than control mice (**Figures 1B,C**, Student's *t*- test, $p < 0.001$) suggesting an increased number of cells in the cell cycle.

We next examined the effect of Dox treatment on immature neurons expressing DCX. Dox treatment significantly increased the number of immature neurons (**Figures 1D,E**, Student's *t*-test, $p < 0.001$). Thus, Dox treatment enhanced proliferation in the adult hippocampus and increased the number of immature neurons. To test whether the increased number of Ki-67- and DCX-expressing cells could be caused by a change in hippocampal volume upon Dox treatment, we measured the volume of the granule cell layer of all mice. We did not detect a difference between treated and untreated animals ($0.16 \pm 0.05\ mm^3$ vs. $0.15 \pm 0.01\ mm^3$, respectively, $n = 5$ and Student's *t*-test, $p = 0.7$), indicating that the increased number of Ki-67 and DCX-immunolabeled cells reflected an increase in proliferation.

We then investigated the effect of Dox on the two main types of proliferative cells: RGL cells and TAPs. RGL cells were identified using nestin-GFP (**Figures 2A,B**) and GFAP-GFP (**Figures 2C,D**) mice, which are commonly used mouse models in studies of adult neurogenesis (Huttmann et al., 2003; Mignone et al., 2004; Beckervordersandforth et al., 2010). In both mouse lines, RGL cells are readily identifiable by their specific morphology (Kriegstein and Alvarez-Buylla, 2009), consisting of a nucleus in the SGZ and a large process extending through the granule cell layer and branching into the proximal molecular layer (**Figures 2B,D**, insets). With immunostaining, we confirmed that

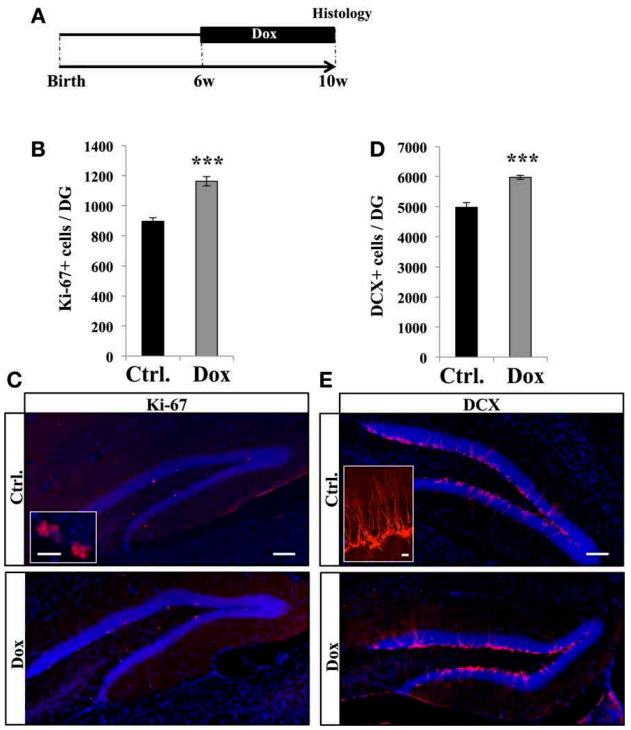

FIGURE 1 | Dox effect on cell proliferation. (A) Experimental timeline: C57Bl/6 mice were treated with control food (Ctrl.) or food containing Dox for 4 weeks and sacrificed at 10 weeks of age. **(B)** Histogram showing the number of Ki-67–expressing cells in the dentate gyrus. Animals: $n = 5$ per group. **(C)** Confocal micrographs of hippocampal sections immunostained with Ki-67 in control animals (upper panel), and treated animals (lower panel). Inset: Higher magnification confocal micrograph of a Ki-67-expressing cell. **(D)** Histogram showing the number of doublecortin (DCX)-immunolabeled cells in the dentate gyrus. Animals: $n = 5$ per group. **(E)** Confocal micrographs of hippocampal sections immunostained for DCX from control animals (upper panel), and treated animals (lower panel). Inset: Higher magnification confocal micrograph of a DCX-immunolabeled group of cells. Blue: Dapi staining. Scale bars: 100 μm, insets 10 μm, $^{***}p < 0.001$ bilateral Student's *t*-test. Each value represents the mean ± SEM.

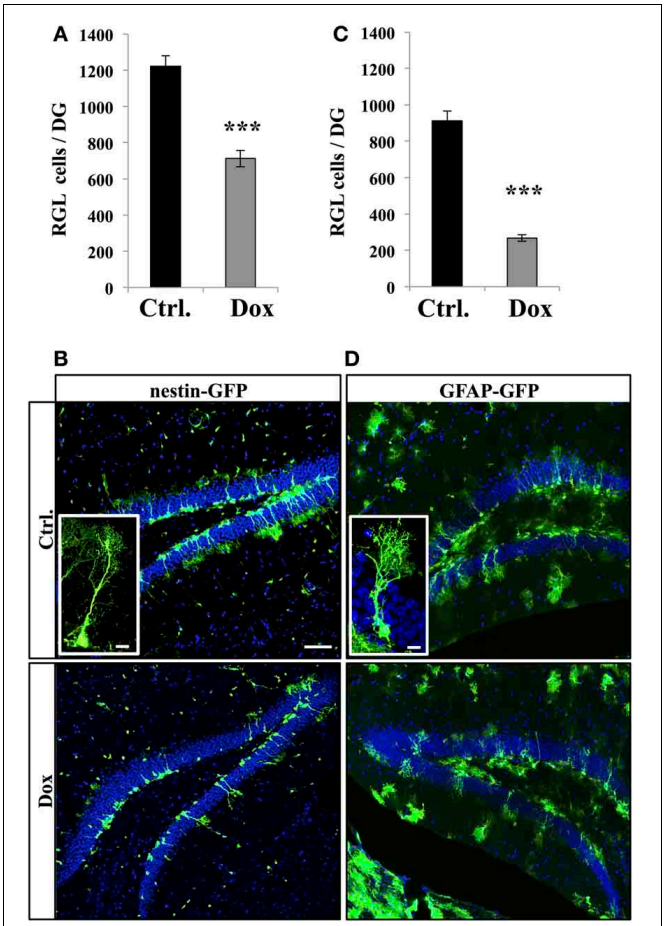

FIGURE 2 | Dox effect on the number of RGL cells in the dentate gyrus. (A) Histogram showing the number of RGL cells in the dentate gyrus of nestin-GFP mice exposed to control (Ctrl.) or Dox treatment. **(B)** Confocal micrographs of hippocampal sections from control (upper panel) and treated animals (lower panel). Inset: higher magnification confocal micrograph of a RGL cell. **(C)** Histogram showing the number of RGL cells in the dentate gyrus of GFAP-GFP mice exposed to control (Ctrl.) or Dox treatment. **(D)** Confocal micrographs of hippocampal sections from control (upper panel) and treated animals (lower panel). Inset: higher magnification confocal micrograph of a RGL cell. Blue: Dapi staining. Animals: $n = 4$ per group, scale bars: 100 μm, insets 10 μm, $^{***}p < 0.001$ bilateral Student's *t*-test. Each value represents the mean ± SEM.

these cells expressed nestin, GFAP, and sox-2 (data not shown). Surprisingly, Dox treatment significantly reduced the number of RGL cells in both the nestin-GFP mice (**Figure 2A**, Student's *t*-test, $p < 0.001$) and the GFAP-GFP mice (**Figure 2C**, Student's *t*-test, $p < 0.001$).

TAPs were identified using immunostaining against Tbr2, (Hodge et al., 2008, **Figure 3**). In untreated nestin-GFP mice, 94.5 ± 1% of TbR2 + cells co-labeled with GFP ($n = 100$ Tbr2+ cells), but 93.1 ± 2% of them did not have RGL morphology (**Figure 3C**). Dox treatment significantly increased the number of Tbr2-expressing cells (**Figure 3A**, Student's *t*-test, $p < 0.001$). Here too, we did not detect any difference in the volume of the granule cell layer between treated and control animals in both nestin-GFP treated and untreated animals ($1.4 \pm 0.09\,mm^3$ vs. $1.51 \pm 0.06\,mm^3$, respectively, $n = 4$ and Student's *t*-test, $p = 0.63$) and treated and untreated GFAP-GFP mice ($1.43 \pm 0.04\,mm^3$ vs. $1.43 \pm 0.01\,mm^3$, respectively, $n = 4$ and Student's *t*-test, $p = 0.97$).

Thus, Dox treatment increased the total number of the highly-proliferative progenitors, but decreased the number of the quiescent, slowly-proliferative RGL cells.

Dox TREATMENT INCREASED ADULT NEUROGENESIS

To examine the effect of Dox treatment on the fate of newborn cells, two groups of adult C57Bl/6 mice were treated with Dox during 4 weeks, after which they received three injections of BrdU (intraperitoneal, 1.0 mg/kg in saline at 2 h intervals). One group of mice was sacrificed 2 h after the last injection, while the second group received another 4 weeks of Dox treatment and was analyzed thereafter to assess neuronal differentiation (**Figure 4A**). The first group showed a higher number of BrdU-expressing cells in the DG as compared to control-treated mice

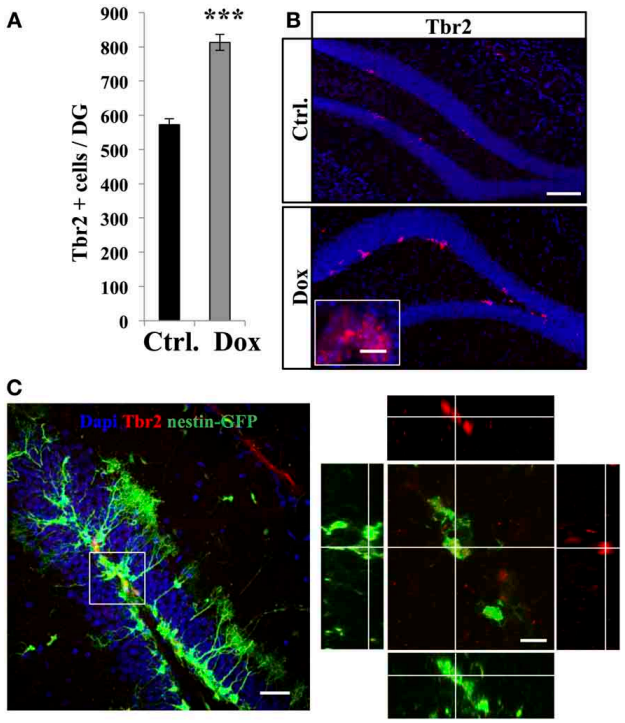

FIGURE 3 | Dox effect on the number of progenitors. (A) Histogram showing the number of Tbr2-expressing cells in the dentate gyrus of nestin-GFP mice exposed to control food (Ctrl.) or Dox treatment. **(B)** Confocal micrographs of hippocampal sections immunostained for Tbr2 from control (upper panel) and treated animals (lower panel) scale bars: 100 μm, inset 10 μm. **(C)** Left panel: Confocal micrograph of a hippocampal section (maximum projection) from a nestin-GFP mouse immunostained for Tbr2 (red) scale bar: 50 μm Right panel: Orthogonal projection of a Tbr2-immunolabeled cell also expressing GFP. Scale bar: 15 μm. Blue: Dapi staining. Animals: $n = 4$ per group, $^{***}p < 0.001$ bilateral Student's *t*-test. Each value represents the mean ± SEM.

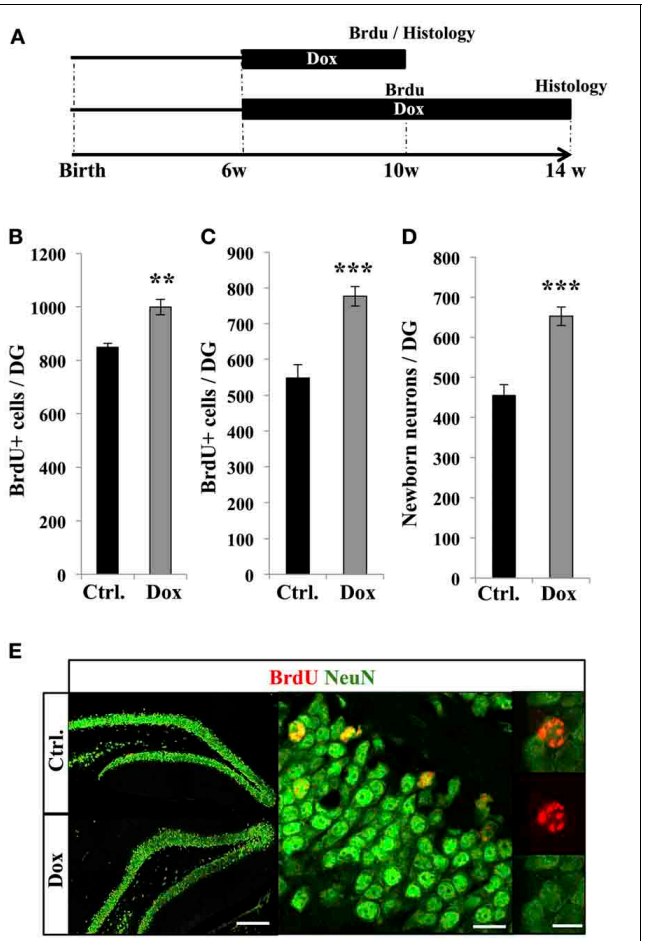

FIGURE 4 | Effect of Dox on the number of new neurons. (A) Experimental timeline: 6 weeks old C57Bl/6 mice were treated with control food (Ctrl.) or food containing Dox for 4 weeks and received BrdU injections. The first group of mice was euthanized 2 h after the BrdU injections to assess the number of proliferative BrdU+ cells. The second group received another 4 weeks of Dox treatment, after which they were euthanized, to measure the number of surviving newborn cells. **(B)** and **(C)** Histogram showing the number of BrdU-expressing cells in the dentate gyrus of animals exposed to control (Ctrl.) or Dox food, the day of injection **(B)** or 4 weeks after BrdU injections **(C)**. Animals: $n = 5$ per group. **(D)** Histogram showing the quantification of cells expressing NeuN relative to the number of BrdU-positive cells, 4 weeks after the last BrdU injection. **(E)** Left: confocal micrographs of hippocampal sections immunostained for BrdU (red) and NeuN (green) in control animals (upper panel) and treated animals (lower panel) scale bar: 100 μm. Right: Higher magnification confocal micrographs of a BrdU-NeuN expressing cells. Scale bar: 10 μm, inset 10 μm. Animals: $n = 3$ per group, 48–69 cells per animal. $^{**}p < 0.01$, $^{***}p < 0.001$ bilateral Student's *t*-test. Each value represents the mean ± SEM.

(**Figure 4B**, Student's *t*-test, $p < 0.01$), supporting our previous observation of increased cell proliferation with Dox treatment (**Figure 1**). Similarly, in the second group (4 weeks after the last BrdU injection), the number of BrdU-expressing cells was higher in Dox-treated mice than in control mice (**Figure 4C**, Student's *t*-test $p < 0.001$). Finally, we assessed the neuronal differentiation of BrdU-labeled cells into neuronal lineage, by co-labeling for BrdU and the neuron-specific marker, NeuN (**Figure 4E**). In control mice, neurons accounted for 83 ± 0.2% of the surviving BrdU-positive cells as compared to 84 ± 0.3% in Dox-treated mice (Student's *t*-test $p > 0.05$), indicating that differentiation was not affected by Dox treatment. All together, these results indicate that Dox-treated mice generate 43.4 ± 0.4% more neurons than non-treated mice (**Figure 4D**, Student's *t*-test, $p < 0.001$).

Dox TREATMENT INCREASED SPINE DENSITY ON NEWBORN NEURONS

The final stage of neurogenesis consists in the integration of the newly-formed neurons into the hippocampal excitatory circuitry and is commonly assessed by measuring dendritic spine density. To this aim, new neurons were identified by viral-mediated gene transfer, with the use of a MoMuLV containing the expression cassette for GFP. C57Bl/6 mice were treated with Dox for 4 weeks and then stereotaxically injected with GFP-retrovirus, followed by 4 weeks of Dox treatment (**Figure 5A**). Dendritic spines were analyzed in the middle-third of the molecular layer, where inputs arise mainly from the entorhinal cortex.

At 30 days post-virus infection, Dox treatment increased spine density (**Figures 5B,D,E**, Student's t-test, $p < 0.001$). Dendritic spine diameter increases with neuronal maturation (Zhao et al., 2006; Toni et al., 2007) and reflects synaptic strength (Murthy et al., 2001). To examine the effect of Dox on dendritic spine maturation, we classified dendritic spines in three categories, based on the maximal diameter of the spine head: filopodia spines $<0.25\,\mu m$, thin spines 0.25–0.45 μm and mushroom spines $>0.45\,\mu m$. Dox treatment did not change the proportion of filopodia, thin and mushroom spines [**Figure 5C**, two way ANOVA $F_{(2,\ 108)} = 1.1$, $p = 0.33$], indicating that this treatment increased spine density but did not affect dendritic spine morphology.

Dox REDUCED MICROGLIA BUT NOT ASTROGLIA *in vivo* AND *in vitro*

Dox is a member of the tetracycline antibiotics group and its analog, minocycline, has been reported to decrease microglia and inhibit microglia activation (Ng et al., 2012). We therefore analyzed the effect of Dox on microglia, identified with immunostaining for the microglia-specific marker Iba1. Four weeks of Dox treatment significantly decreased the number of Iba1-expressing cells in the hippocampus (**Figures 6A,B**, Student's t-test, $p < 0.001$). In contrast, the number of astrocytes, identified with immunohistochemistry for GFAP, was not affected by Dox treatment (**Figures 6C,D**, Student's t-test, $p = 0.59$), indicating that the effect of Dox was specific to microglia. To test the effect of Dox directly on microglia, we performed *in vitro* experiments on purified cell cultures. Microglia was treated with either 1 μg/ml Dox or the equivalent volume of PBS 0.1 M. After 8 days, cells were fixed and immunostained for Iba1. Dox treatment reduced the density of microglia (**Figures 7A,B**, Student's t-test, $p < 0.01$). In contrast, the same treatment did not have any effect on purified astrocytes identified with GFAP immunostaining (**Figures 7C,D**, Student's t-test, $p = 0.2$) or on NPC (**Figures 7E,F**, Student's t-test, $p = 0.26$). Thus, Dox treatment reduced microglia both *in vivo* and *in vitro*.

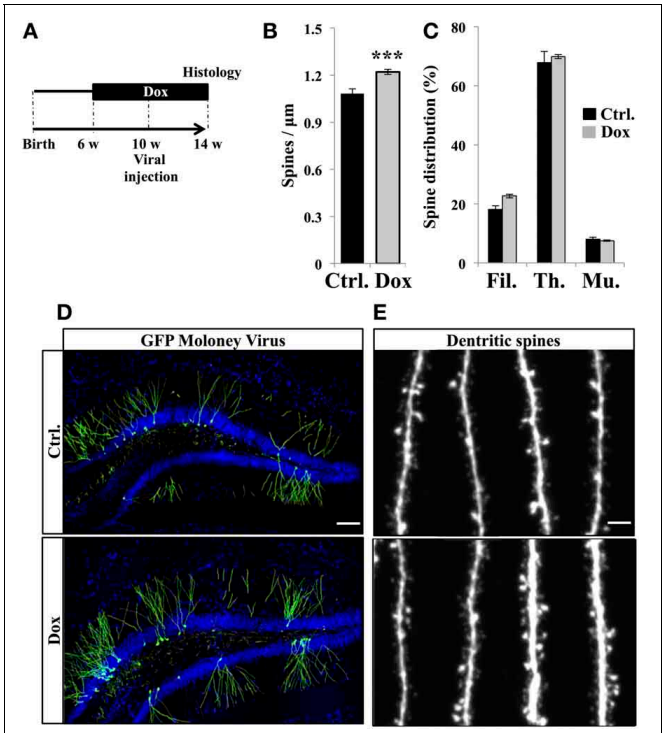

FIGURE 5 | Effect of Dox on the spine density of newborn neurons. (A) Experimental timeline: C57Bl/6 mice were treated with control food (Ctrl.) or food containing Dox for 4 weeks before viral injection. Dox treatment was continued for 4 weeks after viral injection. **(B)** Histogram showing the spine density on newborn neurons from the two experimental conditions, $n = 48$–54 neurons per group, $^{***}p < 0.001$ bilateral Student's t-test. **(C)** Histogram showing the percentage of filopodia (Fil.), thin spines (Th.), and mushroom spines (Mu.) on newborn neurons from control-treated animals (black) and Dox-treated animals (gray) $n = 838$–895 spines per group. **(D)** Confocal micrographs of hippocampal sections of retrovirally-injected mice from control animals (upper panel) and treated animals (lower panel) Blue: Dapi staining, scale bar: 100 μm. **(E)** Confocal micrographs of spiny dendrites from control animals (upper panel) and treated animals (lower panel) scale bars: 10 μm. Each value represents the mean ± SEM.

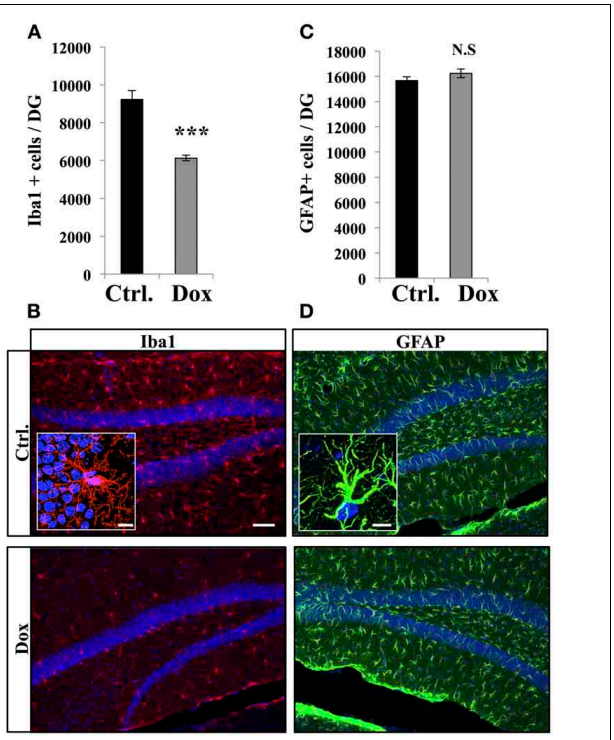

FIGURE 6 | Effect of Dox on the number of microglia and astrocytes in the dentate gyrus. (A) Histogram showing the number of Iba1-expressing cells in the dentate gyrus of mice exposed to control food (Ctrl.) or Dox treatment. Animals: $n = 5$ per group, $^{***}p < 0.001$ bilateral Student's t-test. **(B)** Confocal micrographs of hippocampal sections immunostained for Iba1 from control animals (upper panel), and treated animals (lower panel). Inset: Higher magnification confocal micrograph of an Iba1-immunolabeled cell. **(C)** Histogram of the number of GFAP-expressing astrocytes in the dentate gyrus of mice for each experimental condition. Animals: $n = 3$ per group. **(D)** Confocal micrographs of hippocampal sections immunostained for GFAP from control animals (upper panel), and treated animals (lower panel). Inset: Higher magnification confocal micrograph of a GFAP-immunolabeled cell. Blue: Dapi staining. Scale bars: 100 μm, insets 10 μm. N.S: $p > 0.05$. Each value represents the mean ± SEM.

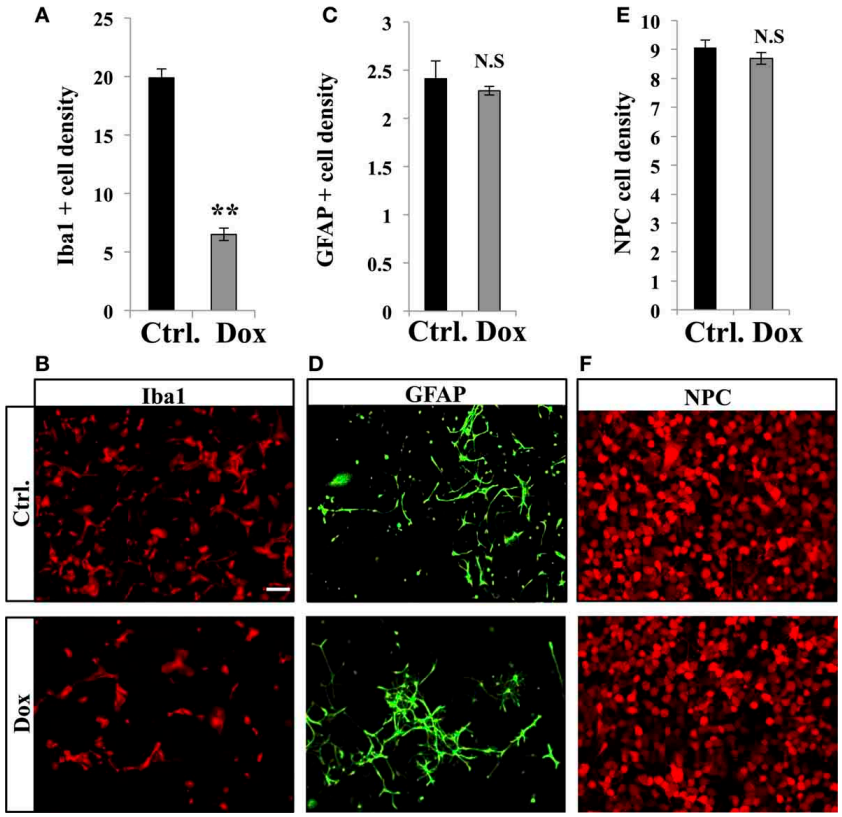

FIGURE 7 | Effect of Dox on microglia, astrocytes and progenitor cells *in vitro*. **(A)** Histogram of the density ($\times 10^{-5}$ cells/μm^2), of Iba1-expressing cells after vehicle (Ctrl.) or Dox treatment of purified microglia cultures. $^{**}p < 0.01$ bilateral Student's *t*-test. **(B)** Confocal micrographs of Iba1-immunostained cultures for control (upper panel) and treated condition (lower panel). **(C)** Histogram of the density ($\times 10^{-4}$ cells/μm^2), of GFAP-expressing cells of purified cultures treated for each condition. **(D)** Confocal micrographs of GFAP-immunostained cells for control (upper panel) and treated condition (lower panel). **(E)** Histogram of the density ($\times 10^{-3}$ cells/μm^2), of purified NPC for each condition. **(F)** Confocal micrographs of RFP-expressing NPC for control (upper panel) and treated condition (lower panel). $n = 3$ culture wells per group. Scale bar: 100 μm. N.S: $p > 0.05$. Each value represents the mean ± SEM.

DISCUSSION

In this study, we tested the effect on adult neurogenesis of a Dox treatment commonly used to regulate gene expression in inducible transgenic mice. Dox reduced the number of RGL cells but increased the number of TAPs in the DG of adult mice. This may result from a shift in fate choice of the RGL cells leading to a depletion of the RGL cells pool in favor of the highly proliferative TAPs (Encinas et al., 2011), a possibility which may be further tested by examining the expression of the proliferation marker Ki-67 and self-renewal transcription factor sox2 in RGL cells of both groups. As a consequence, Dox treatment increased cell proliferation and resulted in a net increase in neurogenesis. Although cell counts were performed without the use of guard zones, which may lead to possible bias in the counting of cells at the edge of each section, this bias was spread across both groups and may affect the absolute number of cells, but not the intergroup difference. In addition, Dox increased dendritic protrusions density on the neurons formed during the treatment. Concomitantly, microglia but not astrocytes were reduced by Dox. These results indicate that Dox has multiple effects on adult neurogenesis.

Although the mechanism of action of Dox is unclear, the dramatic reduction of microglia *in vitro* and *in vivo*, and the lack of effect of Dox on astrocytes and NPC *in vitro*, raises the possibility that the effect of this drug on adult neurogenesis may be mediated by microglia. In support of this possibility, inflammatory microglia inhibit adult neurogenesis (Monje et al., 2002; Ekdahl et al., 2003; Liu et al., 2007; Kohman et al., 2012) and the exercise-induced increase and the age-dependent decline in neurogenesis are mediated by microglia, possibly through CX3CR1-receptor activity (Vukovic et al., 2012). Furthermore, Dox and its analog minocycline have been shown to inhibit inflammation in models of ischemia, brain trauma, pain or neurodegenerative diseases (Yrjanheikki et al., 1998; Thomas et al., 2003; Buller et al., 2009; Kim and Suh, 2009; Jantzie and Todd, 2010; Lu et al., 2010; Wideroe et al., 2012; Kobayashi et al., 2013). Accordingly, minocycline decrease microglia number and increase adult neurogenesis (Kohman et al., 2013). Thus, an extensive reduction in microglia, such as observed with Dox treatment, may interfere with adult neurogenesis. However, the effects of Dox on microglia and neurogenesis may be unrelated and further experiments will

be necessary to examine the causality between reduced microglia and increased neurogenesis upon Dox treatment.

In addition to its effect on microglia, Dox is known to also inhibit Matrix Metalloproteinases (MMPs) (Burggraf et al., 2007; Lee et al., 2009). MMPs are soluble or membrane-bound proteases capable of degrading cell-surface receptors and extracellular matrix proteins, which play a role in tissue remodeling and receptor activation. MMPs are involved in several aspects of neurogenesis: MMP-17 prevents neurogenesis by shedding the ligand for, and activating EGFR (Epidermal growth factor receptor) and its inhibition results in increased neurogenesis (Romero-Grimaldi et al., 2011). MMP-3 and MMP-9 promote the differentiation and migration of neural progenitors (Barkho et al., 2008). Also, MMPs are involved in synaptic plasticity (Bozdagi et al., 2007) and synaptogenesis (Ethell and Ethell, 2007) by the cleavage of trans-synaptic adhesion molecules (Huntley, 2012; Peixoto et al., 2012) and the inhibition of MMP-9 inhibits the LTP-induced spine enlargement and stabilization (Wang et al., 2008). Finally, MMPs are involved in inflammation and the genetic deletion of MMP-9 results in decreased inflammation and neuroprotection in a mouse model of hypoxia (Svedin et al., 2007). Thus, the inhibition of MMPs by Dox may result in increased neurogenesis. However, the involvement of MMPs or microglia on the Dox-mediated increase in neurogenesis remains unclear and additional experiments may elucidate the mode of action of Dox.

Together, our observations indicate that Dox decreased microglia and increased adult neurogenesis, a combination of effects that can introduce confounding factors in studies of adult neurogenesis or brain inflammation. Together with the recent observation that Dox reduced alcohol consumption in mice and increased the sensitivity to alcohol-induced motor impairment (McIver et al., 2012), the present study suggests that, at doses necessary for the induction of gene expression in transgenic mice with tetracycline-responsive promoters, Dox has multiple effects on the central nervous system. Further experiments will be needed to determine whether shorter Dox treatments or other routes of administration, such as intraperitoneal injections, or administration in water induce similar effects on adult neurogenesis and microglia. However, the best experimental design to circumvent the caveats of using tetracycline-responsive promoters relies on the appropriate use of Tet-on or Tet-off systems to enable the experimental tests to be performed in absence of Dox. Alternatively, it is recommended that control experiments include Dox-treated animals. Gene expression control is a critical and increasingly used tool for our understanding of brain physiology and future developments will enable the use of this technology with more specific approaches, thereby reducing confounding factors. In this perspective, the recent introduction of new Tet activators with enhanced sensitivity to Dox represents an interesting effort aimed at using lower doses of Dox, thereby reducing effects on brain physiology (Zhou et al., 2006).

AUTHOR CONTRIBUTIONS

Conceived and designed the experiments: Sebastien Sultan, Elias Gebara, and Nicolas Toni. Performed the experiments: Elias Gebara, Sebastien Sultan. Analyzed the data: Sebastien Sultan and Elias Gebara. Wrote the paper: Sebastien Sultan, Elias Gebara, and Nicolas Toni.

ACKNOWLEDGMENTS

The authors wish to thank Romain Gosselin (Department of Fundamental Neurosciences, University of Lausanne, Switzerland) for critical insight on *in vitro* experiments and Coralie Rummel and Florian Udry for technical assistance. Images acquisition was performed at the Cellular Imaging Facility of the university of Lausanne (Lausanne, Switzerland). This work was supported by the Swiss National Science Foundation.

REFERENCES

Altman, J. (1969). Autoradiographic and histological studies of postnatal neurogenesis. 3. Dating the time of production and onset of differentiation of cerebellar microneurons in rats. *J. Comp. Neurol.* 136, 269–293. doi: 10.1002/cne.901360303

Barkho, B. Z., Munoz, A. E., Li, X., Li, L., Cunningham, L. A., and Zhao, X. (2008). Endogenous matrix metalloproteinase (MMP)-3 and MMP-9 promote the differentiation and migration of adult neural progenitor cells in response to chemokines. *Stem Cells* 26, 3139–3149. doi: 10.1634/stemcells.2008-0519

Beckervordersandforth, R., Tripathi, P., Ninkovic, J., Bayam, E., Lepier, A., Stempfhuber, B., et al. (2010). *In vivo* fate mapping and expression analysis reveals molecular hallmarks of prospectively isolated adult neural stem cells. *Cell Stem Cell* 7, 744–758. doi: 10.1016/j.stem.2010.11.017

Bozdagi, O., Nagy, V., Kwei, K. T., and Huntley, G. W. (2007). *In vivo* roles for matrix metalloproteinase-9 in mature hippocampal synaptic physiology and plasticity. *J. Neurophysiol.* 98, 334–344. doi: 10.1152/jn.00202.2007

Buller, K. M., Carty, M. L., Reinebrant, H. E., and Wixey, J. A. (2009). Minocycline: a neuroprotective agent for hypoxic-ischemic brain injury in the neonate? *J. Neurosci. Res.* 87, 599–608. doi: 10.1002/jnr.21890

Burggraf, D., Trinkl, A., Dichgans, M., and Hamann, G. F. (2007). Doxycycline inhibits MMPs via modulation of plasminogen activators in focal cerebral ischemia. *Neurobiol. Dis.* 25, 506–513. doi: 10.1016/j.nbd.2006.10.013

Cho, Y., Son, H. J., Kim, E. M., Choi, J. H., Kim, S. T., Ji, I. J., et al. (2009). Doxycycline is neuroprotective against nigral dopaminergic degeneration by a dual mechanism involving MMP-3. *Neurotox. Res.* 16, 361–371. doi: 10.1007/s12640-009-9078-1

Chow, J. D. Y., Price, J. T., Bills, M. M., Simpson, E. R., and Boon, W. C. (2012). A doxycycline-inducible, tissue-specific aromatase-expressing transgenic mouse. *Transgenic Res.* 21, 415–428. doi: 10.1007/s11248-011-9525-7

Clark, W. M., Lessov, N., Lauten, J. D., and Hazel, K. (1997). Doxycycline treatment reduces ischemic brain damage in transient middle cerebral artery occlusion in the rat. *J. Mol. Neurosci.* 9, 103–108. doi: 10.1007/BF02736854

Dupret, D., Fabre, A., Döbrössy, M. D., Panatier, A., Rodríguez, J. J., Lamarque, S., et al. (2007). Spatial learning depends on both the addition and removal of new hippocampal neurons. *PLoS Biol.* 5:e214. doi: 10.1371/journal.pbio.0050214

Ehninger, D., and Kempermann, G. (2008). Neurogenesis in the adult hippocampus. *Cell Tissue Res.* 331, 243–250. doi: 10.1007/s00441-007-0478-3

Ekdahl, C. T., Claasen, J. H., Bonde, S., Kokaia, Z., and Lindvall, O. (2003). Inflammation is detrimental for neurogenesis in adult brain. *Proc. Natl. Acad. Sci. U.S.A.* 100, 13632–13637. doi: 10.1073/pnas.2234031100

Encinas, J. M., Michurina, T. V., Peunova, N., Park, J. H., Tordo, J., Peterson, D. A., et al. (2011). Division-coupled astrocytic differentiation and age-related depletion of neural stem cells in the adult hippocampus. *Cell Stem Cell* 8, 566–579. doi: 10.1016/j.stem.2011.03.010

Ethell, I. M., and Ethell, D. W. (2007). Matrix metalloproteinases in brain development and remodeling: synaptic functions and targets. *J. Neurosci. Res.* 85, 2813–2823. doi: 10.1002/jnr.21273

Gage, F. H. (2000). Mammalian neural stem cells. *Science* 287, 1433–1438. doi: 10.1126/science.287.5457.1433

Gao, X., and Chen, J. (2013). Moderate traumatic brain injury promotes neural precursor proliferation without increasing neurogenesis in the adult hippocampus. *Exp. Neurol.* 239, 38–48. doi: 10.1016/j.expneurol.2012.09.012

Ge, S., Sailor, K. A., Ming, G. L., and Song, H. (2008). Synaptic integration and plasticity of new neurons in the adult hippocampus. *J. Physiol.* 586, 3759–3765. doi: 10.1113/jphysiol.2008.155655

Gossen, M., and Bujard, H. (1992). Tight control of gene expression in mammalian cells by tetracycline-responsive promoters. *Proc. Natl. Acad. Sci. U.S.A.* 89, 5547–5551. doi: 10.1073/pnas.89.12.5547

Gu, Y., Arruda-Carvalho, M., Wang, J., Janoschka, S. R., Josselyn, S. A., Frankland, P. W., et al. (2012). Optical controlling reveals time-dependent roles for adult-born dentate granule cells. *Nat. Neurosci.* 15, 1700–1706. doi: 10.1038/nn.3260

Hodge, R. D., Kowalczyk, T. D., Wolf, S. A., Encinas, J. M., Rippey, C., Enikolopov, G., et al. (2008). Intermediate progenitors in adult hippocampal neurogenesis: Tbr2 expression and coordinate regulation of neuronal output. *J. Neurosci.* 28, 3707–3717. doi: 10.1523/JNEUROSCI.4280-07.2008

Huntley, G. W. (2012). Synaptic circuit remodelling by matrix metalloproteinases in health and disease. *Nat. Rev. Neurosci.* 13, 743–757. doi: 10.1038/nrn3320

Huttmann, K., Sadgrove, M., Wallraff, A., Hinterkeuser, S., Kirchhoff, F., Steinhauser, C., et al. (2003). Seizures preferentially stimulate proliferation of radial glia-like astrocytes in the adult dentate gyrus: functional and immunocytochemical analysis. *Eur. J. Neurosci.* 18, 2769–2778. doi: 10.1111/j.1460-9568.2003.03002.x

Jantzie, L. L., and Todd, K. G. (2010). Doxycycline inhibits proinflammatory cytokines but not acute cerebral cytogenesis after hypoxia-ischemia in neonatal rats. *J. Psychiatry Neurosci.* 35, 20–32. doi: 10.1503/jpn.090061

Kee, N., Sivalingam, S., Boonstra, R., and Wojtowicz, J. M. (2002). The utility of Ki-67 and BrdU as proliferative markers of adult neurogenesis. *J. Neurosci. Methods* 115, 97–105. doi: 10.1016/S0165-0270(02)00007-9

Kim, H. S., and Suh, Y. H. (2009). Minocycline and neurodegenerative diseases. *Behav. Brain Res.* 196, 168–179. doi: 10.1016/j.bbr.2008.09.040

Kobayashi, K., Imagama, S., Ohgomori, T., Hirano, K., Uchimura, K., Sakamoto, K., et al. (2013). Minocycline selectively inhibits M1 polarization of microglia. *Cell Death Dis.* 4, e525. doi: 10.1038/cddis.2013.54

Kohman, R. A., Bhattacharya, T. K., Kilby, C., Bucko, P., and Rhodes, J. S. (2013). Effects of minocycline on spatial learning, hippocampal neurogenesis and microglia in aged and adult mice. *Behav. Brain Res.* 242, 17–24. doi: 10.1016/j.bbr.2012.12.032

Kohman, R. A., Deyoung, E. K., Bhattacharya, T. K., Peterson, L. N., and Rhodes, J. S. (2012). Wheel running attenuates microglia proliferation and increases expression of a proneurogenic phenotype in the hippocampus of aged mice. *Brain Behav. Immun.* 26, 803–810. doi: 10.1016/j.bbi.2011.10.006

Kriegstein, A., and Alvarez-Buylla, A. (2009). The glial nature of embryonic and adult neural stem cells. *Annu. Rev. Neurosci.* 32, 149–184. doi: 10.1146/annurev.neuro.051508.135600

Krzisch, M., Sultan, S., Sandell, J., Demeter, K., Vutskits, L., and Toni, N. (2013). Propofol Anesthesia impairs the maturation and survival of adult-born hippocampal neurons. *Anesthesiology* 118, 602–610. doi: 10.1097/ALN.0b013e3182815948

Laplagne, D. A., Espósito, M. S., Piatti, V. C., Morgenstern, N. A., Zhao, C., Van Praag, H., et al. (2006). Functional convergence of neurons generated in the developing and adult hippocampus. *PLoS Biol.* 4:e409. doi: 10.1371/journal.pbio.0040409

Lee, H., Park, J. W., Kim, S. P., Lo, E. H., and Lee, S. R. (2009). Doxycycline inhibits matrix metalloproteinase-9 and laminin degradation after transient global cerebral ischemia. *Neurobiol. Dis.* 34, 189–198. doi: 10.1016/j.nbd.2008.12.012

Liu, Z., Fan, Y., Won, S. J., Neumann, M., Hu, D., Zhou, L., et al. (2007). Chronic treatment with minocycline preserves adult new neurons and reduces functional impairment after focal cerebral ischemia. *Stroke* 38, 146–152. doi: 10.1161/01.STR.0000251791.64910.cd

Lu, L., Li, F., and Wang, X. (2010). Novel anti-inflammatory and neuroprotective agents for Parkinson's disease. *CNS Neurol. Disord. Drug Targets* 9, 232–240. doi: 10.2174/187152710791012035

Ma, D. K., Bonaguidi, M. A., Ming, G.-L., and Song, H. (2009). Adult neural stem cells in the mammalian central nervous system. *Cell Res.* 19, 672–682. doi: 10.1038/cr.2009.56

Mandyam, C. D., Harburg, G. C., and Eisch, A. J. (2007). Determination of key aspects of precursor cell proliferation, cell cycle length and kinetics in the adult mouse subgranular zone. *Neuroscience* 146, 108–122. doi: 10.1016/j.neuroscience.2006.12.064

Massa, F., Koehl, M., Wiesner, T., Grosjean, N., Revest, J. M., Piazza, P. V., et al. (2011). Conditional reduction of adult neurogenesis impairs bidirectional hippocampal synaptic plasticity. *Proc. Natl. Acad. Sci. U.S.A.* 108, 6644–6649. doi: 10.1073/pnas.1016928108

McIver, S. R., Muccigrosso, M. M., and Haydon, P. G. (2012). The effect of doxycycline on alcohol consumption and sensitivity: consideration for inducible transgenic mouse models. *Exp. Biol. Med. (Maywood)* 237, 1129–1133. doi: 10.1258/ebm.2012.012029

Mignone, J. L., Kukekov, V., Chiang, A. S., Steindler, D., and Enikolopov, G. (2004). Neural stem and progenitor cells in nestin-GFP transgenic mice. *J. Comp. Neurol.* 469, 311–324. doi: 10.1002/cne.10964

Monje, M. L., Mizumatsu, S., Fike, J. R., and Palmer, T. D. (2002). Irradiation induces neural precursor-cell dysfunction. *Nat. Med.* 8, 955–962. doi: 10.1038/nm749

Murthy, V. N., Schikorski, T., Stevens, C. F., and Zhu, Y. (2001). Inactivity produces increases in neurotransmitter release and synapse size. *Neuron* 32, 673–682. doi: 10.1016/S0896-6273(01)00500-1

Ng, S. Y., Semple, B. D., Morganti-Kossmann, M. C., and Bye, N. (2012). Attenuation of microglial activation with minocycline is not associated with changes in neurogenesis after focal traumatic brain injury in adult mice. *J. Neurotrauma* 29, 1410–1425. doi: 10.1089/neu.2011.2188

Nolte, C., Matyash, M., Pivneva, T., Schipke, C. G., Ohlemeyer, C., Hanisch, U. K., et al. (2001). GFAP promoter-controlled EGFP-expressing transgenic mice: a tool to visualize astrocytes and astrogliosis in living brain tissue. *Glia* 33, 72–86.

Palmer, T. D., Takahashi, J., and Gage, F. H. (1997). The adult rat hippocampus contains primordial neural stem cells. *Mol. Cell. Neurosci.* 8, 389–404. doi: 10.1006/mcne.1996.0595

Peixoto, R. T., Kunz, P. A., Kwon, H., Mabb, A. M., Sabatini, B. L., Philpot, B. D., et al. (2012). Transsynaptic signaling by activity-dependent cleavage of neuroligin-1. *Neuron* 76, 396–409. doi: 10.1016/j.neuron.2012.07.006

Richter, C., Thieme, S., Bandola, J., Laugsch, M., Anastassiadis, K., and Brenner, S. (2013). Generation of inducible immortalized dendritic cells with proper immune function *in vitro* and *in vivo*. *PLoS ONE* 8:e62621. doi: 10.1371/journal.pone.0062621

Romero-Grimaldi, C., Murillo-Carretero, M., Lopez-Toledano, M. A., Carrasco, M., Castro, C., and Estrada, C. (2011). ADAM-17/tumor necrosis factor-alpha-converting enzyme inhibits neurogenesis and promotes gliogenesis from neural stem cells. *Stem Cells* 29, 1628–1639. doi: 10.1002/stem.710

Samuels, B. A., and Hen, R. (2011). Neurogenesis and affective disorders. *Eur. J. Neurosci.* 33, 1152–1159. doi: 10.1111/j.1460-9568.2011.07614.x

Santarelli, L., Saxe, M., Gross, C., Surget, A., Battaglia, F., Dulawa, S., et al. (2003). Requirement of hippocampal neurogenesis for the behavioral effects of antidepressants. *Science* 301, 805–809. doi: 10.1126/science.1083328

Saxe, M. D., Battaglia, F., Wang, J. W., Malleret, G., David, D. J., Monckton, J. E., et al. (2006). Ablation of hippocampal neurogenesis impairs contextual fear conditioning and synaptic plasticity in the dentate gyrus. *Proc. Natl. Acad. Sci. U.S.A.* 103, 17501–17506. doi: 10.1073/pnas.0607207103

Saxe, M. D., Malleret, G., Vronskaya, S., Mendez, I., Garcia, A. D., Sofroniew, M. V., et al. (2007). Paradoxical influence of hippocampal neurogenesis on working memory. *Proc. Natl. Acad. Sci. U.S.A.* 104, 4642–4646. doi: 10.1073/pnas.0611718104

Shors, T. J., Anderson, M. L., Curlik, D. M., 2nd, and Nokia, M. S. (2012). Use it or lose it: how neurogenesis keeps the brain fit for learning. *Behav. Brain Res.* 227, 450–458. doi: 10.1016/j.bbr.2011.04.023

Stegmeier, F., Hu, G., Rickles, R. J., Hannon, G. J., and Elledge, S. J. (2005). A lentiviral microRNA-based system for single-copy polymerase II-regulated RNA interference in mammalian cells. *Proc. Natl. Acad. Sci. U.S.A.* 102, 13212–13217. doi: 10.1073/pnas.0506306102

Svedin, P., Hagberg, H., Savman, K., Zhu, C., and Mallard, C. (2007). Matrix metalloproteinase-9 gene knock-out protects the immature brain after cerebral hypoxia-ischemia. *J. Neurosci.* 27, 1511–1518. doi: 10.1523/JNEUROSCI.4391-06.2007

Taupin, P. (2007). BrdU immunohistochemistry for studying adult neurogenesis: paradigms, pitfalls, limitations, and validation. *Brain Res. Rev.* 53, 198–214. doi: 10.1016/j.brainresrev.2006.08.002

Thomas, M., Le, W. D., and Jankovic, J. (2003). Minocycline and other tetracycline derivatives: a neuroprotective strategy in Parkinson's disease and Huntington's disease. *Clin. Neuropharmacol.* 26, 18–23. doi: 10.1097/00002826-200301000-00005

Thuret, S., Toni, N., Aigner, S., Yeo, G. W., and Gage, F. H. (2009). Hippocampus-dependent learning is associated with adult neurogenesis in MRL/MpJ mice. *Hippocampus* 19, 658–669. doi: 10.1002/hipo.20550

Toni, N., Laplagne, D. A., Zhao, C., Lombardi, G., Ribak, C. E., Gage, F. H., et al. (2008). Neurons born in the adult dentate gyrus form functional synapses with target cells. *Nat. Neurosci.* 11, 901–907. doi: 10.1038/nn.2156

Toni, N., and Sultan, S. (2011). Synapse formation on adult-born hippocampal neurons. *Eur. J. Neurosci.* 33, 1062–1068. doi: 10.1111/j.1460-9568.2011.07604.x

Toni, N., Teng, E. M., Bushong, E. A., Aimone, J. B., Zhao, C., Consiglio, A., et al. (2007). Synapse formation on neurons born in the adult hippocampus. *Nat. Neurosci.* 10, 727–734. doi: 10.1038/nn1908

Tronel, S., Belnoue, L., Grosjean, N., Revest, J. M., Piazza, P. V., Koehl, M., et al. (2012). Adult-born neurons are necessary for extended contextual discrimination. *Hippocampus* 22, 292–298. doi: 10.1002/hipo.20895

Trouche, S., Bontempi, B., Roullet, P., and Rampon, C. (2009). Recruitment of adult-generated neurons into functional hippocampal networks contributes to updating and strengthening of spatial memory. *Proc. Natl. Acad. Sci. U.S.A.* 106, 5919–5924. doi: 10.1073/pnas.0811054106

Van Praag, H., Kempermann, G., and Gage, F. H. (1999). Running increases cell proliferation and neurogenesis in the adult mouse dentate gyrus. *Nat. Neurosci.* 2, 266–270. doi: 10.1038/6368

Van Praag, H., Schinder, A. F., Christie, B. R., Toni, N., Palmer, T. D., and Gage, F. H. (2002). Functional neurogenesis in the adult hippocampus. *Nature* 415, 1030–1034. doi: 10.1038/4151030a

Vukovic, J., Colditz, M. J., Blackmore, D. G., Ruitenberg, M. J., and Bartlett, P. F. (2012). Microglia modulate hippocampal neural precursor activity in response to exercise and aging. *J. Neurosci.* 32, 6435–6443. doi: 10.1523/JNEUROSCI.5925-11.2012

Wang, X. B., Bozdagi, O., Nikitczuk, J. S., Zhai, Z. W., Zhou, Q., and Huntley, G. W. (2008). Extracellular proteolysis by matrix metalloproteinase-9 drives dendritic spine enlargement and long-term potentiation coordinately. *Proc. Natl. Acad. Sci. U.S.A.* 105, 19520–19525. doi: 10.1073/pnas.0807248105

Wideroe, M., Havnes, M. B., Morken, T. S., Skranes, J., Goa, P. E., and Brubakk, A. M. (2012). Doxycycline treatment in a neonatal rat model of hypoxia-ischemia reduces cerebral tissue and white matter injury: a longitudinal magnetic resonance imaging study. *Eur. J. Neurosci.* 36, 2006–2016. doi: 10.1111/j.1460-9568.2012.08114.x

Yamaguchi, M., Saito, H., Suzuki, M., and Mori, K. (2000). Visualization of neurogenesis in the central nervous system using nestin promoter-GFP transgenic mice. *Neuroreport* 11, 1991–1996. doi: 10.1097/00001756-200006260-00037

Yang, C. P., Gilley, J. A., Zhang, G., and Kernie, S. G. (2011). ApoE is required for maintenance of the dentate gyrus neural progenitor pool. *Development* 138, 4351–4362. doi: 10.1242/dev.065540

Yao, J., Mu, Y., and Gage, F. H. (2012). Neural stem cells: mechanisms and modeling. *Protein Cell* 3, 251–261. doi: 10.1007/s13238-012-2033-6

Yoon, S. Y., Patel, D., and Dougherty, P. M. (2012). Minocycline blocks lipopolysaccharide induced hyperalgesia by suppression of microglia but not astrocytes. *Neuroscience* 221, 214–224. doi: 10.1016/j.neuroscience.2012.06.024

Yrjanheikki, J., Keinanen, R., Pellikka, M., Hokfelt, T., and Koistinaho, J. (1998). Tetracyclines inhibit microglial activation and are neuroprotective in global brain ischemia. *Proc. Natl. Acad. Sci. U.S.A.* 95, 15769–15774. doi: 10.1073/pnas.95.26.15769

Zhao, C., Teng, E. M., Summers, R. G. Jr., Ming, G. L., and Gage, F. H. (2006). Distinct morphological stages of dentate granule neuron maturation in the adult mouse hippocampus. *J. Neurosci.* 26, 3–11. doi: 10.1523/JNEUROSCI.3648-05.2006

Zhou, X., Vink, M., Klaver, B., Berkhout, B., and Das, A. T. (2006). Optimization of the Tet-On system for regulated gene expression through viral evolution. *Gene Ther.* 13, 1382–1390. doi: 10.1038/sj.gt.3302780

Conflict of Interest Statement: The authors declare that the research was conducted in the absence of any commercial or financial relationships that could be construed as a potential conflict of interest.

Received: 24 May 2013; paper pending published: 13 June 2013; accepted: 08 July 2013; published online: 25 July 2013.
*Citation: Sultan S, Gebara E and Toni N (2013) Doxycycline increases neurogenesis and reduces microglia in the adult hippocampus. Front. Neurosci. **7**:131. doi: 10.3389/fnins.2013.00131*
This article was submitted to Frontiers in Neurogenesis, a specialty of Frontiers in Neuroscience.

A5

D-serine increases adult hippocampal neurogenesis

frontiers in
NEUROSCIENCE

ORIGINAL RESEARCH ARTICLE
published: 29 August 2013
doi: 10.3389/fnins.2013.00155

D-serine increases adult hippocampal neurogenesis

Sebastien Sultan†, Elias G. Gebara†, Kristell Moullec and Nicolas Toni*

Department of Fundamental Neurosciences, University of Lausanne, Lausanne, Switzerland

Edited by:
Angelique Bordey, Yale University School of Medicine, USA

Reviewed by:
Francesca Ciccolini, University of Heidelberg, Germany
Jean-Claude Platel, University Joseph Fourrier, France

***Correspondence:**
Nicolas Toni, Department of Fundamental Neurosciences, University of Lausanne, 9, Rue du Bugnon, 1005 Lausanne, Switzerland
e-mail: nicolas.toni@unil.ch
† These authors have contributed equally to this work.

Adult hippocampal neurogenesis results in the continuous formation of new neurons and is a process of brain plasticity involved in learning and memory. The neurogenic niche regulates the stem cell proliferation and the differentiation and survival of new neurons and a major contributor to the neurogenic niche are astrocytes. Among the molecules secreted by astrocytes, D-serine is an important gliotransmitter and is a co-agonist of the glutamate, N-methyl-D-aspartate (NMDA) receptor. D-serine has been shown to enhance the proliferation of neural stem cells *in vitro*, but its effect on adult neurogenesis *in vivo* is unknown. Here, we tested the effect of exogenous administration of D-serine on adult neurogenesis in the mouse dentate gyrus. We found that 1 week of treatment with D-serine increased cell proliferation *in vivo* and *in vitro* and increased the density of neural stem cells and transit amplifying progenitors. Furthermore, D-serine increased the survival of newborn neurons. Together, these results indicate that D-serine treatment resulted in the improvement of several steps of adult neurogenesis *in vivo*.

Keywords: adult neurogenesis, dentate gyrus, d-serine, stem cell niche, stem cell factor, astrocytes

INTRODUCTION

Adult mammalian neurogenesis results in the formation of new neurons principally in the olfactory bulb and the dentate gyrus (DG) of the hippocampus (Altman, 1969). The process of hippocampal neurogenesis consists in several steps: (1) Cell proliferation: Neural stem cells reside in the subgranular zone (SGZ) of the DG, have a radial glia-like (RGL) morphology and express the glial fibrillary acidic protein (GFAP) and nestin. They give rise to GFAP-negative, nestin-positive, Tbr2-positive transit-amplifying progenitors (TAP) (Gage, 2000; Yao et al., 2012). These highly proliferative TAPs then give rise to neuroblasts. (2) The differentiation of the newly formed cells into neuronal lineage by the expression of the immature neuronal marker doublecortin (DCX) followed by the mature neuronal marker Neu-N, the cell polarization and extension of dendrites and axons (Gage, 2000; Van Praag et al., 2002; Laplagne et al., 2006; Yao et al., 2012). (3) The migration of the new neurons into the granule cell layer. (4) The activity-dependent survival of the newly formed neurons (Tashiro et al., 2006). (5) Their functional integration into the hippocampal network (Toni et al., 2007, 2008; Toni and Sultan, 2011) and participation to mechanisms of learning and memory (Aimone et al., 2010).

Each of these steps is highly regulated by signals within the stem cells' specialized environment, called the neurogenic niche. The niche is constituted by several cell types, including astrocytes, the stem cell's progenies, oligodendrocytes, endothelial cells, microglia, mature and immature neurons (Shihabuddin et al., 2000; Song et al., 2002; Zhao et al., 2008; Bonaguidi et al., 2011). All together these cells release specific factors, like Transforming Growth Factor-β (TGF-β) (Kreutzberg, 1996a,b), basic Fibroblast Growth Factor (bFGF) (Wagner et al., 1999), Vascular Endothelial Growth Factor (VEGF) and also Brain Derived Neurotrophic Factor (BDNF) (Bergami et al., 2008; Lee and Son, 2009), which are all involved in the regulation of the niche homeostasis. Of particular interest, astrocytes seem to play a special role in the regulation of the neurogenic niche, by expressing membrane-associated or secreted pro-neurogenic factors involved in the proliferation or neuronal differentiation of adult neural stem cells (Song et al., 2002; Lie et al., 2005; Platel et al., 2010; Ashton et al., 2012).

A particularly interesting factor secreted by astrocytes, D-serine is abundant in the hippocampus and especially in hippocampal astrocytes (Schell et al., 1995) where it is stored in vesicles (Bergersen et al., 2012; Martineau et al., 2013). D-serine is a co-agonist of the NMDA receptor (Mothet et al., 2000) and its calcium-dependent release participates to the expression of long-term potentiation (LTP) in the hippocampus (Yang et al., 2003; Henneberger et al., 2010). D-serine crosses the blood-brain barrier, since the exogenous administration of D-serine increases extracellular and intracellular brain D-serine levels (Pernot et al., 2012). Interestingly, D-serine administration enables LTP (Bashir et al., 1990; Oliver et al., 1990; Watanabe et al., 1992; Duffy et al., 2008) and can reverse the aging-related deficits in LTP expression and learning performances (Mothet et al., 2006; Devito et al., 2011), suggesting that D-serine could be targeted as a cognitive enhancer (Collingridge et al., 2013).

Here, we investigated the effect of exogenous D-serine administration on adult neurogenesis. We found that administration for 8 days increased cell proliferation, the number of RGL cells and the number of TAPs in the dentate gyrus of adult mice. Similarly, *in vitro*, D-serine increased the number of stem/progenitor

cells. Finally, when administered during the fourth week after cell division, D-serine increased the survival of new neurons.

EXPERIMENTAL PROCEDURES

ANIMALS AND D-SERINE ADMINISTRATION

All experimental protocols were approved by the Swiss animal experimentation authorities (Service de la consommation et des affaires vétérinaires, Chemin des Boveresses 155, 1066; Epalinges, Switzerland, permit number: 2301). Every effort was made to minimize the number of animals used and their suffering. Animals used for the study were adult male of 8 weeks of age at the beginning of the experiment. All animals were housed in a 12 h light/12 h dark cycle with free access to food and water and controlled temperature (22°C) conditions. C57Bl/6j mice were purchased from Janvier (le Genest Saint Isle, France), nestin-GFP mice were a kind gift from the laboratory of K. Mori (PRESTO, Kyoto, Japan) (Yamaguchi et al., 2000). These mice express the green fluorescent protein (GFP) under the stem cell-specific promoter nestin. GFAP-GFP mice were a kind gift from the laboratory of Helmut Kettenmann (Max-Delbruck center, Berlin, Germany) (Nolte et al., 2001). They express GFP under the control of the astrocyte-specific promoter GFAP. D-serine was prepared fresh every day and diluted in water containing 0.9% NaCl. Mice were injected intraperitoneally every day with 50 mg/kg of D-serine (Sigma-Aldrich) for 8 consecutive days or with vehicle (0.9% NaCl in water).

BrdU ADMINISTRATION AND IMMUNOHISTOCHEMISTRY

Mice were injected intraperitoneally with 5-bromo-2-deoxyuridine (BrdU, Sigma-Aldrich, Buchs, Switzerland) at a concentration of 100 mg/kg in saline, 3 times at 2-h intervals. Two hours after the last injection, mice were sacrificed to examine cell proliferation (Mandyam et al., 2007; Taupin, 2007; Yang et al., 2011; Gao and Chen, 2013; Sultan et al., 2013). Briefly, mice were injected intraperitoneally with a lethal dose of pentobarbital (10 mL/kg, Sigma, Switzerland) and then perfused with 50 ml of 0.9% saline solution followed by 100 mL of 4% paraformaldehyde (Sigma-Aldrich, USA) dissolved in 0.1 M Phosphate Saline Buffer (PBS, pH 7.4). Their brains were dissected, postfixed overnight at 4°C, cryoprotected 24 h in 30% sucrose solution (Sigma-Aldrich, USA) and rapidly frozen. Then coronal sections were performed at a thickness of 40 μm with a microtome-cryostat (Leica MC 3050S) and slices were stored in cryoprotectant (30% ethylene glycol and 25% glycerin in PBS 0.1 M) at −20°C until processing for immunostaining as previously described (Thuret et al., 2009). Immunochemistry was performed on every 6th sections of the dentate gyrus. Briefly, sections were washed 3 times in PBS 0.1 M and blocking of non-specific binding was achieved by incubating in PBS 0.1 M containing 0.3% Triton-X 100 and 10% normal serum. BrdU immunohistochemistry was preceded by DNA denaturation by incubation in formic acid 50% formamide/ 50% 2X SSC buffer (2X SSC is 0.3 M NaCl and 0.03 M sodium citrate, pH 7.0) at 65°C for 2 h, rinsed twice in 2X SSC buffer, incubated in 2 M HCl for 30 min at 37°C, and rinsed in 0.1 M borate buffer pH 8.5 for 10 min. Then, sections were incubated at 4°C with one of the following primary antibodies: mouse monoclonal anti-BrdU (48 h, 1:250, Chemicon International, Dietikon, Switzerland), goat anti-DCX (1:500, Santa Cruz biotechnology, sc-8066), rabbit anti-Ki-67 (48 h, 1:200, Abcam, ab15580), rabbit anti-Tbr2 (1:200, Abcam, ab23345), rabbit anti-GFAP (1:500, Invitrogen, 180063) mouse anti-Neu-N (Chemicon international 1:1000). Sections were then incubated for 2 h at room temperature with the following fluorescent secondary antibody: goat anti-mouse Alexa-594 (1:250, Invitrogen), goat anti-rabbit 594 (1:250, Invitrogen), donkey anti-goat Alexa-555 (1:250 Invitrogen). After immunostaining, one minute incubation of slices into 4,6 diamidino-2-phenylindole (DAPI) was used to reveal nuclei.

IMAGE ANALYSIS

Images were collected with a Zeiss confocal microscope (Zeiss LSM 710 Quasar Carl Zeiss, Oberkochen, Germany) and cell counts were performed using stereology, as previously described (Thuret et al., 2009). Briefly, for each animal, a 1-in-6 series of section between −1.3 and −2.9 mm from the Bregma was stained with the nucleus marker DAPI and used to measure the volume of the granule cell layer. The granule cell area was traced using Axiovision (Zeiss, Germany) software and the granule cell reference volume was determined by multiplying the area of the granule cell layer by the distance between the sections sampled (240 μm). All cells were counted in the entire thickness of the sections in a 1-in-6 series of section (240 μm apart) with a 40× objective. All cells were counted blind with regard to the mouse status. The number of immunolabeled cells was then related to granule cell layer sectional volume and multiplied by the reference volume to estimate the total number of immunolabeled cells. Cells expressing BrdU, Ki-67, DCX or Tbr2 were counted in the granule cell layer, whereas cells expressing GFAP (**Figures 3C,D**) were counted in the whole dentate gyrus. BrdU colocalization with the neuronal marker Neu-N was analyzed by confocal microscopy and was confirmed on single optical sections, for 50–60 cells per animal. The proportion of double-labeled cells was then obtained for each animal and then averaged for each group.

CELL CULTURE

Astroyctes primary culture: Cerebral cortices from 3 postnatal day 0 (P0) rats were mechanically dissociated for homogenization, cells were pooled and seeded onto 75 cm^2 flasks in Dulbecco's Modified Eagle Medium (DMEM) glutamax (Invitrogen, USA), 15% foetal bovine serum with penicillin/streptomycin (Invitrogen, USA). Cells were grown for 10–12 days in a humidified 5% CO_2 incubator at 37°C. At confluence, flasks were shaken at 250 rpm on an orbital shaker for 2 h to remove microglia. Adult neural progenitor cells (NPCs) expressing the red fluorescent protein (RFP) are a kind gift from the laboratory of Fred Gage (Salk Institute, San Diego, USA). They were originally isolated from the dentate gyrus of adult Fisher 344 rats and cultured as previously described (Ray and Gage, 2006). RFP expressing NPCs were plated on coated 12 mm coverslips in a 24-well culture plate, at a density of 2,000,000

cells/mL (80 μL per well). Medium was changed daily and supplemented with 2 μM FGF2. Three wells per condition were used. In a first experiment, the effect of D-serine was tested on NPCs and then, in a second, independent experiment, on NPCs-astrocytes co-cultures. Twenty-four hours after plating, the medium was replaced by fresh culture medium, and then treated daily with D-serine (50 μM, diluted in culture media) during 8 days. Control cultures were treated with the same volume of vehicle. After this, cells were fixed with 4% paraformaldehyde for 20 min, washed and the coverslips were immunostained and mounted.

In vitro CELL QUANTIFICATION

Images were acquired using confocal microscopy. The number of RFP+ and GFAP+ cells was counted in 4 selected fields, systematically placed in the same positions relative to the coverslips' edges. The total number of cells was divided by the total area of the selected fields to obtain an average cell density per well that was then multiplied by the total surface area of the coverslip to obtain an estimate of the total number of cells per coverslip. This number of cells was then compared to the number of cells that were plated in the wells to obtain a percentage of increase in cell number (Gebara et al., 2013).

STATISTICAL ANALYSIS

Hypothesis testing was two-tailed. All analyses were performed using JMP10 software. First, Shapiro-Wilk tests were performed on each group of data to test for distribution normality. The distribution was normal for all data. The analysis was performed using parametric tests (One-Way ANOVA followed by a *post hoc* bilateral Student's *t*-test). For two-sample comparisons, the equality of variances of the groups was tested and the adequate unpaired *t*-test was used. Data is presented as mean ± SEM.

RESULTS

D-SERINE INCREASED CELL PROLIFERATION IN THE DENTATE GYRUS

We first examined the effect of D-serine on cell proliferation in the dentate gyrus of adult C57Bl/6 mice. Eight-week-old mice were injected with one daily intraperitonal injection of D-serine (50 mg/kg), for 8 days, as this regimen is known to increase extracellular D-serine brain levels (Fukushima et al., 2004; Ferraris et al., 2008) and improve learning performances in mice (Bado et al., 2011; Filali and Lalonde, 2013) (**Figure 1A**). Control mice were injected with the same volume of the vehicle (0.9% NaCl), or received no injection. One day after the last injection, all mice received 3 intraperitoneal injections of the cell proliferation tracer BrdU (100 mg/kg) at 2-h intervals and were sacrificed 2 h after the last BrdU injection. Brains were sectioned and immunostained for BrdU and the proliferation marker Ki-67 and the number of immunoreactive cells was counted in the granule cell layer of the dentate gyrus. D-serine injections significantly increased the number of BrdU-expressing cells [**Figures 1B,C**, One-Way ANOVA, $F_{(2,\ 11)} = 20.64$, $p < 0.001$; *post-hoc* bilateral Student's *t*-test between groups $p < 0.001$] and the number of Ki-67-expressing cells [**Figures 1D,E**, One-Way ANOVA, $F_{(2,\ 11)} = 24.90$, $p < 0.001$; *post-hoc* bilateral Student's *t*-test between groups, $p < 0.001$]. To test whether the D-serine-induced increase in cell proliferation was specific to the dentate gyrus, we counted the number of Ki-67-expressing cells in the S1 area of the somatosensory cortex. D-serine treatment did not change the density of Ki-67+ cells in the somatosensory cortex (NaCl: $2.54 \pm 0.14 \times 10^{-6}$ cells/μm^3 vs. D-serine: $2.83 \pm 0.28 \times 10^{-6}$ cells/μm^3, Student's *t*-test $p = 0.3$). No difference was found between non-injected and NaCl-injected animals (*post-hoc* bilateral Student's *t*-test $p = 0.21$ for BrdU+ cells and $p = 0.58$ for Ki-67+ cells). To test whether the increased number of BrdU- or Ki-67-expressing cells could be caused by a change in hippocampal volume upon D-serine treatment, we measured the volume of the granule cell layer of all mice. We did not detect any difference between treated and control animals [One-Way ANOVA, $F_{(2,\ 11)} = 2.20$, $p = 0.166$, control animals: $0.17 \pm 0.006\ mm^3$, animals injected with NaCl $0.18 \pm 0.04\ mm^3$, injected with D-serine $0.17 \pm 0.03\ mm^3$ respectively, $n = 4$ animals per group], indicating that the increased numbers of BrdU and Ki-67 cells reflected an increase in cell proliferation.

We then examined the effect of D-serine on the main proliferative cells in the SGZ: the type-1 radial glia-like (RGL) stem cells and TAPs (TAPs; **Figures 2**, **3**). To identify RGL cells, we used a transgenic mouse expressing GFP under the stem cell-specific promoter nestin (Yamaguchi et al., 2000). GFP-expressing RGL cells of the dentate gyrus were readily identifiable by their morphology, consisting of a nucleus located in the subgranular zone, a large processes extending through the granule cell layer and branching into the proximal part of the molecular layer (Kriegstein and Alvarez-Buylla, 2009), (**Figure 2B**). With immunostaining, we confirmed that these cells expressed nestin, GFAP, and sox-2 (data not shown). D-serine treatment significantly increased the number of RGL cells in the dentate gyrus as compared to control or vehicle treatment [**Figure 2A**, One-Way ANOVA, $F_{(2,\ 11)} = 90.36$, $p < 0.001$; *post-hoc* bilateral Student's *t*-test between groups $p < 0.001$]. RGL cells were also identified in GFAP-GFP mice (Nolte et al., 2001; **Figure 2D**). Similarly, in GFAP-GFP mice, D-serine induced an increase in RGL cell number in the subgranular zone [**Figures 2C,D**, One-Way ANOVA, $F_{(2,\ 11)} = 35.20$, $p < 0.001$; *post-hoc* bilateral Student's *t*-test between groups $p < 0.001$]. Here too, we did not detect any difference in the volume of the granule cell layer between treated and control animals in both nestin-GFP and GFAP-GFP mice [nestin-GFP mice: One-Way ANOVA, $F_{(2,\ 11)} = 0.34$, $p = 0.7$ and GFAP-GFP mice One-Way ANOVA, $F_{(2,\ 11)} = 1.6$, $p = 0.24$, respectively $n = 4$ animals per group]. To examine whether the proliferation potential of the RGL cells was modified by treatment, we labeled GFAP-GFP mice with the proliferation marker Ki-67. We analyzed 4 mice per group and a total of 615 RGL cells for the D-serine group and 317 RGL cells for the NaCl group. D-serine treatment showed a significant increase of the percentage RGL cells that expressed Ki-67 as compared to NaCl treatment (Data not shown, D-serine treatment 5.54% ± 0.15 vs. NaCl 4.16% ± 0.43, Student's *t*-test $p < 0.05$).

We next examined the effect of D-serine on TAPs identified by immunohistochemistry against T-brain gene-2 (Hodge

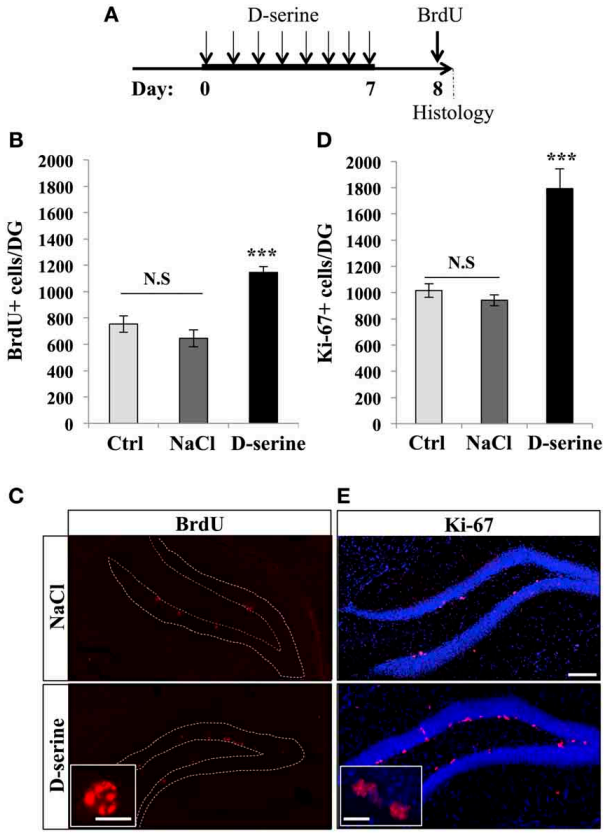

FIGURE 1 | D-serine increased cell proliferation in the dentate gyrus. (A) Experimental timeline: Mice were injected intraperitoneally every day with 50 mg/kg of D-serine, for 8 consecutive days. One day after the last injection, mice were pulsed with BrdU (100 mg/kg, 3 injections every 2 h) and, 2 h later, euthanized and prepared for immunohistochemistry. **(B)** Histogram showing the number of BrdU-expressing cells per dentate gyrus of animals injected with D-serine, NaCl or not injected (Ctrl). Animals: $n = 4$ per group. **(C)** Confocal maximal projection micrographs of hippocampal sections immunostained for BrdU in the two injected groups (D-serine and NaCl). Inset: Higher magnification micrograph of a BrdU-expressing cell. **(D)** Histogram showing the number of Ki-67–expressing cells. Animals: $n = 4$ per group. **(E)** Confocal maximal projection micrographs of hippocampal sections immunostained for Ki-67 in the two experimental groups (D-serine and NaCl). Inset: Higher magnification micrograph of Ki-67-expressing cells. Blue: Dapi staining. Each value represents the mean ± SEM; *post-hoc* bilateral Student's *t*-test, (***$p < 0.001$), N.S., non-significant ($p > 0.05$). Scale bar: 100 μm, insets 10 μm.

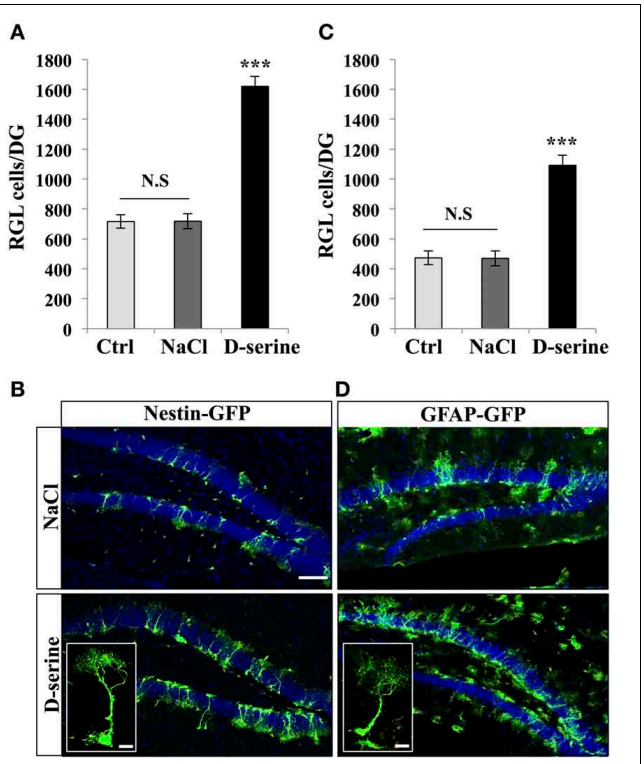

FIGURE 2 | D-serine increased the number of RGL cells. (A) Histogram showing the number of RGL cells per dentate gyrus of nestin-GFP mice injected with D-serine, NaCl or not injected (Ctrl). Animals $n = 4$ per group. **(B)** Confocal maximal projection micrographs of hippocampal sections in the two injected groups (D-serine and NaCl). Inset: higher magnification confocal micrograph of a RGL cell. **(C)** Histograms showing the number of RGL cells in the dentate gyrus of GFAP-GFP mice injected with D-serine, NaCl and in control, non-injected animals (Ctrl). Animals: $n = 4$ animals per groups. **(D)** Confocal maximal projection micrographs of hippocampal sections from the two experimental groups. Inset: higher magnification micrograph of a RGL cell. Blue: Dapi staining. Each value represents the mean ± SEM; *post-hoc* bilateral Student's *t*-test, (***$p < 0.001$), N.S., non-significant ($p > 0.05$). Scale bar: 100 μm. Insets 10 μm.

et al., 2008). D-serine significantly increased the number of Tbr2-expressing cells in the granule cell layer [**Figures 3A,B**, One-Way ANOVA, $F_{(2, 11)} = 7.18$, $p = 0.013$; *post-hoc* bilateral Student's *t*-test between groups $p < 0.01$]. The effect was specific to proliferating cells, since D-serine treatment did not change the number of GFAP-immunolabeled astrocytes of the whole dentate gyrus, i.e., including hilus, granule cell layer and molecular layer [**Figures 3C,D**, One-Way ANOVA, $F_{(2, 11)} = 0.54$, $p = 0.59$]. Together, these results indicate that D-serine increased cell proliferation in the SGZ and increased the number of RGL cells and TAPs.

D-SERINE INCREASED THE PROLIFERATION OF NPCs *in vitro*

To test the effect of D-serine directly on progenitor cells, we performed *in vitro* experiments on purified NPCs. We plated the same number of RFP-expressing NPCs from the adult dentate gyrus in each well, treated them for 8 days with D-serine (50 μM, daily) or vehicle (culture medium) and then counted the number of remaining NPCs, that we then expressed as the proportion of increase in cell number from the plated cell number. D-serine significantly increased the number of NPCs (**Figures 4A,B**, bilateral Student's *t*-test $p < 0.001$). On another set of experiments, we tested the effect of D-serine on NPCs in presence of astrocytes, by examining the effect of D-serine on co-cultures of astrocytes with NPCs. Similarly to purified cultures, co-cultures treated for 8 days with D-serine showed a greater number of NPCs (**Figures 4C,E**, bilateral Student's *t*-test $p < 0.01$). However, the number of GFAP-immunolabeled astrocytes remained unchanged as compared to control co-cultures (**Figures 4D,E**, bilateral Student's

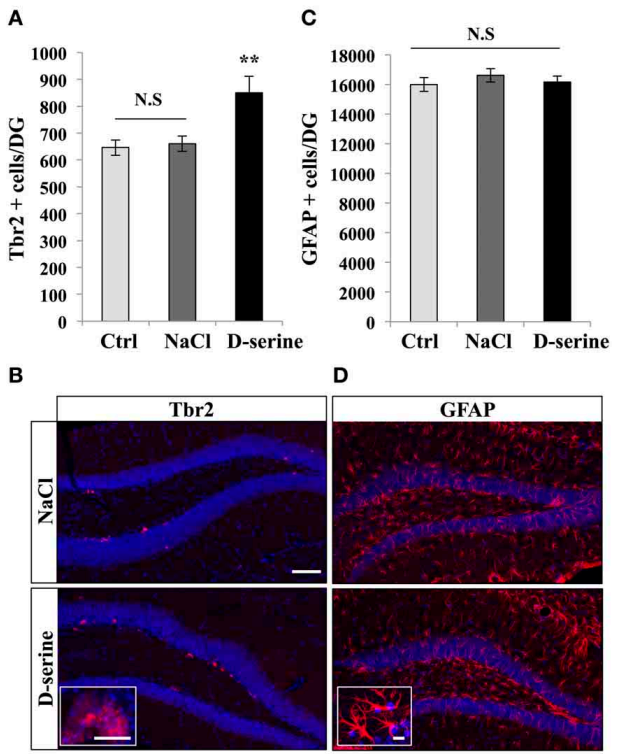

FIGURE 3 | D-serine increased the number of Tbr-2-expressing cells. (A) Histogram showing the number of Tbr2-expressing cells in the granule cell layer of the dentate gyrus of mice injected with D-serine or NaCl and in control, non-injected animals (Ctrl). Animals: $n = 4$ animals per group. **(B)** Confocal maximal projection micrographs of hippocampal sections immunostained for Tbr2 from the two injected groups. Inset: higher magnification micrograph of Tbr-2-immunolabeled cells. **(C)** Histogram showing the number of GFAP-expressing cells per dentate gyrus of injected mice (D-serine and NaCl) and in control, non-injected animals (Ctrl). Animals: $n = 4$ per groups. **(D)** Confocal maximal projection micrographs of hippocampal sections immunostained for GFAP from the two experimental groups. Inset: higher magnification micrograph of a GFAP-immunostained cell. Blue: Dapi staining. Each value represents the mean ± SEM; *post-hoc* bilateral Student's *t*-test, (**$p < 0.01$), N.S., Non-significant ($p > 0.05$). Scale bar: 100 μm, insets 10 μm.

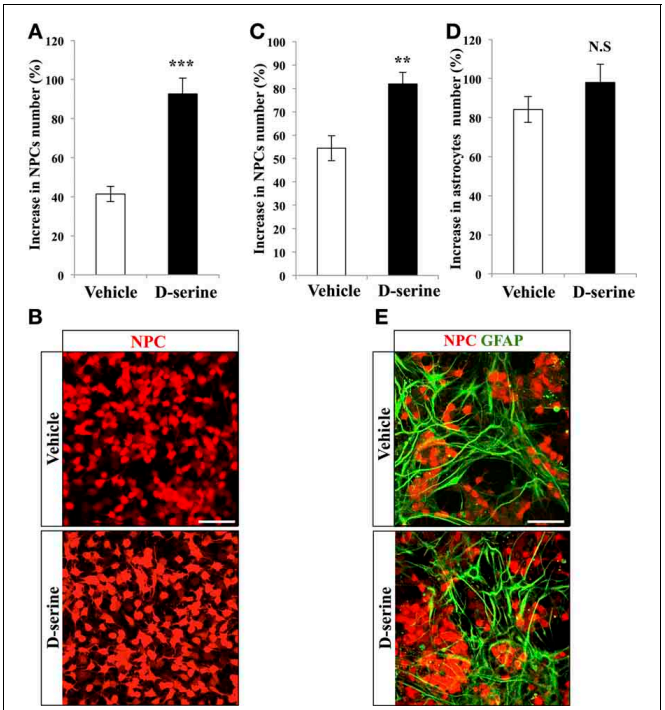

FIGURE 4 | D-serine increased the number of NPCs *in vitro*. (A) Histogram of the increase in NPCs number (% of the number of plated cells), upon treatment with D-serine or vehicle. **(B)** Confocal maximal projection micrographs of RFP-expressing NPCs for each condition. **(C,D)** Histograms showing the proportion of increase in NPCs **(C)** and in GFAP-expressing astrocytes **(D)** in co-cultures treated with D-serine or vehicle. **(E)** Confocal maximal projection micrographs of NPCs-Astrocytes co-cultures in the two conditions. Each value represents the mean ± SEM; *post-hoc* bilateral Student's *t*- test, (***$p < 0.001$, **$p < 0.01$), N.S., non-significant ($p > 0.05$). Scale bars: 100 μm.

t-test $p = 0.19$). Thus, D-serine increased the number of NPCs, but not of astrocytes.

D-SERINE INCREASED THE NUMBER OF IMMATURE NEURONS AND THE SURVIVAL OF NEWBORN NEURONS

Next, to test whether D-serine affected neuronal differentiation and survival, we examined the number of immature neurons and the fate of the dividing cells, which matured under a D-serine treatment. Adult mice were injected with BrdU (intraperitoneal at 100 mg/kg, 3 injections at 2-h intervals) and were treated with D-serine from 22 to 29 days after the last BrdU injection. One day after the last injection, mice were sacrificed and brain sections were immunostained for the immature neuronal marker doublecortin (DCX), the mature neuronal marker Neu-N and BrdU (**Figure 5**). D-serine significantly increased the number of DCX-expressing cells [**Figures 5B,C**, One-Way ANOVA, $F_{(2,\ 11)} = 227.30$, $p < 0.001$; *post-hoc* bilateral Student's *t*-test $p < 0.001$], whereas the volume of the granule cell layer did not change between groups [one-way ANOVA, $F_{(2,\ 11)} = 1.51$, $p = 0.27$]. In order to test whether the D-serine treatment also increased the proliferation of neuroblasts, we immunostained for DCX and Ki-67 and measured the percentage of double labeled cells. Compared to NaCl, D-serine treatment showed no significant difference in the proportion of DCX-expressing cells which also expressed Ki-67 (NaCl 5.72% ± 0.85 vs. D-serine 4.36% ± 0.73, Student's *t*-test $p = 0.33$, data not shown). Thus, D-serine increased the number of immature neurons but not the proliferation of neuroblasts. The number of BrdU-labeled cells was significantly increased in D-serine injected animals [**Figures 5D,E**, One-Way ANOVA, $F_{(2,\ 11)} = 10.73$, $p < 0.01$; *post-hoc* bilateral Student's *t*-test $p < 0.01$], indicating an effect of D-serine on the survival of newborn cells. Finally, we examined differentiation of new cells into neuronal lineage by measuring the proportion of BrdU-labeled cells that also expressed Neu-N (**Figures 5F,G**). In control and NaCl mice, neurons accounted respectively for 86 ± 2% and 85 ± 1.7% of the surviving BrdU-positive cells as compared to 91 ± 1% in D-serine-treated mice [One-Way ANOVA, $F_{(2,\ 8)} = 1.8$, $p = 0.24$], indicating that D-serine did not significantly increase neuronal differentiation. When the

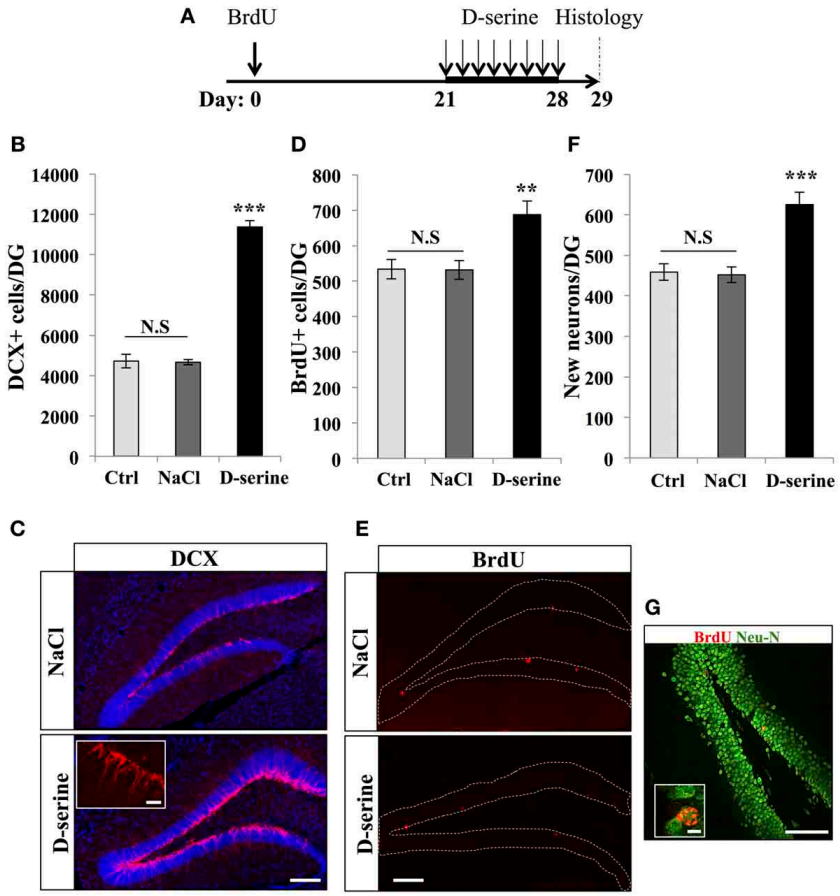

FIGURE 5 | D-serine increased the number of DCX-expressing cells and the survival of new neurons. (A) Experimental timeline: Mice were injected with BrdU (100 mg/kg) 3 times at 2 h interval. Twenty-one days later, mice received one injection of D-serine (50 mg/kg) every day for 8 consecutive days. One day after the last injection, mice were euthanized and prepared for histology. **(B)** Histogram showing the number of DCX-immunolabeled cells in the dentate gyrus of mice injected with D-serine or NaCl and in control, non-injected animals (Ctrl). Animals: $n = 4$ per groups. **(C)** Confocal maximal projection micrographs of hippocampal sections immunostained for DCX from the two experimental groups. Inset: higher magnification micrograph of a DCX-immunolabeled group of cells. **(D)** Histogram of the number of BrdU-immunolabeled cells in the dentate gyrus of mice injected with D-serine or NaCl and non-injected animals (Ctrl). Animals: $n = 4$ per groups. **(E)** Confocal maximal projection micrographs of hippocampal sections immunostained for BrdU from the two experimental groups. **(F)** Histogram showing the number of new born neurons in the dentate gyrus of each group. Animals: $n = 4$ per group. **(G)** Single optical section confocal micrograph of BrdU- and Neu-N-immunolabeled cells in the dentate gyrus. Inset: higher magnification confocal micrograph of a BrdU-labeled cell expressing Neu-N. Blue: dapi staining. Each value represents the mean ± SEM; *post-hoc* bilateral Student's *t*-test (**$p < 0.01$, ***$p < 0.001$), N.S., non-significant ($p > 0.05$). Scale bars: 100 μm, insets 10 μm.

number of surviving cells was multiplied by the fraction of cells that differentiated into neurons, we found that D-serine-treated mice had 39.8 ± 1.1% more newly-formed neurons than non-treated mice [**Figure 5F**, One-Way ANOVA $F_{(2,\ 11)} = 16.67$, $p < 0.001$; *post-hoc* bilateral Student's *t*-test $p < 0.001$]. Thus, D-serine treatment during the fourth week after cell division increased the survival of new neurons, but did not modify their differentiation.

DISCUSSION

In this study, we tested the effect of repeated injections of D-serine on hippocampal adult neurogenesis. We found that *in vivo*, 8 days of D-serine administration increased cell proliferation as well as the number of both RGL cells (type-1) and TAP cells (type-2) and slightly increased the proliferation of RGL cells. D-serine applied to adult hippocampal neural progenitors in culture also increased cell number suggesting a direct effect of D-serine on adult NSCs. Finally, when administered during the critical phase for activity-dependent survival, D-serine increased the survival of newborn neurons. Since this critical phase lasts until the end of the first month after cell division (Kempermann et al., 2003), the surviving neurons observed after D-serine treatment are expected to survive throughout the entire life of the animals. Thus, D-serine increased adult neurogenesis by acting on several steps of this process and may result in long-lasting changes in the granule cell layer.

Together, these results are relevant to the effect of D-serine on learning and memory. Indeed, newborn neurons in the

hippocampus are involved in hippocampal dependent learning and memory (Dupret et al., 2007; Ming and Song, 2011; Gu et al., 2012). The performances of animals in hippocampal-learning tasks are highly correlated with the rate of adult neurogenesis in the hippocampus. For example, voluntary running strongly increases the proliferation of adult neural stem cells in the dentate gyrus and newborn neurons survival (Van Praag et al., 1999b; Snyder et al., 2009) and improves the performance of animals in a water maze (Van Praag et al., 1999a). Inversely, ablation studies lead to decreased performances in hippocampal-dependent learning (Saxe et al., 2006; Dupret et al., 2007; Imayoshi et al., 2008; Massa et al., 2011; Lemaire et al., 2012) and more recently, the optogenetic inactivation or stimulation of new neurons induced memory deficits or improvements, respectively (Alonso et al., 2012; Gu et al., 2012). Thus, by increasing neurogenesis, D-serine may improve learning performances. Further behavioral experiments combined with D-serine treatment and ablation of neurogenesis will enable to test the role of adult neurogenesis in the D-serine-mediated learning improvements.

The effect of D-serine on neuronal survival is consistent with the role of NMDA receptor activation in the survival of adult-born neurone: Neurons generated during adulthood undergo a critical time-window for their survival during the third week after cell division, during which the cell-specific knockout of the NR1 subunit in adult-born neurons dramatically decreases their survival (Tashiro et al., 2006). Inversely, increased activity correlates with increased survival (Kempermann et al., 1998), an effect that may be due to glutamate, since this neurotransmitter enhances neuronal survival (Platel et al., 2010; Kelsch et al., 2012) and D-aspartate, a NMDA receptor agonist produced by newborn neurons, induces the dendritic maturation and survival of these cells (Kim et al., 2010). Thus, the effect of D-serine on new neurons survival may be mediated by an increase in NMDA receptors activity on these cells.

In contrast, the mechanism of action of D-serine on cell proliferation remains less clear and could be mediated by an indirect effect of D-serine on hippocampal network activity or by a direct effect on neural stem/progenitor cells, or both. In favor of the former possibility, adult NSCs proliferation and newborn neurons survival are tightly regulated by hippocampal network activity: High frequency stimulations of the perforant path increase NSCs proliferation and newborn neurons survival (Bruel-Jungerman et al., 2006; Chun et al., 2006; Stone et al., 2011). Moreover, mice placed in an enriched environment showed an increase of both proliferation and survival of newborn neurons in the DG (Kempermann et al., 1997; Van Praag et al., 2000; Tashiro et al., 2007). Inversely, a decrease in neuronal activity decreases neurogenesis (Li et al., 2009; Sun et al., 2009; Krzisch et al., 2013). Thus, by increasing NMDA-dependent neuronal activity (Wake et al., 2001; Xie et al., 2005), D-serine treatment could result in increased cell proliferation. Alternatively, in favor of the hypothesis of a direct action of D-serine on the NMDA receptors of stem/progenitor cells, studies using electrophysiological recordings have shown that RGL cells express NMDA receptors (Wang et al., 2005; Nacher et al., 2007) and our experiments showed that D-serine increased RGL cells proliferation *in vivo* and NPCs proliferation *in vitro*. However, previous studies have shown that, in the SGZ, NSC proliferation is strongly decreased by NMDAR activation (Cameron et al., 1995). Furthermore, a recent study (Huang et al., 2012) showed that D-serine treatment did not change the proliferation of early progenitor cells *in vitro*, although the discrepancy between this earlier study and our observations may arise from the treatment duration (48 h vs. 8 days, respectively) or the origin of the cells (mouse vs. rat). Thus, the mode of action of D-serine remains unclear and the insight gained *in vitro* studies for the understanding of the regulation of the neurogenic niche remains limited and, further *in vivo* experiments using cell autonomous approaches will be necessary to determine the origin and the targets of D-serine in the neurogenic niche.

Together, our results indicate that D-serine administration increases the proliferation of stem/progenitor cells and the survival of new neurons. It remains, however, unclear whether *in vivo*, D-serine release plays a role in the regulation of adult neurogenesis. (Huang et al., 2012) have shown that stem/progenitor cells in the subventricular zone release D-serine and that a blockade of D-serine synthesis reduces cell proliferation *in vitro*, suggesting an autocrine regulation mechanism. However, D-serine has been reported to be secreted by other cells, including astrocytes and neurons (Radzishevsky et al., 2013). Of particular interest, the release of D-serine from astrocytes is triggered by the activation of astrocytic AMPA/kainate receptors (Schell et al., 1995). In the hippocampus, astrocytic territories span tens of micrometers (Bushong et al., 2002) and can extend from the hilus or the molecular layer to the subgranular zone of the dentate gyrus. These cells are therefore ideally located to relay signaling between synaptic activity and the neurogenic niche. Although still speculative, the controlled release of D-serine by astrocytes in the neurogenic niche may be a mechanism coupling neuronal activity in specific territories of the dentate gyrus with the local proliferation of stem/progenitor cells. Future experiments aimed at interfering with astrocytic D-serine synthesis or release may shed light on the regulation of endogenous D-serine in the adult hippocampus and on the processes regulating adult neurogenesis. These mechanisms are relevant to our understanding of the regulation of adult neurogenesis and its use as a target for cognitive impairment.

AUTHOR CONTRIBUTIONS

Conceived and designed the experiments: Sebastien Sultan, Elias G. Gebara and Nicolas Toni. Performed the experiments: Elias G. Gebara, Sebastien Sultan and Kristell Moullec. Analyzed the data: Sebastien Sultan and Elias G. Gebara. Wrote the paper: Sebastien Sultan, Elias G. Gebara and Nicolas Toni.

ACKNOWLEDGMENTS

Images acquisition was performed at the Cellular Imaging Facility of the university of Lausanne (Lausanne, Switzerland). This work was supported by the Swiss National Science Foundation, grant No: PP0033-119026.

REFERENCES

Aimone, J. B., Deng, W., and Gage, F. H. (2010). Adult neurogenesis: integrating theories and separating functions. *Trends Cogn. Sci.* 14, 325–337. doi: 10.1016/j.tics.2010.04.003

Alonso, M., Lepousez, G., Sebastien, W., Bardy, C., Gabellec, M. M., Torquet, N., et al. (2012). Activation of adult-born neurons facilitates learning and memory. *Nat. Neurosci.* 15, 897–904. doi: 10.1038/nn.3108

Altman, J. (1969). Autoradiographic and histological studies of postnatal neurogenesis. 3. Dating the time of production and onset of differentiation of cerebellar microneurons in rats. *J. Comp. Neurol.* 136, 269–293. doi: 10.1002/cne.901360303

Ashton, R. S., Conway, A., Pangarkar, C., Bergen, J., Lim, K. I., Shah, P., et al. (2012). Astrocytes regulate adult hippocampal neurogenesis through ephrin-B signaling. *Nat. Neurosci.* 15, 1399–1406. doi: 10.1038/nn.3212

Bado, P., Madeira, C., Vargas-Lopes, C., Moulin, T. C., Wasilewska-Sampaio, A. P., Maretti, L., et al. (2011). Effects of low-dose D-serine on recognition and working memory in mice. *Psychopharmacology* 218, 461–470. doi: 10.1007/s00213-011-2330-4

Bashir, Z. I., Tam, B., and Collingridge, G. L. (1990). Activation of the glycine site in the NMDA receptor is necessary for the induction of LTP. *Neurosci. Lett.* 108, 261–266. doi: 10.1016/0304-3940(90)90651-O

Bergami, M., Rimondini, R., Santi, S., Blum, R., Gotz, M., and Canossa, M. (2008). Deletion of TrkB in adult progenitors alters newborn neuron integration into hippocampal circuits and increases anxiety-like behavior. *Proc. Natl. Acad. Sci. U.S.A.* 105, 15570–15575. doi: 10.1073/pnas.0803702105

Bergersen, L. H., Morland, C., Ormel, L., Rinholm, J. E., Larsson, M., Wold, J. F., et al. (2012). Immunogold detection of L-glutamate and D-serine in small synaptic-like microvesicles in adult hippocampal astrocytes. *Cereb. Cortex* 22, 1690–1697. doi: 10.1093/cercor/bhr254

Bonaguidi, M. A., Wheeler, M. A., Shapiro, J. S., Stadel, R. P., Sun, G. J., Ming, G. L., et al. (2011). *In vivo* clonal analysis reveals self-renewing and multipotent adult neural stem cell characteristics. *Cell* 145, 1142–1155. doi: 10.1016/j.cell.2011.05.024

Bruel-Jungerman, E., Davis, S., Rampon, C., and Laroche, S. (2006). Long-term potentiation enhances neurogenesis in the adult dentate gyrus. *J. Neurosci.* 26, 5888–5893. doi: 10.1523/JNEUROSCI.0782-06.2006

Bushong, E. A., Martone, M. E., Jones, Y. Z., and Ellisman, M. H. (2002). Protoplasmic astrocytes in CA1 stratum radiatum occupy separate anatomical domains. *J. Neurosci.* 22, 183–192.

Cameron, H. A., McEwen, B. S., and Gould, E. (1995). Regulation of adult neurogenesis by excitatory input and NMDA receptor activation in the dentate gyrus. *J. Neurosci.* 15, 4687–4692.

Chun, S. K., Sun, W., Park, J. J., and Jung, M. W. (2006). Enhanced proliferation of progenitor cells following long-term potentiation induction in the rat dentate gyrus. *Neurobiol. Learn. Mem.* 86, 322–329. doi: 10.1016/j.nlm.2006.05.005

Collingridge, G. L., Volianskis, A., Bannister, N., France, G., Hanna, L., Mercier, M., et al. (2013). The NMDA receptor as a target for cognitive enhancement. *Neuropharmacology* 64, 13–26. doi: 10.1016/j.neuropharm.2012.06.051

Devito, L. M., Balu, D. T., Kanter, B. R., Lykken, C., Basu, A. C., Coyle, J. T., et al. (2011). Serine racemase deletion disrupts memory for order and alters cortical dendritic morphology. *Genes Brain Behav.* 10, 210–222. doi: 10.1111/j.1601-183X.2010.00656.x

Duffy, S., Labrie, V., and Roder, J. C. (2008). D-serine augments NMDA-NR2B receptor-dependent hippocampal long-term depression and spatial reversal learning. *Neuropsychopharmacology* 33, 1004–1018. doi: 10.1038/sj.npp.1301486

Dupret, D., Fabre, A., Döbrössy, M. D., Panatier, A., Rodríguez, J. J., Lamarque, S., et al. (2007). Spatial learning depends on both the addition and removal of new hippocampal neurons. *PLoS Biol.* 5:e214. doi: 10.1371/journal.pbio.0050214

Ferraris, D., Duvall, B., Ko, Y. S., Thomas, A. G., Rojas, C., Majer, P., et al. (2008). Synthesis and biological evaluation of D-amino acid oxidase inhibitors. *J. Med. Chem.* 51, 3357–3359. doi: 10.1021/jm800200u

Filali, M., and Lalonde, R. (2013). The effects of subchronic d-serine on left-right discrimination learning, social interaction, and exploratory activity in APPswe/PS1 mice. *Eur. J. Pharmacol.* 701, 152–158. doi: 10.1016/j.ejphar.2012.12.018

Fukushima, T., Kawai, J., Imai, K., and Toyo'oka, T. (2004). Simultaneous determination of D- and L-serine in rat brain microdialysis sample using a column-switching HPLC with fluorimetric detection. *Biomed. Chromatogr.* 18, 813–819. doi: 10.1002/bmc.394

Gage, F. H. (2000). Mammalian neural stem cells. *Science* 287, 1433–1438. doi: 10.1126/science.287.5457.1433

Gao, X., and Chen, J. (2013). Moderate traumatic brain injury promotes neural precursor proliferation without increasing neurogenesis in the adult hippocampus. *Exp. Neurol.* 239, 38–48. doi: 10.1016/j.expneurol.2012.09.012

Gebara, E. G., Sultan, S., Kocher-Braissant, J., and Toni, N. (2013). Adult hippocampal neurogenesis inversely correlates with microglia in conditions of voluntary running and aging. *Front. Neurosci.* 7:145. doi: 10.3389/fnins.2013.00145

Gu, Y., Arruda-Carvalho, M., Wang, J., Janoschka, S. R., Josselyn, S. A., Frankland, P. W., et al. (2012). Optical controlling reveals time-dependent roles for adult-born dentate granule cells. *Nat. Neurosci.* 15, 1700–1706. doi: 10.1038/nn.3260

Henneberger, C., Papouin, T., Oliet, S. H., and Rusakov, D. A. (2010). Long-term potentiation depends on release of D-serine from astrocytes. *Nature* 463, 232–236. doi: 10.1038/nature08673

Hodge, R. D., Kowalczyk, T. D., Wolf, S. A., Encinas, J. M., Rippey, C., Enikolopov, G., et al. (2008). Intermediate progenitors in adult hippocampal neurogenesis: tbr2 expression and coordinate regulation of neuronal output. *J. Neurosci.* 28, 3707–3717. doi: 10.1523/JNEUROSCI.4280-07.2008

Huang, X., Kong, H., Tang, M., Lu, M., Ding, J. H., and Hu, G. (2012). D-Serine regulates proliferation and neuronal differentiation of neural stem cells from postnatal mouse forebrain. *CNS Neurosci. Ther.* 18, 4–13. doi: 10.1111/j.1755-5949.2011.00276.x

Imayoshi, I., Sakamoto, M., Ohtsuka, T., Takao, K., Miyakawa, T., Yamaguchi, M., et al. (2008). Roles of continuous neurogenesis in the structural and functional integrity of the adult forebrain. *Nat. Neurosci.* 11, 1153–1161. doi: 10.1038/nn.2185

Kelsch, W., Li, Z., Eliava, M., Goengrich, C., and Monyer, H. (2012). GluN2B-containing NMDA receptors promote wiring of adult-born neurons into olfactory bulb circuits. *J. Neurosci.* 32, 12603–12611. doi: 10.1523/JNEUROSCI.1459-12.2012

Kempermann, G., Gast, D., Kronenberg, G., Yamaguchi, M., and Gage, F. H. (2003). Early determination and long-term persistence of adult-generated new neurons in the hippocampus of mice. *Development* 130, 391–399. doi: 10.1242/dev.00203

Kempermann, G., Kuhn, H. G., and Gage, F. H. (1997). More hippocampal neurons in adult mice living in an enriched environment. *Nature* 386, 493–495. doi: 10.1038/386493a0

Kempermann, G., Kuhn, H. G., and Gage, F. H. (1998). Experience-induced neurogenesis in the senescent dentate gyrus. *J. Neurosci.* 18, 3206–3212.

Kim, P. M., Duan, X., Huang, A. S., Liu, C. Y., Ming, G. L., Song, H., et al. (2010). Aspartate racemase, generating neuronal D-aspartate, regulates adult neurogenesis. *Proc. Natl. Acad. Sci. U.S.A.* 107, 3175–3179. doi: 10.1073/pnas.0914706107

Kreutzberg, G. W. (1996a). Microglia: a sensor for pathological events in the CNS. *Trends Neurosci.* 19, 312–318. doi: 10.1016/0166-2236(96)10049-7

Kreutzberg, G. W. (1996b). Principles of neuronal regeneration. *Acta Neurochir. Suppl.* 66, 103–106.

Kriegstein, A., and Alvarez-Buylla, A. (2009). The glial nature of embryonic and adult neural stem cells. *Annu. Rev. Neurosci.* 32, 149–184. doi: 10.1146/annurev.neuro.051508.135600

Krzisch, M., Sultan, S., Sandell, J., Demeter, K., Vutskits, L., and Toni, N. (2013). Propofol Anesthesia impairs the maturation and survival of adult-born hippocampal neurons. *Anesthesiology* 118, 602–610. doi: 10.1097/ALN.0b013e3182815948

Laplagne, D. A., Espósito, M. S., Piatti, V. C., Morgenstern, N. A., Zhao, C., Van Praag, H., et al. (2006). Functional convergence of neurons generated in the developing and adult hippocampus. *PLoS Biol.* 4:e409. doi: 10.1371/journal.pbio.0040409

Lee, E., and Son, H. (2009). Adult hippocampal neurogenesis and related neurotrophic factors. *BMB Rep.* 42, 239–244. doi: 10.5483/BMBRep.2009.42.5.239

Lemaire, V., Tronel, S., Montaron, M. F., Fabre, A., Dugast, E., and Abrous, D. N. (2012). Long-lasting plasticity of hippocampal adult-born neurons.

J. Neurosci. 32, 3101–3108. doi: 10.1523/JNEUROSCI.4731-11.2012

Li, G., Bien-Ly, N., Andrews-Zwilling, Y., Xu, Q., Bernardo, A., Ring, K., et al. (2009). GABAergic interneuron dysfunction impairs hippocampal neurogenesis in adult apolipoprotein E4 knockin mice. *Cell Stem Cell* 5, 634–645. doi: 10.1016/j.stem.2009.10.015

Lie, D. C., Colamarino, S. A., Song, H. J., Desire, L., Mira, H., Consiglio, A., et al. (2005). Wnt signalling regulates adult hippocampal neurogenesis. *Nature* 437, 1370–1375. doi: 10.1038/nature04108

Mandyam, C. D., Harburg, G. C., and Eisch, A. J. (2007). Determination of key aspects of precursor cell proliferation, cell cycle length and kinetics in the adult mouse subgranular zone. *Neuroscience* 146, 108–122. doi: 10.1016/j.neuroscience.2006.12.064

Martineau, M., Shi, T., Puyal, J., Knolhoff, A. M., Dulong, J., Gasnier, B., et al. (2013). Storage and uptake of D-serine into astrocytic synaptic-like vesicles specify gliotransmission. *J. Neurosci*. 33, 3413–3423. doi: 10.1523/JNEUROSCI.3497-12.2013

Massa, F., Koehl, M., Wiesner, T., Grosjean, N., Revest, J. M., Piazza, P. V., et al. (2011). Conditional reduction of adult neurogenesis impairs bidirectional hippocampal synaptic plasticity. *Proc. Natl. Acad. Sci. U.S.A*. 108, 6644–6649. doi: 10.1073/pnas.1016928108

Ming, G. L., and Song, H. (2011). Adult neurogenesis in the mammalian brain: significant answers and significant questions. *Neuron* 70, 687–702. doi: 10.1016/j.neuron.2011.05.001

Mothet, J. P., Parent, A. T., Wolosker, H., Brady, R. O., Jr., Linden, D. J., et al. (2000). D-serine is an endogenous ligand for the glycine site of the N-methyl-D-aspartate receptor. *Proc. Natl. Acad. Sci. U.S.A*. 97, 4926–4931. doi: 10.1073/pnas.97.9.4926

Mothet, J. P., Rouaud, E., Sinet, P. M., Potier, B., Jouvenceau, A., Dutar, P., et al. (2006). A critical role for the glial-derived neuromodulator D-serine in the age-related deficits of cellular mechanisms of learning and memory. *Aging Cell* 5, 267–274. doi: 10.1111/j.1474-9726.2006.00216.x

Nacher, J., Varea, E., Miguel Blasco-Ibanez, J., Gomez-Climent, M. A., Castillo-Gomez, E., Crespo, C., et al. (2007). N-methyl-d-aspartate receptor expression during adult neurogenesis in the rat dentate gyrus. *Neuroscience* 144, 855–864. doi: 10.1016/j.neuroscience.2006.10.021

Nolte, C., Matyash, M., Pivneva, T., Schipke, C. G., Ohlemeyer, C., Hanisch, U. K., et al. (2001). GFAP promoter-controlled EGFP-expressing transgenic mice: a tool to visualize astrocytes and astrogliosis in living brain tissue. *Glia* 33, 72–86.

Oliver, M. W., Kessler, M., Larson, J., Schottler, F., and Lynch, G. (1990). Glycine site associated with the NMDA receptor modulates long-term potentiation. *Synapse*. 5, 265–270. doi: 10.1002/syn.890050403

Pernot, P., Maucler, C., Tholance, Y., Vasylieva, N., Debilly, G., Pollegioni, L., et al. (2012). d-Serine diffusion through the blood-brain barrier: effect on d-serine compartmentalization and storage. *Neurochem. Int*. 60, 837–845. doi: 10.1016/j.neuint.2012.03.008

Platel, J. C., Dave, K. A., Gordon, V., Lacar, B., Rubio, M. E., and Bordey, A. (2010). NMDA receptors activated by subventricular zone astrocytic glutamate are critical for neuroblast survival prior to entering a synaptic network. *Neuron* 65, 859–872. doi: 10.1016/j.neuron.2010.03.009

Radzishevsky, I., Sason, H., and Wolosker, H. (2013). D-serine: physiology and pathology. *Curr. Opin. Clin. Nutr. Metab. Care* 16, 72–75. doi: 10.1097/MCO.0b013e32835a3466

Ray, J., and Gage, F. H. (2006). Differential properties of adult rat and mouse brain-derived neural stem/progenitor cells. *Mol. Cell. Neurosci*. 31, 560–573. doi: 10.1016/j.mcn.2005.11.010

Saxe, M. D., Battaglia, F., Wang, J. W., Malleret, G., David, D. J., Monckton, J. E., et al. (2006). Ablation of hippocampal neurogenesis impairs contextual fear conditioning and synaptic plasticity in the dentate gyrus. *Proc. Natl. Acad. Sci. U.S.A*. 103, 17501–17506. doi: 10.1073/pnas.0607207103

Schell, M. J., Molliver, M. E., and Snyder, S. H. (1995). D-serine, an endogenous synaptic modulator: localization to astrocytes and glutamate-stimulated release. *Proc. Natl. Acad. Sci. U.S.A*. 92, 3948–3952. doi: 10.1073/pnas.92.9.3948

Shihabuddin, L. S., Horner, P. J., Ray, J., and Gage, F. H. (2000). Adult spinal cord stem cells generate neurons after transplantation in the adult dentate gyrus. *J. Neurosci*. 20, 8727–8735.

Snyder, J. S., Glover, L. R., Sanzone, K. M., Kamhi, J. F., and Cameron, H. A. (2009). The effects of exercise and stress on the survival and maturation of adult-generated granule cells. *Hippocampus* 19, 898–906. doi: 10.1002/hipo.20552

Song, H., Stevens, C. F., and Gage, F. H. (2002). Astroglia induce neurogenesis from adult neural stem cells. *Nature* 417, 39–44. doi: 10.1038/417039a

Stone, S. S., Teixeira, C. M., Devito, L. M., Zaslavsky, K., Josselyn, S. A., Lozano, A. M., et al. (2011). Stimulation of entorhinal cortex promotes adult neurogenesis and facilitates spatial memory. *J. Neurosci*. 31, 13469–13484. doi: 10.1523/JNEUROSCI.3100-11.2011

Sultan, S., Gebara, E., and Toni, N. (2013). Doxycycline increases neurogenesis and reduces microglia in the adult hippocampus. *Front. Neurosci*. 7:131. doi: 10.3389/fnins.2013.00131

Sun, B., Halabisky, B., Zhou, Y., Palop, J. J., Yu, G., Mucke, L., et al. (2009). Imbalance between GABAergic and glutamatergic transmission impairs adult neurogenesis in an animal model of alzheimer's disease. *Cell Stem Cell* 5, 624–633. doi: 10.1016/j.stem.2009.10.003

Tashiro, A., Makino, H., and Gage, F. H. (2007). Experience-specific functional modification of the dentate gyrus through adult neurogenesis: a critical period during an immature stage. *J. Neurosci*. 27, 3252–3259. doi: 10.1523/JNEUROSCI.4941-06.2007

Tashiro, A., Sandler, V. M., Toni, N., Zhao, C., and Gage, F. H. (2006). NMDA-receptor-mediated, cell-specific integration of new neurons in adult dentate gyrus. *Nature* 442, 929–933. doi: 10.1038/nature05028

Taupin, P. (2007). BrdU immunohistochemistry for studying adult neurogenesis: paradigms, pitfalls, limitations, and validation. *Brain Res. Rev*. 53, 198–214. doi: 10.1016/j.brainresrev.2006.08.002

Thuret, S., Toni, N., Aigner, S., Yeo, G. W., and Gage, F. H. (2009). Hippocampus-dependent learning is associated with adult neurogenesis in MRL/MpJ mice. *Hippocampus* 19, 658–669. doi: 10.1002/hipo.20550

Toni, N., Laplagne, D. A., Zhao, C., Lombardi, G., Ribak, C. E., Gage, F. H., et al. (2008). Neurons born in the adult dentate gyrus form functional synapses with target cells. *Nat. Neurosci*. 11, 901–907. doi: 10.1038/nn.2156

Toni, N., and Sultan, S. (2011). Synapse formation on adult-born hippocampal neurons. *Eur. J. Neurosci*. 33, 1062–1068. doi: 10.1111/j.1460-9568.2011.07604.x

Toni, N., Teng, E. M., Bushong, E. A., Aimone, J. B., Zhao, C., Consiglio, A., et al. (2007). Synapse formation on neurons born in the adult hippocampus. *Nat. Neurosci*. 10, 727–734. doi: 10.1038/nn1908

Van Praag, H., Christie, B. R., Sejnowski, T. J., and Gage, F. H. (1999a). Running enhances neurogenesis, learning, and long-term potentiation in mice. *Proc. Natl. Acad. Sci. U.S.A*. 96, 13427–13431. doi: 10.1073/pnas.96.23.13427

Van Praag, H., Kempermann, G., and Gage, F. H. (1999b). Running increases cell proliferation and neurogenesis in the adult mouse dentate gyrus. *Nat. Neurosci*. 2, 266–270. doi: 10.1038/6368

Van Praag, H., Kempermann, G., and Gage, F. H. (2000). Neural consequences of environmental enrichment. *Nat. Rev. Neurosci*. 1, 191–198. doi: 10.1038/35044558

Van Praag, H., Schinder, A. F., Christie, B. R., Toni, N., Palmer, T. D., and Gage, F. H. (2002). Functional neurogenesis in the adult hippocampus. *Nature* 415, 1030–1034. doi: 10.1038/4151030a

Wagner, J. P., Black, I. B., and Dicicco-Bloom, E. (1999). Stimulation of neonatal and adult brain neurogenesis by subcutaneous injection of basic fibroblast growth factor. *J. Neurosci*. 19, 6006–6016.

Wake, K., Yamazaki, H., Hanzawa, S., Konno, R., Sakio, H., Niwa, A., et al. (2001). Exaggerated responses to chronic nociceptive stimuli and enhancement of N-methyl-D-aspartate receptor-mediated synaptic transmission in mutant mice lacking D-amino-acid oxidase. *Neurosci. Lett*. 297, 25–28. doi: 10.1016/S0304-3940(00)01658-X

Wang, L. P., Kempermann, G., and Kettenmann, H. (2005). A subpopulation of precursor cells in the mouse dentate gyrus receives synaptic GABAergic input. *Mol. Cell. Neurosci*. 29, 181–189. doi: 10.1016/j.mcn.2005.02.002

Watanabe, Y., Saito, H., and Abe, K. (1992). Effects of glycine and structurally related amino acids on generation of long-term potentiation in rat hippocampal slices. *Eur. J. Pharmacol*. 223, 179–184. doi: 10.1016/0014-2999(92)94837-L

Xie, X., Dumas, T., Tang, L., Brennan, T., Reeder, T., Thomas, W., et al. (2005). Lack of

the alanine-serine-cysteine transporter 1 causes tremors, seizures, and early postnatal death in mice. *Brain Res.* 1052, 212–221. doi: 10.1016/j.brainres.2005.06.039

Yamaguchi, M., Saito, H., Suzuki, M., and Mori, K. (2000). Visualization of neurogenesis in the central nervous system using nestin promoter-GFP transgenic mice. *Neuroreport* 11, 1991–1996. doi: 10.1097/00001756-200006260-00037

Yang, C. P., Gilley, J. A., Zhang, G., and Kernie, S. G. (2011). ApoE is required for maintenance of the dentate gyrus neural progenitor pool. *Development* 138, 4351–4362. doi: 10.1242/dev.065540

Yang, Y., Ge, W., Chen, Y., Zhang, Z., Shen, W., Wu, C., et al. (2003). Contribution of astrocytes to hippocampal long-term potentiation through release of D-serine. *Proc. Natl. Acad. Sci. U.S.A.* 100, 15194–15199. doi: 10.1073/pnas.2431073100

Yao, J., Mu, Y., and Gage, F. H. (2012). Neural stem cells: mechanisms and modeling. *Protein Cell* 3, 251–261. doi: 10.1007/s13238-012-2033-6

Zhao, C., Deng, W., and Gage, F. H. (2008). Mechanisms and functional implications of adult neurogenesis. *Cell* 132, 645–660. doi: 10.1016/j.cell.2008.01.033

Conflict of Interest Statement: The authors declare that the research was conducted in the absence of any commercial or financial relationships that could be construed as a potential conflict of interest.

Received: 03 June 2013; accepted: 12 August 2013; published online: 29 August 2013.

*Citation: Sultan S, Gebara EG, Moullec K and Toni N (2013) D-serine increases adult hippocampal neurogenesis. Front. Neurosci. **7**:155. doi: 10.3389/fnins.2013.00155*

This article was submitted to Neurogenesis, a section of the journal Frontiers in Neuroscience.

A6

Taurine increases hippocampal neurogenesis in aging mice

Stem Cell Research (2015) 14, 369–379

Available online at www.sciencedirect.com

ScienceDirect

www.elsevier.com/locate/scr

Taurine increases hippocampal neurogenesis in aging mice

Elias Gebara, Florian Udry, Sébastien Sultan, Nicolas Toni*

Department of Fundamental Neurosciences, University of Lausanne, 9 rue du Bugnon, 1005 Lausanne, Switzerland

Received 19 December 2014; received in revised form 31 March 2015; accepted 1 April 2015
Availabla online 10 April 2015

Abstract Aging is associated with increased inflammation and reduced hippocampal neurogenesis, which may in turn contribute to cognitive impairment. Taurine is a free amino acid found in numerous diets, with anti-inflammatory properties. Although abundant in the young brain, the decrease in taurine concentration with age may underlie reduced neurogenesis. Here, we assessed the effect of taurine on hippocampal neurogenesis in middle-aged mice. We found that taurine increased cell proliferation in the dentate gyrus through the activation of quiescent stem cells, resulting in increased number of stem cells and intermediate neural progenitors. Taurine had a direct effect on stem/progenitor cells proliferation, as observed *in vitro*, and also reduced activated microglia. Furthermore, taurine increased the survival of newborn neurons, resulting in a net increase in adult neurogenesis. Together, these results show that taurine increases several steps of adult neurogenesis and support a beneficial role of taurine on hippocampal neurogenesis in the context of brain aging.

Introduction

Neurogenesis persists during adulthood in the dentate gyrus (DG) of the hippocampus in most mammals (Altman & Das, 1965). Adult neural stem cells reside in the subgranular zone of the DG, where they give rise to intermediate progenitor cells. These progenitors proliferate rapidly to give rise to neurons, which migrate into the granule cell layer (Kronenberg et al., 2003). With their increased plasticity (Schmidt-Hieber et al., 2004), new neurons enhance synaptic plasticity in the hippocampus and participate to the mechanisms of learning and memory as well as mood control (Kheirbek et al., 2012). The age-dependent reduction in adult neurogenesis (Gebara et al., 2013; Kuhn et al., 1996; Encinas & Sierra, 2012) is associated with decreased learning performances (Gil-Mohapel et al., 2013), which can be restored by increasing adult neurogenesis with voluntary exercise (van Praag et al., 2005). Thus, manipulations aimed at increasing adult neurogenesis represent a promising approach for alleviating disease- or age-related cognitive impairment (Bolognin et al., 2014) as well as mood disorders (Drew & Hen, 2007). In this context, nutritional supplements acting on adult neurogenesis have been proposed as a beneficial approach to prevent or reduce age-related cognitive loss (van Praag et al., 2007).

Taurine is a free sulfur amino acid that is not incorporated in proteins. It is synthesized from methionine and cysteine by the rate-limiting enzyme cysteinesulfinic acid decarboxylase (CSD) that is found in the liver, the kidney and the brain,

* Corresponding author.
E-mail addresses: eliasgeorges.gebara@unil.ch (E. Gebara), florian.udry@fa2.ch (F. Udry), sebastien.sultan@unil.ch (S. Sultan), Nicolas.toni@unil.ch (N. Toni).

http://dx.doi.org/10.1016/j.scr.2015.04.001

where it is localized in glial cells (Ripps & Shen, 2012). In the liver, CSD activity is increased by protein-rich diet (Bella et al., 1999) whereas in the brain, glutamate increases CSD activity (Wu et al., 1998). Taurine is also found in high concentrations in numerous diets such as meat and seafood (Huxtable, 1992) and crosses the blood brain barrier using a specific beta amino acid transporter TAUT (TAUrine Transporter (Benrabh et al., 1995)). Taurine is 3–4 times more abundant in the developing than in the mature brain (Miller et al., 2000) and its concentration decreases with aging (Banay-Schwartz et al., 1989), suggesting that taurine plays a role during brain development. Consistent with this, dietary taurine deficiency during gestation leads to impaired development of the cerebellum and the visual cortex of newborn cats (Sturman et al., 1985). Intriguingly, taurine also seems to play a role in the adult and aging brain: Chronic administration of taurine in aged mice (El Idrissi, 2008; Neuwirth et al., 2013) or in a mouse model of Alzheimer's disease (Kim et al., 2014) increases hippocampus-dependent learning and retention and reduces anxiety and depression (Chen et al., 2004). The mechanisms by which taurine increases learning performances are unclear, but recent work showed that taurine increases the proliferation of adult neural stem/progenitor cells from the subventricular zone *in vitro* (Ramos-Mandujano et al., 2014; Hernandez-Benitez et al., 2012), suggesting that the effect of taurine may be mediated by an increase in adult neurogenesis. However, these studies did not address whether taurine increased net hippocampal neurogenesis *in vivo*.

Here, we directly assessed the effect of taurine on the age-related decline of adult hippocampal neurogenesis. To this aim, we tested the effect of taurine injections on 10-month-old mice, an age at which adult neurogenesis has reached its minimal activity (Kuhn et al., 1996; Gil-Mohapel et al., 2013). Using the incorporation of the proliferation marker 5-bromo-2-deoxyuridine (BrdU), combined with the genetic and immunohistochemical identification of adult hippocampal stem cells, intermediate progenitors, newborn mature and immature neurons, we examined the effect of taurine on several steps of the formation of new neurons in the aging hippocampus.

Methods

Ethics statement

This study was carried out in strict accordance with the recommendations in the Guidance for the Care and Use of Laboratory Animals of the National Institutes of Health. All experimental protocols were approved by the Swiss animal experimentation authorities (Service de la consommation et des affaires vétérinaires, Chemin des Boveresses 155, 1066 Epalinges, Switzerland). Every effort was made to minimize the number of animals used and their suffering.

Animals and taurine administration

Animals used for the study were male mice of 2, 4, 6, 8 and 10 months of age at the beginning of the experiments. C57Bl/6j mice were purchased from Janvier (le Genest Saint Isle, France), nestin-GFP mice were a kind gift from the laboratory of K. Mori (PRESTO, Kyoto, Japan) (Yamaguchi et al., 2000). These mice express the green fluorescent protein (GFP) under the stem cell-specific promoter nestin. All animals were housed in a 12 h light/12 h dark cycle with free access to food and water and controlled temperature (22 °C) conditions. Taurine was prepared fresh every day and diluted in water containing 0.9% NaCl. 10-month-old mice were injected intraperitoneally every day for 40 consecutive days either with 0.2 ml of taurine (265 mg/kg, Sigma-Aldrich) or with 0.2 ml of vehicle (0.9% NaCl in water) for control animals.

BrdU administration

Mice were injected intraperitoneally with 5-bromo-2-deoxyuridine (Sigma-Aldrich, Buchs, Switzerland) at a concentration of 100 mg/kg in saline, 3 times per day at 2-h intervals, for 3 days. For proliferation studies, taurine was injected for 40 days and BrdU injection started 24 h after the last taurine injection. Mice were then sacrificed 24 h after the last BrdU injection. For survival studies, BrdU was injected for 3 days and 24 h after the last BrdU injection, taurine was injected for 40 days. 24 h after the last taurine injection, mice were sacrificed and analyzed (Chen et al., 2004).

Tissue collection and preparation

At the end of the experiment, mice received a lethal dose of pentobarbital (10 ml/kg, Sigma-Aldrich, Buchs, Switzerland) and were perfusion-fixed with 50 ml of 0.9% saline followed by 100 ml of 4% paraformaldehyde (Sigma-Aldrich, Switzerland) dissolved in phosphate buffer saline (PBS 0.1 M, pH 7.4). Brains were then collected, postfixed overnight at 4 °C, cryoprotected 24 h in 30% sucrose and rapidly frozen. Coronal frozen sections of a thickness of 40 μm were cut with a microtome-cryostat (Leica MC 3050S) and slices were kept in cryoprotectant (30% ethylene glycol and 25% glycerin in 1× PBS) at −20 °C until processed for immunostaining.

Immunohistochemistry

Immunochemistry was performed as previously described (Gebara et al., 2013). Briefly, sections were washed 3 times in PBS 0.1 M. BrdU detection required formic acid pretreatment (formamide 50% in 2× SSC buffer; 2× SSC is 0.3 M NaCl and 0.03 M sodium citrate, pH 7.0) at 65 °C for 2 h followed by DNA denaturation for 30 min in 2 M HCl for 30 min at 37 °C and rinsed in 0.1 M borate buffer pH 8.5 for 10 min. Then, slices were incubated in blocking solution containing 0.3% Triton-X100 and 15% normal serum normal goat serum (Gibco, 16210-064) or normal donkey serum (Sigma Aldrich, D-9663), depending on the secondary antibody in PBS 0.1 M. Slices were then incubated 40 h at 4 °C with the following primary antibodies: mouse monoclonal anti-BrdU (48 h, 1:250, Chemicon International, Dietikon, Switzerland), goat anti-DCX (1:500, Santa Cruz Biotechnology, sc-8066), rabbit anti-Ki-67 (48 h, 1:200, Abcam, ab15580), rabbit anti-Tbr2 (1:200, Abcam, ab23345), goat anti-Iba1 (1:200, Abcam, ab5076), mouse anti-MHC-II (1:200, Abcam, ab23990) rabbit anti-GFAP (1:500, Invitrogen, 180063) mouse anti-Neu-N (Chemicon International 1:1000). The sections were then incubated for 2 h in either of the secondary antibodies: goat anti-mouse Alexa-594 (1:250, Invitrogen), goat anti-mouse Alexa-660

(1:250, Invitrogen), goat anti-rabbit 594 (1:250, Invitrogen), donkey anti-goat Alexa-555 (1:250, Invitrogen). After immunostaining, slices were incubated for 1 min into 4,6 diamidino-2-phenylindole (1:1000, DAPI) to reveal nuclei.

Cell culture

Adult neural progenitor cells (NPCs) were a kind gift from the laboratory of Fred Gage (Salk Institute, San Diego, USA). They were isolated from the DG of adult Fisher 344 rats and cultured as previously described (Palmer et al., 1997) at a density of 20,000 cells per well. Three wells per condition were used and experiments were replicated 3 times. Twenty-four hours after plating, the medium was supplemented with 10 mM taurine (Sigma-Aldrich) every day, for 7 days (Hernandez-Benitez et al., 2012). On the eighth day, medium was supplemented with 5 μM BrdU for 30 min then washed and fixed with 4% paraformaldehyde for 20 min, briefly washed, immunostained for BrdU and mounted.

Image analysis

All images were acquired using a Zeiss confocal microscope (Zeiss LSM 710 Quasar Carl Zeiss, Oberkochen, Germany). The total numbers of immunoreactive cells throughout the entire granule cell layer were estimated using stereological sampling, as previously described (Thuret et al., 2009), between −1.3 and −2.9 mm from the Bregma. However, no guard zones were used, which may lead to possible bias in the counting of cells at the edge of each section, spread across control and taurine groups. For each animal, a 1-in-6 series of sections was stained with the nucleus marker DAPI and used to measure the volume of the granule cell layer. The granule cell area was traced using Axiovision (Zeiss, Germany) software and the granule cell volume was determined by multiplying the traced granule cell layer area by the thickness of the corresponding section and the distance between the sections sampled (240 μm). For all the mice analyzed in this study, no difference was found between taurine-treated and control animals in the volume of the granule cell layer. All cells were counted blind with regard to the mouse status. The total number of immunolabeled cells were counted in the entire thickness of the sections in a 1-in-6 series of section (240 μm apart), for a total of 8 sections, with a 40× objective. The number of cells was then related to granule cell layer sectional volume and multiplied by the reference volume to estimate the total number of immunolabeled cells (Gebara et al., 2013; Thuret et al., 2009). Cells expressing BrdU, Ki-67, DCX or Tbr2 were counted in the granule cell layer and the subgranular zone, whereas cells expressing Iba-1 (microglia), MHC II and cells expressing GFAP with a prototypical stellar astrocyte morphology were counted in the whole dentate gyrus, as these cell types are scarce in the granule cell layer. BrdU colocalization with the neuronal marker NeuN was analyzed on confocal microscope image stacks and was confirmed on single optical sections, for 52–70 cells per animal. The proportion of double-labeled cells was then obtained for each animal and then averaged for each group (Gebara et al., 2013). 3D reconstructions were performed using Imaris 7.6.1 (Bitplane, South Windsor, CT, USA).

For *in vitro* cell quantification, images were acquired using confocal microscopy. The number of BrdU labeled NPCs was counted in 4 selected fields, systematically placed in the same position relative to the coverslips' edges. The number of BrdU labeled NPCs was reported to the total number of NPCs in each selected field to obtain a percentage of proliferation in each condition.

Statistical analysis

Hypothesis testing was two-tailed. All analyses were performed using JMP10 software. First, Shapiro–Wilk tests were performed on each group of data to test for distribution normality. For normal distribution, the equality of variances of the groups was tested and a bilateral Student t-test was performed. For non-normal distribution, we performed the Wilcoxon test. Data are presented as mean ± SEM.

Results

Taurine increased stem cell proliferation in the DG

We first examined the effect of taurine on cell proliferation in the DG. Ten-month-old nestin-GFP mice were injected daily for 40 days with either taurine (i.p. 265 mg/kg), or with the same volume (0.2 ml) of vehicle (0.9% NaCl) as control. This regimen has previously been shown to reduce inflammation (Yamaguchi et al., 2000) and the inflammation-induced inhibition of adult hippocampal neurogenesis (Palmer et al., 1997). Nestin-GFP mice express the GFP reporter under the control of the stem cell-specific nestin promoter thereby enabling the identification of adult neural stem cells (Kim et al., 2014). Twenty-four hours after the last taurine injection, all mice received 3 injections per day at 2-h intervals for 3 days of the synthetic thymidine analog 5-bromo-2-deoxyuridine (BrdU, i.p., 100 mg/kg) and were sacrificed 24 h after the last BrdU injection (Fig. 1A). Mice were perfused, the brains collected, sectioned and immunostained for BrdU and the endogenous proliferation marker Ki-67. The total number of immunoreactive cells was counted in the granule cell layer (GCL) and the subgranular zone of the DG. Taurine significantly increased the number of BrdU-expressing cells (Fig. 1B–C, bilateral Student's t-test $p < 0.001$) and the number of Ki-67-expressing cells (Fig. 1D–E, bilateral Student's t-test $p < 0.001$). To test whether the increased number of BrdU- or Ki-67-expressing cells could be caused by a change in hippocampal volume upon taurine treatment, we measured the volume of the GCL of all mice. There was no difference between groups (controls: 0.17 ± 0.08 mm^3; Taurine: 0.17 ± 0.07 mm^3, n = 5, bilateral Student's t-test $p = 0.26$). These results indicate that taurine increased cell proliferation in the subgranular zone of the DG.

We next identified the cell types contributing to the taurine-induced increase in cell proliferation, using immunohistochemistry and morphology. Two main types of proliferative cells co-exist in the subgranular zone: The radial glia-like (RGL), nestin-expressing stem cells, readily identifiable by their morphology consisting of a nucleus located in the subgranular zone, a large process extending through the GCL and branching into the proximal part of the molecular layer; and the intermediate neural progenitor cells, with short

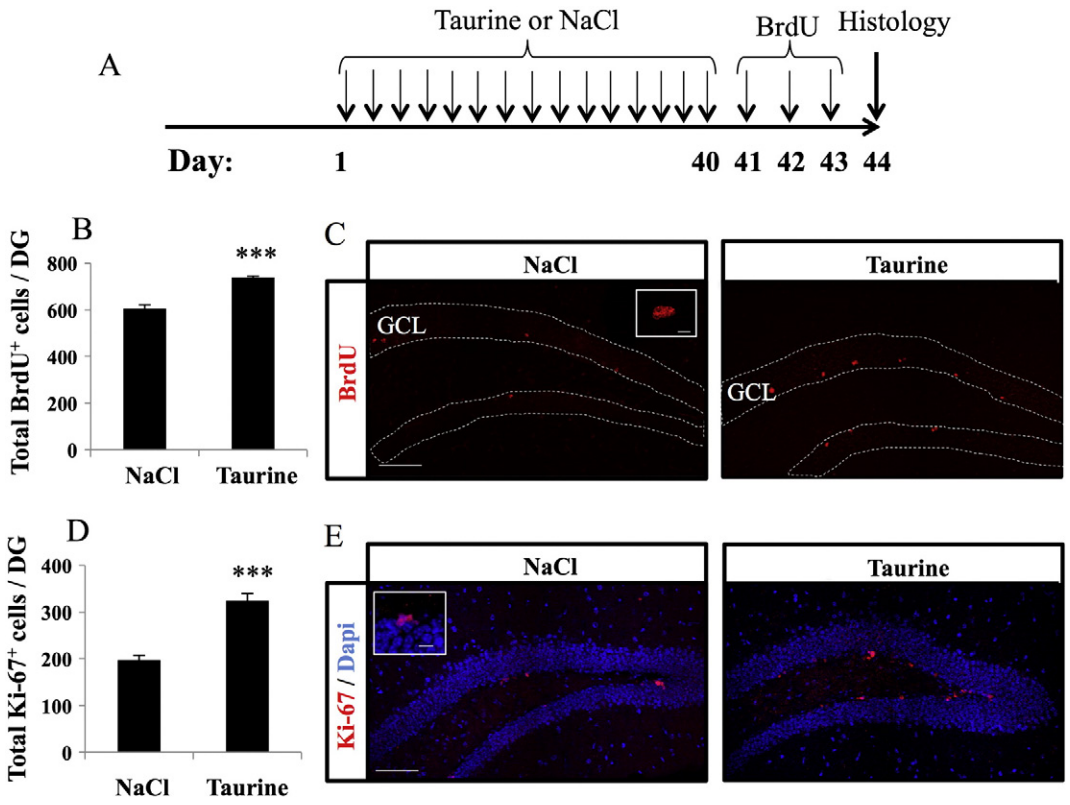

Figure 1 Taurine increased cell proliferation in the DG. (A) Experimental timeline: Mice were injected with taurine or vehicle (NaCl) for 40 days, followed immediately by 3 BrdU (5-bromo-2-deoxyuridine) injections per day for 3 days. Twenty-four hours after the last injection, brain slices were processed for histology. (B) Histogram of the total number of BrdU-immunopositive cells in the granule cell layer of the DG. (C) Confocal maximal projection micrographs of hippocampal sections immunostained for BrdU. Inset: Higher magnification confocal micrograph of a BrdU-positive cell. (D) Histogram of the total number of Ki-67-expressing cells in the GCL of the DG. (E) Confocal maximal projection micrographs of hippocampal sections immunostained for Ki-67. Inset: Higher magnification confocal micrograph of a Ki-67 expressing cell. Blue: Dapi staining. Animals, n = 5 per group. Scale bars: 100 μm, insets 10 μm, bilateral Student's t-test ***$p < 0.001$. Each value represents the mean ± SEM.

processes extending into subgranular zone/GCL area. Both cell types express the T-box brain gene-2 transcription factor (Tbr2 (Hodge et al., 2008)), but they can be differentiated by their distinct morphology. Taurine increased the number of RGL stem cells in the subgranular zone of the DG as compared to NaCl (Fig. 2A–B, bilateral Student's t-test $p < 0.001$). To test whether taurine increased the division of RGL stem cells, mitigated the age-related reduction in RGL stem cells number or both, we measured RGL stem cell number at 2, 4, 6, 8 and 10 months of age. Consistent with previous reports (Encinas et al., 2011; Walter et al., 2011; Bonaguidi et al., 2011), RGL stem cells' number decreased over time and reached its minima at 8 months (Fig. 2C). There was no significant difference between 8 months and NaCl-treated animals (*i.e.* 11.5 months, $p = 0.42$). In stark contrast, taurine treatment on 10 month-old mice restored the number of RGL stem cells to values found in 2-months-old mice (bilateral Student's t-test $p = 0.22$). This effect may be mediated by the proliferation of RGL stem cells, since taurine increased the percentage of BrdU-expressing RGL stem cells (Fig. 2D-E, bilateral Student's t-test $p < 0.05$). Taurine also significantly increased the total number of Tbr2-expressing cells (Fig. 2F–G, bilateral Student's t-test $p < 0.01$), but did not increase the proportion of Tbr2-expressing cells that incorporated BrdU (Fig. 2b H–I, bilateral Student's t-test $p = 0.6$). These results suggest that taurine increased the proliferation of RGL stem cells, resulting in an increase of both RGL stem cells and Tbr2$^+$ progenitor cells populations.

Taurine increased the number of immature neurons

The increased number of Tbr2$^+$ progenitors may result in increased neuronal production. We next examined the effect of taurine on immature new neurons, identified by the expression of the immature neuronal marker doublecortin (DCX). Taurine increased the total number of DCX-immunostained neuronal soma in the subgranular zone/GCL (Fig. 3A–B, bilateral Student's t-test $p < 0.001$). Furthermore, upon taurine treatment, immature neurons displayed increased proportion of dendritic branches extending into the molecular layer, suggesting increased maturation (Fig. 3C–D, Bilateral Student's t-test for 125 μm from the GCL: $p < 0.05$). To further investigate the effect of taurine on new neurons' maturation, we quantified the three categories of DCX-expressing cells (Seri et al., 2004): cells without process, known to be the most immature subtype with the highest proliferative activity, cells with horizontal processes and cells with a radial process,

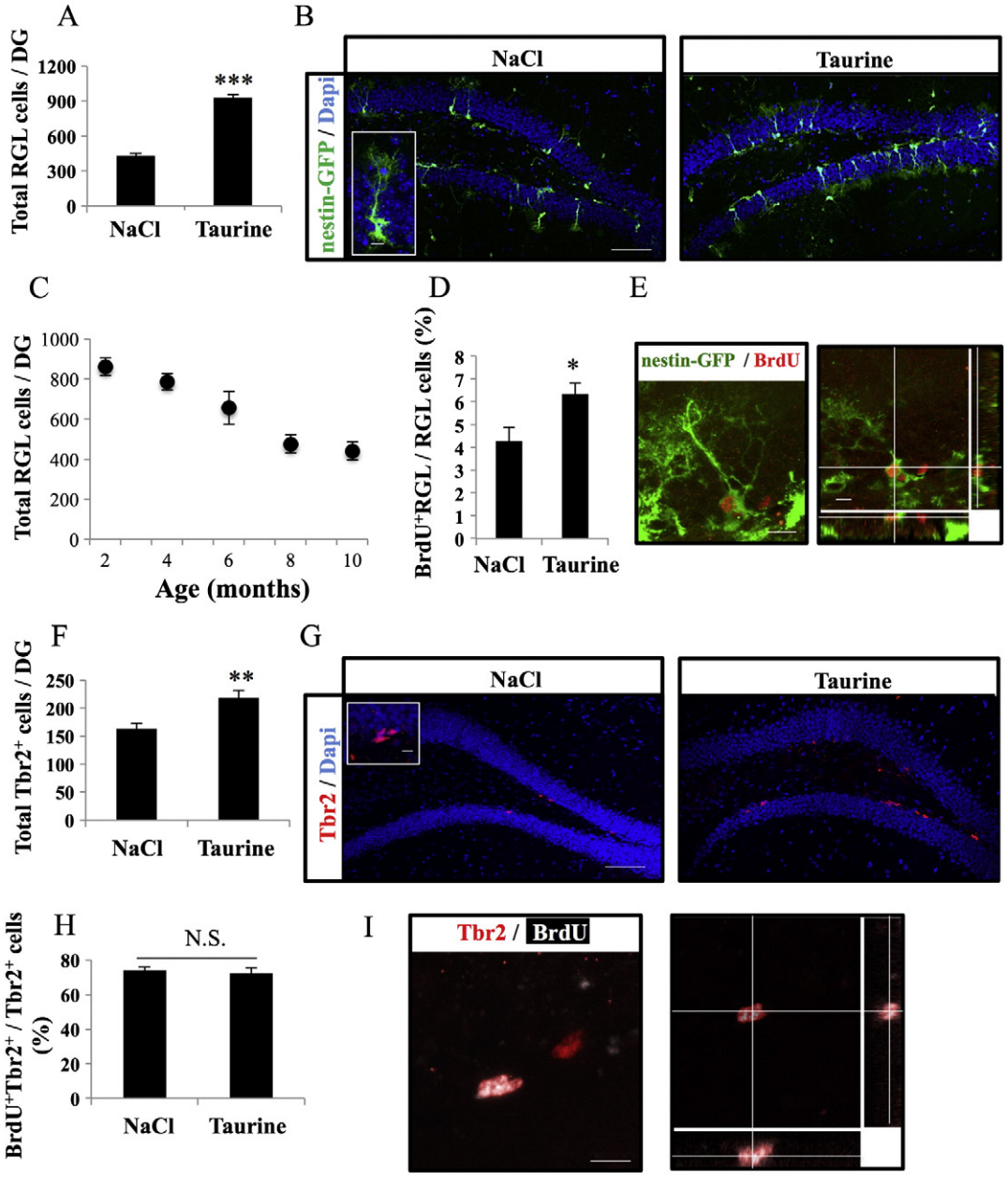

Figure 2 Taurine increased the proliferation of RGL stem cells. (A) Quantification of the total number of nestin-GFP stem cells with RGL (radial glia-like) morphology in the subgranular zone of the DG. (B) Confocal maximal projection micrographs of hippocampal sections of nestin-GFP mice. Inset: Higher magnification confocal micrograph of a GFP-expressing RGL stem cell. Scale bars: 100 μm, inset 10 μm. (C) Time course of the total number of RGL in 2, 4, 6, 8 and 10 month old mice. (D) Histogram showing the percentage of BrdU-immunostained RGL stem cells over the total number of RGL cells. (E) Left panel: Confocal micrograph of a hippocampal section (maximal projection) immunostained for BrdU (red) and GFP (green). Scale bar: 10 μm. Right panel: Orthogonal projections of the same RGL stem cell. (F) Histogram of the total number of Tbr2-expressing intermediate progenitor cells in the GCL of the DG. (G) Confocal maximal projection micrographs of hippocampal sections immunostained for Tbr2. Inset: Higher magnification confocal micrograph of a Tbr2-expressing cell. Blue: Dapi staining. Scale bars: 100 μm, inset 10 μm. (H) Histogram of the percentage of $BrdU^+$ $Tbr2^+$ cells over the total number of $Tbr2^+$ cells. (I) Left panel: Confocal micrograph of a hippocampal section (maximal projection) immunostained for Tbr2 (red) and BrdU (white). Scale bar: 10 μm. Right panel: Orthogonal projections of a $BrdU^+$ $Tbr2^+$-immunolabeled cell. Animals, n = 5 per group. Bilateral Student's t-test N.S.: $p > 0.05$ *$p < 0.05$ **$p < 0.01$ ***$p < 0.001$. Each value represents the mean ± SEM.

representing the most mature phenotype (Fig. 3E). Taurine significantly increased the proportion of DCX-expressing cells with a process (Student's t-test: $p < 0.001$), an effect that was almost entirely due to an increase in cells with a radial process (Fig. 3F, Student's t-test: $p < 0.001$). All together, these results suggest that taurine increased the number of new, immature

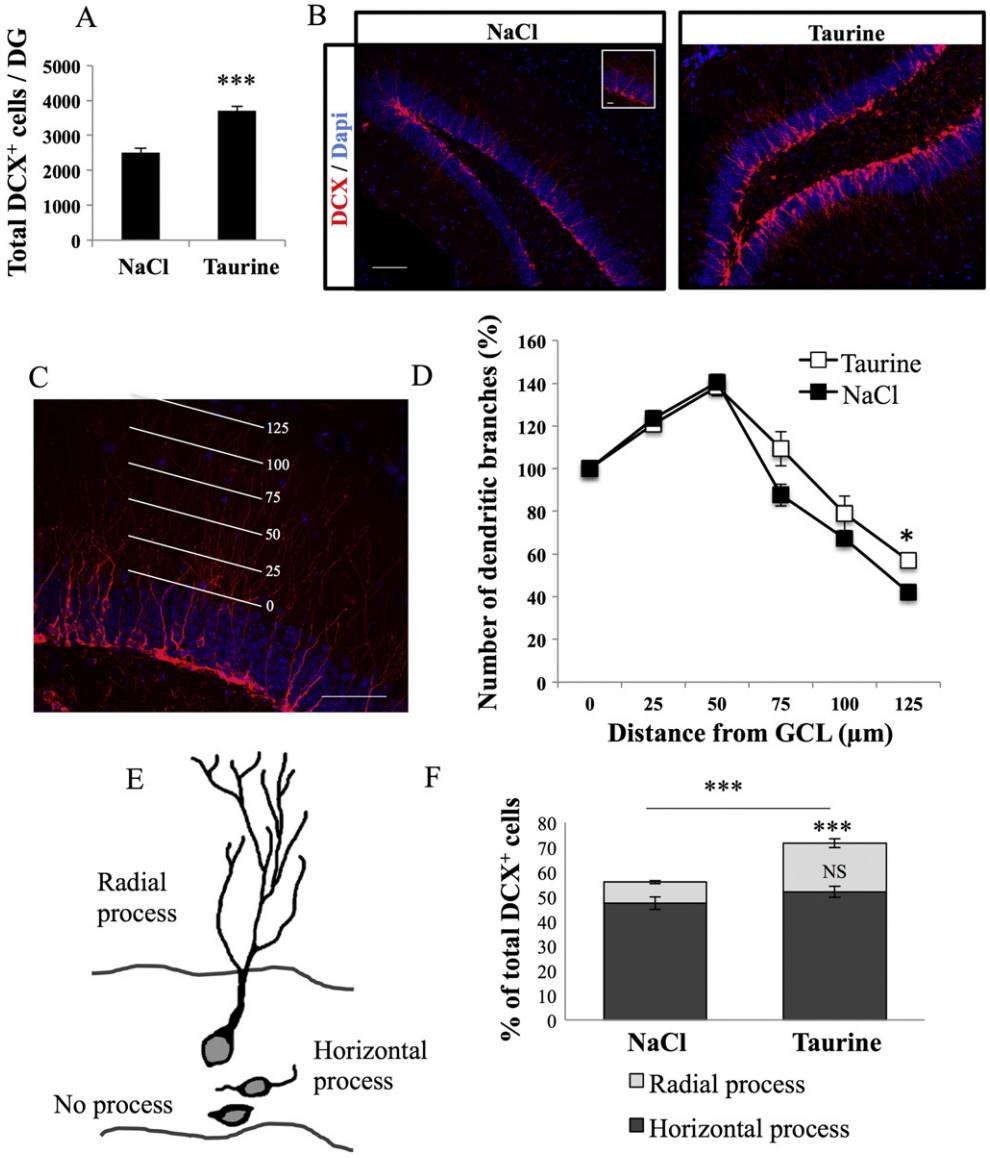

Figure 3 Taurine increased the number of immature neurons. (A) Histogram of the number of DCX^+ cells in the GCL of the DG. (B) Confocal maximal projection micrographs of hippocampal sections immunostained for DCX. Inset: Higher magnification confocal micrograph of a DCX-positive cell. Dapi staining. Scale bars: 100 μm, insets 10 μm. (C) Confocal micrograph of DCX^+ cells, extending dendrites in the molecular layer. Scale bar: 100 μm. (D) The number of dendritic branches crossing each white bar (shown in C) was counted and normalized to the value measured at 0 μm, to account for the increased number of cells. (E) Schematic illustration of the three subtypes of DCX expressing cells, based on the presence and orientation of their processes. (F) Histogram showing the proportion of DCX expressing cells without process, with a radial or a horizontal process in NaCl and taurine-treated animals. Animals, n = 5 per group. Bilateral Student's t-test N.S.: $p > 0.05$ *$p < 0.05$ ***$p < 0.001$. Each value represents the mean ± SEM.

neurons and increased the proportion of cells with mature morphological characteristics.

Taurine increased neurogenesis

We next examined the effect of taurine on the fate of newly-divided cells. Ten-month-old C57Bl/6 mice were injected with BrdU for 3 days (i.p., 100 mg/kg, 3 injections per day at 2-h intervals) and 24 h after the last injection, were treated with daily injections of taurine for 40 days. Owing to the short half-life of BrdU (11 min (Taupin, 2007)), this protocol ensures that BrdU is not incorporated into cells after 24 h (Sultan et al., 2013a). One day after the last taurine injection, mice were sacrificed, the brains removed, sliced and immunostained against BrdU and the mature neuronal marker Neu-N (Fig. 4A). The number of BrdU-labeled cells was significantly increased by 66% in taurine-injected animals (Fig. 4B bilateral Student's t-test $p < 0.05$). BrdU can be retained in daughter cells after several divisions. Since taurine increased proliferation by 22% (Fig. 1B), the effect observed here is consistent with an increase in both proliferation and survival of the new cells.

We then assessed the neuronal differentiation of newborn cells into neuronal lineage by measuring the proportion of BrdU-labeled cells that also expressed NeuN (Fig. 4C–E). In taurine-treated mice, neurons accounted for 85 ± 8% of the surviving BrdU-positive cells as compared to 60.5 ± 10% in NaCl mice. This difference was however not significant (Wilcoxon test, $p = 0.07$, Fig. 4C), indicating that taurine did not significantly increase neuronal differentiation. Nonetheless, when the number of surviving cells was multiplied by the fraction of cells that differentiated into neurons, taurine-treated mice had about 128% more newly-formed neurons than vehicle-treated mice (Fig. 4D, bilateral Student's t-test $p < 0.01$). Thus taurine increased net adult neurogenesis.

Taurine decreased microglia

Taurine is known to have anti-inflammatory properties (Menzie et al., 2013; Kim & Cha, 2014) and we recently found that the number of microglia in the dentate gyrus is inversely correlated with the proliferation of stem/progenitor cells in aged mice (Gebara et al., 2013). To test the effect of taurine on microglia in the DG, we examined microglia using immunostaining against the microglia-specific marker Iba1 (Fig. 5). Taurine significantly decreased the total number of Iba1-expressing microglia in the DG (Fig. 5A–B, bilateral Student's t-test $p < 0.001$), but did not affect the number of GFAP-immunolabeled astrocytes (Supplementary Fig. 1, bilateral Student's t-test $p = 0.57$), indicating that the effect of taurine was specific for microglia. Brain inflammation results in morphological changes of microglia upon activation: Resting microglia (stage I) have rod-shaped cell bodies with fine, ramified processes whereas activated microglia (stage II) have elongated cell bodies with long thick processes (Fig. 5C) (Mathieu et al., 2010; Preissler et al., 2015; Streit et al., 1999). We therefore examined the morphology of microglia in taurine-treated and control animals. Taurine decreased the soma area (Fig. 5D, bilateral Student's t-test $p < 0.001$), increased the territory projection area (Fig. 5E, bilateral Student's t-test $p < 0.001$) and the number of branches (Fig. 5F, bilateral Student's t-test $p < 0.001$) of microglia.

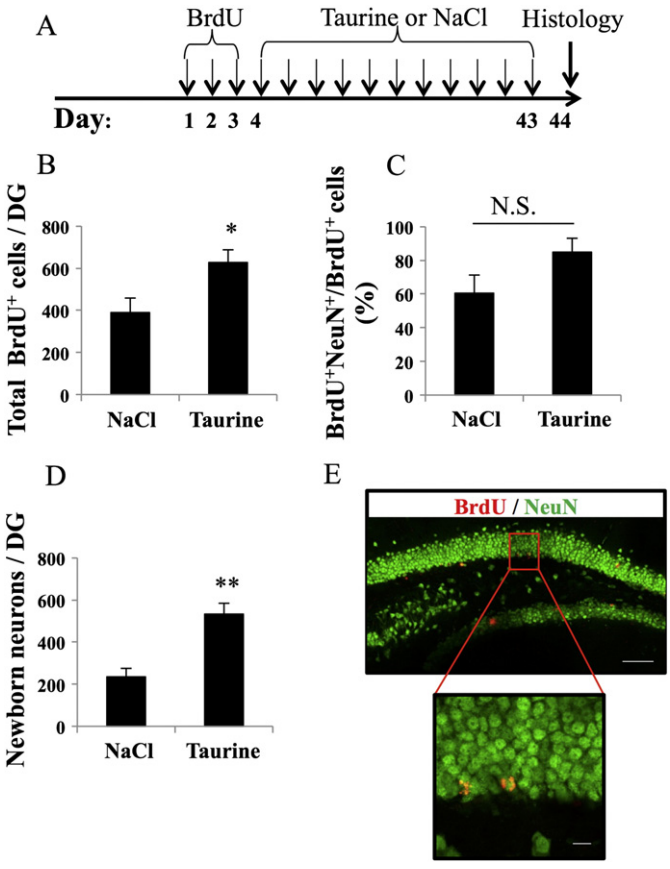

Figure 4 Taurine increased the survival of new-born neurons. (A) Experimental timeline: Mice were injected with BrdU 3 times a day for 3 days. 24 h after the last BrdU injection, mice were injected with taurine or NaCl (n = 5 mice per group) daily for 40 days. 24 h after the last taurine injection, mice were sacrificed and their brains processed for histology (B) Histogram showing the total number of BrdU-expressing cells. (C) Histogram showing the percentage of $BrdU^+$ $NeuN^+$ new neurons over the total number of $BrdU^+$ cells. Wilcoxon test N.S.: $p = 0.07$ (D) Histogram of the total number of new, $BrdU^+$ newborn neurons. (E) Upper panel: confocal micrograph of a hippocampal section immunostained for BrdU (red) and NeuN (green). Lower panel. Higher magnification micrograph of BrdU-NeuN expressing cells. Scale bar: 100 μm, inset 10 μm. For the NeuN–BrdU co-localization study, we analyzed 3 animals per group and 52–70 cells per animal. Bilateral Student's t-test: $^*p < 0.05$, $^{**}p < 0.01$. Each value represents the mean ± SEM.

These morphological modifications are consistent with a decreased activation state of microglia upon taurine treatment. Consistently, activated microglial cells accounted for 8.2 ± 0.75% of the total number of microglia in taurine-treated animals and for 37.8 ± 1.8% in NaCl-treated animals (bilateral Student's t-test $p < 0.001$). Finally, the expression of the activated microglia marker MHC-II (Frank et al., 2006) was significantly reduced in the DG of taurine-treated mice (Fig. 5G–H, bilateral Student's t-test $p < 0.001$). Thus, consistently with previous studies (Menzie et al., 2013; Kim & Cha, 2014; Kim & Kim, 2005; Chan et al., 2014) these results suggest that taurine decreased microglia number.

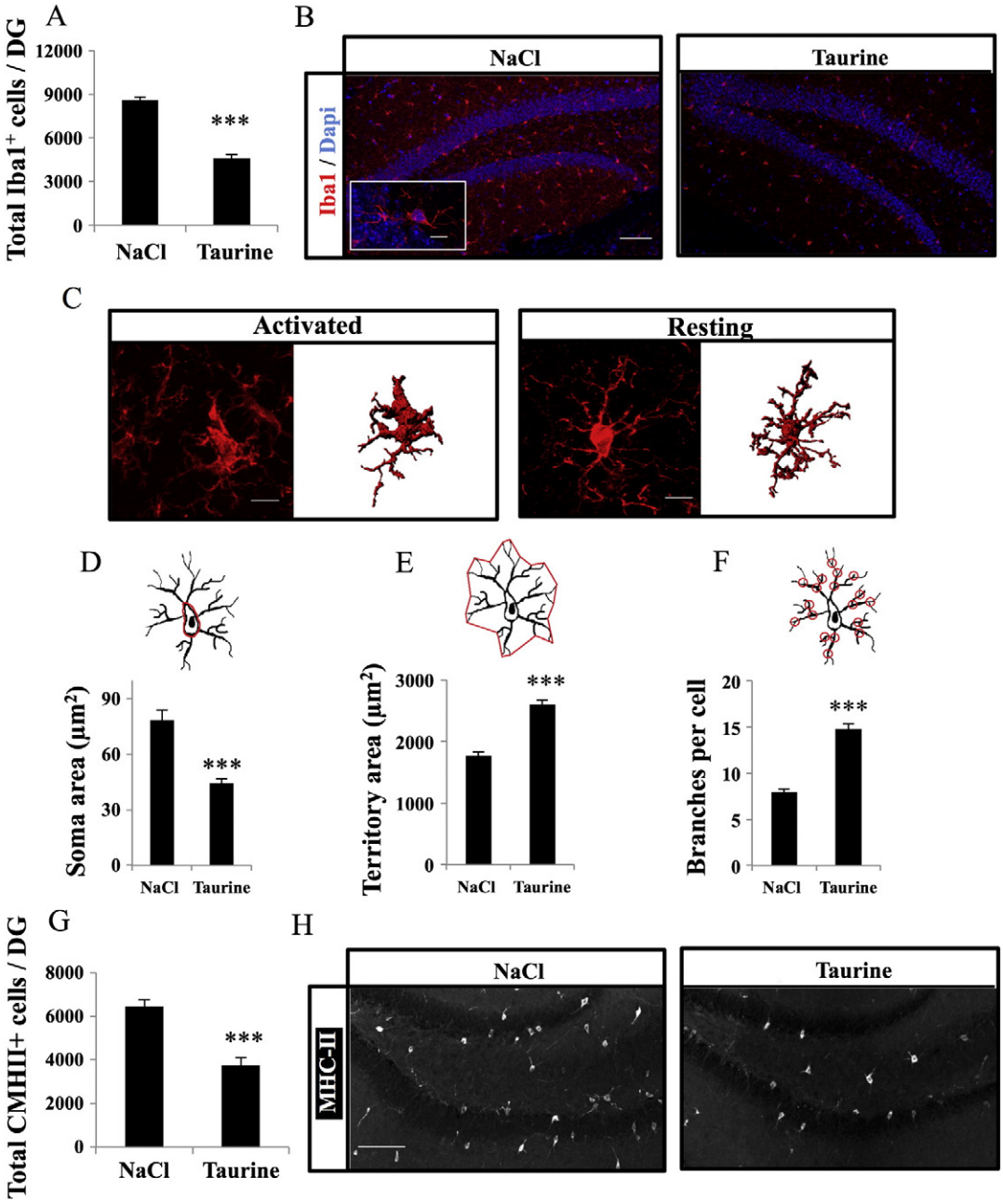

Figure 5 Taurine decreased microglia number and markers of microglia activation. (A) Histogram showing the total number of Iba1-expressing cells in the DG. (B) Confocal micrographs (maximal projections) of hippocampal sections immunostained for Iba1. Inset: Higher magnification confocal micrograph of an Iba1-immunolabeled cell. (C) Confocal micrographs and 3D reconstruction of microglia in activated (left) and resting state (right). (D) Drawing (upper panel) and histogram (lower panel) showing the soma area of microglia. (E) Drawing and histogram showing the territory area of microglia. (F) Drawing and histogram showing the number of branches per microglia. (G) Histogram showing the total number of MHC-II-expressing microglia in the DG. (H) Confocal micrographs (maximal projections) of hippocampal sections immunostained for MHC-II. Blue: Dapi staining. Animals: n = 5 per group. Scale bars: 100 µm, inset 10 µm. Bilateral Student's t-test ***$p < 0.001$. Each value represents the mean ± SEM.

Taurine increased the proliferation of neural stem/progenitor cells in vitro

Finally, we examined whether taurine may have a direct effect on stem/progenitor cells. For this, we performed *in vitro* experiments on purified adult hippocampal stem/progenitor cells (NPCs). 20,000 NPCs per well were plated and treated everyday with either 10 mM taurine or the equivalent volume of PBS 0.1 M for half an hour. After 7 days, the medium was supplemented with 5 μM BrdU for 30 min then washed and immediately fixed and immunostained for BrdU (Hernandez-Benitez et al., 2012). Taurine increased the proportion of NPCs that incorporated BrdU (Fig. 6A–B, Student's t-test, $p < 0.01$), indicating that taurine directly increased the proliferation of NPCs.

Discussion

In the present study, we tested the effect of chronic administration of taurine on hippocampal neurogenesis in aging mice. We found that taurine increased cell proliferation in the DG. More specifically, RGL stem cells showed enhanced proliferation that resulted in an increase in the number of RGL stem cells, $Tbr2^+$ intermediate progenitors and DCX^+ immature neurons. Moreover, taurine increased the survival of new neurons, resulting in a net increase in adult neurogenesis. Taurine also a reduced microglia number, morphological parameters associated with activation, MHC-II expression and increased stem/progenitor cell proliferation *in vitro*. Together, these results indicate that, in the aging brain, taurine increases the production of new neurons by stimulating several steps of adult neurogenesis and plays a role in microglia function.

Taurine is known to be involved in variety of cellular processes, including calcium homeostasis (El Idrissi, 2008; Wu et al., 2005; Foos & Wu, 2002), protection from glutamate excitotoxicity and apoptosis (Foos & Wu, 2002; Leon et al., 2009), inflammation (Kim & Cha, 2014), oxidative stress (Menzie et al., 2013), and epilepsy (El Idrissi et al., 2003), all of which contribute to the regulation of adult neurogenesis. However, since there is currently no known taurine receptor, its role as an osmolyte is believed to participate to these processes. Our results suggest that taurine can regulate adult neurogenesis both through an indirect effect on microglia and a direct effect on stem/progenitor cells.

The indirect effect of taurine on adult neurogenesis may be mediated by its anti-inflammatory properties: taurine reduces the production of inflammatory cytokines such as TNFα or IL-1β (Kim & Cha, 2014) and its derivative, taurine-chloramine, reduces the activation of NFkb in several models of inflammation (Kim & Kim, 2005). In the brain, taurine administration reduces cell damage and cytokines expression after traumatic brain injury (Chan et al., 2014) and mitigates lipopolysaccharide-induced inflammation and microglia activation (Menzie et al., 2013). In physiological conditions, brain aging is accompanied by increased expression of genes involved in cellular stress and inflammation (Sturman et al., 1985) and increased microglia proliferation and activity (Kohman, 2012). In turn, this increased inflammation negatively correlates with hippocampal RGL stem cells proliferation (Gebara et al., 2013). Thus, the increased inflammation in the aging brain inhibits hippocampal neurogenesis and conversely, anti-inflammatory treatments that reduce microglia activation, increase adult neurogenesis (Gebara et al., 2013; Sultan et al., 2013b). Consistent with these observations, taurine partially restores cell proliferation in the DG after lipopolysaccharide-induced inflammation (Menzie et al., 2013). Altogether, these results suggest that the effect of taurine on adult neurogenesis that we observed in the aging brain may be, at least partially, mediated by a reduction in microglia activation. Although we did not directly measure levels of inflammatory cytokines in this study, this possibility is consistent with our observations of decreased microglia number, reduced morphological markers that are normally associated with activation and reduced MHC-II expression upon taurine treatment.

In addition to its indirect effect, taurine directly increased the proliferation of purified adult hippocampal stem/progenitor cells *in vitro*, similarly to what was previously observed on subventricular zone progenitors (Ramos-Mandujano et al., 2014). The antioxidant (Schaffer et al., 2009) and antiapoptotic properties of taurine (Taupin, 2007; Sultan et al., 2013a), can potentially contribute to the increased proliferation and survival rate of the highly proliferative and metabolically active neural stem cells and new neurons. Of particular interest, taurine has recently been shown to interact with the polyamine site of the NMDA receptor and modulate the activity of the NMDA receptor (Chan et al., 2014). NMDA receptors are expressed by RGL stem cells and regulate their activity (Muth-Kohne et al., 2010), as demonstrated by the increased proliferation induced

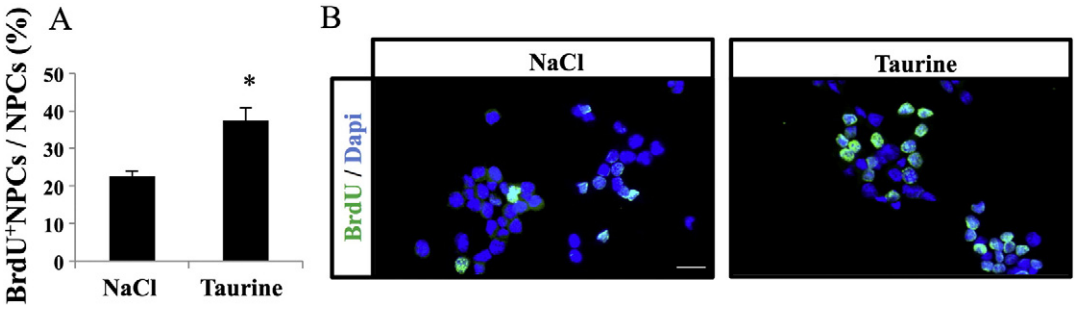

Figure 6 Taurine increased the proliferation of adult hippocampal stem/progenitor cells (NPCs) *in vitro*. (A) Histogram showing the percentage of NPCs immunostained for BrdU over the total number of NPCs. (B) Confocal micrographs of NPCs treated with NaCl (left panel) or taurine (right panel). n = 3 culture wells per group. *$p < 0.05$. Each value represents the mean ± SEM. Scale bar: 20 μm.

by the NMDA receptor antagonists memantine or MK-801 (Namba et al., 2009), and the co-agonist D-serine (Sultan et al., 2013a). NMDA receptors are also expressed on immature adult-born hippocampal neurons and are required for the survival of these cells (Tashiro et al., 2006). Thus, by directly modulating NMDA receptor activity on RGL stem cells and on immature neurons, taurine may increase the proliferation of the former and the survival of the latter and thereby contribute to the increased neurogenesis we observed. Endogenous taurine is released by astrocytes (Choe et al., 2012) and may contribute to the regulation of adult neurogenesis by the microenvironment. With age, the dysregulation of the neurogenic niche (Bernal & Peterson, 2011; Katsimpardi et al., 2014) may involve a reduction of astrocytic function, leading to reduced taurine production, thereby causing age-related impaired neurogenesis.

Reduced adult neurogenesis contributes to age-related cognitive impairment and several therapeutic approaches for stroke or neurodegenerative disorders target adult neurogenesis. The renewal of stem cells in the adult brain being limited (Calzolari et al., 2015), approaches that increase the stem cell pool may yield a more promising outcome for restoring neurogenesis in the aged brain, than targeting later stages of the process. In light of our results, the potent activating effect of taurine on RGL stem cells may underlie its beneficial cognitive effects and may represent a promising approach for the treatment of age-related reduction in adult neurogenesis and cognition.

Supplementary data to this article can be found online at http://dx.doi.org/10.1016/j.scr.2015.04.001.

Author contribution

E.G., F.U., S.S. and N.T. designed the experiment. E.G., F.U. and S.S. performed the experiments and analyzed the data. E.G., F.U. and N.T. prepared the manuscript, N.T. provided financial support.

Acknowledgments

The authors wish to thank Jacqueline Kocher-Braissant for technical help. Images acquisition was performed at the Cellular Imaging Facility of the University of Lausanne (Switzerland). This work was supported by the Swiss National Science Foundation and the Synapsis foundation.

References

Altman, J., Das, G.D., 1965. Post-natal origin of microneurones in the rat brain. Nature 207, 953–956.

Banay-Schwartz, M., Lajtha, A., Palkovits, M., 1989. Changes with aging in the levels of amino acids in rat CNS structural elements. II. Taurine and small neutral amino acids. Neurochem. Res. 14, 563–570.

Bella, D.L., Hirschberger, L.L., Hosokawa, Y., Stipanuk, M.H., 1999. Mechanisms involved in the regulation of key enzymes of cysteine metabolism in rat liver in vivo. Am. J. Physiol. 276, E326–335.

Benrabh, H., Bourre, J.M., Lefauconnier, J.M., 1995. Taurine transport at the blood-brain barrier: an in vivo brain perfusion study. Brain Res. 692, 57–65.

Bernal, G.M., Peterson, D.A., 2011. Phenotypic and gene expression modification with normal brain aging in GFAP-positive astrocytes and neural stem cells. Aging Cell 10, 466–482.

Bolognin, S., Buffelli, M., Puolivali, J., Iqbal, K., 2014. Rescue of cognitive-aging by administration of a neurogenic and/or neurotrophic compound. Neurobiol. Aging 35, 2134–2146.

Bonaguidi, M.A., Wheeler, M.A., Shapiro, J.S., Stadel, R.P., Sun, G.J., Ming, G.L., Song, H., 2011. In vivo clonal analysis reveals self-renewing and multipotent adult neural stem cell characteristics. Cell 145, 1142–1155.

Calzolari, F., Michel, J., Baumgart, E.V., Theis, F., Gotz, M., Ninkovic, J., 2015. Fast clonal expansion and limited neural stem cell self-renewal in the adult subependymal zone. Nat. Neurosci. 18, 490–492.

Chan, C.Y., Sun, H.S., Shah, S.M., Agovic, M.S., Friedman, E., Banerjee, S.P., 2014. Modes of direct modulation by taurine of the glutamate NMDA receptor in rat cortex. Eur. J. Pharmacol. 728, 167–175.

Chen, S.W., Kong, W.X., Zhang, Y.J., Li, Y.L., Mi, X.J., Mu, X.S., 2004. Possible anxiolytic effects of taurine in the mouse elevated plus-maze. Life Sci. 75, 1503–1511.

Choe, K.Y., Olson, J.E., Bourque, C.W., 2012. Taurine release by astrocytes modulates osmosensitive glycine receptor tone and excitability in the adult supraoptic nucleus. J. Neurosci. 32, 12518–12527.

Drew, M.R., Hen, R., 2007. Adult hippocampal neurogenesis as target for the treatment of depression. CNS Neurol. Disord. Drug Targets 6, 205–218.

El Idrissi, A., 2008. Taurine improves learning and retention in aged mice. Neurosci. Lett. 436, 19–22.

El Idrissi, A., Messing, J., Scalia, J., Trenkner, E., 2003. Prevention of epileptic seizures by taurine. Adv. Exp. Med. Biol. 526, 515–525.

Encinas, J.M., Sierra, A., 2012. Neural stem cell deforestation as the main force driving the age-related decline in adult hippocampal neurogenesis. Behav. Brain Res. 227, 433–439.

Encinas, J.M., Michurina, T.V., Peunova, N., Park, J.H., Tordo, J., Peterson, D.A., Fishell, G., Koulakov, A., Enikolopov, G., 2011. Division-coupled astrocytic differentiation and age-related depletion of neural stem cells in the adult hippocampus. Cell Stem Cell 8, 566–579.

Foos, T.M., Wu, J.Y., 2002. The role of taurine in the central nervous system and the modulation of intracellular calcium homeostasis. Neurochem. Res. 27, 21–26.

Frank, M.G., Barrientos, R.M., Biedenkapp, J.C., Rudy, J.W., Watkins, L.R., Maier, S.F., 2006. mRNA up-regulation of MHC II and pivotal pro-inflammatory genes in normal brain aging. Neurobiol. Aging 27, 717–722.

Gebara, E., Sultan, S., Kocher-Braissant, J., Toni, N., 2013. Adult hippocampal neurogenesis inversely correlates with microglia in conditions of voluntary running and aging. Front. Neurosci. 7, 145.

Gil-Mohapel, J., Brocardo, P.S., Choquette, W., Gothard, R., Simpson, J.M., Christie, B.R., 2013. Hippocampal neurogenesis levels predict WATERMAZE search strategies in the aging brain. PLoS One 8, e75125.

Hernandez-Benitez, R., Ramos-Mandujano, G., Pasantes-Morales, H., 2012. Taurine stimulates proliferation and promotes neurogenesis of mouse adult cultured neural stem/progenitor cells. Stem Cell Res. 9, 24–34.

Hodge, R.D., Kowalczyk, T.D., Wolf, S.A., Encinas, J.M., Rippey, C., Enikolopov, G., Kempermann, G., Hevner, R.F., 2008. Intermediate progenitors in adult hippocampal neurogenesis: Tbr2 expression and coordinate regulation of neuronal output. J. Neurosci. 28, 3707–3717.

Huxtable, R.J., 1992. Physiological actions of taurine. Physiol. Rev. 72, 101–163.

Katsimpardi, L., Litterman, N.K., Schein, P.A., Miller, C.M., Loffredo, F.S., Wojtkiewicz, G.R., Chen, J.W., Lee, R.T., Wagers, A.J.,

Rubin, L.L., 2014. Vascular and neurogenic rejuvenation of the aging mouse brain by young systemic factors. Science 344, 630–634.
Kheirbek, M.A., Klemenhagen, K.C., Sahay, A., Hen, R., 2012. Neurogenesis and generalization: a new approach to stratify and treat anxiety disorders. Nat. Neurosci. 15, 1613–1620.
Kim, C., Cha, Y.N., 2014. Taurine chloramine produced from taurine under inflammation provides anti-inflammatory and cytoprotective effects. Amino Acids 46, 89–100.
Kim, J.W., Kim, C., 2005. Inhibition of LPS-induced NO production by taurine chloramine in macrophages is mediated though Ras-ERK-NF-kappaB. Biochem. Pharmacol. 70, 1352–1360.
Kim, H.Y., Kim, H.V., Yoon, J.H., Kang, B.R., Cho, S.M., Lee, S., Kim, J.Y., Kim, J.W., Cho, Y., Woo, J., Kim, Y., 2014. Taurine in drinking water recovers learning and memory in the adult APP/PS1 mouse model of Alzheimer's disease. Sci. Rep. 4, 7467.
Kohman, R.A., 2012. Aging microglia: relevance to cognition and neural plasticity. Methods Mol. Biol. 934, 193–218.
Kronenberg, G., Reuter, K., Steiner, B., Brandt, M.D., Jessberger, S., Yamaguchi, M., Kempermann, G., 2003. Subpopulations of proliferating cells of the adult hippocampus respond differently to physiologic neurogenic stimuli. J. Comp. Neurol. 467, 455–463.
Kuhn, H.G., Dickinson-Anson, H., Gage, F.H., 1996. Neurogenesis in the dentate gyrus of the adult rat: age-related decrease of neuronal progenitor proliferation. J. Neurosci. 16, 2027–2033.
Leon, R., Wu, H., Jin, Y., Wei, J., Buddhala, C., Prentice, H., Wu, J.Y., 2009. Protective function of taurine in glutamate-induced apoptosis in cultured neurons. J. Neurosci. Res. 87, 1185–1194.
Mathieu, P., Battista, D., Depino, A., Roca, V., Graciarena, M., Pitossi, F., 2010. The more you have, the less you get: the functional role of inflammation on neuronal differentiation of endogenous and transplanted neural stem cells in the adult brain. J. Neurochem. 112, 1368–1385.
Menzie, J., Prentice, H., Wu, J.Y., 2013. Neuroprotective mechanisms of taurine against ischemic stroke. Brain Sci. 3, 877–907.
Miller, T.J., Hanson, R.D., Yancey, P.H., 2000. Developmental changes in organic osmolytes in prenatal and postnatal rat tissues. Comp. Biochem. Physiol. A Mol. Integr. Physiol. 125, 45–56.
Muth-Kohne, E., Pachernegg, S., Karus, M., Faissner, A., Hollmann, M., 2010. Expression of NMDA receptors and Ca2 + -impermeable AMPA receptors requires neuronal differentiation and allows discrimination between two different types of neural stem cells. Cell. Physiol. Biochem. 26, 935–946.
Namba, T., Maekawa, M., Yuasa, S., Kohsaka, S., Uchino, S., 2009. The Alzheimer's disease drug memantine increases the number of radial glia-like progenitor cells in adult hippocampus. Glia 57, 1082–1090.
Neuwirth, L.S., Volpe, N.P., El Idrissi, A., 2013. Taurine effects on emotional learning and memory in aged mice: neurochemical alterations and differentiation in auditory cued fear and context conditioning. Adv. Exp. Med. Biol. 775, 195–214.
Palmer, T.D., Takahashi, J., Gage, F.H., 1997. The adult rat hippocampus contains primordial neural stem cells. Mol. Cell. Neurosci. 8, 389–404.
Preissler, J., Grosche, A., Lede, V., Le Duc, D., Krugel, K., Matyash, V., Szulzewsky, F., Kallendrusch, S., Immig, K., Kettenmann, H., Bechmann, I., Schoneberg, T., Schulz, A., 2015. Altered microglial phagocytosis in GPR34-deficient mice. Glia 63, 206–215.
Ramos-Mandujano, G., Hernandez-Benitez, R., Pasantes-Morales, H., 2014. Multiple mechanisms mediate the taurine-induced proliferation of neural stem/progenitor cells from the subventricular zone of the adult mouse. Stem Cell Res. 12, 690–702.
Ripps, H., Shen, W., 2012. Review: taurine: a "very essential" amino acid. Mol. Vis. 18, 2673–2686.
Schaffer, S.W., Azuma, J., Mozaffari, M., 2009. Role of antioxidant activity of taurine in diabetes. Can. J. Physiol. Pharmacol. 87, 91–99.
Schmidt-Hieber, C., Jonas, P., Bischofberger, J., 2004. Enhanced synaptic plasticity in newly generated granule cells of the adult hippocampus. Nature 429, 184–187.
Seri, B., Garcia-Verdugo, J.M., Collado-Morente, L., McEwen, B.S., Alvarez-Buylla, A., 2004. Cell types, lineage, and architecture of the germinal zone in the adult dentate gyrus. J. Comp. Neurol. 478, 359–378.
Streit, W.J., Walter, S.A., Pennell, N.A., 1999. Reactive microgliosis. Prog. Neurobiol. 57, 563–581.
Sturman, J.A., Moretz, R.C., French, J.H., Wisniewski, H.M., 1985. Postnatal taurine deficiency in the kitten results in a persistence of the cerebellar external granule cell layer: correction by taurine feeding. J. Neurosci. Res. 13, 521–528.
Sultan, S., Gebara, E.G., Moullec, K., Toni, N., 2013a. D-serine increases adult hippocampal neurogenesis. Front. Neurosci. 7, 155.
Sultan, S., Gebara, E., Toni, N., 2013b. Doxycycline increases neurogenesis and reduces microglia in the adult hippocampus. Front. Neurosci. 7, 131.
Tashiro, A., Sandler, V.M., Toni, N., Zhao, C., Gage, F.H., 2006. NMDA-receptor-mediated, cell-specific integration of new neurons in adult dentate gyrus. Nature 442, 929–933.
Taupin, P., 2007. BrdU immunohistochemistry for studying adult neurogenesis: paradigms, pitfalls, limitations, and validation. Brain Res. Rev. 53, 198–214.
Thuret, S., Toni, N., Aigner, S., Yeo, G.W., Gage, F.H., 2009. Hippocampus-dependent learning is associated with adult neurogenesis in MRL/MpJ mice. Hippocampus 19, 658–669.
van Praag, H., Shubert, T., Zhao, C., Gage, F.H., 2005. Exercise enhances learning and hippocampal neurogenesis in aged mice. J. Neurosci. 25, 8680–8685.
van Praag, H., Lucero, M.J., Yeo, G.W., Stecker, K., Heivand, N., Zhao, C., Yip, E., Afanador, M., Schroeter, H., Hammerstone, J., Gage, F.H., 2007. Plant-derived flavanol (-)epicatechin enhances angiogenesis and retention of spatial memory in mice. J. Neurosci. 27, 5869–5878.
Walter, J., Keiner, S., Witte, O.W., Redecker, C., 2011. Age-related effects on hippocampal precursor cell subpopulations and neurogenesis. Neurobiol. Aging 32, 1906–1914.
Wu, J.Y., Tang, X.W., Schloss, J.V., Faiman, M.D., 1998. Regulation of taurine biosynthesis and its physiological significance in the brain. Adv. Exp. Med. Biol. 442, 339–345.
Wu, H., Jin, Y., Wei, J., Jin, H., Sha, D., Wu, J.Y., 2005. Mode of action of taurine as a neuroprotector. Brain Res. 1038, 123–131.
Yamaguchi, M., Saito, H., Suzuki, M., Mori, K., 2000. Visualization of neurogenesis in the central nervous system using nestin promoter-GFP transgenic mice. Neuroreport 11, 1991–1996.